31515

THE NOVAYA ZEMLYA EVENT OF 31 DECEMBER 1992 AND SEISMIC IDENTIFICATION ISSUES

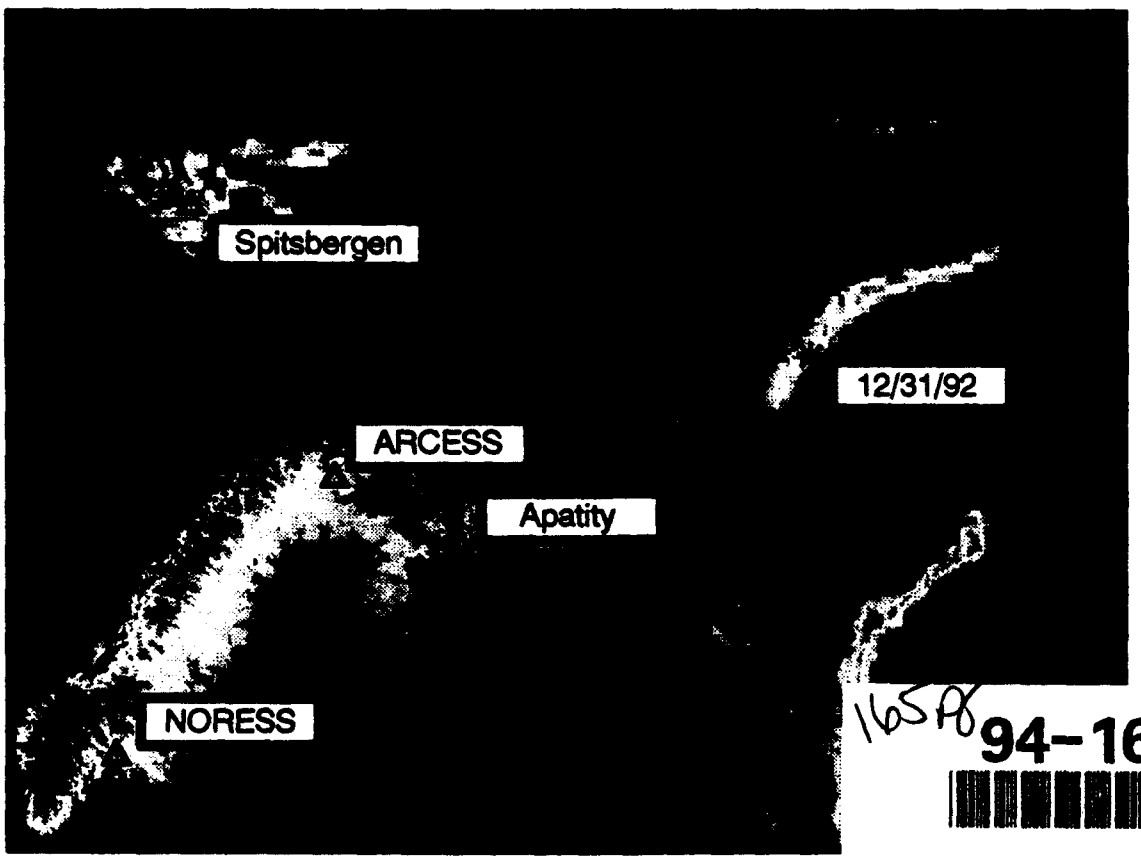

*Original contains color plates: All DTIC reproductions will be in black and white.

15th Annual
Seismic Research Symposium
8 - 10 September 1993
Vail, Colorado

THE NOVAYA ZEMLYA EVENT OF 31 DECEMBER 1992 AND SEISMIC IDENTIFICATION ISSUES

15th Annual
Seismic Research Symposium
8 - 10 September 1993
Vail, Colorado

TABLE OF CONTENTS

TABLE OF CONTENTS
(Continued)

EXECUTIVE SUMMARY

THE NOVAYA ZEMLYA EVENT OF DECEMBER 31, 1992 AND SEISMIC IDENTIFICATION ISSUES

Executive Summary

Alan S. Ryall , Jr.
ARPA/NMRO

Introduction

On December 31, 1992 a small (mb 2.5) event (hereafter "921231") was detected on Novaya Zemlya by the Threshold Monitor (TM) system developed and operated by NORSAR (Ringdal and Kvaerna, 1989; Kvaerna, 1991; 1992). The TM system uses data from the on-line array network to continuously monitor seismic amplitude levels for a number of specified experimental target sites, including the Russian nuclear test range on Novaya Zemlya. The method involves continuous beamforming (i.e., time-aligning and summing the traces for each regional array) for the target beam-steering points, to extract parameters of the beams for a continuous assessment of the upper magnitude limit of events at the target site that would go undetected by the Scandinavian array network. When events occur that are above the network noise level, they appear as peaks on the TM beams and are thus tagged for detailed off-line analysis. The 921231 event was detected in this way and was identified as an event that might be of particular interest to ARPA.

On receipt of the information ARPA decided to use the 921231 event as an example to test the effectiveness of seismic identification tools and systems that are being developed within the nuclear monitoring research community. The reason for focusing on this particular event is that it had a number of characteristics that might be typical of events that would be of concern in a future CTBT or NPT monitoring environment:

- it was in an area where nuclear testing had been conducted;
- it was in an area of very low seismicity;
- it occurred during a testing moratorium;
- it had magnitude appropriate for a fully decoupled 1 kiloton nuclear test;
- it was detected by only a few highly sensitive arrays at far-regional distances, due to its small magnitude and the sparse station distribution in the region.

A number of ARPA contractors who have been involved in seismic identification research and/or the development of identification subsystems for the Intelligent Monitoring System were asked to attempt to identify the 921231 event and write a short report on their results. These contractors included T.J. Sereno (SAIC), D.R. Baumgardt (ENSCO), T.J. Bennett (S-Cubed), J.J. Pulli (Radix) and M.D.

Fisk (Mission Research). In addition, information on tectonic structure of Novaya Zemlya was supplied by R. Matzko (U.S. Geological Survey), and Hans Israelsson (SAIC) reanalyzed the location of the event. The analysis reports received from these individuals are attached as separate sections of this report. Together they comprise an interesting case study, and one which illustrates the point that identification of small seismic events is not yet a solved problem. They also show the value of a team approach to resolving the remaining issues of seismic identification, as each of the seismologists analyzing the 921231 event had a different view of the problem stemming from his particular experience in this research area, and these views together present a more complete picture than any of the analyses by itself.

Location of the event

The initial location of the 921231 event provided by NORSAR was 73.6 deg N, 55.2 deg E, depth 0.0 km (fixed), with an error-ellipse semi-major axis of 47.8 km oriented N 69 W, and a semi-minor axis of 20.2 km. This location is on the north island, north of Matochkin Shar Strait and east of Mityushikha Fjord; the error ellipse is almost entirely on land. In an April 1993 communication the NORSAR group reports:

> "We have concluded extensive analysis of the mb = 2.5 seismic event at Novaya Zemlya at 09.29.25 GMT on 31 December 1992. This event was detected by ARCESS (P and S), Spitsbergen (P and S), NORESS (P) and Apatity (S). In addition, the Kola Centre provided readings for the station Amderma (Pg and Sn) made from analog recordings. Our results indicate that the epicenter was slightly to the north of the test site. However, there are some uncertainties in the travel time tables, and an on-site location cannot entirely be ruled out."

At ARPA's request, the event location was also analyzed by the research group at the ARPA Center for Seismic Studies (CSS), and a report by Hans Israelsson (1993) covering this reanalysis is included as a following section. The CSS analysis involves a master-event relocation of the 921231 event, using as a reference event a well-recorded nuclear test on October 24, 1990. The analysis focuses on the problem of timing low-amplitude signals obscured by noise, and discusses the scatter in picks made independently by four analysts. This scatter was used to estimate uncertainties in the arrival times used in the master-event calculation. The analysis also involved the use of different earth models, including a Scandinavian crustal model that has been used at the CSS since 1990, and the 1991 IASPEI model (Kennett, 1991). Because the Spitsbergen array did not record the reference event, the Spitsbergen arrival times were compared with P and S readings for the reference event at station KBS, which is about 100 km farther from Novaya Zemlya than the Spitsbergen array. Israelsson's final location of the event was 73.46 deg N, 55.48 deg E, with an error ellipse having semi-major axis of 12 km oriented N 113 deg E, and semi-minor axis of 8 km. The uncertainty in the location is largely controlled by the

assumed standard error of the Sn reading at ARCESS. The event depth was assumed to be zero, lacking any evidence to the contrary.

Israelsson's analysis and that of the NORSAR group illustrate the difficulties associated with attempting to accurately locate a small event that is poorly recorded by only a few stations, at far-regional distance and with poor azimuthal distribution -- even, as in this case, where a region has been calibrated by large, well-located nuclear explosions. It points up the need for research to determine earth structure and/or traveltime and azimuth corrections in areas of concern to treaty monitoring. Research is also needed to evaluate and improve current location methods, and to develop reliable techniques for determining focal depth using regional seismic data.

Tectonic structure

A summary of the tectonic structure of Novaya Zemlya was provided in a 1993 communication by Rod Matzko of the U.S. Geological Survey. A small-scale geologic map included with the communication clearly indicates a NNE-trending fault zone about 20 km west of the eastern side of the island. According to Matzko:

> "The trend of this fault is parallel to the trend of the elongate fold structures of the island; this is the same trend followed by the Main Novozemel'skii fault, which runs the length of Novaya Zemlya along the west coast. Sidorenko (1970, p. 189) says that the majority of Mesozoic-Cenozoic faults are steep in nature, directed along the strike of fold structures with sharp dip angles. Another feature of some of these faults is a significant horizontal component in their movement. The age of the fault in question is not known, but the map suggests that it cuts rocks of lower to upper Carboniferous age. Sidorenko also states that gulfs and river valleys are "intimately traversed by transverse and diagonal faults," and that the straits of Matochkin Shar, Karskiye Vorota and Yugorski Shar at the southern tip of Novaya Zemlya, are all fault controlled. It is reasonable to expect that the river valleys and gulfs that trend perpendicular to these straits are controlled by faults running parallel to the structural trend of the islands."

Identification

Developing the capability to identify, with high confidence, small events in areas of low seismicity and sparse station distribution remains as a major obstacle to effective monitoring of a CTBT or NPT, and the 921231 event provides a good illustration of the difficulty this problem poses for the research community. To visualize this problem consider Figure 1, which shows spectrograms (provided by Anne Suteau-Henson of CSS) for the 921231 event, a nuclear test in 1990, a mid-Atlantic Ridge earthquake in 1989, and a Novaya Zemlya earthquake in 1986. ARCESS had the clearest signals for the 921231 event, and two of the reference events were also recorded at ARCESS. However, the nuclear test was much larger

than the 921231 event, and the 1989 earthquake, while only somewhat larger and slightly farther from the array than the 921231 event, was in a completely different azimuth. The 1986 Novaya Zemlya event was concluded to be a probable earthquake because of its Ms:mb ratio, but since ARCESS was not operating in 1986 only a NORESS recording is available for both events, and NORESS is twice the distance of ARCESS from Novaya Zemlya. The 1986 event was also larger than the 921231 event by more than two units of magnitude. Thus, while recordings of a large number of historic nuclear tests are available for Novaya Zemlya, an adequate sample of small earthquakes, chemical explosions and small nuclear explosions does not exist to construct an identification "training set" for this case. A similar situation will obtain in numerous areas of concern to CTBT and/or NPT monitoring around the world, and ways must be found to transport identification techniques from one region to another without complete degradation of confidence in the results.

Figure 1 shows differences and similarities between the four events. For example, the 921231 event has relatively more high-frequency energy in both P and S than any of the other events. The event displays significant spectral variance, but not the distinct, time-independent features observed by Henson (1989) and Hedlin et al. (1990) for ripple-fired quarry blasts recorded at shorter distance ranges. The 1989 mid-Atlantic Ridge earthquake has less spectral variance and smaller S/P amplitude ratio than the 921231 event. The 1986 Novaya Zemlya earthquake also had small S/P ratio, and most of its P energy is concentrated in a large peak at 2 Hz. The 1990 nuclear explosion has less spectral variance than either the 1992 or 1989 events and an S/P ratio close to 1; however, the S energy is shifted to lower frequency by almost 2 Hz relative to the frequency band for the P wave. For the other three events this shift in frequency between P and S is not observed. Because of possible effects due to differences in event size, distance, azimuth and source radiation pattern, it is not possible to characterize specific features on these spectrograms as being due to differences in source type (earthquake, nuclear test, mine blast). The 921231 spectrogram has some features that are similar to each of the other events, and some that are different.

Similar conclusions were reached in the more extensive analyses presented in other sections of this report. The section by Sereno and Wahl (1993) describes an automated event identification subsystem (EVID) that has been operated as part of the Intelligent Monitoring System (IMS) at the Center for Seismic Studies (CSS). The authors characterize EVID as a "novel-event detector," which can be used to screen a sample of seismic signals to reject events that are identified with high confidence to be earthquakes or mine explosions. This would then allow the analysts to focus their effort primarily on events that the system has not been able to identify, searching in particular for nuclear tests conducted under evasive conditions. The EVID analyzes *contextual discriminants* (event depth, location, magnitude, and seismicity of the epicentral region) and *regional discriminants* (including but not limited to source multiplicity, cepstral analysis, spectral variance, presence of Rg, S/P amplitude ratio), and also tries *script matching* (waveform

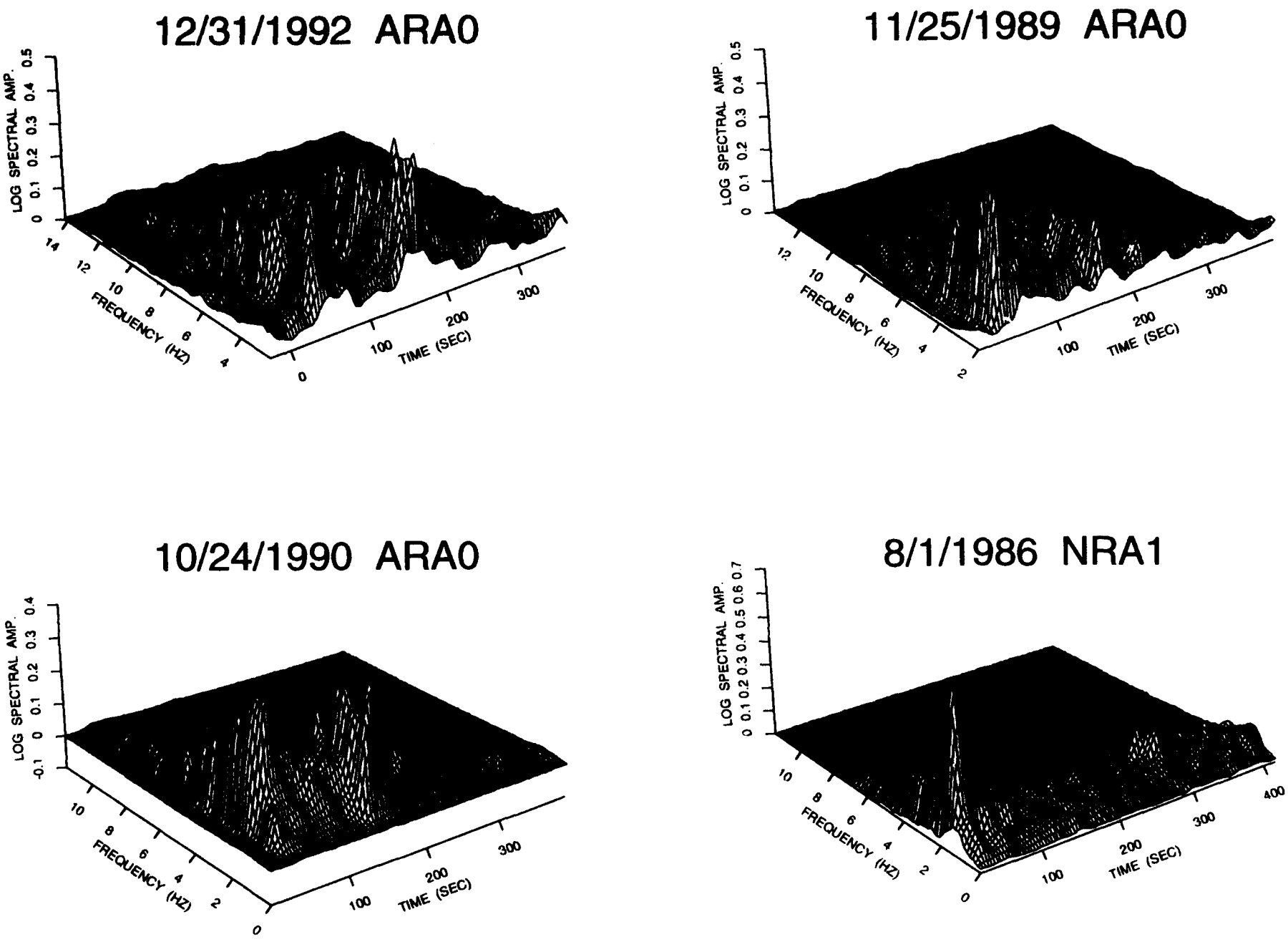

Figure 1. Spectrogram of the December 31, 1992, Novaya Zemlya event (upper left, ML 2.3), compared with an mb 5.7 nuclear test on October 24, 1990 (lower left), an ML 2.2 mid-Atlantic Ridge earthquake on November 25, 1989 (upper right), and an mb 4.6 Novaya Zemlya earthquake on August 1, 1986. The latter was recorded at NORESS, Δ = 20.6 deg; the others are from ARCESS, Δ = 10.0-11.9 deg.

correlation) for events located in areas that have repeated mine explosions. For some of the discriminants a "fuzzy logic" approach is used that permits an event to have membership in two classes simultaneously (e.g., 40% deep, 60% shallow focal depth). EVID can be expanded to include a wide range of discriminants, and its performance can be improved with time if region-specific knowledge is added to the system to make the methods more effective.

In the case of the 921231 event, almost all of the EVID discriminants were ineffective: the location (on land in a generally aseismic region), the small magnitude and uncertain focal depth gave an indeterminate identification. Some of the regional discriminants (lack of cepstral evidence for source multiplicity, lack of spectral variance, lack of an Rg phase) may have been indeterminate because of the small SNR and large epicentral distance -- ARCESS, the nearest array, was more than 1,100 km from the event. The depth of the event could not be determined because it was recorded by only a few stations in a limited, far-regional distance range. Script matching could not be used because a set of previously recorded small earthquakes and mine blasts on Novaya Zemlya did not exist. One discriminant that showed a distinct difference between the 921231 event and three previous nuclear tests recorded by ARCESS was the high-frequency S/P amplitude ratio, which was smaller for the nuclear tests than for the 921231 event. However, the nuclear tests were three units of magnitude larger than the 921231 event, and the shift to lower frequencies for the S wave may have been a function of the event size. Sereno and Wahl (1993) conclude that neither the contextual nor the regional discriminants are sufficient to identify the 921231 event, and "an obvious conclusion is that other and better regional discriminants are needed to identify this type of event." They also point out that transporting discriminants from calibrated to uncalibrated regions "requires an extensive amount of observational data for which ground-truth information is available. Therefore, efforts to acquire large regional data sets in areas of interest with ground truth information are important. Unfortunately, relatively aseismic areas like Novaya Zemlya have few data for calibration. Therefore, accurate identification of events in these areas will depend heavily on our ability to transport *model-based* discriminants."

The 921231 event was also studied by Baumgardt (1993) using an Intelligent Seismic Event Identification System (ISEIS) developed by ENSCO. Like EVID, ISEIS was developed as a post-processor to be used after the detection and location of an event, and it incorporates both regional and teleseismic discriminants. The system can be used in either an interactive or automated mode, and includes a front-end signal analysis capability as well as feature extraction to make measurements used by the discriminants. Discrimination processing in ISEIS involves initial data status assessment to determine if sufficient data are present to identify the event, followed by event identification. As with EVID the latter includes both a comparison of waveforms with reference events and an identification processor based on a number of discriminants (P/S ratio, spectral ratio, ripple-fire analyzer, dynamic time-warp, and other methods).

Baumgardt's analysis of the 921231 event included comparison of its signal features with those of reference data sets, including a large number of earthquakes and mine blasts around Scandinavia and on the Kola peninsula, a signal from a submarine sinking off the coast of Norway, and nuclear tests on Novaya Zemlya. The 921231 NORESS signal was also compared with that of the August 1, 1986 Novaya Zemlya earthquake. The data processing included incoherent beam analysis, spectral analysis, Pn/Sn amplitude ratios for different frequency bands, Sn spectral ratios, and analysis of spectral scalloping. The 921231 event was found to have high-frequency Pn/Sn amplitude ratio smaller than the nuclear tests but somewhat larger than those produced by small earthquakes in the same distance (but different azimuth) range. The Pn/Sn ratio in the 8-10 Hz band was the same for the 911231 event as for mine explosions on the Kola Peninsula (same azimuth, different distance). Lack of spectral scalloping suggested that the event was not ripple-fired, although some ripple-fired mine blasts have been observed to lack spectral scalloping.

In a detailed comparison with the 1986 Novaya Zemlya earthquake, Baumgardt presents a scaling analysis in which narrow-band Pn/Sn amplitude ratios for a number of nuclear explosions are scaled to the 921231 event (ARCESS recordings) and to the 1986 Novaya Zemlya earthquake (NORESS recordings). This scaling was done for four frequency bands, and the factor required to scale the Pn/Sn ratio for the nuclear tests to the 921231 event was found to be about the same as that needed to scale the nuclear tests to the 1986 earthquake, after compensating for differential attenuation of P and S waves. This provided indirect evidence that the 921231 event was also an earthquake. Baumgardt concludes that careful consideration of propagation-path differences is essential in comparing known earthquakes and explosions with events of unknown identity. If propagation path differences were not taken into account, comparison of the 921231 Pn/Sn ratio with that of Kola mine explosions would have led to the conclusion that the 921231 event was a mine blast.

Bennett et al. (1993) compare their analysis of the 921231 event with previous S-Cubed studies of nuclear tests, earthquakes, mine explosions and rockbursts in different parts of the world. They observe that Lg/P and S/P ratios for nuclear explosions*in many different areas and over a wide range of magnitude* are commonly 1.0 or greater at frequencies less than about 2 Hz, but these ratios drop to significantly lower values at higher frequencies. This substantiates the conclusion that the relatively high Sn/Pn ratio for the ARCESS recording of the 921231 event is inconsistent with the event having been an underground nuclear test. However, the authors were unable to make a definitive distinction between three alternative source types: earthquake, rockburst or chemical explosion. As an additional complication, Bennett (1993, personal communication) is studying cavity-decoupled nuclear explosions (the 0.38 kt Sterling experiment in 1966 and an 11.5 kt shot in Azgir in 1976), and observes that the high-frequency S/P ratio is larger (i.e., more similar to earthquakes and quarry blasts) for the decoupled explosions than for fully coupled nuclear explosions at the same test site.

Pulli and Dysart (1993) apply a *hybrid machine learning* technique to the identification problem, with a back propagation neural network using measured parameters of the Pn and Sn waves recorded by ARCESS: broadband plus three different narrowband Pn/Sn spectral ratios, and the Pn and Sn cepstral variances. The neural network was trained with NORESS recordings of explosions and earthquakes around Scandinavia, and when the 921231 event was input to the trained network it was clearly within the chemical explosion population. However, the authors note that in examining the six parameters separately, the high-frequency (10-20 Hz) Pn/Sn spectral ratio for the 921231 event was more consistent with the earthquake measurements than with those for the mine explosions. This result is opposite to that of Baumgardt (1993), who found that the high-frequency Pn/Sn ratio for the 921231 event was identical to that for the explosion sample used, and significantly higher than the earthquake values. This underscores Baumgardt's comments about the importance of taking path effects into account, and calls for caution in training automated analysis systems on discriminants that may be specific to regions other than the one being monitored.

In the last section, Fisk and Gray (1993) use Baumgardt's analysis of narrowband Pn/Sn ratios to illustrate a statistical approach to the identification problem. The method, which involves the generalized likelihood ratio (GLR) and the bootstrap technique, can be applied to statistically classifying events in regions where only a handful of previously recorded events may exist, and may also be used to test training sets for possible contamination. Application of a GLR *outlier test* rejected the 921231 event as an outlier of the 3-event Novaya Zemlya nuclear test population, a group of 24 earthquakes near Steigen, Norway, or a group of 5 Mid-Atlantic Ridge earthquakes. However, the outlier test indicated that the 921231 event could be rejected as a member of the Kola quarry blast group (53 events) only if we were willing to reject a third of the Kola blasts as members of the group. Using a GLR *classification test* trained on the four reference event groups, the 921231 event was again rejected as a member of the nuclear test, Mid-Atlantic Ridge earthquake or Steigen earthquake populations, but was accepted as a member of the Kola quarry blast group. The authors point out that their results do not imply that the 921231 event was a Kola quarry blast, only that this classification is preferred over the alternatives and there is insufficient evidence to reject it as a Kola event based on the training data. They also noted that a key question in regard to this analysis is whether the discriminants used are truly characteristic of the source, and suggest that the extent to which such discriminants are influenced by propagation effects should be the subject of further investigation.

As a final note, on 9 February 1993 the Seismological Service of the Ministry of Defense, Russian Federation, was contacted and asked if they had any information as to the origin of the 921231 event. The response from Col. V.V. Kovalenko on 18 March 1993 was that on the date in question there were no blasting activities, either for military or construction purposes, on the territory of the Novaya Zemlya test range.

Conclusions

Only one relatively firm conclusion appears to be possible from the analyses and comparisons presented in this report, and that is a finding that the 921231 event had high-frequency P/S amplitude and spectral ratios that are inconsistent with large, fully-coupled nuclear explosions on Novaya Zemlya, and with nuclear explosions having a range of yields in other regions. Because of its small size the 911231 event was recorded by only a few sensitive stations, none of which were close to the epicenter, and as a result of poor SNR and possibly distance effects most of the regional and teleseismic discriminants that are used for larger events could not be applied or were indeterminate in this case. Careful analysis showed that signal features for this event were variously consistent with those observed for earthquakes, mine explosions, and possibly even decoupled nuclear explosions in other regions.

Part of the difficulty in identifying this event stems from the fact that our experience with Novaya Zemlya is almost entirely limited to recordings of large, fully coupled nuclear tests, a single exception being a small earthquake near Novaya Zemlya in 1986 (recorded by the NORESS array but not by newer arrays that recorded the 921231 event). Lacking an adequate database of known earthquakes and mine explosions on Novaya Zemlya, identification of the 921231 event could only be attempted by comparing its signal characteristics with earthquakes and mine blasts in other regions -- at different distance ranges, different azimuths, different earth structure and different magnitudes than the event of interest. Because features of seismic signals are functions not only of source type but also of event size and earth structure along the propagation path, classification of small events in a poorly calibrated region based on signal characteristics observed elsewhere is a process that, at our current level of understanding, is attended by more than slight uncertainty.

Recommendations

To add a political/programmatic dimension to this discussion, Congress in the July 1992 Hatfield-Mitchell-Exon amendment to HR5373 required the administration to negotiate a multilateral Comprehensive Test Ban Treaty by September 1996. Toward this end, the United Nations Conference on Disarmament is now preparing to negotiate such a treaty. The treaty will include a regime of international verification drawing on the work of the CD's Group of Scientific Experts, especially in the use of the prototype international monitoring system that is now being tested and that will be fully operational in 1995.

The analyses summarized above and discussed in detail in the following sections underscore the point that seismic identification remains as the primary technical obstacle to our ability to adequately monitor a CTBT. In particular, we urgently need to develop the capability to accurately locate and to identify *with high confidence* any small nuclear tests that may be conducted in the future under

evasive conditions anywhere in the world. ARPA is undertaking immediately an aggressive R&D effort to address this problem.

Rather than tackle the identification problem on a global basis the ARPA research program will focus on specific region -- the Middle East -- with the objective of demonstrating that over a relatively short period of time both the tools and the knowledge base can be acquired for effective treaty verification in a region that has previously not been a focus of U.S. monitoring efforts. The database for this research will consist of recordings from a number of new seismic arrays and broadband stations that are being deployed in the Middle East and Eurasia in connection with the upcoming GSE monitoring experiment, and that are planned to be operational by the end of 1993. In addition, there are a large number of local and regional network stations already operating in various Middle Eastern countries, and an attempt will be made to acquire data from these networks as such data is needed to help with calibration of earth structure and propagation characteristics.

Research conducted under the ARPA plan will be closely coordinated to avoid duplication and to provide for optimum communication between the contractors and the government. The program will be evaluated at regular intervals by an ARPA advisory panel, to help with coordination and to provide guidance on the most promising research directions. The technologies developed under this program will be incorporated into the Intelligent Monitoring System, automated using expert system techniques being developed in a complementary effort, tested in routine analysis of data during and after the GSE Technical Test, and continuously evaluated to insure that the capability of the system to accurately locate and identify detected events continues to improve with experience.

Elements of the ARPA identification research program are shown by the chart in Figure 2. Because event location is an important ingredient of identification, the top part of the chart shows the components needed to develop a knowledge base with sufficient information on earth structure, characteristics of seismic propagation, station traveltime, amplitude corrections and other parameters for accurate location of seismic events. Construction of a geophysical information system for the Middle East (Fielding et al., 1993) has been undertaken by workers at Cornell University; this system will reside at Cornell and will be accessible via network connections to the CSS over Internet. Theoretical waveform modeling, inversion of broadband recordings of moderate-sized events in the region, and data from local and regional networks will be used to improve knowledge of the structure of the lithosphere and to identify secondary arrivals detected by regional seismic stations. All of this information will be incorporated into automated event location routines and the location results will be evaluated to insure that the accuracy of IMS event locations for the Middle East continues to improve.

The lower part of Figure 2 shows components of a program to demonstrate an improved capability to identify small Middle Eastern seismic events detected by the new seismic arrays in that region. In general the various research areas correspond

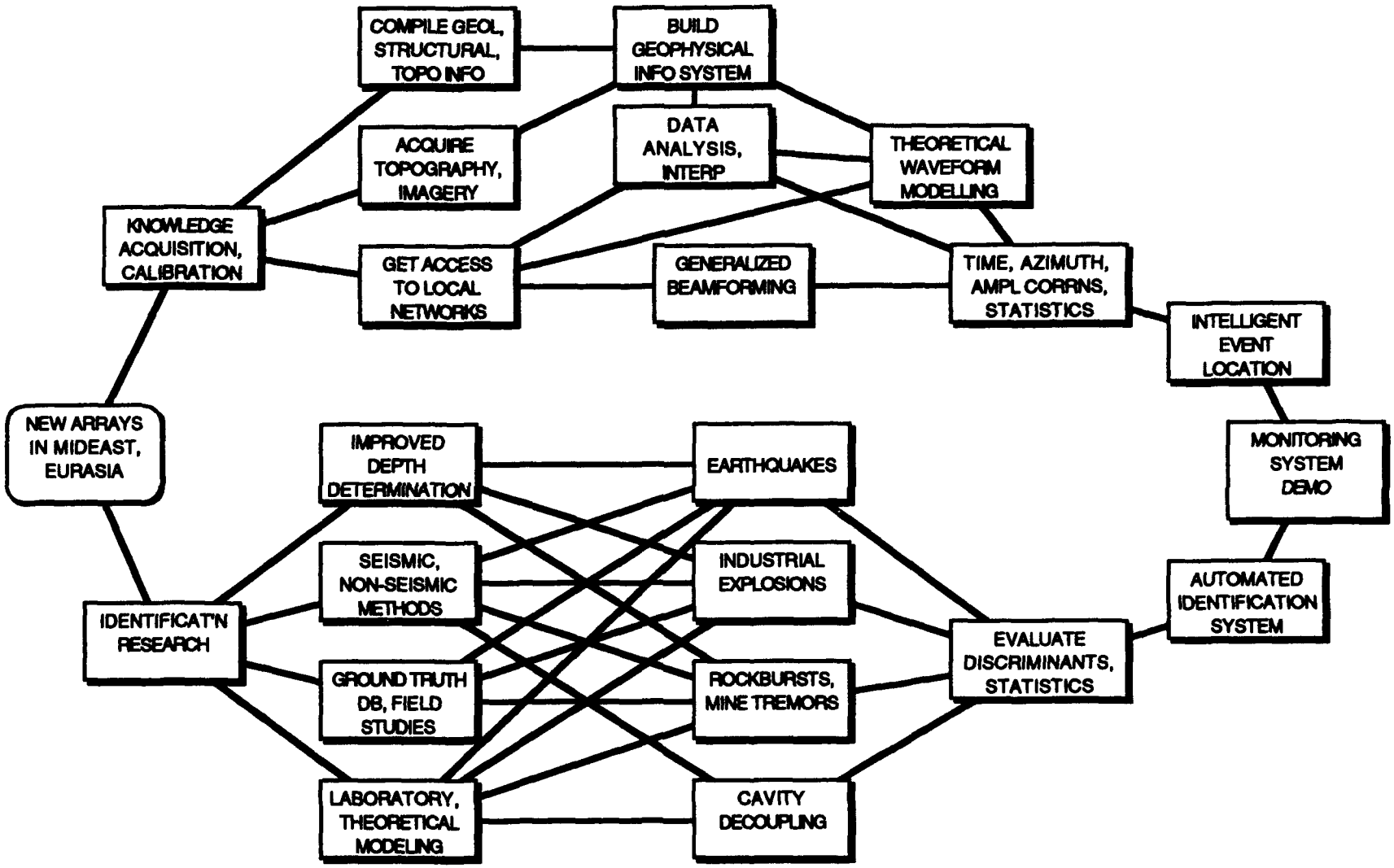

Figure 2. Elements of an ARPA research program aimed at achieving automated event location and identification by September 1996

to those recommended by an ARPA advisory panel in 1992, following an ARPA Seismic Identification Workshop (Blandford, et al., 1992; distributed at the 14th Annual PL/ARPA Seismic Research Symposium in Tucson). Research to improve depth determination is included in the identification research program on Figure 2 because of the importance of accurate focal depth to seismic identification. The research will also include testing of known discriminants and development of new seismic identification tools, insofar as possible tailored to the area of interest. Non-seismic techniques such as infrasonic measurements will be explored. Laboratory studies, theoretical waveform modeling and field studies will all be employed to develop a better understanding of the various types of seismic sources (earthquakes, mine explosions, rockbursts, mine tremors) that may be observed in the Middle East, and to develop a more complete picture of the tradeoffs between effects due to event type, depth, size, structure along the path, and other factors. Because it is unlikely that nuclear explosions will be conducted in this region, every effort will be made to save all the information that is now available for such events in other regions, and to make it available to the research community. Synthetic data may be the only means of evaluating evasion scenarios, and such data will be generated for decoupling scenarios in structures analogous to those in the Middle East, and will be stored at the CSS for use by the research community. Research will continue on the development of a rigorous statistical framework for an automated identification system, including a system of metrics by which the various discriminants can be judged to succeed or fail.

The analyses and interpretations presented in the following sections of this report indicate that the problem of identifying small, poorly-recorded seismic events in previously uncalibrated regions will be, in colloquial terms, a tough nut to crack. On the other hand the approach planned by ARPA, by focusing an intensive, highly coordinated, multi-agency research effort on a specified region of interest, should offer a far more vigorous attack on the problem than trying to glean bits and pieces of knowledge from the loose collection of basic and applied investigations that constituted the discrimination research program of years past. With the likelihood that negotiations will begin soon on a CTBT, and that these negotiations will focus on protocols to establish an effective monitoring regime for this treaty, the urgency of this research should be quite clear.

References

Baumgardt, D.R. (1993). Seismic waveform feature analysis and discrimination of the December 31, 1992 Novaya Zemlya event, *this report,* 30 pp.

Bennett, T.J., J. R. Murphy, M.E. Marshall and B.W. Barker (1993). A preliminary regional seismic discrimination of the Novaya Zemlya event of December 31, 1992, *this report,* 22 pp.

Blandford, R.R., A. Dainty, R. Lacoss, R. Maxion, A. Ryall, B. Stump, C. Thurber, T. Wallace (1992). *Report on the DARPA Seismic Identification Workshop,* DARPA Spec. Rpt., 28 pp.

Fielding, E., M. Barazangi and B. Isacks (1993). A network-accessible geological and geophysical database for Eurasia, North Africa and the Middle East, *Proc. 15th Annual Seismic Research Symposium,* in press.

Fisk, M.D. and H.L. Gray (1993). Event identification analysis of the Novaya Zemlya event on 31 December 1992 using outlier and classification likelihood ratio tests, *this report,* 25 pp.

Grant, L., J. Coyne and F. Ryall (1993). GSS Ground-Truth database: Update and case study, *Proc. 15th Annual Seismic Research Symposium,* in press.

Gray, H.L., W.A. Woodward and G.D. McCartor (1993). A bootstrap generalized likelihood ratio test in discriminant analysis, *Proc. 15th Annual Seismic Research Symposium,* in press.

Hedlin, M., J. Orcutt, B. Minster and H. Gurrola (1990). An automatic means to discriminate between earthquakes and quarry blasts, *Bull. Seism. Soc Am., 80(B),* 2143-2160.

Henson, Anne (1989). Summary of spectrogram characterization of regional events, *Tech. Rept. C89-02 for 1 October 1987-30 September 1989, Center for Seismic Studies, SAIC,* Section 3, 2-5.

Israelsson, Hans (1993). Estimates of the epicenter uncertainty for a small Novaya Zemlya event Dec. 31 1992, *this report.* 18 pp.

Kennett, B.L.N., editor (1991). *IASPEI 1991 Seismological Tables,* Research School of Earth Sci., Australian Nat. University, Canberra, Australia, 167 pp.

Kvaerna, Tormud (1991). Threshold monitoring of Novaya Zemlya: A scaling experiment, *Semiannual Tech. Summary, 1 Oct 1990-31 Mar 1991,* NORSAR Sci. Rept. 2-90/91, NORSAR, Kjeller, Norway.

Kvaerna, Tormud (1992). Continuous threshold monitoring of the northern Novaya Zemlya test site: Long-term operational characteristics, *Sci. Rept. 12, 1Nov 1991-31 Jan 1992,* NORSAR Sci. Rept., NORSAR, Kjeller, Norway.

Pulli, J.J. and P.S. Dysart (1993). Identification analysis of the Dec. 31, 1992 Novaya Zemlya event, *this report,* 16 pp.

Ringdal, F. and T. Kvaerna (1989). A multi-channel processing approach to real-time network detection, phase association and threshold monitoring, *Bull. Seism. Soc. Am., 79,* 1927-1940.

Sereno, T.J. and D.D. Wahl (1993). A fuzzy-logic approach to regional seismic event identification: application to the Novaya Zemlya event on 31 December 1992, *this report,* 24 pp.

Sidorenko, , A.V. (1970). *Geologiya SSSR, T. XXVI, Ostrova Sovetskoi Arktiki, Geologicheskoye Opisaniye (Geology of the USSR, Vol. XXVI, Islands of the Arctic, Geologic Descriptions),* "Nedra," Moscow, 547 pp.

ESTIMATES OF THE EPICENTER UNCERTAINTY FOR A SMALL NOVAYA ZEMLYA EVENT DEC 31 1992

Report #

ESTIMATES OF THE EPICENTER UNCERTAINTY FOR A SMALL NOVAYA ZEMLYA EVENT DEC 31 1992

Hans Israelsson

Science Applications International Corporation
Center for Seismic Studies
1300 N. 17th Street, Suite 1450
Arlington, VA 22209

May 14, 1993

Scientific Report No. 1

INTRODUCTION

The purpose of the analysis in this note was to estimate the epicenter and its associated uncertainties of a small seismic event in the Novaya Zemlya region on 92/12/31 with an origin time around 09:29. To this end waveform data recorded at the mini arrays ARA0 and NRA0 were analyzed relative to waveform data from a reference event, a nuclear explosion at the Novaya Zemlya testing grounds on 90/10/24 (14:58:00, 73.32 N and 54.78 E). In addition waveform data for the 92/12/31 event at the mini array SPA0 was used together with arrival time data reported from the station KBS for the reference event.

Figure 1 shows the relative location of Novaya Zemlya and the seismic stations. The loca-

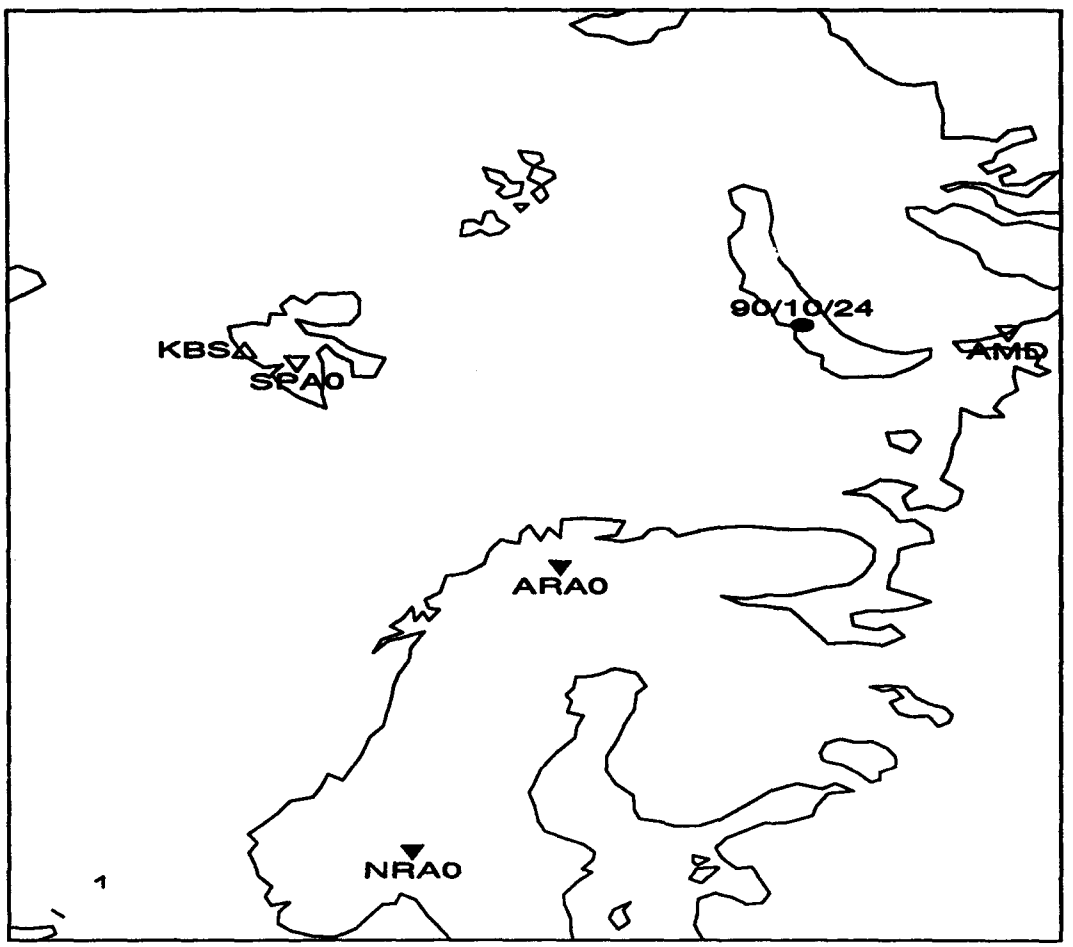

Figure 1: *The map shows the locations of the Novaya Zemlya explosion on 90/10/24 and of the seismic stations for which data were analyzed.*

tion of the 90/10/24 explosion is also marked on the map and so is the location of the sta-

tion Amderma, AMD, in northern Russia, for which arrival time data were available for the 92/12/31 event, but not for the 90/10/24 event.

For the estimation we attempted to assess the accuracy of the arrival time readings, select a travel time model, and apply reference event location techniques. The dimensions of the estimated epicenter confidence ellipse of the 92/12/31 event were also compared with location errors calculated for some similar arrival time data sets of nuclear explosions at Novaya Zemlya and for locations based on data only at the two arrays, ARA0 and NRA0.

ARRIVAL TIME MEASUREMENTS

Arrival times of Pn and Sn phases at ARA0 and of the Pn phase at NRA0 and SPA0 were measured by four analysts. One of the analysts made two sets of independent measurements. The measurements for ARA0 and NRA0 were made in relative sense for the reference event 90/10/24 and the 92/12/31 event. The readings are summarized in Table 1, where the analysts are numbered 1-4 and the two measurements of analyst 1 are labeled 1a and 1b.

The standard deviations of the relative time differences, $\Delta t_A = (Sn - Pn)_{92/12/31} - (Sn - Pn)_{90/10/24}$ and $\Delta t_N = (Pn(NRA0) - Pn(ARA0))_{92/12/31} - (Pn(NRA0)-Pn(ARA0))_{90/10/24}$ were used as measures of scatter in the analysts readings, being 0.8 and 0.1 s respectively. The standard deviation of Δt_A is a close approximation of the standard deviation of the difference in the Sn times, as the standard deviation in the Pn times is so much smaller. The standard deviation of the arrival time of Pn at SPA0 was less than 0.1 s.

Table 1: Arrival time measurements

Date	Station	Phase	Time	Analyst #
90/10/24	ARA0	Pn	15:00:21.8	2
			15:00:22.76	3
			15:00:22.79	4
			15:00:22.83	1b
			15:00:22.85	1a
92/12/31	ARA0	Pn	09:31:48.1	2
			09:31:49.4	1a
			09:31:49.45	1b
			9:31:48.84	3
			9:31:49.20	4
90/10/24	ARA0	Sn	15:02:06.74	4
			15:02:07.40	1a
			15:02:07.6	2
			15:02:08.05	1b
			15:02:10.29	3
92/12/31	ARA0	Sn	09:33:36.6	2
			09:33:36.70	1a
			09:33:36.82	1b
			9:33:36.60	4
			9:33:37.70	3
90/10/24	NRA0	Pn	15:02:36.7	2
			15:02:37.98	3
			15:02:38.14	4
			15:02:38.16	1a
			15:02:38.25	1b

Table 1: Arrival time measurements

Date	Station	Phase	Time	Analyst #
92/12/31	NRA0	Pn	09:34:02.4	2
			09:34:04.1	1a
			09:34:04.22	1b
			9:34:03.52	3
			9:34:04.02	4
92/12/31	SPA0	Pn	09:31:50.6	2
			09:31:50.73	1a
			09:31:50.76	1b
			9:31:50.58	4
			9:31:50.78	3

Figure 2 and 3 shows the arrival time picks for Pn and Sn marked on the waveform seg-

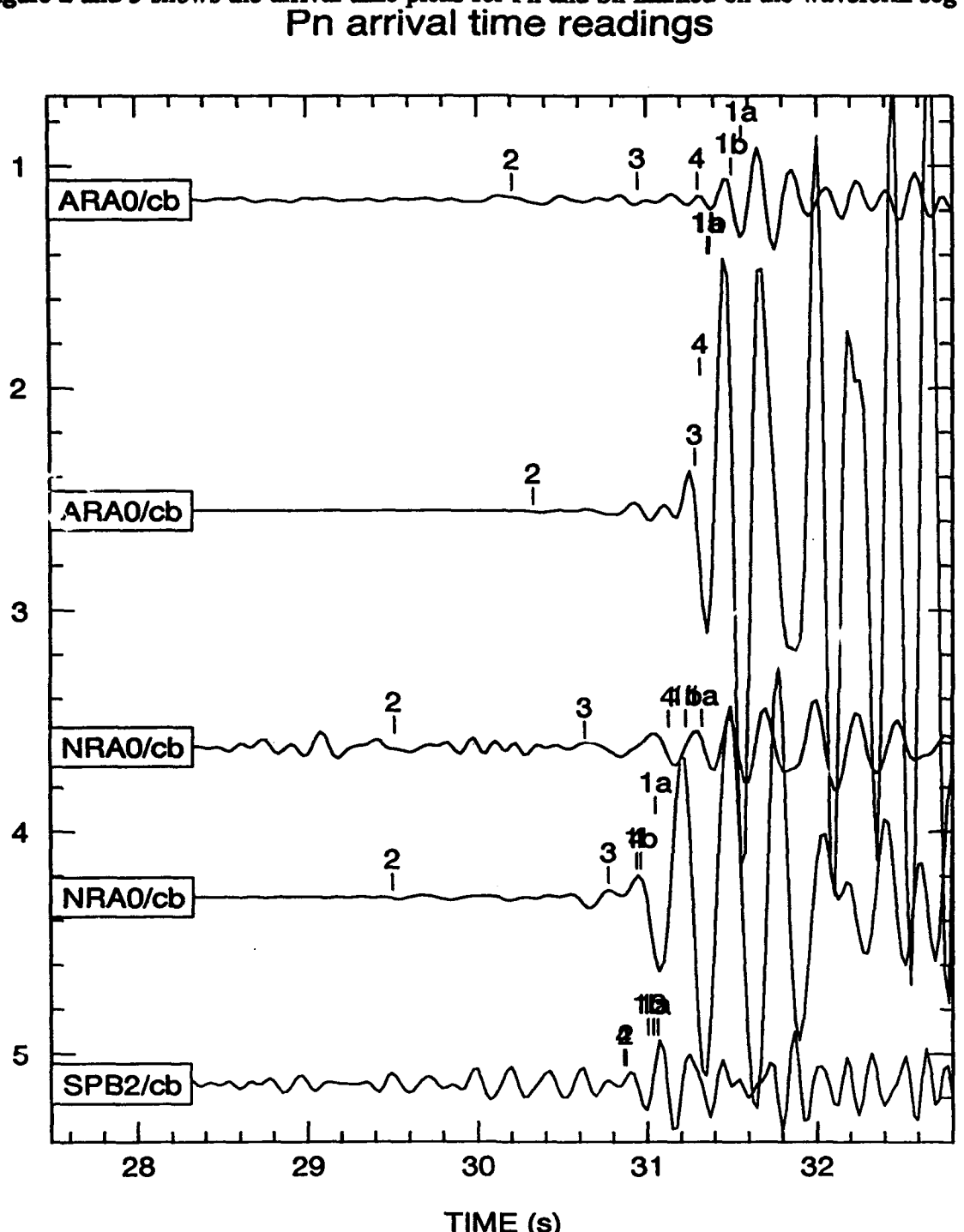

Figure 2: *The seismogram section compares the Pn arrival time readings by the analysts. The lower traces for ARA0 and NRA0 are from the reference event 90/10/24, and the other traces are from the event on 92/12/31.*

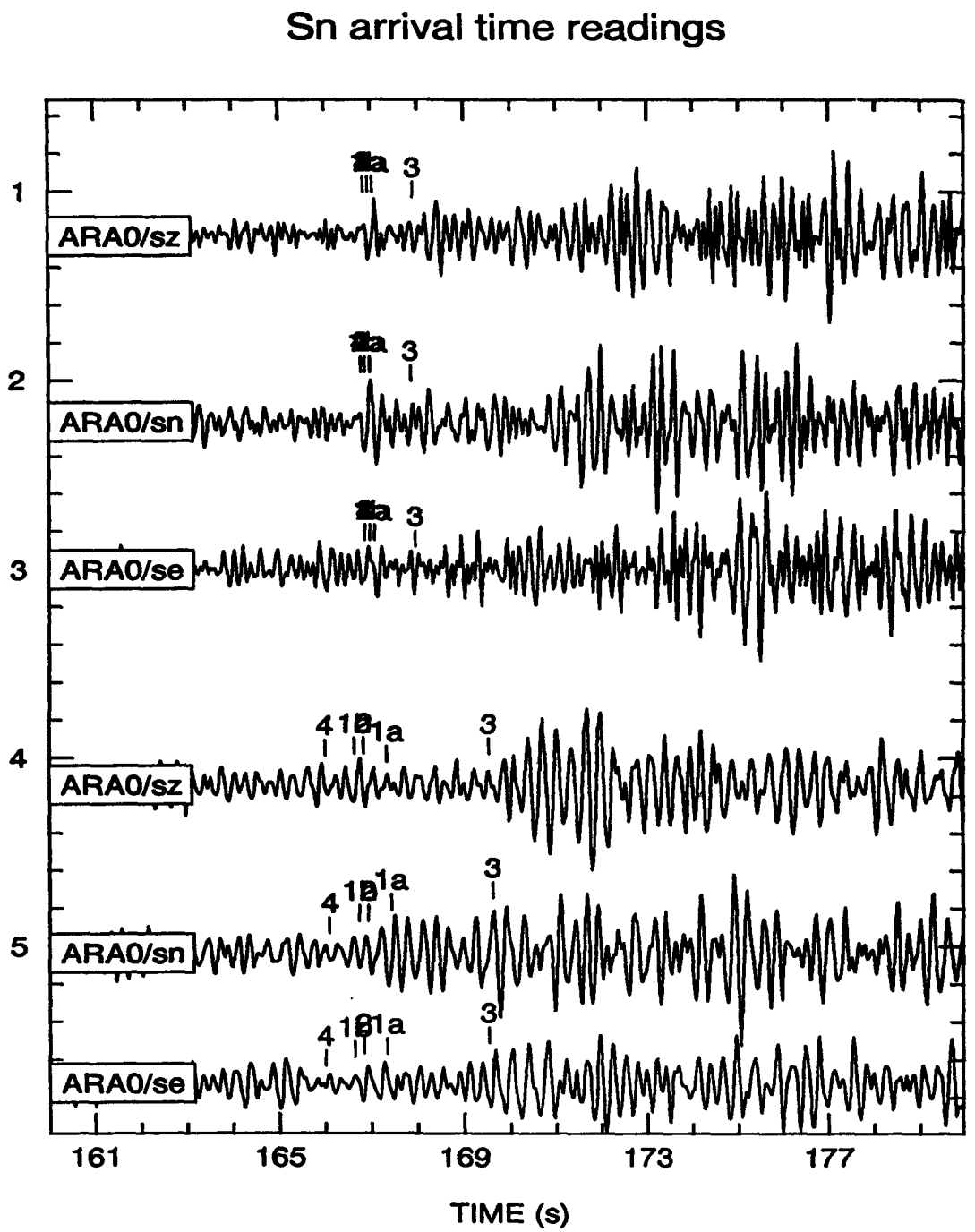

Figure 3: *The seismogram section compares Sn arrival time readings of the analysts. The three lower and upper traces are from the reference event 90/10/24 and the 92/12/31 event respectively.*

ments It should be noted that the measurements were not made from the records in Figure 2 and 3 which only serve to illustrate graphically the scatter in the measurements. Each analyst selected his own channels and filtering and made the measurements independently. The seismogram section in Figure 4 shows the variation across the C-ring at ARA0 of the

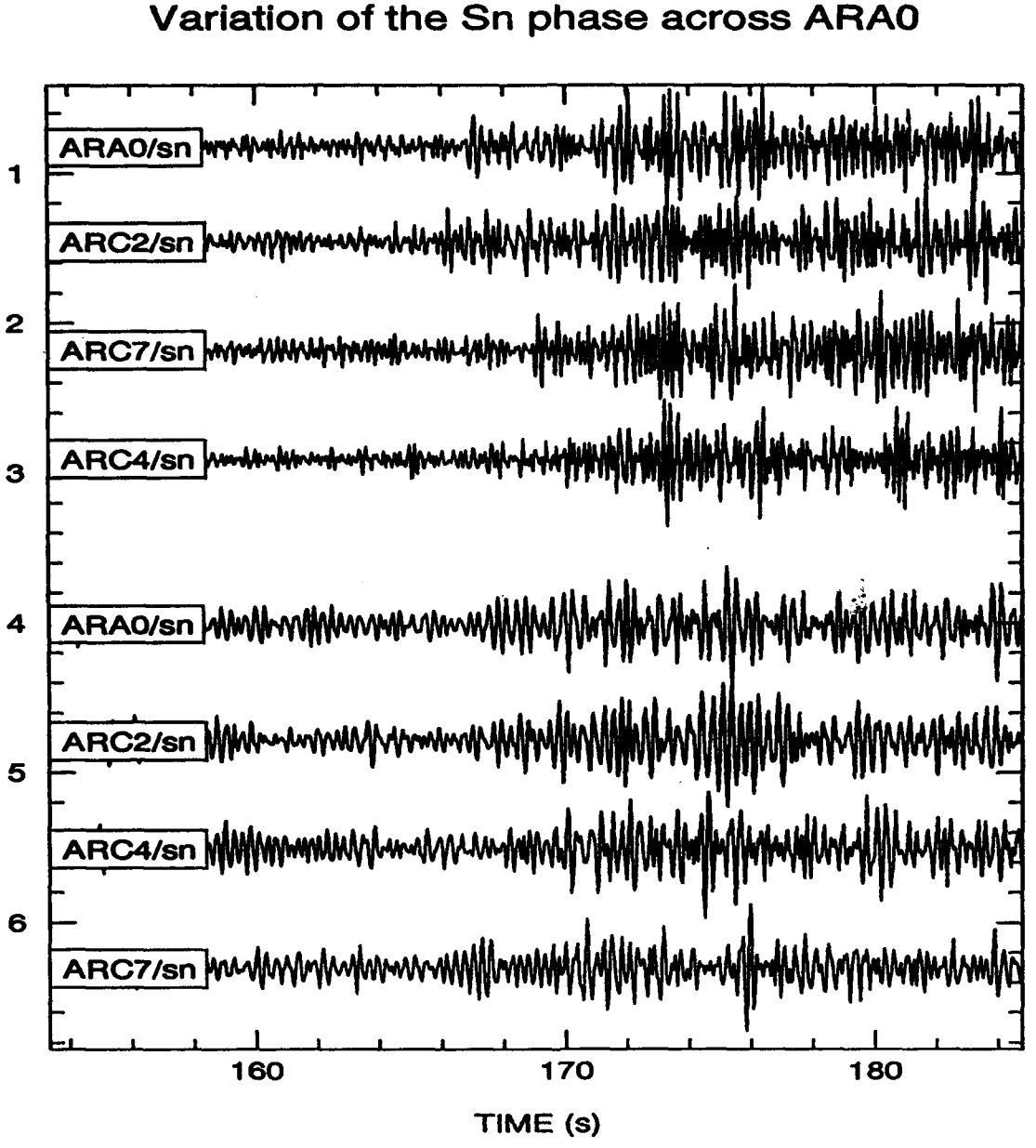

Figure 4: *The seismogram section shows the variation of the Sn phase on the NS components of the ARA0 and C ring elements.*

NE component of the Sn phases for the two events and indicate the difficulty in defining a clear unambiguous arrival times for the Sn phase.

TRAVELTIME MODEL

Preliminary locations showed differences in epicentral estimates of more than 10 km depending on which travel time model was used - the IASPEI 91 and the standard model employed since 1990 by the IMS. In order to establish which tables would provide the most accurate locations of the 92/12/31 event, comparisons were made with JED solutions of other Novaya Zemlya events in the mid 70's and early 80's (Lilwall and Marshall, 1986). Arrival time data reported to the ISC from stations in Scandinavia and Finland for five events that span the cluster of the JED solutions across the Novaya Zemlya testing grounds were used in these comparisons. The five events were located with both IASPEI and IMS travel time tables using data form several combinations of stations and with the 90/10/24 event as a reference event. The epicenters obtained with the IASPEI tables were consistently in the closest agreement with the JED solutions.

For example, with Pn at 7-9 Scandinavian stations the distances to the JED epicenters range between 5-32 for IMS and 4-18 km for IASPEI locations. The larger distances were obtained when data was limited to stations with a narrow azimuthal coverage from the events. For events, for which Pn at KBS were available, the distances varied between 5-13 and 4-6 km respectively. The fewer the number of stations the more pronounced were the differences between IASPEI and IMS results.

The 4-6 km distances for the IASPEI tables with Pn at KBS data included indicate also that these tables would perform with a high accuracy, in an absolute sense, for our reference event location of the 92/12/31 event; location errors would primarily be dominated by errors in the arrival time measurements and not by errors in travel time tables. The fact that the distances are not smaller than 4-6 km could well be due to the circumstance that the IASPEI locations were based on independent arrival time measurements relative to one single reference event, whereas in JED solutions station corrections are usually based on data from more than one event.

REFERENCE EVENT LOCATION

For the locations we used the computer program LocSAT that is used in the IMS. The program estimates a confidence ellipse that depends on *a priori* or assumed standard deviations of the arrival time errors.

Assumed Arrival Time Errors

For the reference event location of the 92/12/31 event we used *a priori* standard deviations of 0.1, 0.2, 0.4, and 0.8 s respectively for ARA0 Pn, NRA0 Pn, SPA0 Pn, and ARA0 Sn respectively.

The assumed values for Pn at ARA0 and NRA0 may be somewhat conservative considering the consistency in the arrival time readings. However, as they are so small anyway they will not have any significant influence on the size of the confidence ellipse. The largest standard error, for Sn at ARA0, which determines to a high degree the length of the major axis was based on the standard deviation in the Sn-Pn arrival times, Δt_A, calculated above. If that can be reduced, the size of the confidence ellipse will be reduced accordingly.

Finally, the value for Pn at SPA0 may, considering the consistency in the analysts picks, appear overly conservative. The chosen value is based on the circumstance that the SPA0 Pn measurement is not a truly relative measurement as are those for ARA0 and NRA0 phases. The correction to the reference event for Pn at SPA0 is based on a reported arrival time at KBS, which is turn is subject to uncertainties in two ways. Firstly there may be an error in the KBS measurement for the 90/12/31 event and secondly there may be systematic differences between KBS and SPA0, which are separated by about 100 km, in instrument phase response, filtering or other local effects.

Figure 5 shows the observed travel times to KBS for the JED events as a function of distance. The JED solutions for the explosions on 88/05/07, 88/12/04, and 90/12/24 were obtained from Marshall (personal communication). The arrival time for the 90/10/24 explosion fits well with the mean trend of the data, although the standard deviation of the travel residuals relative to a slowness of 13.69 s/degree (from IASPEI) is about 0.5 s omitting the outlying value for the 88/05/07 event.

Due to lack of events with data recorded at both KBS and SPA0 at the present time, the second type of uncertainty - systematic differences between KBS and SPA0 - cannot be established with a similar confidence. At this point, only two events could be found with data at both stations (based on bulletin data for KBS through Dec 1992). The calculated travel times and measured arrival times for these two events are summarized by Table 2:The difference between the observed and the calculated (ISAPEI) arrival times for the two stations would represent their station corrections. And the difference between the two station corrections (KBS-SPA0) is for the two events, -0.1 and -0.3s. Clearly this is no proof of equal or nearly equal station corrections for the two stations for Pn, but the small differences at least do not contradict the possibility of such a similarity.

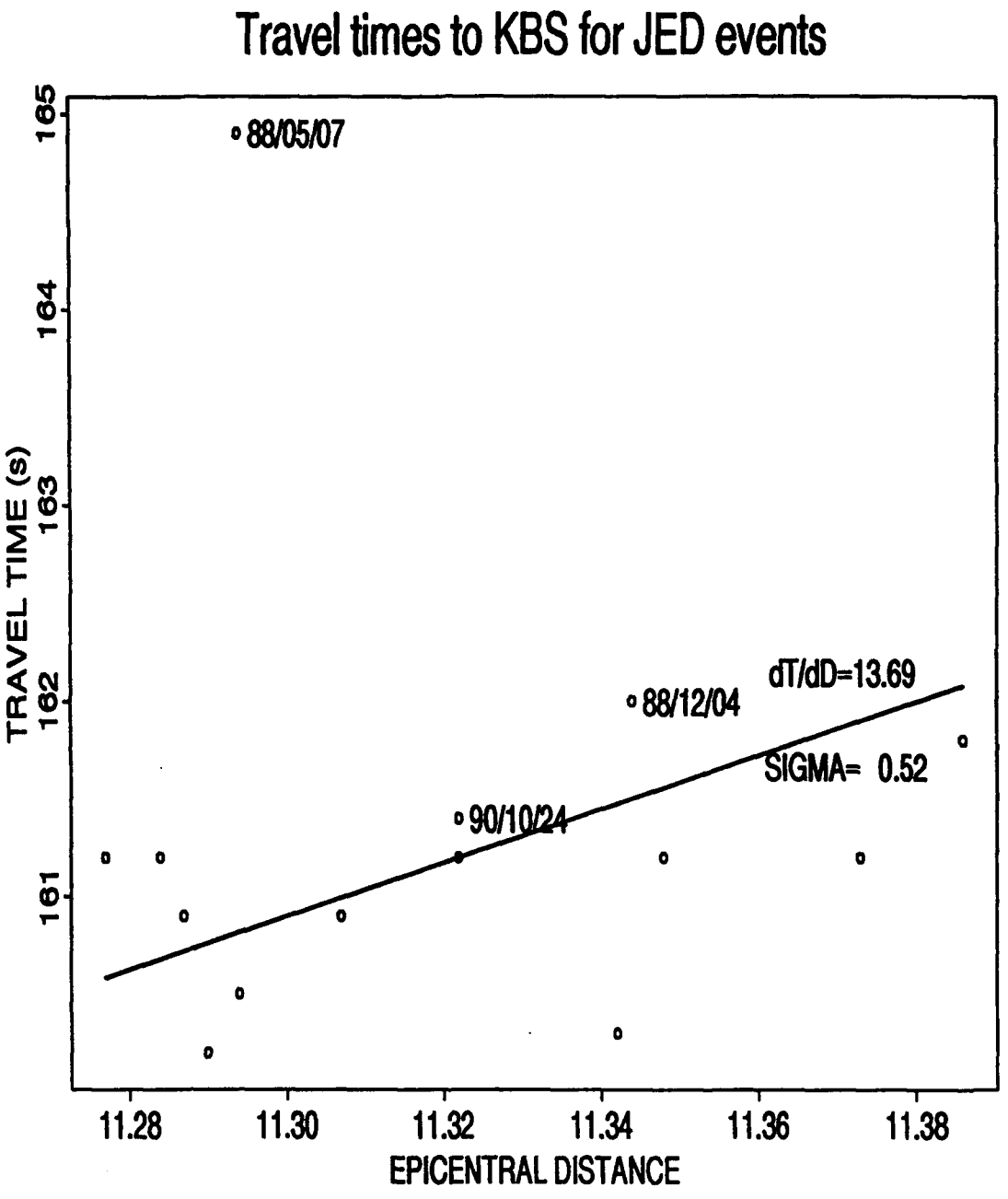

Figure 5: *The travel times at KBS as a function of epicentral distance for JED solutions of Novaya Zemlya explosions (Lilwall and Marshall, 1986,; Marshall personal communications). The line represent a slowness of 13.69 s/degree and the "SIGMA" value in the diagram represent the standard deviation of the travel times around this line (the data point for the event 88/05/07 not included). The travel times for the events on 88/05/07, 88/12/04 and 90/10/24 are identified in the diagram.*

Table 2: Calculated travel and observed arrival times to KBS and SPA0

Date	time	Epicenter		Distance		Travel time		Arrival time	
				KBS	SPA0	KBS	SPA0	KBS	SPA0
92/12/17	10:39	25.89N	61.46E	57.266	56.115	589.22	581.02	10:49:15.3	10:49:07.4
92/12/19	12:14	51.87N	158.51E	47.706	47.924	518.26	519.95	12:22:56.0	12:22:57.8

Confidence Ellipse

Arrival time residuals were calculated from the reference event 90/12/24 and those were added to the measured arrival times for the 92/12/31 events and the location program was then applied to these corrected arrival times.

Figure 6 shows the epicenters determined in this manner using the different analysts picks. They are all within an area of 10 km, and are all covered by the 90% confidence ellipse calculated for the median solution, 73.46N 55.48E, defined from the analyst readings as the one with the median of the Sn-Pn time difference, Δt_A. The lengths of the semi axes are 12 and 8 km, and the strike of the major axis is N 113.3 degrees E from the north.

The median solution gave residuals of 0.02, -0.12, -0.04, and 0.42 s for ARA0 Pn, NRA0 Pn, SPA0 Pn, and ARA0 Sn respectively.

Residuals for arrival time readings - ePg and iSn - available for the station AMD were calculated for the median solution. The Pg readings had large residuals, of the order of 10 s, relative to both assumed Pg and Pn phases. The residual for the Sn phase, however, was about 1.2 s. Including the Sn arrival at AMD in the reference event location would not change the solution in any significant degree, as this arrival time has to be assigned a large assumed standard deviation due to lack of data from the reference event.

COMPARISONS WITH SOME OTHER EVENT LOCATIONS

For the sake of comparison some reference locations relative to the event 90/10/24 were also made for JED events (Lilwall and Marshall, 1986). On the assumption that the JEDs are very close to the true epicenters, the distances between the reference event locations and the JEDs correspond to location errors.

Novaya Zemlya explosion Dec 4 1988

Arrival times for Pn and Sn at ARA0 and Pn at NRA0 were read from waveform data for a nuclear explosion on 88/12/04 in a similar manner (only one analyst though) as for the

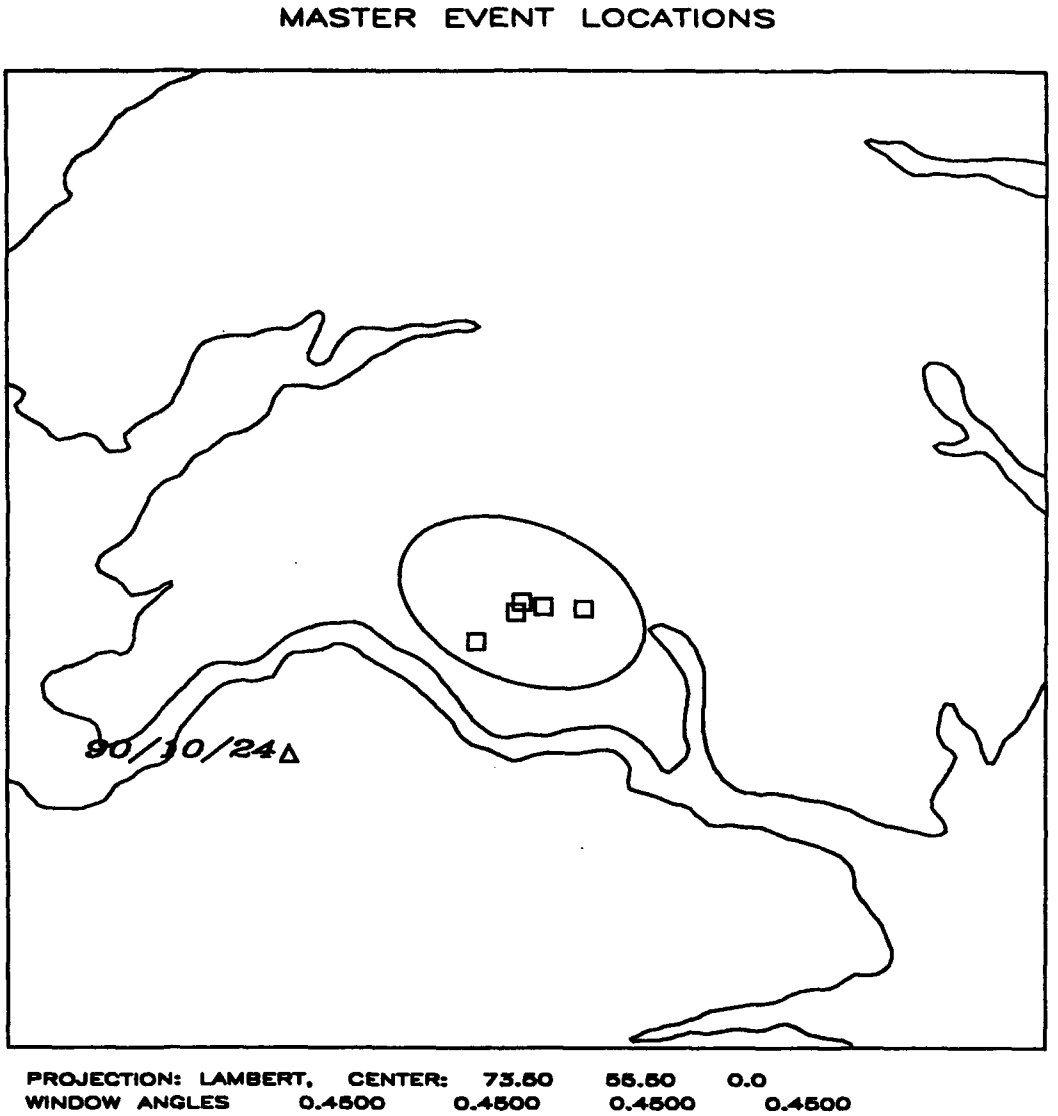

Figure 6: *The squared symbols show the reference event locations for the readings of the analysts and the 90% confidence ellipse for the median solution is marked. The location of the reference event 90/10/24 is indicated with a triangle.The distance horizontally and vertically across the map is100 km.*

90/10/24 and 92/12/31 events. These were combined with the arrival time reported for KBS (see Figure 5) for this explosion in a reference event location just as for the 92/12/31 event. The only difference being that we used the KBS reading instead of the SPA0 reading from the 92/12/31 event. The resulting epicenter, 73.373 N 54.676 E is about 10 km away from the JED of this event, 73.364 N 55.013 E (Marshall, personal communication).

Arrival times measured for ARA0 and NRA0 of the Novaya Zemlya explosion on 88/05/07 could not be combined with the reported KBS to obtain a reliable solution, as the KBS arrival time appear to have a too large residual, inconsistent with those for other Novaya Zemlya explosions (see Figure 5).

JED events by Lilwall and Marshall (1986)

reference event locations were made with various subsets of reported Pn and Sn readings at stations in Scandinavia and Finland for a few of the JED events. And the distances between the reference and JED solutions were calculated. Table 3 compares the distances to the JED solutions for the two cases, both with 4 observations. In one case the locations are based on 4 Pn phases and in the other on 3 Pn and 1 Sn phase.

Table 3: Distances to JED solutions (km)

Date of Event	Arrival time data used	
	Pn at KBS, UPP and Pn and Sn at NUR	Pn at KBS, KEV, NUR, UPP
76/09/26	24	7
78/08/10		5
81/10/01	46	12

The case based on 1 Sn phase has the largest disagreement with the JED solutions. Calculations for other cases with and without Sn phases showed similar results.

TWO STATION LOCATIONS

The confidence region of the event location is dependent on the assumption that the standard error of the Pn phase at SPA0 is 0.4 s. As data is currently not available to test with a high degree of confidence the hypothesis that the station corrections for SPA0 and KBS are equal, locations based on data at only ARA0 and NRA0 were also attempted. These were based on the changes in distances to the two arrays to the 92/12/31 event, δ_A and δ_N for ARA0 and NRA0, from the distances to the reference event, Δ_A and Δ_N, using the for-

mulas:

$$\delta_A = \Delta t_A / (dT/d\Delta_{S_n} - dT/d\Delta_{P_n})$$

$$\delta_N = (\Delta t_N + \delta_A \cdot dT/d\Delta_{P_n(A)}) / dT/d\Delta_{P_n(N)}$$

Δt_A and Δt_N are the relative time differences of Sn-Pn and Pn-Pn times introduced above and index A and N on slownesses refer to ARA0 and NRA0. An epicenter is then defined from one of the crossing points of the distance circles, $\Delta_A+\delta_A$ and $\Delta_N+\delta_N$, to ARA0 and to NRA0 respectively. The map in Figure 7 shows the crossing points obtained from the time differences for the five analyst's readings with a scatter of about 50 km. Similarly the map in Figure 8 shows the crossing points for the two nuclear explosions 88/05/07 and 88/12/04 (one analyst only) with distances of about 10 and 30 km to the JED solutions.

ATTEMPT TO IMPROVE Sn READING ACCURACY

Measurements of arrival times of Sn waves from RMS trace envelopes as opposed to standard waveforms were attempted to reduce the scatter. Although such measurements on the 4 array elements at ARA0 with three component instrumentation showed fairly high consistency, the locations based on such envelope readings were clearly separated from those based on readings from regular waveforms. Furthermore, the location of the 88/12/04 based on picks from RMS traces was further away from the JED solution than that based on picks from regular waveforms.

CONCLUDING REMARKS

With reference event location techniques we obtain an epicenter estimate of 73.46 N and 55.48 E for the event 92/12/31 with the lengths of the semi axes of the 90% confidence ellipse being 12 and 8 km and the strike of the major axis being N 113.3 degrees E. The dimensions of the error ellipse is determined by the assumed standard deviations of the four defining phases. The length of the major axis is largely controlled by the standard deviation of the Sn phase at ARA0 (0.8s), which, as for the Pn at ARA0 and NRA0, were estimated from the scatter in the readings of relative arrival times for the reference and the

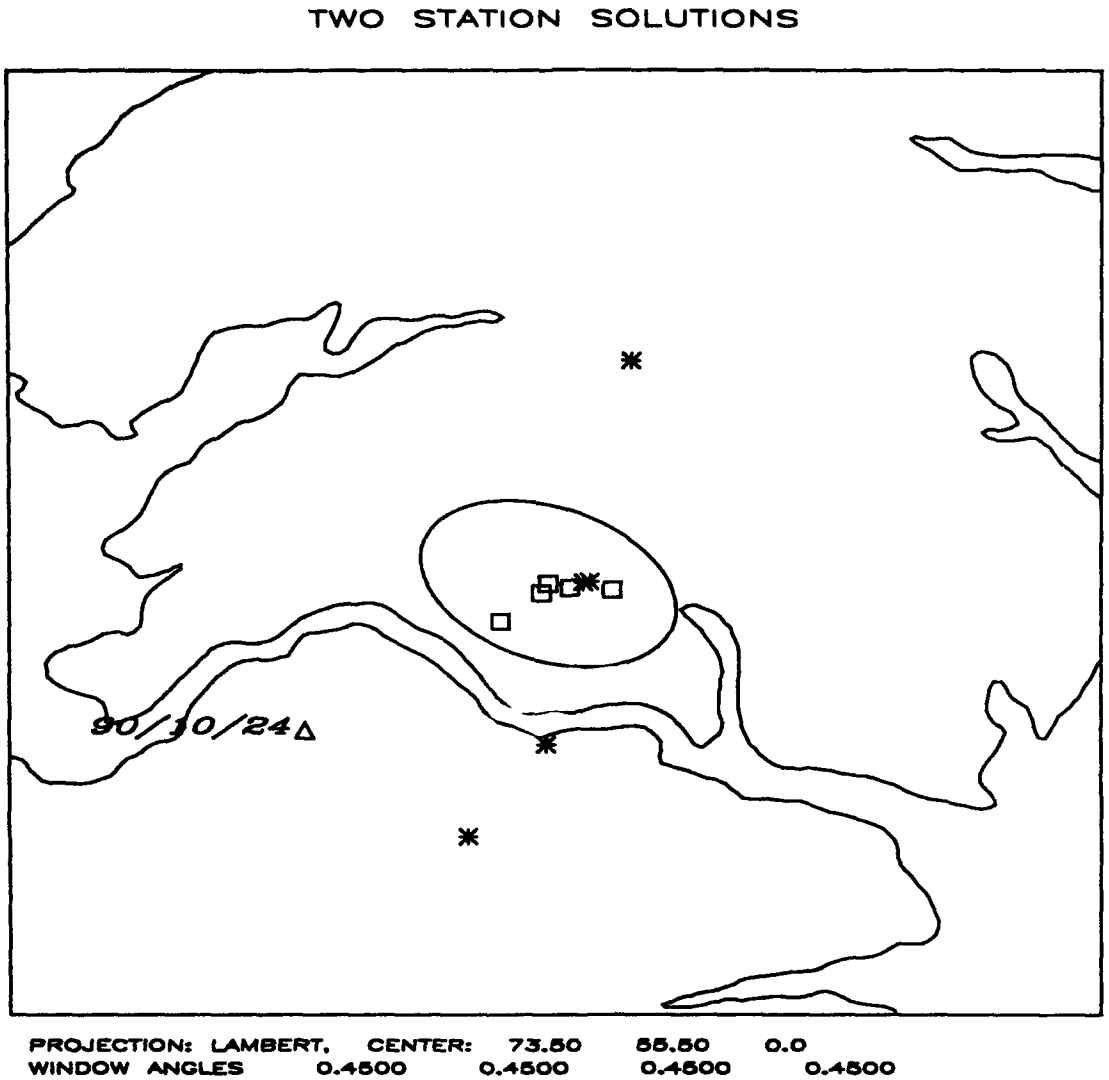

Figure 7: *The asterisk symbols show the two station locations based on the readings of the analysts of the event 92/12/31. The 90% confidence ellipse and the 3 station solutions from Figure 6 are included for comparison. The location of the reference event 90/10/24 is indicated with a triangle.The distance horizontally and vertically across the map is100 km.*

92/12/31 event. The standard deviation for the Pn phase at SPA0, however, could not be estimated directly from relative measurements, but had to be assigned. This value, 0.4 s, was based on the small standard deviation of the arrival readings at SPA0 for the 92/12/31 event and the consistency of the KBS arrival time of the reference event in relation to other Novaya Zemlya explosions. Furthermore, the data available for two other events, both recorded at KBS and SPA0 did not indicate any systematic difference in station cor-

Figure 8: *he asterisk symbols show the two station locations based on the readings of an analyst of the events on 88/05/07 and 88/12/04. The locations of the JEDs for these two events are marked with squared symbols.The location of the reference event 90/10/24 is indicated with a triangle. The distance horizontally and vertically across the map is100 km.*

rections between the two stations. If the standard deviation for Pn at SPA0 were doubled to 0.8 s, i.e. equal to that of Sn for ARA0, the lengths of the semi axes would increase to 16 and 12 km respectively.

The estimation of epicenters here is based on the premise of zero or very shallow focus depth.

REFERENCE

Lilwall, R. C. and P.D. Marshall (1986), Body wave magnitudes and locations of Soviet underground nuclear explosions at the Novaya Zemlya Test Site, AWRE, MOD(PE), Aldermaston, Berks. UK, Report AWRE O 17/86

A FUZZY-LOGIC APPROACH TO REGIONAL SEISMIC EVENT IDENTIFICATION: APPLICATION TO THE NOVAYA ZEMLYA EVENT ON 31 DECEMBER 1992

A Fuzzy-Logic Approach to Regional Seismic Event Identification: Application to the Novaya Zemlya Event on 31 December 1992

Thomas J. Sereno, Jr. and Darrin D. Wahl
Science Applications International Corporation
10260 Campus Point Drive
San Diego, CA 92121

ABSTRACT

A novel approach based on fuzzy logic was developed for identifying regional seismic events. This approach combines evidence from regional discriminants applied to the seismic signals with evidence from contextual discriminants (event depth and magnitude, previous natural seismicity, and whether the event is onshore or offshore) to derive a composite identification. The Event Identification System for the Intelligent Monitoring System (IMS) is based on this fuzzy-logic approach. It consists of a module for automated regional event identification and graphical tools for analyst review of the automated solutions. This system was applied to >6000 events recorded in Scandinavia, and >800 of these were identified in a bulletin produced by the University of Helsinki. Of the events in the Helsinki Bulletin, 92% were identified correctly as explosion or earthquakes, 2% were misidentified (most of these were earthquakes that were identified as explosions), and 6% could not be identified by the IMS. At the request of the Nuclear Monitoring Research Office (NMRO) of ARPA, the IMS Event Identification System was also applied to an event at Novaya Zemlya that occurred on 31 December 1992. This event appears to have been shallow, onshore, and in a relatively aseismic area. The regional discriminants provide some evidence that the event is an earthquake, but the confidence is low. The composite identification including the contextual discriminants could not be determined by the IMS. The system was also applied to three known nuclear explosions at Novaya Zemlya and an earthquake on the Mid-Atlantic Ridge. The regional discriminants give similar results for all five events (the waveforms and spectra are also similar), but the system correctly identifies the known events, primarily on the basis of the contextual discriminants. The IMS Event Identification System is unable to identify the 31 December 1992 event, but it provides valuable information regarding its spectral characteristics and the relative excitation of P and S waves. This event is difficult to identify even with careful off-line analysis. Therefore, new regional discriminants must be developed before events like this can be identified by an automated system.

1.0 OBJECTIVES

The objectives of the IMS Event Identification System fall into three categories:

- Automated Event Identification
- Analyst Review of the Automated Solutions
- Knowledge Acquisition

Automated Identification

The objective of the IMS Event Identification System is to automate as much as possible the identification of all regional events with magnitudes ≥ 2.5. Some human participation will undoubtedly be required, but our objective is to screen events to focus attention on key features of a small number of suspicious events. The system first tries to separate events into earthquakes and explosions. Next, a case-based approach is used to identify the common sources of man-made seismicity (e.g., mining explosions). The events that remain are either unidentified, or they

are identified as having explosion-like characteristics. In either case, these events might be underground nuclear tests. This subset requires further review by a seismologist. With this procedure, the system identifies most events automatically and focuses attention on novel events that are difficult to identify.

The IMS Event Identification System can be characterized as a "novel-event detector." As with all detectors, there is a trade-off between the probability of detecting real signals and the number of false alarms. Our system is configured to have a high probability of detecting real signals (*i.e.*, novel events that could be nuclear tests), at the cost of more false alarms (generally misidentified earthquakes). These false alarms will be reviewed by a seismologist. Therefore, the penalty for a false alarm is an increased workload for a seismologist, but the penalty for missing a novel event could be a missed nuclear test. Because of this, we expect relatively high false-alarm rates, especially as nuclear monitoring is expanded into new areas. Therefore, we have put considerable effort into the development of analysis tools to minimize the effort required to review the automated solutions. We are also working to reduce the false alarms to manageable numbers by adding new discriminants to the IMS Event Identification System. Several of these new discriminants are under development by researchers supported by ARPA's R&D Program.

Analyst Review of the Automated Solutions

The IMS Event Identification System provides convenient analysis tools for validating, rejecting or modifying the automated event identification solutions. These include an explanation facility for each discriminant and the composite identification. They also include tools for waveform display and manipulation, signal processing, calculation and display of spectra and spectrograms, and an interactive map program. Most of these tools were developed for other parts of the IMS (e.g., for analyst-review of automated phase association and event location). We use our Software Integration Platform *[Given et al., 1993]* to connect these separately-developed modules in a distributed processing environment. The system architecture is described in more detail in Section 3.2. The end-result is that all of these review functions are available to a seismologist through a convenient graphical user-interface.

Knowledge Acquisition

A mechanism must be provided for analyzing and improving the performance of the automated system as experience is gained. This is accomplished in two ways. First, all relevant details about the automated and analyst solutions for each event are saved in our database management system. Comparison of the two provides a basis for analyzing the performance of each of the discriminants and our method for combining their results. This comparison is used to acquire new seismological knowledge to improve the performance of the existing automated system. Second, the architecture of the IMS Event Identification System was designed to facilitate rapid integration of new discriminants.

2.0 FUZZY-LOGIC APPROACH

A fuzzy system typically consists of a small number of IF-THEN rules that are based on linguistic variables. These linguistic variables are common terms that describe a fuzzy set. Examples include DEEP, SHALLOW, HIGH, LOW or MEDIUM. The degree-of-membership is the confidence, expressed as a number from 0 to 1, that a particular value belongs in a fuzzy set. For example, a seismic event at zero depth has a degree-of-membership equal to one in the fuzzy set described as SHALLOW. However, an event at 5-10 km may have degree-of-membership between 0 and 1 in both classes, DEEP and SHALLOW. The mathematical relationship between an input variable and its degree-of-membership in one or more fuzzy sets is called a membership

function. The process of converting input variables to classes and degree-of-memberships is called "fuzzification." The response of each IF-THEN rule is weighted according to the degree-of-membership of its input variables. The combined result of multiple rules is a fuzzy response. "Defuzzification" techniques are used for converting this fuzzy response into a specific one.

The fuzzy-logic approach provides a framework for representing the kind of reasoning used by seismic analysts to identify events. It has intuitive rules that are defined in terms of linguistic variables (e.g., If the depth is DEEP, then the event is an EARTHQUAKE) with imprecise definitions of class boundaries (e.g., DEEP and SHALLOW). Since the uncertainty is isolated in the representation of class boundaries, fuzzy systems are characterized by smaller and simpler rule bases than more conventional rule-based systems. Among other advantages, this makes it much easier to add new input variables (i.e., discriminants) to the system. We believe the IMS Event Identification System is the first application of fuzzy logic to a seismic data interpretation problem. General descriptions of fuzzy logic and diverse applications of it are described in various textbooks and review articles [e.g., *Zadeh*, 1965; *Yeager*, 1981; *Negoita*, 1985; *Kandel*, 1986; *Caudill*, 1990; *Self*, 1990; *Kosko*, 1992].

A simple example is useful for illustrating these concepts. Suppose we have a fuzzy system with the following two rules:

Rule 1: If a seismic event is DEEP, then its identification is HIGH-CONFIDENCE EARTHQUAKE

Rule 2: If a seismic event is SHALLOW, then its identification is INDETERMINATE.

The left side of Figure 1 is an example of membership functions for event depth. If the depth is <5 km, the degree-of-membership is 1.0 in SHALLOW and 0.0 in DEEP. The converse is true if the depth is >10 km. However, depths between 5 and 10 km have partial membership in both classes. If the depth is 7.0 km in this example, then the event is DEEP to degree 0.4 and SHALLOW to degree 0.6 (Figure 1). In this case, the response of Rule 1 will be assigned a weight of 0.4 and the response of Rule 2 will be assigned a weight of 0.6. The combined fuzzy response is shown graphically in the right panel of Figure 1. We use a "centroid defuzzification" technique to obtain a specific output class and confidence [e.g., *Kosko*, 1992]. In this technique, the class and confidence are determined from the centroid of the of fuzzy response. The centroid is then mapped to a confidence measure from 0.5 for INDETERMINATE to 1.0 for HIGH-CONFIDENCE. For the example in Figure 1, the centroid is in the class LOW-CONFIDENCE EARTHQUAKE (LQ), and the confidence is 0.7.

3.0 IMS EVENT IDENTIFICATION SYSTEM

The IMS Event Identification System is described in two parts. Section 3.1 describes the fuzzy-logic automated event identification module, and Section 3.2 describes the system architecture and analysis tools.

3.1 Automated Event Identification

The automated event identification module uses fuzzy logic to combine evidence from multiple regional discriminants based on seismic signals with contextual discriminants (event depth and magnitude, previous natural seismicity, and whether the event is onshore or offshore) to derive a composite identification. This is done in two stages. First, fuzzy logic is used to combine the regional discriminants independent of the contextual discriminants. The result is an estimate of the degree-of-membership in EARTHQUAKE and EXPLOSION classes (i.e., the extent to which the signal characteristics are earthquake- or explosion-like). Next, fuzzy logic is used to combine

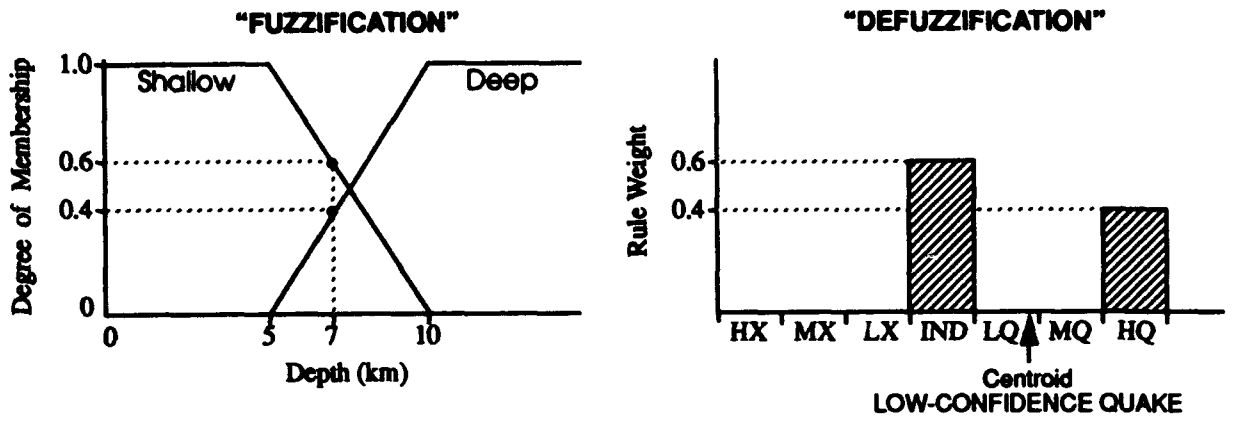

Figure 1. *This is an illustrative example of a simple fuzzy system for identifying seismic events on the basis of depth.*

this with contextual discriminants to derive a composite identification. The composite identification is described in Section 3.1.1, and the system to combine the regional discriminants is described in Section 3.1.2.

3.1.1 Composite Identification

The contextual discriminants are depth, location, magnitude and natural seismicity. For depth we use the membership function shown in Figure 1, except that we use depth minus an estimate of the depth error at the 90% confidence level. The location classes are OFFSHORE and ONSHORE, and membership is based on the location error ellipse. A weighted sum of samples taken at the epicenter and on error ellipses at three different confidence levels is used to determine class membership in ONSHORE and OFFSHORE. The magnitude classes are HIGH and LOW. These classes overlap in the range M_L 2.5-3.5. Magnitudes outside of this range have degree-of-membership equal to 1.0 in one of the two classes. Natural seismicity is parameterized on a 1°x1° geographical grid. This grid consists of the average number of events per year with $mb \geq 4.0$ in a 20,000 km^2 area (approximately 80 km radius) around each grid point. It is based on events in the PDE bulletin between 1960 and 1990. The natural seismicity grid is plotted in Figure 2. The locations with full membership in the class HIGH are plotted with red symbols, and the locations with partial membership in this class are plotted with green symbols. All other locations have full membership in the class LOW.

The rules for deriving the composite identification are listed in Table 1. The input variables are the four contextual discriminants and the results of applying the regional discriminants. A dash in any column indicates that the rule is independent of that input variable. For example, the first rule states that if an event is deep (where depth is defined as the estimated depth minus the depth uncertainty at the 90% confidence level), then it is identified as a HIGH-CONFIDENCE EARTHQUAKE (HQ). This is independent of the regional discriminants or other contextual discriminants. Rule 2.0 states that a shallow event in a seismically active area with signal characteristics that are earthquake-like is also identified as a HIGH-CONFIDENCE EARTHQUAKE. Rule 3.0 reduces the confidence to moderate if the magnitude is low and the event is located in an aseismic area.

Two basic principles are applied for Rules 4.0-7.0. First, large events in aseismic regions are unlikely to be earthquakes. Second, offshore events in seismically active areas are more likely to be earthquakes than explosions. Rule 8.0 acknowledges that small offshore explosions can occur.

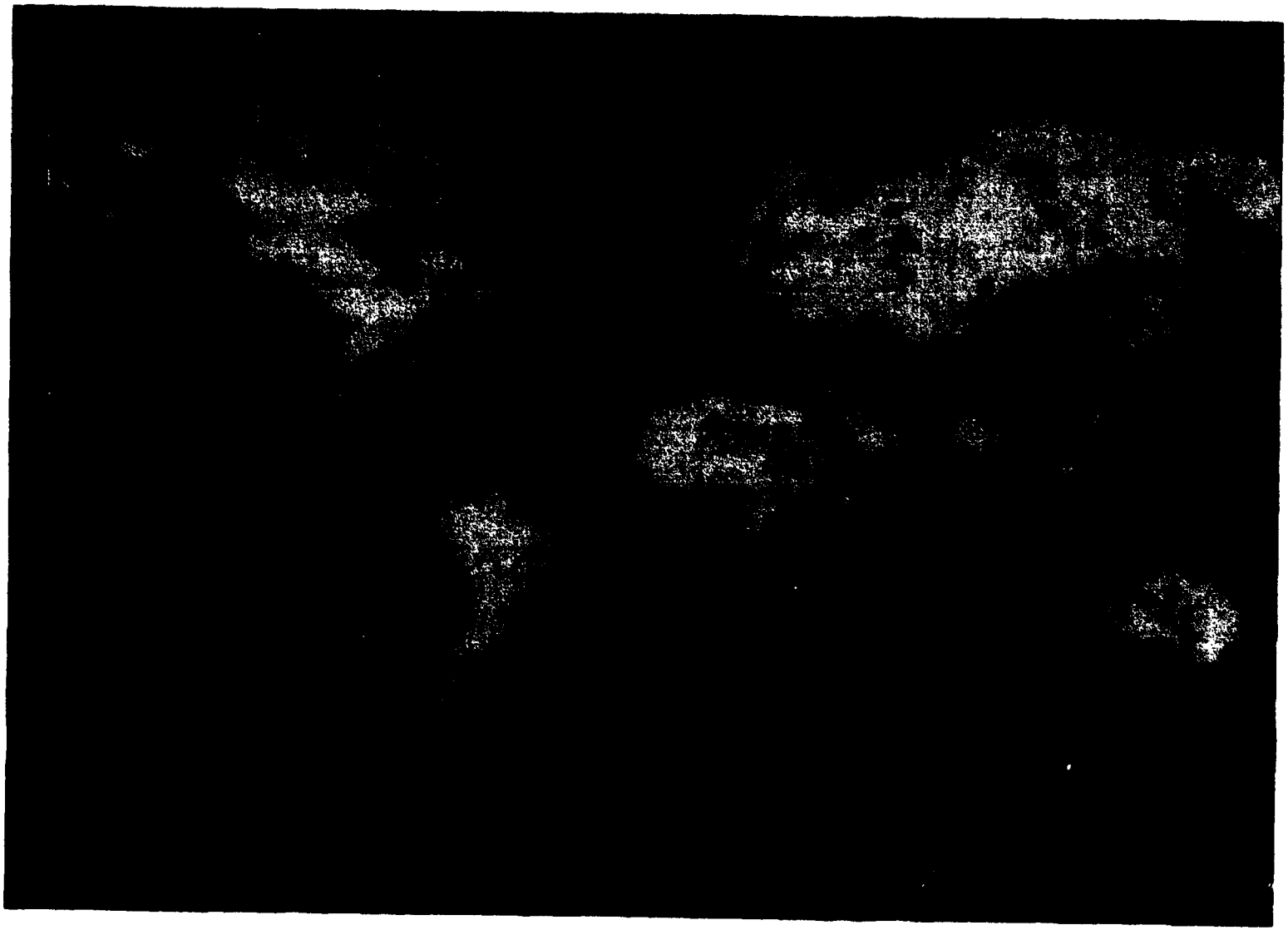

Figure 2. *This map shows locations that are characterized by high (red) and moderate (green) natural seismicity.*

In fact, there are many examples of these in the IMS database. Finally, Rule 9.0 states that onshore events with explosion-like characteristics are identified as HIGH-CONFIDENCE EXPLOSIONS (HX).

Table 1: Rules for Composite Identification

Rule	Depth	Location	Magnitude	Seismicity	Regional Discriminants	Conclusion*
1.0	DEEP	-	-	-	-	HQ
2.0	SHALLOW	-	-	HIGH	EARTHQUAKE	HQ
3.0	SHALLOW	-	LOW	LOW	EARTHQUAKE	MQ
4.0	SHALLOW	OFFSHORE	HIGH	HIGH	EXPLOSION	MQ
5.0	SHALLOW	-	HIGH	LOW	EARTHQUAKE	IND
6.0	SHALLOW	OFFSHORE	HIGH	LOW	EXPLOSION	IND
7.0	SHALLOW	OFFSHORE	LOW	HIGH	EXPLOSION	MX
8.0	SHALLOW	OFFSHORE	LOW	LOW	EXPLOSION	HX
9.0	SHALLOW	ONSHORE	-	-	EXPLOSION	HX

* (HQ = HIGH-CONFIDENCE EARTHQUAKE; MQ = MODERATE-CONFIDENCE EARTHQUAKE; IND = INDETERMINATE; MX = MODERATE-CONFIDENCE EXPLOSION; HX = HIGH-CONFIDENCE EXPLOSION)

The conclusions in the fuzzy rule base specify the composite identification if each input variable has full membership in only one class. Fuzzy logic is used to interpolate between these end-members when the input variables have partial membership in multiple classes (e.g., if the magnitude is in between HIGH and LOW). This is accomplished by assigning a weight to the conclusion of each rule. This weight is the minimum of the degree-of-memberships of all of its input variables. The logical "and" is replaced by the minimum operator. For example, the weight assigned to the conclusion of Rule 3.0 is:

$$weight = min\,[m(depth, SHALLOW),\ m(magnitude, LOW),\ m(seismicity, LOW),\ m(discriminants, EARTHQUAKE)] \quad (1)$$

where the membership function $m(x, Y)$ defines the degree-of-membership of input variable x in class Y. Several rules may fire with varying weights, and the final result (identification and confidence) is obtained by "centroid defuzzification" as described in Section 2.0. The result is a smooth and continuous transition across class boundaries. For example, Figure 3 plots earthquake confidence as a function of M_L for a shallow event in an aseismic region that has earthquake-like signal characteristics (this uses Rules 3.0 and 5.0). Large events are identified as INDETERMINATE, and small events are identified as MODERATE-CONFIDENCE EARTHQUAKES. The earthquake confidence decreases continuously from moderate to indeterminate as the M_L increases from LOW to HIGH. A more conventional rule-based approach would require many more rules to achieve the same continuous transition. Also, adding another input variable to a fuzzy system (e.g., population density may be a valuable contextual discriminant) requires only the addition of a new membership function and a few associated rules. This is usually much easier than adding a new input variable to a more conventional rule-based system.

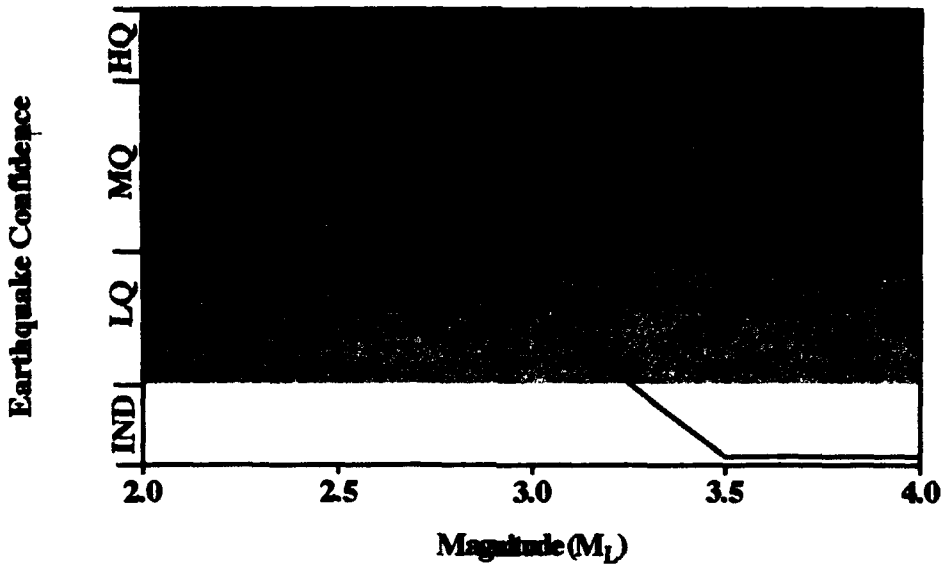

Figure 3. *Earthquake confidence is plotted as a function of M_L for a shallow event in an aseismic region whose signal characteristics indicate that it is an earthquake.*

3.1.2 Regional Discriminants

This section briefly describes the regional discriminants that are currently included in the IMS Event Identification System. These discriminants were developed primarily by researchers supported by ARPA's R&D Program. Our work has focussed on developing the fuzzy-logic infrastructure for combining evidence from multiple discriminants. As described above, a major advantage of the fuzzy-logic approach is that it is relatively easy to add new discriminants as they become available. We are in the process of adding several new discriminants to the system, and these are described at the end of this section.

The current regional discriminants in the IMS Event Identification System are:

- Source Multiplicity
- Spectral Variance
- Rg
- Ms - Mp
- Script Match

Source Multiplicity

Cepstral analysis is performed on each associated phase. Consistent cepstral peaks among phases at one station or among multiple stations are interpreted as evidence of "ripple-firing" which is a common blasting technique used in commercial mining [e.g, *Baumgardt and Ziegler*, 1988, 1989; *Smith*, 1989; *Hedlin et al.*, 1990]. Two classes are recognized by the fuzzy-logic system: CEPSTRAL-PEAKS and NO-CEPSTRAL-PEAKS. Membership depends on the amplitude of the consistent cepstral peaks, and whether these peaks are consistent among phases at one station or among multiple stations. In general, cepstral peaks provide evidence that the event is an explosion, and their absence provides no evidence for identification.

Spectral Variance

The variance of the detrended log spectrum is calculated for each associated phase. Mining explosions recorded at NORESS tend to have higher spectral variance than earthquakes [*Dysart and Pulli*, 1987; *Baumgardt and Zeigler*, 1989]. This is a secondary feature for identification of ripple-firing [*Baumgardt et al.*, 1991]. The spectral modulations that cause cepstral peaks may be difficult to detect if there is significant variance in the delay times or if the shots are detonated in complex spatial patterns [e.g., *Stump and Reinke*, 1988; *Smith*, 1989]. However, the spectra from these events commonly have a high variance. The fuzzy-logic system recognizes three classes for spectral variance: HIGH, LOW, and NOT-AVAILABLE (N/A). Membership is based on the minimum spectral variance of all associated phases. High variance is interpreted as evidence that the event is an explosion, and low variance is interpreted as evidence that the event is an earthquake. If spectral variance data are unavailable (e.g., the signal-to-noise ratio is too low), then this discriminant provides no evidence for identification.

Rg

The presence of an Rg phase (defined as a fundamental-mode Rayleigh wave with period between 0.4 and 2.5 s) in a regional seismogram provides strong evidence that the event is very shallow, and these phases are particularly prominent for quarry blasts [*Kafka*, 1990]. The fuzzy-logic system recognizes two classes: RG-PRESENT and RG-NOT-PRESENT. Membership in the current implementation is crisp (as opposed to fuzzy) since an Rg phase is either reported by the IMS location analyst or it isn't. A reported Rg phase at any station is interpreted as evidence that the event is an explosion, and the absence of Rg provides no evidence for identification. Unfortunately, the absence of Rg cannot generally be considered as evidence that the event is deep, since its propagation depends on shallow crustal structure which can have significant regional variations. Our current implementation of this discriminant is not entirely satisfactory since the presence of Rg only indicates the source is very shallow (not that it is an explosion). Therefore, we intend to replace this crisp definition with a fuzzy one that depends on Rg/Lg amplitude ratios [*Kafka*, 1990].

Ms-Mp

Regional P-wave magnitudes (Mp) are estimated from Pn and Pg amplitudes, and regional S-wave magnitudes (Ms) are estimated from Sn and Lg amplitudes. The amplitudes are measured in a 2-4 Hz band, and the magnitudes are based on distance corrections developed for paths in Scandinavia [*Bache et al.*, 1991]. The difference between Ms and Mp reflects the relative excitation of P- and S-waves, but it also includes the source radiation pattern since most of the small regional events are recorded by only a few stations. The fuzzy-logic system recognizes two classes for Ms-Mp: HIGH and LOW-OR-N/A. N/A indicates the data required for the calculation of either Ms or Mp were not available. A high value is interpreted as evidence that the event is an earthquake, and a low or missing value provides no evidence for identification. Low values can occur for earthquakes if the recording stations are near a node in the S-wave radiation pattern.

Script Match

Script matching is a case-based approach to recognizing repeated mining explosions. The scripts consist of an estimate of the mean and standard deviation of many signal parameters derived from previous events at known mine sites. New events are compared to these scripts to determine the extent to which they are similar to the previous mining events. This approach was originally introduced to seismic monitoring by *Baumgardt* [1987]. We modified the implementation to include data from multiple phases and stations in the same statistical test, but the basic concept

was not changed. The two classes for the script match are HIGH and LOW-OR-N/A. Membership in these classes is based on the results of a chi-squared test. A high value for the script match is interpreted as evidence that the event is a mining explosion, and a low or missing value provides no evidence for identification. An event will not be identified as a mining explosion by the IMS Event Identification System unless it passes this case-based test.

Combination of Regional Discriminants

The rule base for combining the regional discriminants is currently designed to give each of them approximately equal weight. The only exception is low spectral variance. This discriminant was derived from earthquakes and mining explosions which are commonly "ripple-fired". However, it is likely than an isolated explosion would a have lower spectral variance than is commonly observed for mining explosions. To account for this, the rules are weighted such that low spectral variance contributes less than a high value of Ms-Mp to the identification of earthquakes. The final step in applying the discriminants is to estimate the degree-of-membership in the EXPLOSION and EARTHQUAKE classes. This is calculated from the centroid, and it is used for the composite identification described in the previous section.

New discriminants

We are adding three new regional discriminants to the IMS Event Identification System. The first is a case-based approach for identifying repeated events on the basis of waveform correlation [*Riviere and Grant*, 1992]. This is similar to the script match discriminant except that the scripts are replaced by reference waveforms. The waveform at the closest station is correlated with the waveform from an event that represents a cluster. If the correlation is high, where the classes HIGH and LOW are defined empirically by membership functions, then the new event is assigned to that cluster. An automated clustering algorithm was used that does not require the identification of the past events. If the reference waveform for a cluster can be identified (e.g., as a mining explosion or as part of an earthquake sequence) then this information will be used in the rules. Even if the reference waveform is not identified, the correlation provides important data that suggest the event in question is similar to past events and therefore is unlikely to be an underground nuclear test.

The other two discriminants are based on frequency-dependent amplitudes of regional phases. One of these is an Lg spectral ratio [*Bennett and Murphy*, 1986; *Taylor et al.*, 1988b; *Baumgardt et al.*, 1992]. Previous studies indicate that the high-frequency/low-frequency (HF/LF) Lg spectral ratio is typically higher for earthquakes than it is for explosions, and this is probably related to depth. The other discriminant is the amplitude ratio of regional S and P phases at high-frequency [*Dysart and Pulli*, 1987; *Chan et al.*, 1990; *Lynnes and Baumstark*, 1991; *Baumgardt et al.*, 1992; *Bennett et al.*, 1992]. The HF S/P ratio is generally higher for earthquakes, and the separation appears to increase with increasing frequency (at least up to 8-10 Hz). Unfortunately, these ratios can depend strongly on distance since high-frequency regional P and S phases attenuate at different rates. For example, we found that distance-corrected ratios in the 8-10 Hz band were much more effective at separating explosions and earthquakes recorded at the GERESS array than uncorrected ratios. Generally, discriminants that are based on HF regional phase amplitudes have been successful for localized source regions, but meaningful extrapolation to new areas requires detailed region-specific knowledge.

3.2 System Architecture

The IMS Event Identification System includes a software module for the automated event identification described in the previous section and many graphical tools for analyst-review of the

automated system. It is built on the IMS Software Integration Platform (SIP) which allows separately-developed modules to be connected using Interprocess Communication (IPC) in a distributed processing environment. The SIP is described in detail by *Given et al.* [1993].

Figure 4 is a schematic view of the system architecture. The Event Server is a forms-based interface to a database management system that allows the user to select events on the basis of parameters such as latitude, longitude, origin time, magnitude, and event identification. The Event Server returns in a "results window" a selectable list of events satisfying the user's query. A key feature of the SIP is that all IMS applications (including the Event Server) have a consistent Data Management System Interface (DMSI). This facilitates the development of new applications and makes the system easier to maintain. Events can be selected from the "results window" and sent by pull-down menu to other applications. An IPC message containing unique identifiers (database keys) for the events is sent from the Event Server to the various applications. The IPC and distributed processing are managed by the Distributed Applications and Control System (DACS), which is another key element of the SIP [*Given et al.*, 1993]. If an application is not currently running, the DACS will start it automatically and deliver the IPC message. The most important applications for review of the automated event identification are the IMS Analyst Review Station (ARS) for waveform display and manipulation, the IMS Map program, and the IMS EventID program.

Waveforms can be displayed by selecting an event from the Event Server "results window" and sending it to the IMS Analyst Review Station [*Wang et al.*, 1993]. ARS reads and displays the relevant waveform and parametric data. It provides internal features for filtering, waveform manipulation (zooming and scrolling), phase association, and event location. In addition to these, a variety of separately-developed Analyst Tools are available through pull-down menus or user-defined buttons (similar to the "ToolBar" found in many window-based PC programs). When one of these tools is selected, an IPC message is sent to the application. This message includes pointers to data that are needed for that application. For example, a time window and channel or a seismic detection can be selected from ARS and sent to programs for calculating and displaying spectra, spectrograms, *f-k* power spectra, or event beams. Examples of these displays are included in Section 5.0.

Events selected from either the Event Server "results window" or ARS can also be sent to the IMS Map program or EventID program. The Map program is used to display the event location and error ellipse with a variety of projections and scales. It has an interface to the database that can be used to display station locations or the locations of previous events. IPC messages sent to the EventID program are routed through the Process Manager. The Process Manager is primarily used to initiate batch-type processing. It converts the IPC message into command-line parameters and passes them to applications through a configurable Application Programmer's Interface (API). The order in which the applications are executed is specified through the interpretive Scheme-based API (Scheme is a dialect of the Lisp language). The API supports conditional, serial, and parallel processing. In this way, the Process Manager and API allow a high-level configuration of a data processing pipeline. Each of the applications required for EventID include a Command-Line Interface (CLI). The first application queries the database to see if the calculations that are needed for the regional discriminants have been performed. If they haven't, then the relevant applications are executed in parallel on a variety of host machines. The distributed processing is managed by the DACS. The EventID program for combining these results is executed after all of these applications have finished.

The EventID program has a graphical interface that allows the user to accept, reject or modify the results of the automated system. The analyst results are saved to a separate database table so that

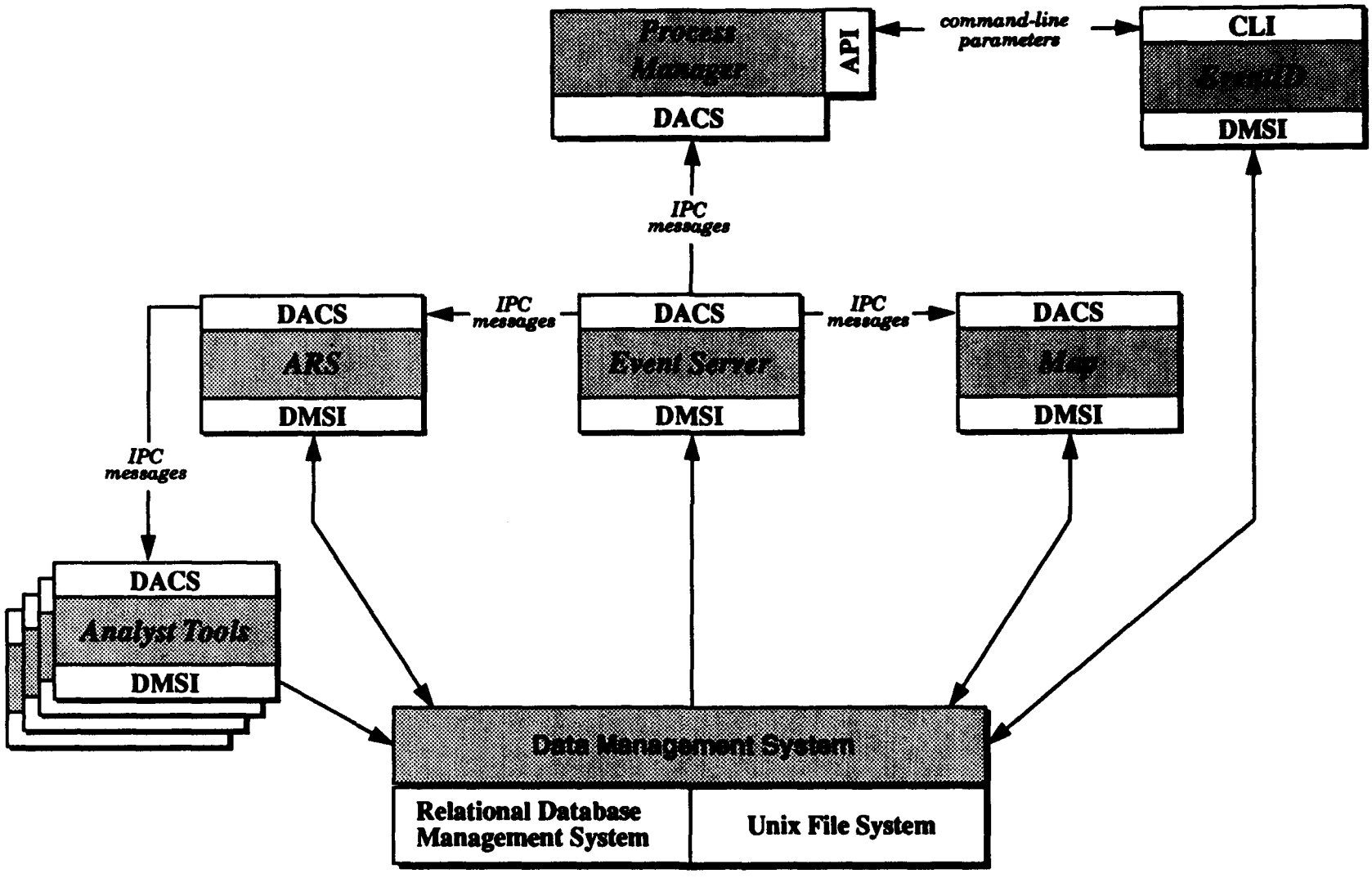

Figure 4. *This is a schematic diagram of the architecture of the IMS Event Identification System.*

these can be compared to the automated results after many events have been analyzed. The EventID program includes separate explanation facilities for the composite identification and the discriminants. These explanations include a listing of all the rules that fired and their weights, the class memberships for each of the input variables, and more details for each discriminant. It also provides the capability to activate or deactivate any of the regional discriminants and recompute the composite identification.

4.0 IMS RESULTS

The IMS Event Identification System was applied to >6000 regional events recorded by the NORESS, ARCESS and FINESA arrays in Scandinavia, and >800 of these have independent identification in a bulletin produced by the University of Helsinki. The events in the Helsinki Bulletin are identified by experienced analysts based on data from a dense network of seismic stations in northern Europe. Many of the events in this bulletin are not identified, which leads us to believe that the identification only appears in the bulletin if the analyst is confident of it.

Table 2 compares the University of Helsinki identifications to those determined by the IMS Event Identification System for 824 regional events. Only 2 of 759 Helsinki mine blasts were identified as earthquakes by IMS, and these were both single-station events with $M_L < 2.0$. However, 23% of the Helsinki earthquakes were identified as explosions by IMS. We believe that most or all of them are actually earthquakes. The current IMS Event Identification System only includes two discriminants that can provide evidence that an event is an earthquake (high Ms-Mp and low spectral variance). We expect to achieve higher identification accuracy for earthquakes once the new discriminants based on frequency-dependent regional wave amplitudes are implemented.

Table 2: Comparison of IMS and University of Helsinki Regional Event Identifications

Helsinki Identification	IMS EventID System				
	Mine Blast	Explosion	Earthquake	Indeterminate	Total
Mine Blast	528	185	2	44	759
Earthquake	1	14	41	9	65
Total	529	199	43	53	824

About 70% of the 759 Helsinki mine blasts were identified as such by IMS, and 185 (24%) were identified as explosions but were not identified as mine blasts because they did not match scripts. We expect that about 10% of the blasts at any given mine will not match the script because this is how we defined the membership functions for script matching. In addition, many of the Helsinki mine blasts occurred in mines for which we did not have enough data to generate scripts. Even without the scripts for these mines, only 30% of the events in the Helsinki Bulletin were identified as EXPLOSION or INDETERMINATE which are the events that require further review by a seismologist. This percentage should decrease further as new discriminants are added to the system.

The system was applied to another 5200 events for which we had no independent information on the event identification. Most of the events that were identified as earthquakes were located in seismic areas (the Mid-Atlantic Ridge and the southwest coast of Norway). The events identified by IMS as mining events were located near known mines, but this is expected since azimuth and relative arrival times are included in the scripts. The events with $M_L \geq 2.0$ that were identified as explosions generally occurred in clusters. Some clusters are probably explosions at mines for which we don't have scripts. Others are probably mining explosions at sites for which we have scripts but the parameters did not match (i.e., the 10% that we expect to be in this category). There

are also four other clusters that appear to be underwater explosions because they have distinctive spectral modulations that are a characteristic signature of a bubble-pulse. There are some events that are obviously misidentified (e.g., several events on the Mid-Atlantic Ridge were identified by IMS as explosions), but this was evident from the comparison to the Helsinki Bulletin in Table 2.

We also applied the Event Identification System to several hundred events recorded by GERESS, though only a small ground-truth database exists for this region [*Grant and Coyne*, 1992]. Our initial results for this region are not very good. Many of the events that we believe are earthquakes because of their locations and magnitudes are identified by IMS as EXPLOSIONS or INDETERMINATE. However, we believe that the new discriminant based on distance-corrected HF S/P amplitude ratios will improve the identification accuracy for earthquakes in this region. Unfortunately, it will be difficult to make a quantitative performance assessment like the one in Table 2 because of the limited amount of ground-truth data that are currently available.

5.0 APPLICATION TO NOVAYA ZEMLYA

The IMS Event Identification System was applied to an event at Novaya Zemlya that occurred on 31 December 1992. This is exactly the type of low-magnitude seismic event that would be important for monitoring nuclear explosion testing at low-yield thresholds.

5.1 Data Quality and the IMS Event Location

Single-channel waveform data and the IMS location solution for this event are shown in Figure 5. It was recorded by four of the IMS regional arrays (ARCESS, NORESS, and the two new 9-element arrays in Apatity and Spitzbergen). The IMS event location is listed in Table 3. Three of the arrays are 9°–10° from the event, and the distance to NORESS is about 20°. High-quality Pn and Sn signals are observed at ARCESS for frequencies above 4 Hz. Only three of the array elements at Spitzbergen had Pn and Sn signals with similar quality to the one shown in Figure 5 (SPA3). The other elements were dominated by noise, so the data quality was too low to get reliable slowness or azimuth estimates from frequency-wavenumber (*f-k*) analysis. The data on all nine elements of the Apatity array were similar to the one shown. The Sn phase has low signal-to-noise ratio (*snr*) on the single-channels, but it can be observed on a coherent beam. However, the *f-k* power spectrum does not have an obvious peak that would indicate that this is an Sn phase from Novaya Zemlya. The NORESS data are filtered between 1 and 3 Hz in Figure 5. The *snr* is low for the single channels, but the *f-k* power spectrum for the P phase has a clear peak at a teleseismic slowness and azimuth to the northeast.

Table 3: IMS Origin Data for the 31 December 1992 Novaya Zemlya Event

Latitude	Longitude	Origin Time (GMT)	Depth	M_L
73.58	55.21	12/31/92 09:29:24	0.0	2.26

The IMS location is based on average travel-time curves for paths in Scandinavia. *Israelsson* [a separate paper in this volume] relocated this event using a well-located nuclear test as a master event. They estimate the location to be about 20 km to the southeast of the IMS location in Table 3. We also relocated this event without including the Spitzbergen or Apatity data so that we could compare to the IMS locations of previous nuclear tests at Novaya Zemlya. Figure 6 shows the original IMS location from Table 3 (labeled "1") and the location without the Spitzbergen or Apatity data (labeled "2"). Excluding these data moved the location about 100 km to the southeast. Also shown in Figure 6 are the IMS locations of three nuclear explosions at Novaya Zemlya. These solutions included data from NORESS and ARCESS, and one of them also included data from

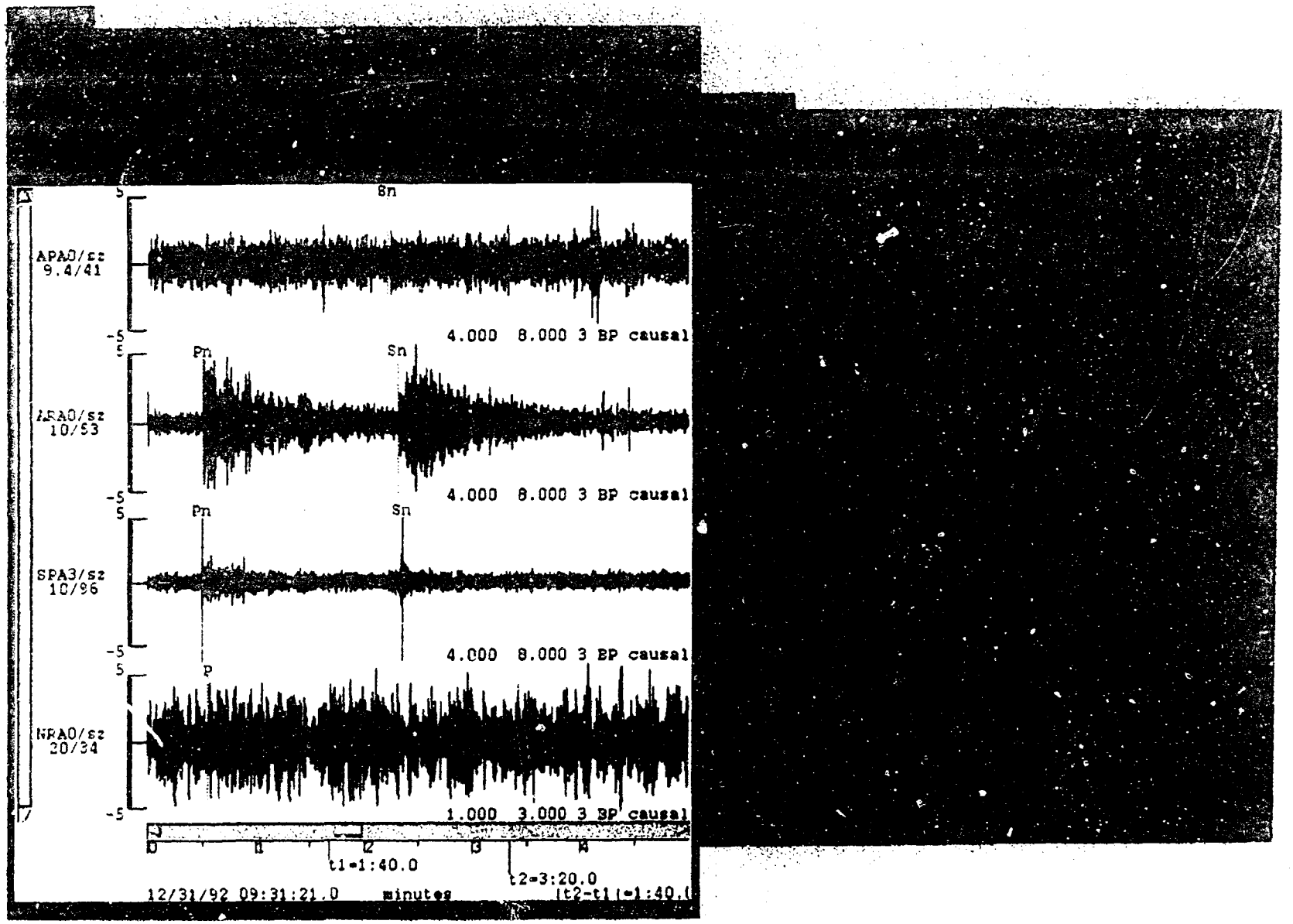

Figure 5. *Single-channel waveform data from the 31 December 1992 event at Novaya Zemlya recorded by the IMS arrays are plotted. The map shows the array locations and the IMS location solution. The measured azimuths at NORESS and ARCESS are shown for each associated phase. Azimuths were not estimated for phases at Spitzbergen or Apatity.*

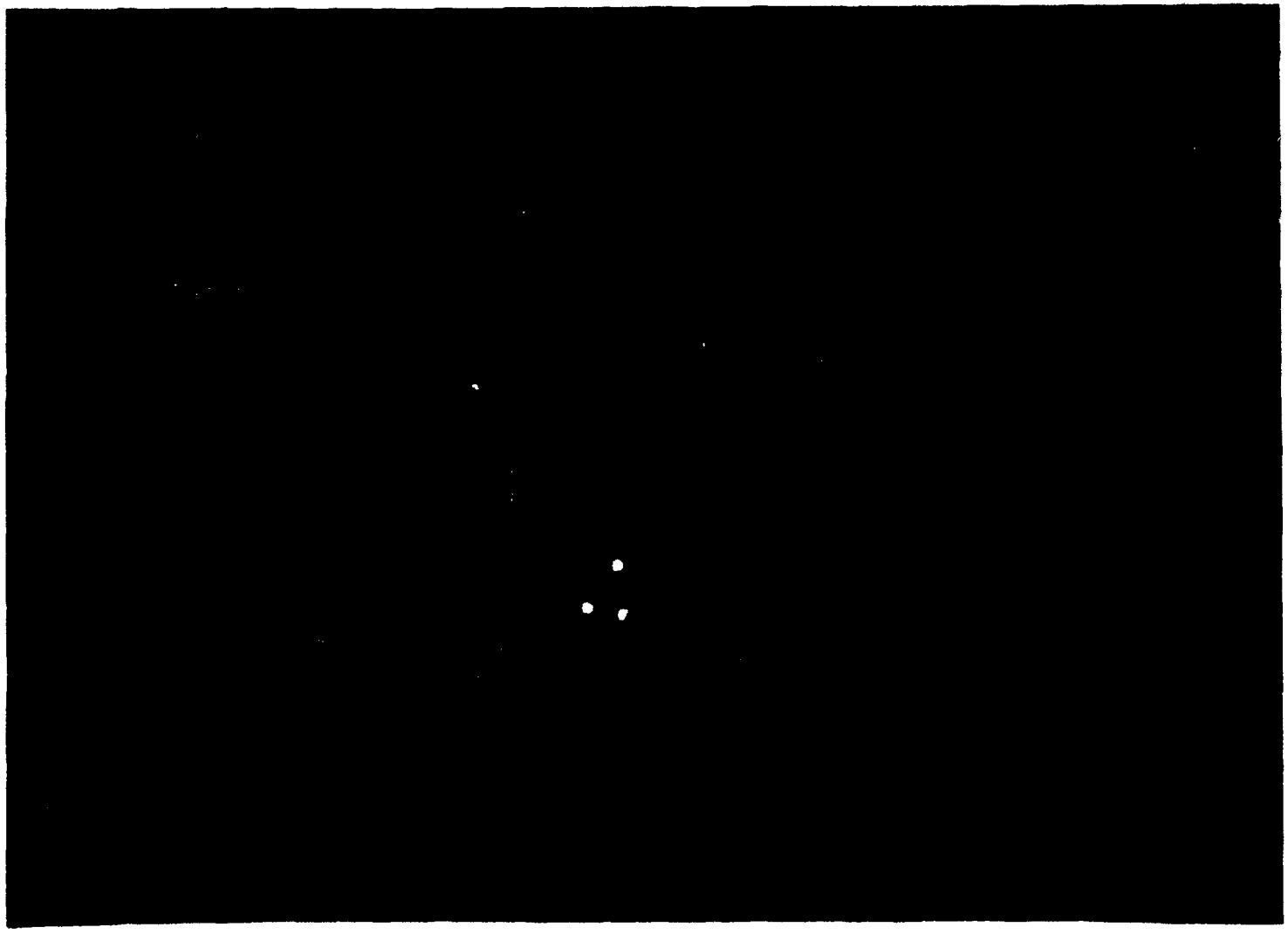

Figure 6. *This map shows the IMS location of the 31 December 1992 event at Novaya Zemlya including data from all four arrays (labeled "1"), and after excluding data from Spitzbergen and Apatity (labeled "2"). The IMS locations of three nuclear explosions are plotted in white. The location of the Novaya Zemlya test site is also plotted ("NZ").*

FINESA. The location of the Novaya Zemlya test site is shown for reference. The IMS locations are about 200 km southeast of the test site.

5.2 Automated Event Identification

The IMS Event Identification System was applied to the 31 December 1992 Novaya Zemlya event. The regional discriminants provided some evidence that the event was an earthquake, but the confidence was low. The contextual discriminants provided evidence that the event was an explosion since it was in an area of low natural seismicity. The composite identification was INDETERMINATE. The contextual and regional discriminants are described below.

Contextual Discriminants

Table 4 lists the contextual discriminants for this event. The event appears to have been shallow, onshore, and in a relatively aseismic area. The event depth was fixed at zero by the NORSAR analyst. If the depth were unconstrained, then the uncertainty would be too large to be useful for event identification. Since the depth has full membership in the class SHALLOW, this discriminant is not relevant for the event identification because shallow events can be explosions or earthquakes. The entire location error ellipse at the 90% confidence level is onshore. This is the case with or without the data from Spitzbergen and Apatity (Figure 6). The IMS local magnitude (M_L) is based on Pn and Sn amplitudes in the 2-4 Hz band. The M_L for the Novaya Zemlya event is 2.26, which gives full membership in the class LOW.

Table 4: Contextual Discriminants for the 31 December 1992 Novaya Zemlya Event

Contextual Discriminant	Class	Degree-of-Membership
depth	SHALLOW	1.0
location	ONSHORE	1.0
magnitude	LOW	1.0
seismicity	LOW	1.0

The contextual discriminants for this event bias the composite identification towards EXPLOSION because the event is in a relatively aseismic region. The two rules used to identify this event are:

Depth	Location	Magnitude	Seismicity	Regional Discriminants	Conclusion
SHALLOW	ONSHORE	LOW	LOW	EXPLOSION	HX
SHALLOW	ONSHORE	LOW	LOW	EARTHQUAKE	MQ

If the regional discriminants did not provide evidence for identification (membership equal to 0.5 in both the EXPLOSION and EARTHQUAKE classes), then the event would be identified as an explosion with confidence = 0.58. This is the centroid between HIGH-CONFIDENCE EXPLOSION (HX) and MODERATE-CONFIDENCE EARTHQUAKE (MQ). The contextual discriminants do not eliminate the possibility that small earthquakes can occur in relatively aseismic regions. For example, if the regional discriminants indicate that the event is an earthquake with high confidence (membership equal to 1.0 in the EARTHQUAKE class), then the composite identification would be MODERATE-CONFIDENCE EARTHQUAKE (MQ).

Regional Discriminants

Table 5 lists the results of applying the regional discriminants. No evidence of source multiplicity (i.e., ripple-firing) was found from data recorded by any of the IMS stations. Therefore, this discriminant provides no evidence for identification. The spectral variance is lower than it is for typical mining events in Scandinavia. Figure 7 compares the Pn and Sn spectra at ARCESS to the spectrum of the noise prior to Pn. The *snr* is above 10 dB for most of the range between 4 and 14 Hz. The variance of the detrended log spectrum is in the region of overlap between explosions and earthquakes, but it is closer to the mean of the earthquake population. Therefore, this discriminant provides some evidence that the event is an earthquake.

Table 5: Regional Discriminants for the 31 December 1992 Novaya Zemlya Event

Regional Discriminant	Class	Degree-of-Membership
Source Multiplicity	NO-CEPSTRAL-PEAKS	1.00
Spectral Variance	LOW	0.76
Spectral Variance	HIGH	0.24
Ms - Mp	LOW	1.00
Rg	NOT-PRESENT	1.00
Script Match	LOW-OR-N/A	1.00

The last three regional discriminants in Table 5 provide no evidence for identification. The local magnitudes were estimated from the data recorded at ARCESS. The difference between the M_L estimated from Sn and the M_L estimated from Pn was only 0.05. This gives full membership in the class LOW. As expected for oceanic paths and long epicentral distances, there were no Rg phases recorded. Also, there are no scripts within 300 km of the Novaya Zemlya event for the script match discriminant. The two rules used to determine membership in the explosion and earthquake classes were:

Source Multiplicity	Spectral Variance	Ms-Mp	Rg	Script Match	Conclusion
NO-CEPSTRAL-PEAKS	HIGH	LOW	NOT-PRESENT	LOW-OR-N/A	LX
NO-CEPSTRAL-PEAKS	LOW	LOW	NOT-PRESENT	LOW-OR-N/A	LQ

The degree-of-membership in the EARTHQUAKE class is 0.59, and it is 0.41 in the EXPLOSION class. The discriminants provide some evidence that the event is an earthquake because the spectral variance is lower than is typical for ripple-fired mining explosions. However, nuclear explosions (or isolated explosions in general) may have lower spectral variance, and we were aware of this trade-off when we developed the rules. If spectral variance is not used, then the discriminants provide no evidence for identification, and the composite identification is EXPLOSION with confidence equal to 0.58.

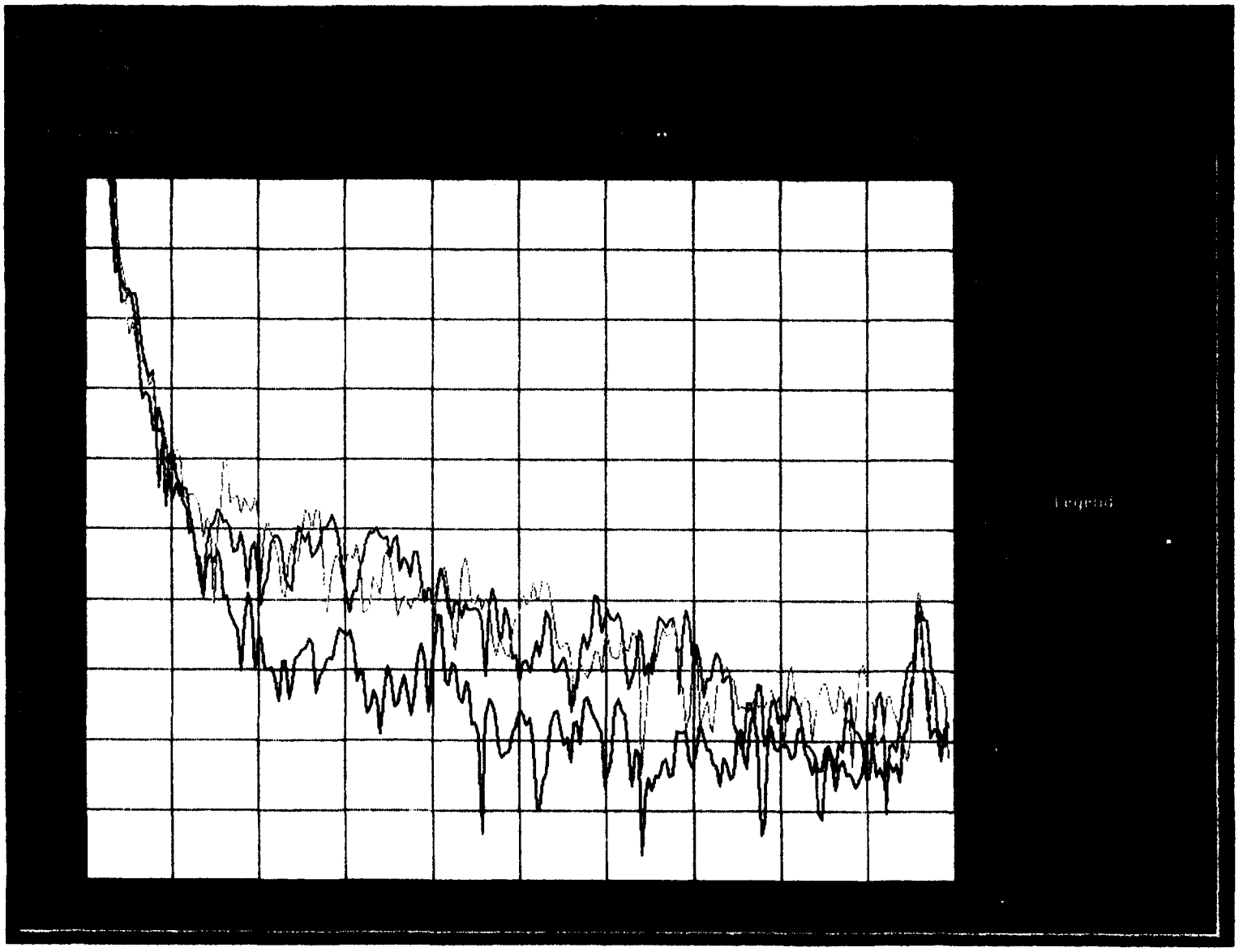

Figure 7. *The spectra of Pn and Sn phases recorded at ARCESS are plotted (green and yellow, respectively). The noise spectrum for a time window before Pn is also plotted (purple). The spectra were computed for 10-s windows, and they were smoothed over a 0.2 Hz bandwidth.*

5.3 Comparison to Other Events

We compared the results of the Event Identification System for the event on 31 December 1992 to the results for three known nuclear explosions at Novaya Zemlya and to an earthquake on the Mid-Atlantic Ridge at a similar epicentral distance to ARCESS (12°). The event parameters are listed in Table 6.

Table 6: Origin Data for Three Nuclear Explosions at Novaya Zemlya and an Earthquake on the Mid-Atlantic Ridge

Latitude	Longitude	Origin Time (GMT)	Type	mb	Ms	M_L	Author
73.364	54.445	05/07/88 22:49:58	Nuclear	5.6	3.8	-	USGS
73.387	54.998	12/04/88 05:19:53	Nuclear	5.9	4.6	-	USGS
73.361	54.707	10/24/90 14:57:58	Nuclear	5.7	4.0	-	USGS
80.020	1.410	06/09/91 10:57:09	Quake	-	-	3.5	IMS

Single-channel waveform data at ARCESS from each of these events are compared to the 31 December 1992 event in Figure 8. The top four panels are the waveforms for the events in Table 6 (in the same order). The bottom panel is the waveform for the 31 December 1992 event. All waveforms are filtered between 4 and 8 Hz. The waveforms are similar for all events. High-frequency (4-8 Hz) Pn and Sn are the dominant regional phases. There are no observed Lg or Rg phases which is typical for oceanic paths. The S/P amplitude ratio (4-8 Hz) is higher for the earthquake and the 31 December 1992 event than it is for any of the nuclear explosions.

The IMS Event Identification System identified all three of the nuclear tests as EXPLOSIONS with moderate to high confidence. The main difference between these events and the 31 December 1992 event is that the nuclear tests had high magnitudes. For example, the explosion on 5/7/88 had nearly identical results for the discriminants as the 31 December 1992 event, but the composite identification was EXPLOSION with confidence = 0.70. The two rules used to identify the three nuclear explosions are:

Depth	Location	Magnitude	Seismicity	Regional Discriminants	Conclusion
SHALLOW	ONSHORE	HIGH	LOW	EXPLOSION	HX
SHALLOW	ONSHORE	HIGH	LOW	EARTHQUAKE	IND

The nuclear explosion was a large event in an aseismic region, and would have been identified as INDETERMINATE by IMS if the regional discriminants had indicated that the event was an earthquake (large earthquakes in aseismic regions are very rare). Since the discriminants had partial membership in both the EARTHQUAKE and EXPLOSION classes, the composite identification was a weighted average between INDETERMINATE (IND) and HIGH-CONFIDENCE EXPLOSION (HX). The 31 December 1992 event had a low magnitude, and its composite identification was a weighted average between MODERATE-CONFIDENCE EARTHQUAKE (MQ) and HIGH-CONFIDENCE EXPLOSION (HX).

The IMS Event Identification System identified the Mid-Atlantic Ridge event as an EARTHQUAKE with confidence = 0.91. The regional discriminants were nearly the same as the 31 December 1992 event, but the composite identification was much different. This is again because of the contextual discriminants. The Mid-Atlantic Ridge event was offshore in a

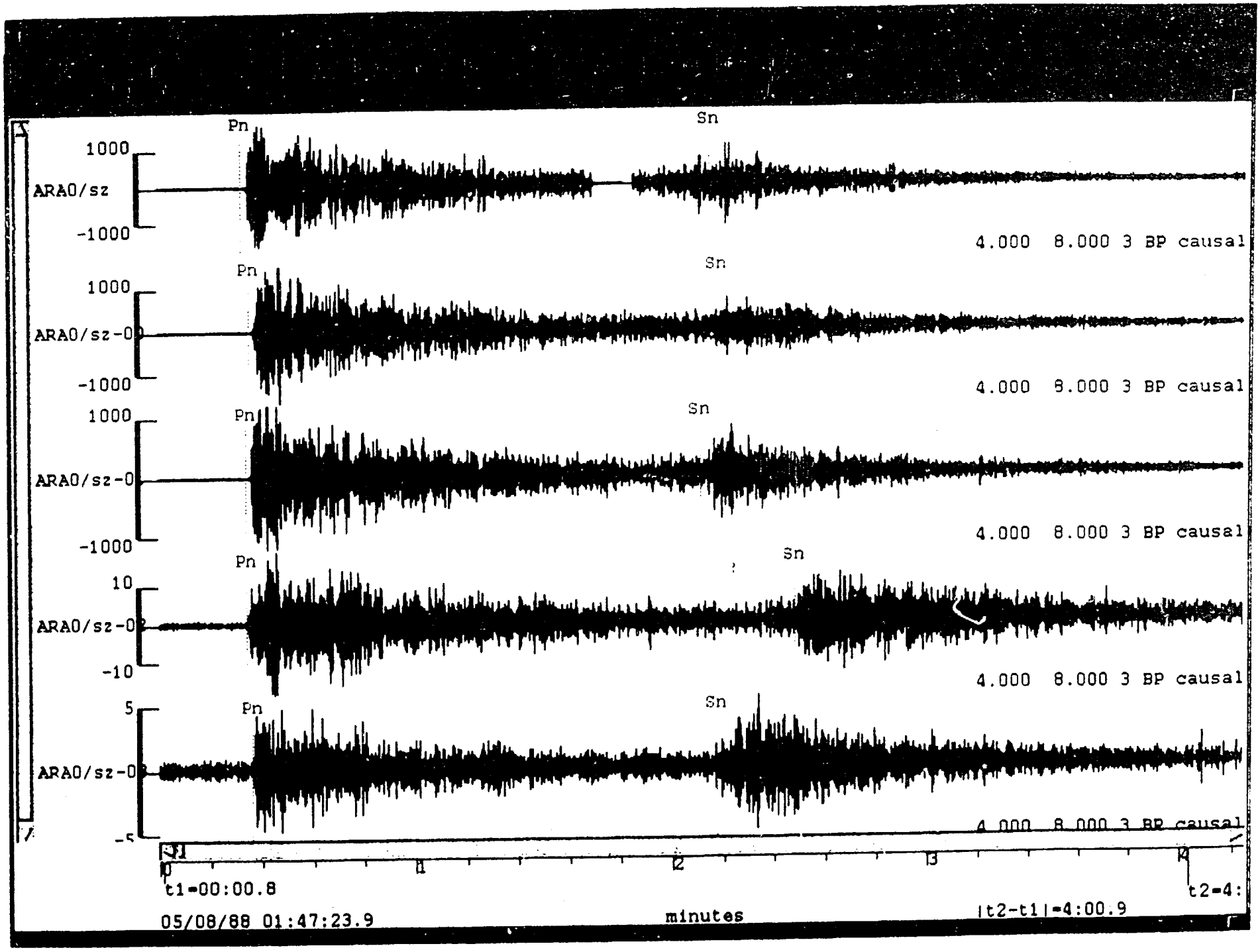

Figure 8. *Single-channel waveform data recorded at ARCESS are plotted for the four events in Table 6 (in the same order) and the 31 December 1992 event at Novaya Zemlya (bottom).*

seismically active area, and it had a high magnitude. Events of this type are identified as HIGH-CONFIDENCE EARTHQUAKE if the regional discriminants indicate that the event is an earthquake, and MODERATE-CONFIDENCE EARTHQUAKE if the regional discriminants indicate that the event is an explosion. The latter rule was developed to improve the identification accuracy of offshore earthquakes. The trade-off is that large nuclear explosions in offshore seismic regions will be misidentified, but it is likely that these events would be detected by hydrophones. However, small events that occur offshore are not automatically identified as earthquakes. In fact, there are many events in the IMS database that are identified as probable underwater explosions.

In summary, the regional discriminants in the IMS Event Identification System gave similar results for all five of the events in this study. The waveforms for these events are very similar, except that the high-frequency S/P amplitude ratios are lower for the nuclear explosions. Even though the discriminants were similar, the three nuclear explosions were identified as EXPLOSIONS with moderate-to-high confidence, the Mid-Atlantic Ridge event was identified as an EARTHQUAKE with high confidence, and the 31 December 1992 event was identified as INDETERMINATE. The main difference is in the contextual discriminants, and these examples demonstrate how important these can be for accurate identification. Even after careful review of all of the data, it is difficult to identify the 31 December 1992 event with much confidence. At high frequency it appears different from the nuclear explosions, and similar to the Mid-Atlantic Ridge earthquake. However, the nuclear explosions are much larger than the event in question, and it is uncertain how this ratio scales with event size. The IMS Event Identification System was successful at focusing attention on this event by identifying it as INDETERMINATE. New regional discriminants must be developed before events like this can be identified by an automated system.

6.0 CONCLUSIONS AND RECOMMENDATIONS

We developed a system for automated identification of regional seismic events. This system is easily expanded to incorporate a wide variety of methods for identifying events and the region-specific knowledge needed to make these methods more effective. A fuzzy-logic paradigm is used to combine the evidence from the various methods. The first operational version of the system was applied to >6000 regional events in Scandinavia, and >800 of these were identified in an independent bulletin. Assuming the latter is correct, the system correctly identified >90% of the events as explosions or earthquakes, and only 2% were misidentified. This system was also applied to a small event at Novaya Zemlya (31 December 1992) which is the type of event that would be important for monitoring a CTBT or a low-yield threshold treaty. Our system was unable to identify this event. However, it properly identified three previous nuclear explosions at Novaya Zemlya and an earthquake on the Mid-Atlantic ridge roughly the same distance from ARCESS. The signal characteristics are very similar for all five of the events, providing little evidence of the source type. The main difference between them is in the contextual discriminants (i.e., their size and location compared to known seismicity). The contextual discriminants are obviously important for identifying events, and our system provides a basis for quantifying this and combining them with other evidence.

The contextual discriminants are not sufficient to identify a low-magnitude event at Novaya Zemlya. Therefore, identification must be based on discriminants computed from the seismic signals. Since the identification could not be determined, an obvious conclusion is that other and better regional discriminants are needed to identify this type of event.

All the signal-character discriminants are based on experience elsewhere. Some are easily transported to new areas, and others require detailed region-specific knowledge. The

transportable discriminants in the current system are cepstral analysis, spectral variance and the presence of Rg. These are valuable for identifying many mine blasts and underwater explosions, but there are also events for which they are inconclusive, such as the Novaya Zemlya event. Previous studies have investigated other transportable discriminants such as the relative excitation of short-period SH waves and methods other than Rg for estimating the depth of regional events. Discriminants based on short-period SH waves have not been successful because scattering produces significant transverse energy in regional seismograms [*Gupta and Blandford*, 1983; *Taylor et al.*, 1988a]. However, time-domain discriminants based on identifying regional depth phases have been successful in the western United States [*Burdick et al.*, 1991]. These, and other methods for estimating the depth of regional events, will be added to our system.

Although depth discriminants may improve our capability to identify small regional events, it is unlikely that these events can be identified accurately enough to monitor low-yield nuclear explosion testing without region-specific knowledge. Empirically-based regional discriminants (e.g., HF S/P amplitude ratios) have been successfully developed for many areas. They are typically based on explosions and earthquakes that are approximately co-located. Since the paths are nearly the same, observational differences can be interpreted in terms of source differences. However, extrapolation of these discriminants to new areas will require region-specific path corrections. Thus, these discriminants must be calibrated for each new area, and this calibration requires an extensive amount of observational data for which ground-truth information is available. Therefore, efforts to acquire large regional data sets in areas of interest with ground-truth information are important. Unfortunately, relatively aseismic areas like Novaya Zemlya have few data for calibration. Therefore, accurate identification of events in these areas will depend heavily on our ability to transport model-based discriminants.

REFERENCES

Bache, T., S. Bratt, J. Given, T. Schroeder, H. Swanger, and J. Wang, The Intelligent Monitoring System Version 2, Quarterly Technical Report #7, SAIC-91/1137, Science Applications International Corporation, San Diego, California, 93 pp., 1991.

Baumgardt, D., Case-based reasoning applied to regional seismic event characterization, Proceedings from the 9th Annual DARPA/AFGL Seismic Research Symposium, Nantucket, Massachusetts, 173-178, 1987.

Baumgardt, D., J. Carney, M. Maxson and S. Carter, Evaluation of regional seismic discriminants using the Intelligent Seismic Event Identification System, Semi-Annual Technical Report SAS-TR-93-38, ENSCO, Inc., Springfield, Virginia, 96 pp., 1992.

Baumgardt, D., G. Young, and K. Ziegler, Design and development of the Intelligent Event Identification System: Design considerations and processing for regional event identification, Scientific Report PL-TR-91-2211, 106 pp., 1991.

Baumgardt, D. and K. Ziegler, Spectral evidence of source multiplicity in explosions: Application to regional discrimination of earthquakes and explosions, Bull. Seismol. Soc. Am., 78, 1773-1795, 1988.

Baumgardt, D. and K. Ziegler, Automatic recognition of economic and underwater blasts using regional array data, Unpublished Report to Science Applications International Corporation, 11-880085-51, ENSCO, Inc., Springfield, Virginia, 24 pp., 1989.

Burdick, L., E. Garnero, C. Saikia and D. Helmberger, Time domain regional discriminants, Scientific Report PL-TR-91-2278, 86 pp., 1991.

Bennett, J., A. Campanella, J. Scheimer, and J. Murphy, Demonstration of regional discrimination of Eurasian seismic events using observations at Soviet IRIS and CDSN stations, Final Report PL-TR-92-2090, 122 pp., March, 1992.

Bennett, T. J., and J. R. Murphy, Analysis of seismic discrimination capabilities using regional data from western United States events, Bull. Seismol. Soc. Am., 76, 1069-1086, 1986.

Caudill, M., Using Neural Nets: Fuzzy Decisions (Part 2), AI Expert, 59-64, April, 1990.

Chan, W., R. Baumstark, and R. Cessaro, Spectral discrimination between explosions and earthquakes in Central Eurasia, Tech. Rep. GL-TR-90-0217, Teledyne Geotech, Alexandria, Virginia, 38 pp., 1990.

Dysart, P. and J. Pulli, Spectral study of regional earthquakes and chemical explosions recorded at the NORESS array, Technical Report C87-03, Center for Seismic Studies, Arlington, Virginia, 34 pp., 1987.

Given, J., W. Fox, J. Wang, and T. Bache, The Intelligent Monitoring System Software Integration Platform, Tech. Rep. SAIC-93/1069, Science Applications International Corporation, San Diego, California, 79 pp., 1993.

Grant, L. and J. Coyne, Ground-truth data for seismic discrimination research, Proceedings from the 14th Annual PL/DARPA Seismic Research Symposium, Tucson, Arizona, 139-145, 1992.

Gupta, I. and R. Blandford, A mechanism for generation of short-period transverse motion from explosions, Bull. Seismol. Soc. Am., 73, 571-592, 1983.

Hedlin, M., J.B. Minster, and J.A. Orcutt, An automatic means to discriminate between earthquakes and quarry blasts, Bull. Seismol. Soc. Am., 80, 2143-2160, 1990.

Israelsson, H., Estimates of the epicenter uncertainty for a small Novaya Zemlya Event Dec. 31 1992, [a paper in this volume], 1993.

Kafka, A., Rg as a depth discriminant for earthquakes and explosions: A case study in New England, Bull. Seismol. Soc. Am., 80, 373-394, 1990.

Kandel, A., *Fuzzy Mathematical Techniques with Applications*, Addison-Wesley, Reading, Massachusetts, 1986.

Kosko, B., *Neural Networks and Fuzzy Systems: A Dynamical Systems Approach to Machine Intelligence*, Prentice-Hall Inc., New Jersey, 1992.

Lynnes, C. and R. Baumstark, Phase and spectral ratio discrimination in North America, Technical Report PL-TR-91-2212(II), Teledyne Geotech, Alexandria, Virginia, 68 pp., 1991.

Negoita, C., *Expert Systems and Fuzzy Systems*, Menlo Park, California: Benjamin/Cummings Publishing, 1985.

Riviere-Barbier, F. and L. Grant, Cluster analysis of closely spaced mining blasts as a method of event location, Final Report PL-TR-92-2006, 54 pp., 1992.

Self, K., Designing with fuzzy logic, IEEE Spectrum, November, 1990.

Smith, A., High-frequency seismic observations and models of chemical explosions: implications for the discrimination of ripple-fired mining blasts, Bull. Seismol. Soc. Am., 79, 1089-1110, 1989.

Stump, B. and R. Reinke, Experimental confirmation of superposition from small-scale explosions, Bull. Seismol. Soc. Am., 78, 1059-1073, 1988.

Taylor, S., M. Denny, E. Vergino and R. Glaser, Regional discrimination between NTS explosions and western U.S. earthquakes, Tech. Rep. UCRL-99790, Lawrence Livermore National Laboratory, Livermore, California, 68 pp., 1988a.

Taylor, S., N. Sherman and M. Denny, Spectral discrimination between NTS explosions and western United States earthquakes at regional distances, Bull. Seismol. Soc. Am., 78, 1563-1579, 1988b.

Wang, J., B. Smithey, and S. Wass, The SAIC Analyst Review Station Architecture and Implementation, Technical Report SAIC-93/1034, Science Applications International Corporation, San Diego, California, 150 pp., 1993.

Yeager, R., Concepts, theory, and techniques: A new methodology for ordinal multi-objective decisions based on fuzzy sets, Decision Sciences, 12(4), 589-600, October, 1981.

Zadeh, L., Fuzzy Sets, Information and Control, 8, 338-353, 1965.

SEISMIC WAVEFORM FEATURE ANALYSIS AND DISCRIMINATION OF THE DECEMBER 31, 1992 NOVAYA ZEMLYA EVENT

SEISMIC WAVEFORM FEATURE ANALYSIS AND DISCRIMINATION OF THE DECEMBER 31, 1992 NOVAYA ZEMLYA EVENT

Douglas R. Baumgardt

July 31, 1993

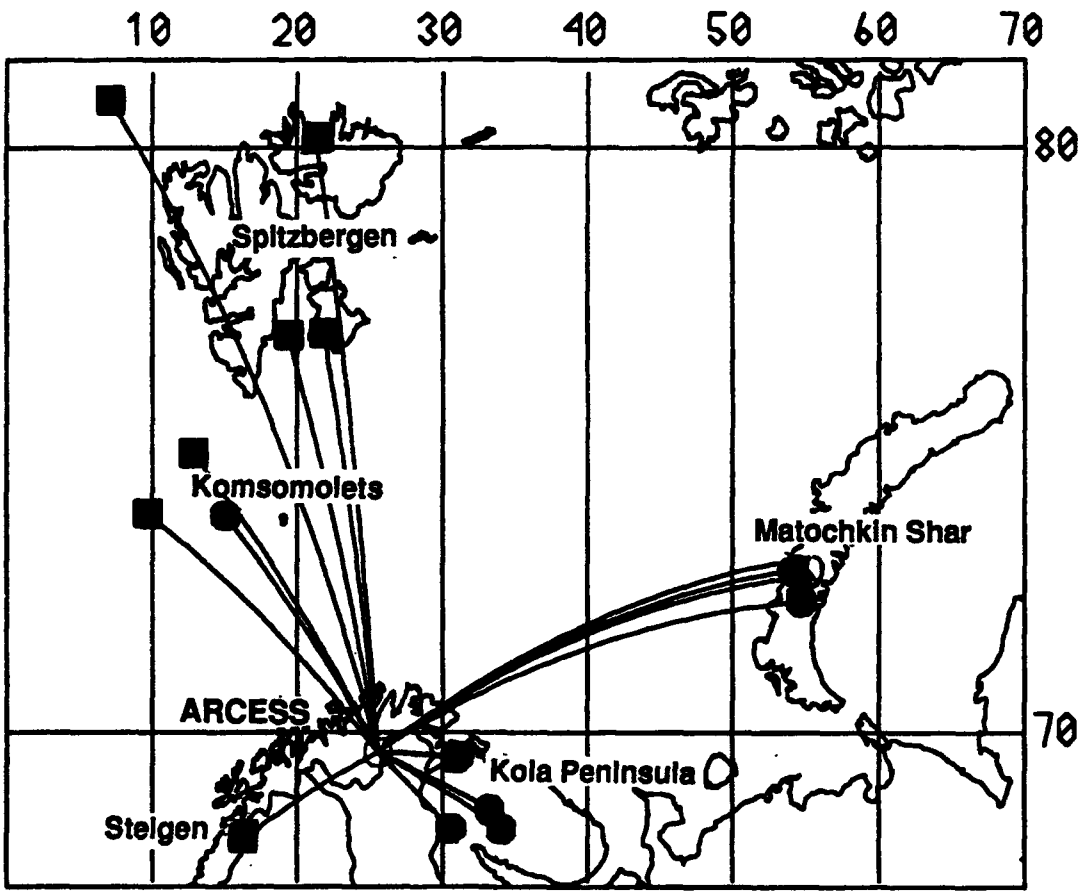

ENSCO, Inc.

SEISMIC WAVEFORM FEATURE ANALYSIS AND DISCRIMINATION OF THE DECEMBER 31, 1992 NOVAYA ZEMLYA EVENT

Douglas R. Baumgardt

ENSCO, Inc
5400 Port Royal Road
Springfield, Va 22151

July 31, 1993

ABSTRACT

The objective of this study iss to characterize and identify, using waveform features, a seismic event that occurred on December 31, 1992 (921231) north of Matochkin Shar near the Russian nuclear test site on Novaya Zemlya. The best signals from the event were recorded at the ARCESS and Spitzbergen arrays, although the waveforms have to be filtered in bands above 2 Hz because of high, long-period microseismic noise levels. The event was detected and located with the Intelligent Monitoring System (IMS) and the waveform features extracted and analyzed by a discrimination research system, the Intelligent Seismic Events Identification System (ISEIS). Comparison of ARCESS waveforms from the 921231 event with historical nuclear explosions at Novaya Zemlya shows that the event generates more *Sn* energy, relative to *Pn* energy, than the nuclear explosions. Nuclear explosions produce very large *Pn/Sn* amplitude ratios in frequency bands above 4 Hz. Ratios for the 921231 event are not as high as those of nuclear explosions but are slightly larger than those produced by earthquakes in the same distance range. The *Pn/Sn* amplitude ratios in the 8 to 10 Hz band are nearly the same as the average value of all the Kola Peninsula events. Spectral analysis of *Pn* and *Sn* indicates that the event is not ripple-fired since the spectra are not scalloped. The *Sn* spectral ratio fails to discriminate between small earthquakes and chemical blasts. Reanalysis of an earlier larger (*mb* = 4.6) Novaya Zemlya ev[illegible], which occurred on August 1, 1986 (860801) and identified as an earthquake, reveals that it has similarities to the 921231 event in terms of its waveform features compared to reference events recorded at NORESS. The 860801 event has an explosion-like impulsive *P* onset, and the *Pn/Sn* ratio at NORESS is close to that observed for mine blasts and a PNE in the White Sea region, but significantly less than the ratios observed for large nuclear explosions at Novaya Zemlya. The 860801 event was not recorded at ARCESS, since the array was not operational at the time, and there were no shear waves recorded at NORESS from the 921231 event because it was too small. However, a statistical comparison was made, relative to the Novaya Zemlya nuclear explosions, of the *Pn/Sn* amplitude ratios in four frequency bands (2- 4 Hz, 2.5-4.5 Hz, 3-5 Hz, 4-6 Hz) of the 921231 event at ARCESS and the 860801 event at NORESS. This analysis shows that the log *Pn/Sn* amplitude ratios scale almost exactly the same relative to the nuclear explosions. Thus, had the 921231 event been large enough to be recorded at NORESS, it would have had the same *Pn/Sn* amplitude ratios as the 860801 event. We conclude that both events are not nuclear explosions and that their *Pn/Sn* ratios are comparable to many observed chemical blasts. However, since the 860801 event has been identified as an earthquake based on other discriminants (location, magnitude, *Ms - mb*), the *Pn/Sn* relative scaling argument indicates that the 921231 event is more likely an earthquake rather than a chemical blast.

INTRODUCTION

On December 31, 1992 (hereafter 921231), a seismic event of unknown identity occurred at Novaya Zemlya near Matochkin Shar, the primary Russian nuclear test site. Natural seismicity has occurred in this region, although it is very rare (W. Leith, personal reference). Thus, proximity to this known test site does not automatically identify the event as an explosion. The objective of the study described in this paper is to characterize the high-frequency waveform signals detected at the Scandinavian regional arrays for this event, to compare them with historical events of known identity, and thereby to determine whether the event was a nuclear explosion, a chemical explosion, or an earthquake.

The 921231 event produced seismic signals at two regional arrays in Scandinavia, NORESS and ARCESS, a sensor called Apatity on the Kola Peninsula, and a newly installed array at Spitzbergen. The signals detected by these sensors were processed by the Intelligent Monitoring System (IMS) (Bache et al, 1990), which located the event and determined its local magnitude to be 2.2. The analysis described in this report utilizes waveform edits produced by the IMS for the event as recorded at the regional arrays.

The approach in this study is to analyze the waveforms in the IMS database at the Center for Seismic Studies (CSS), utilizing a new research discrimination prototype, called the Intelligent Seismic Event Identification System (ISEIS), described by Baumgardt (1991a), Baumgardt et al (1992), and Baumgardt (1993). In brief, the processing steps include: (1) incoherent beam computation in nine primary filter bands, ranging from 0.5-2.5 Hz (for possible Rg phase analysis) to 8-16 Hz; (2) phase selection for key phases and amplitude computation (maximum and average) within preset windows keyed-on IMS phase identifications; (3) regional *P/S* amplitude-ratio computation (same frequency) for selected regional phases; (4) array-stacked spectral density computation in the phase-selection windows; (5) spectral ratio computation for all phases; (6) cepstrum calculation for ripple-fire detection and depth estimation; (7) storage of all key features to an Oracle database; (8) rule-based processing, using rules coded in the NASA expert systems shell, CLIPS, to identify events on the basis of individual discriminants extracted from the database; and (9) overall event identification using a voting scheme.

ISEIS has been designed to accept as input events formed by the IMS, including all associated phase identifications and waveforms, and to make a number of time and frequency domain measurements on the regional seismograms. Interactive graphics interfaces facilitate the comparison of waveform features with the same features measured at the same sensors for historical events which were processed earlier through IMS and ISEIS. In this study, we use ISEIS to compute

and compare waveform features from the 921231 Novaya Zemlya event to those of historical events to determine what kind of source (i.e., chemical blast, nuclear explosion, or earthquake) the event most resembles.

Ideally, the historical events should be the same type as those of interest (i.e., chemical explosions, earthquakes, nuclear explosions) and in the same geographic region as the event we are characterizing in order to factor out effects on the waveforms caused by propagation path differences. However, in the present case, we do not have this ideal arrangement because seismicity is rare, except for nuclear explosions, in the Novaya Zemlya region, and so we must compare the event with historical events in other regions near Novaya Zemlya. However, we try to find historical events whose paths to the sensors are as similar as possible as those for the Novaya Zemlya event. At the least, we try to examine events in the same magnitude range (2.0 to 3.0) as the Novaya Zemlya event and which are at a comparable distance as the Novaya Zemlya event is from the regional arrays. However, even for paths of similar distance, the differences in crustal structure along different paths need to be considered when comparing regional waveform signatures.

In this paper, we first discuss the characteristics of the waveforms of this event and other earthquakes, chemical blasts, and nuclear explosions recorded at the ARCESS. After a review of the processing methods, we discuss the discrimination results for the ARCESS array. At NORESS, the signals were very weak and only a *P* wave was detected. However, we present an analysis of a larger event which occurred in 1986, identified as a possible earthquake (Ryall et al, 1987), and which had strong *Pn* and *Sn* signals recorded at the NORESS array. Although this event occurred before the ARCESS array was installed and cannot be directly compared to the 921231 event, it nevertheless has certain similarities to the 921231 event, which has important ramifications about the identification of both events.

DISCRIMINATION ANALYSIS OF THE 921231 EVENT AT ARCESS

ARCESS Waveforms

Figure 1 shows a map of the locations of the ARCESS arrays relative to Novaya Zemlya. Also shown on the map are the locations of the reference events that were recorded at ARCESS and the great-circle propagation paths. These events consist of previous nuclear explosions at Novaya Zemlya, mine explosions on the Kola Peninsula, earthquakes from a swarm in northern Norway in the Steigen region, the presumed Komsomolets submarine-implosion off the northern coast of Norway (Baumgardt, 1991b), and earthquakes in the Spitzbergen-Greenland Sea regions. Note that the nuclear explosions, mine blasts, and earthquakes all occurred in different regions and the paths from the different events to ARCESS are all different. The distances from ARCESS

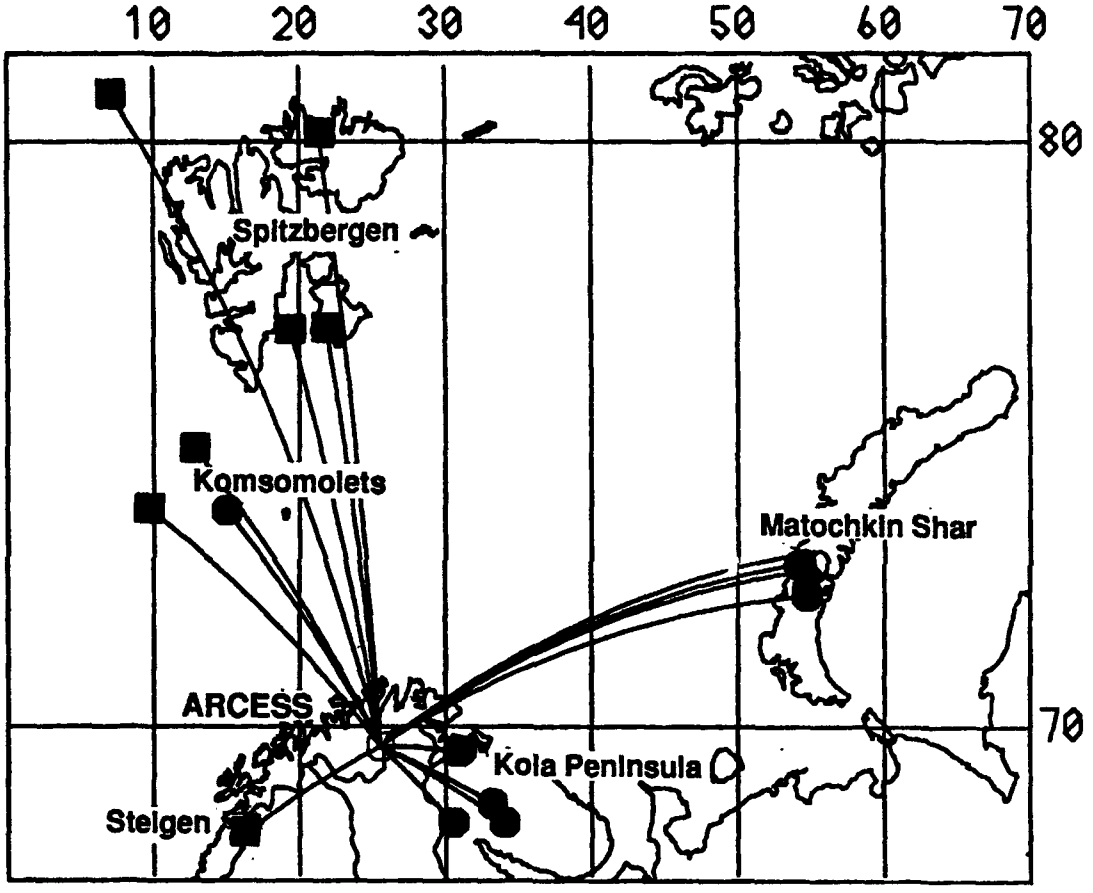

Figure 1: Map showing the locations of the ARCESS and Spitzbergen arrays and the reference events recorded at ARCESS used to characterize the 921231 event. The great circle paths between the 921231 event from the reference events to ARCESS are shown. Square and circle symbols indicate earthquake and explosion locations, respectively.

range from 200 to 300 km for the Kola events, 400 to 500 km for the Steigen earthquakes, and 900 to 1100 km for the Greenland Sea earthquakes and the Novaya Zemlya events. The Spitzbergen-Greenland Sea earthquakes occurred well east of the Mohns-Ridge midoceanic spreading center so that the seismic propagation paths to ARCESS should be similar to those from Novaya Zemlya to ARCESS.

The 921231 Novaya Zemlya event wrote excellent waveforms at ARCESS, although it was necessary to apply bandpass filters to reject the high noise levels. Figures 2, 3, and 4 compare the waveforms recorded on the ARB1sz channel of ARCESS for the 921231 event with selected historical events recorded on the same channel. In each plot, the waveforms have been bandpass-filtered with a recursive Butterworth filter in the 8 to 10 Hz band. (As we shall discuss later, this frequency band was the best for discrimination of the different source types in this region.) Strong signal-to-noise ratios were observed in all bands above 2 Hz, with the highest frequencies near 10 Hz for all events. Two large arrivals were identified as the *Pn* and *Sn* regional phases.

Figure 2 shows a comparison of three Kola Peninsula mine blasts with the 921231 event. The Kola blasts occurred much closer to the ARCESS array than the Novaya Zemlya event, as evidenced by the shorter time delay between *Pn* and *Sn* for these events. However, the presumed mine blasts have nearly the same amount of *Pn* and *Sn* energy in this 8 to 10 Hz band as is also observed for the 921231 event.

Figure 3 compares the three known Novaya Zemlya nuclear explosion tests, which have occurred since ARCESS was installed, with the 921231 event. Although both *Pn* and *Sn* phases are observed at ARCESS for these events, no direct *Lg* waves are observed. Presumably, *Lg* is blocked in its propagation across the Barents Sea from Novaya Zemlya to ARCESS, as discussed by Baumgardt (1991c). (Note: The energy in the coda of the *Sn* observed on the 921231 trace is probably an interfering local event.) This comparison shows that the *Sn* waves are not as strong relative to *Pn* for the nuclear explosions in the 8 to 10 Hz band as for the 921231 event.

Figure 4 compares the ARCESS traces from three Greenland Sea earthquakes with the 921231 event in the 8 to 10 Hz filter band. No *Lg* is observed from these earthquakes or from the Novaya Zemlya events, presumably because of the largely oceanic propagation path from the Greenland Sea region to ARCESS. However, the *Sn* waves from the Greenland Sea earthquakes are strong in the 8 to 10 Hz band. The 921231 event generates more *Pn* energy relative to *Sn* than do the earthquakes. This comparison is significant, because the earthquakes and Novaya Zemlya events are nearly the same distance from ARCESS, albeit on different azimuths. The paths are different, but they should have similar distance dependent effects.

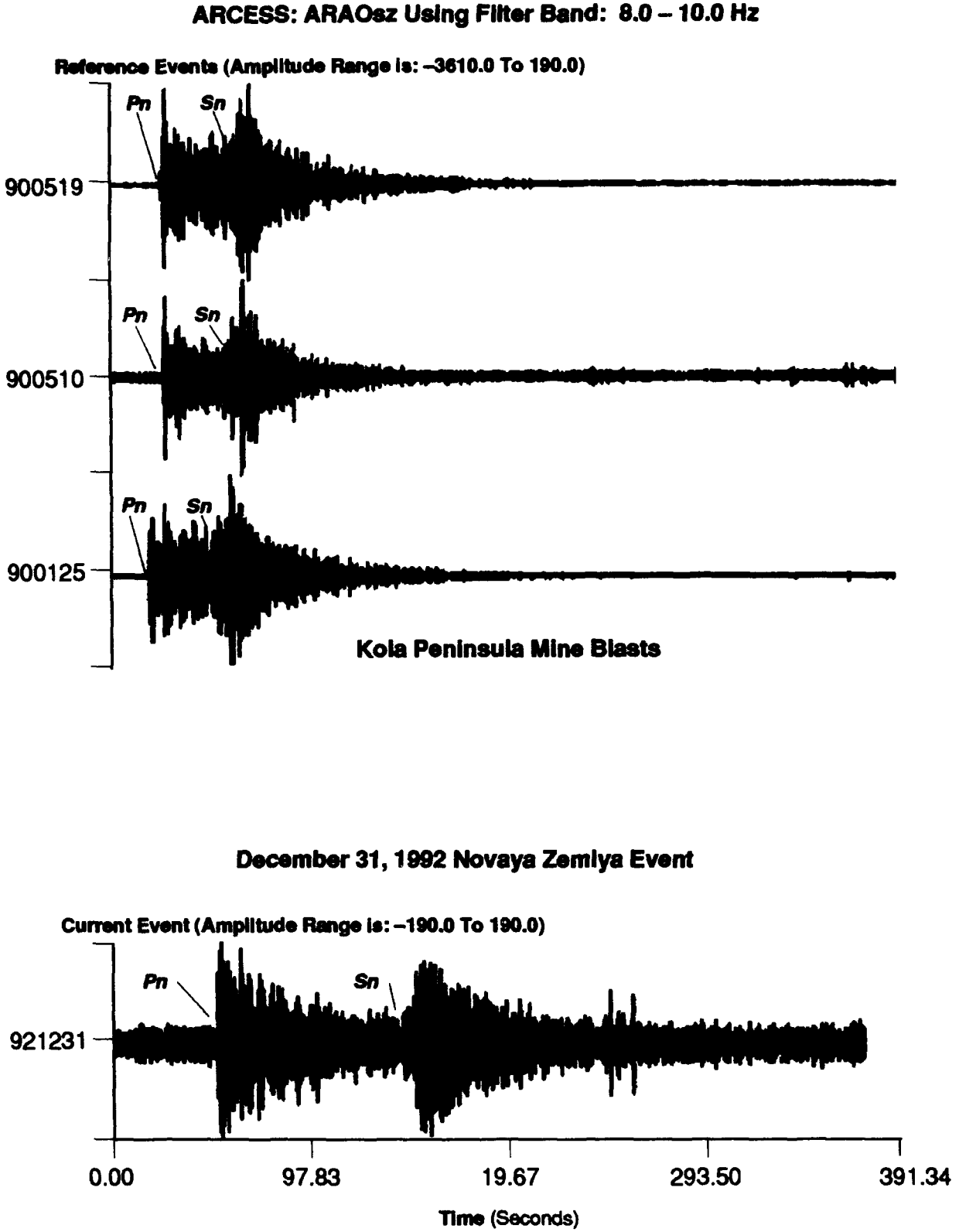

Figure 2: Comparison of waveforms from the 921231 event (bottom) and three Kola Peninsula mine blasts. All traces are bandpass filtered from 8 to 10 Hz.

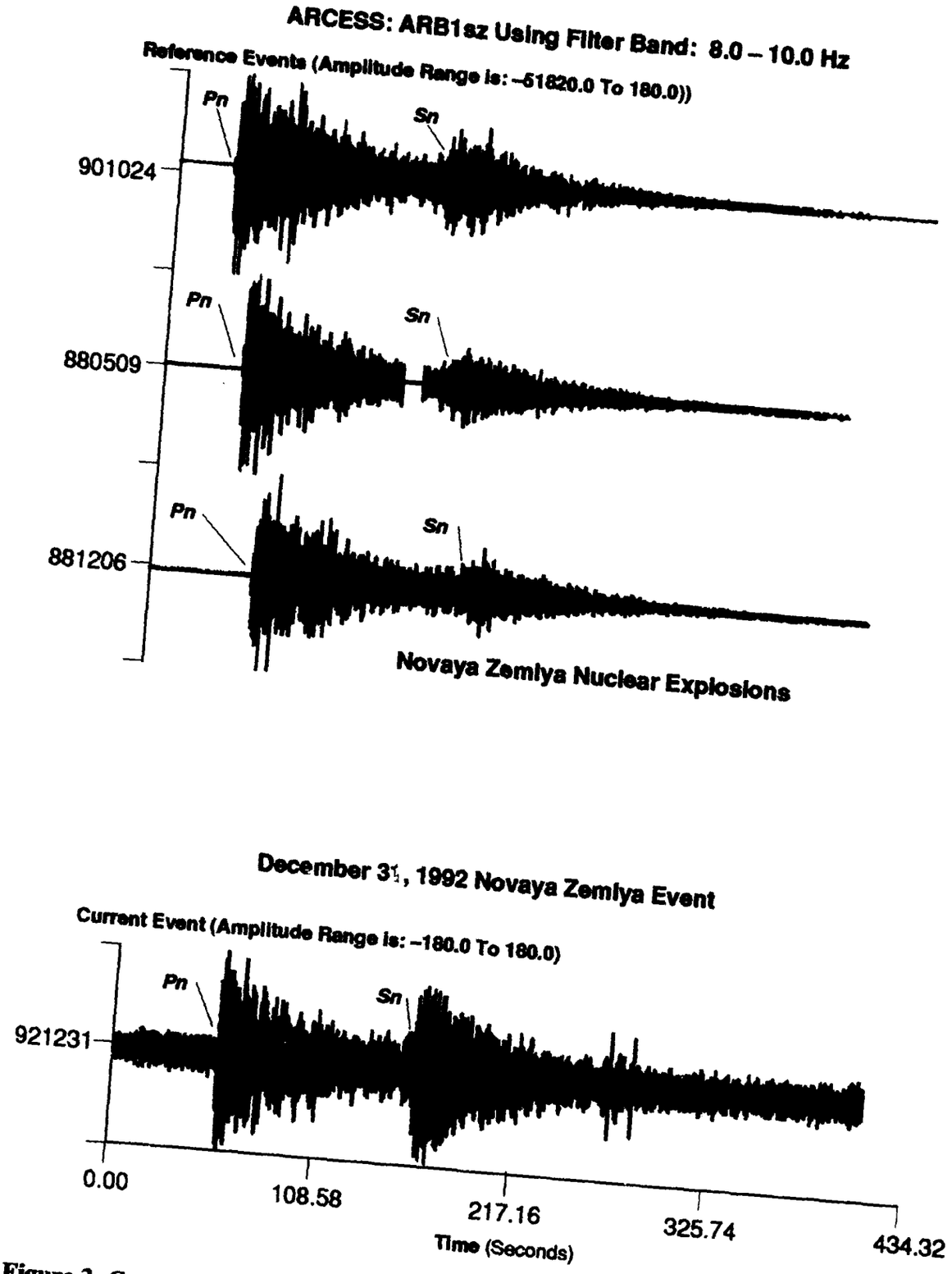

Figure 3: Comparison of waveforms from the 921231 event (bottom) and three Novaya Zemlya nuclear explosions. All traces are bandpass filtered from 8 to 10 Hz.

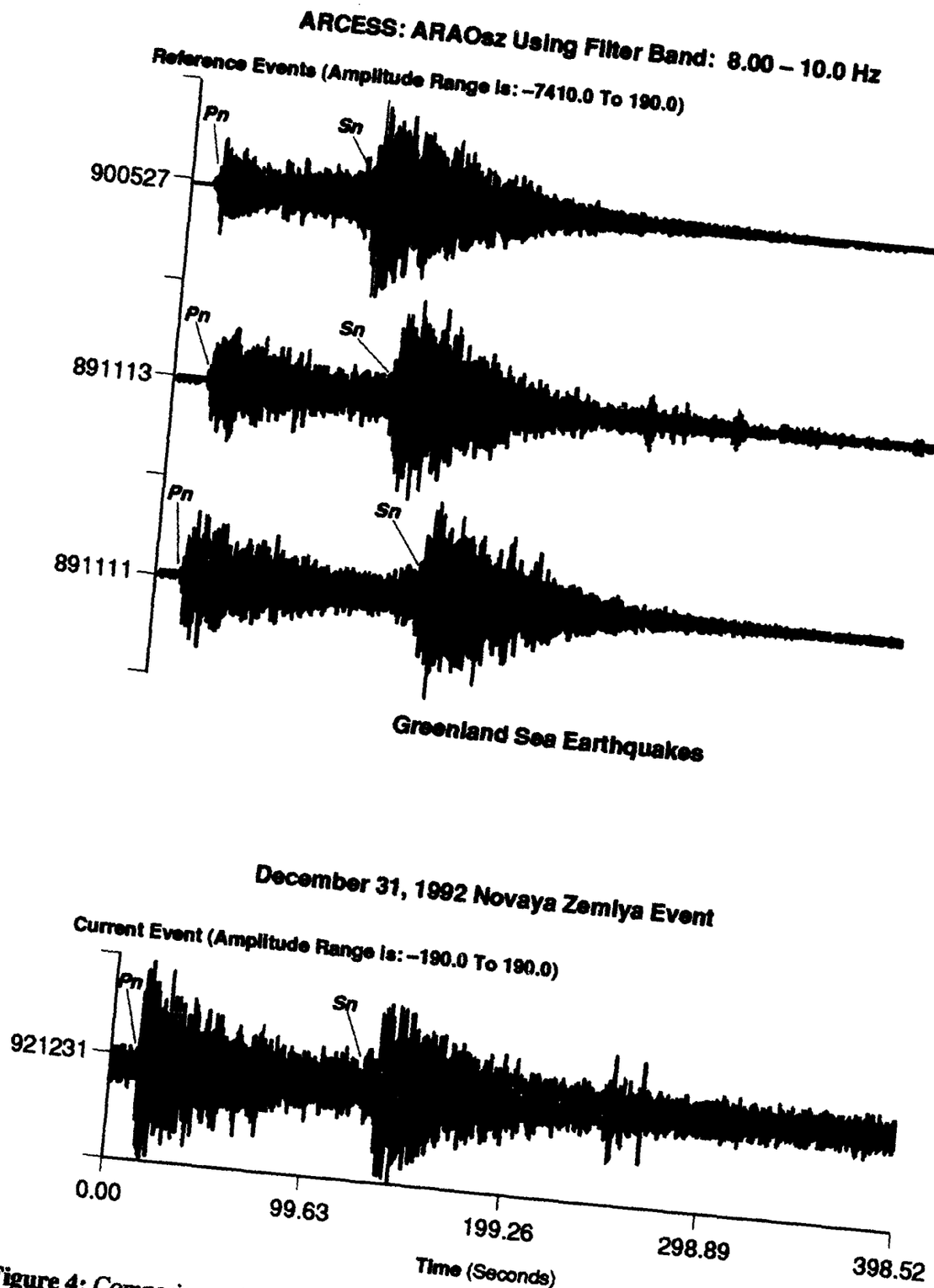

Figure 4: Comparison of waveforms from the 921231 event (bottom) and three earthquakes in the Greenland Sea near the mid Atlantic ridge. All traces are bandpass filtered from 8 to 10 Hz.

These three plots show that the 921231 event does not resemble the nuclear explosions. It most closely resembles the Kola blasts, but there may be significant propagation-path difference effects which must be considered in such a comparison.

Incoherent Beam Analysis at ARCESS

ISEIS feature processing relies extensively on incoherent beams computed on multiple-bandpass-filtered waveform data for regional-phase definition and feature extraction, as discussed by Baumgardt (1991a) and Baumgardt et al (1992). Incoherent beams in ISEIS are computed by first bandpass-filtering the trace in one of nine frequency bands ranging from 0.5 to 2.5 Hz on the low end to 8 to 16 Hz on the high end. Then, on the filtered traces, the average log-rms amplitudes in one second windows, shifted down the trace in one second increments, are computed on each vertical component array element and these log rms amplitudes are averaged across the array.

Figure 5 shows the log-rms incoherent beams in the 8 frequency bands computed for the ARCESS array. The 0.5 to 2.5 Hz beam has not been plotted because it is mostly noise. The beam windows begin about 40 seconds before the onset of *Pn* and extend well into the *Sn* coda. Each beam, corresponding to a different filter band, has been shifted up for viewing purposes. The *Pn* and *Sn* picks of the CSS seismic analyst are shown on top of the incoherent beams. Note that these picks were made by the analyst on the seismogram itself, probably on a coherent beam, and not on the incoherent beam plots in Figure 5. These plots show that both the *Pn* and *Sn* phases are evident in the 2.5 to 4.5 Hz band and up, although the highest signal-to-noise ratios can be found in the 8 to 10 Hz and 8 to 16 Hz bands. The *phase selections* used for RMS amplitude measurements and spectral analysis windows begin at the phase pick times and extend to a specified time, based on an assumed group velocity for each regional phase (8.1-7.8 km/sec for *Pn* and 4.5 to 4.0 km/sec for *Sn*).

Spectral Analysis

As discussed above, with reference to phase selection, ISEIS computes spectra for phase-selection windows defined on the incoherent beams. Each spectrum is computed by windowing the phase on each channel after a cosine taper, computing the FFT, smoothing with a Hanning window convolution in the frequency domain, and then averaging the spectra across all the array channels.

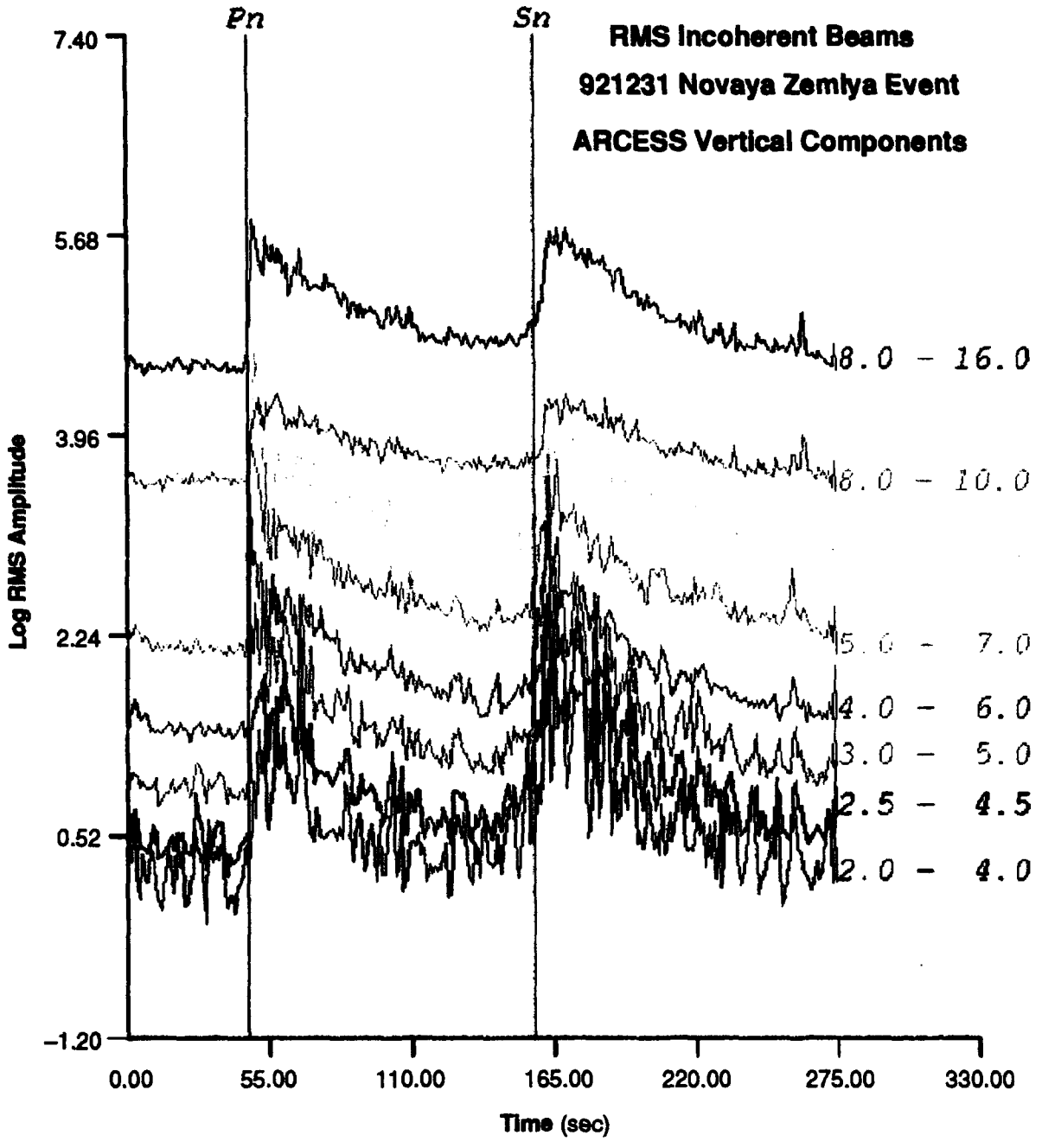

Figure 5: Plots of multifiltered log-rms incoherent beams recorded at ARCESS (ARA0). The *Pn* and *Sn* lines indicate the picks the analyst made on a coherent beam.

Figure 6a shows array-averaged *Pn* and *Sn* spectra for the 921231 event, compared to the noise background to *Pn*. The instrument response for ARCESS has been deconvolved from both the signal and noise spectrum. This plot shows that the signals are above the noise levels above about 2-3 Hz. Both spectra are generally simple, showing a nearly linear drop-off with frequency. There is no evidence of time-independent spectral modulations, which were observed by Baumgardt and Ziegler (1988) for ripple-fired explosions, so the event appears to be a single event.

Figures 6b and 6c, respectively, compare *Pn* and *Sn* zoomed spectra for the 921231 event, plotted yellow, with the same-phase spectra for the Novaya Zemlya explosions, plotted red, and one of the Greenland Sea earthquakes, plotted green. The expected difference in absolute level is evident since the nuclear explosions are at least three orders of magnitude larger than the 921231 event. Also, the high-frequency *Pn* and *Sn* spectral slopes of this event are less than those of the nuclear explosions but comparable to those of the earthquake. These slope differences are probably related to spectral scaling differences caused by the large differences in magnitude. These spectra show that the Novaya Zemlya nuclear explosions and the earthquake are also simple, with no indication of strong spectral modulations, as expected for single sources.

Pn/Sn Amplitude Ratio Features

The amplitude ratio between *P* and *S* type phases has been found to be a very promising discriminant in a number of studies (e.g., Bennett et al, 1989, 1991; Baumgardt and Young, 1990). It is based on an old idea that earthquakes should generate more shear wave energy relative to compressional wave energy and thus, earthquakes should have smaller *P/S* type amplitude ratios than explosions. Recent research has shown that this discriminant seems to work better at high frequency than at low frequency. Baumgardt (1992) and Baumgardt et al (1992) studied this discriminant extensively using ISEIS and data from the Scandinavian arrays and concluded that earthquakes and mine blasts can be discriminated using high-frequency *Pn/Sn* and *Pn/Lg* ratios.

In this study, we compare amplitude ratios of the 921231 event with the same measurements for many mine blasts, earthquakes, and the three nuclear explosions recorded at ARCESS. For Novaya Zemlya events, we must rely entirely on the *Pn/Sn* ratio since virtually no *Lg* energy is recorded at ARCESS (Baumgardt, 1990, 1991).

ISEIS uses phase selection windows to measure features on each phase, where the window starts at the IMS phase-pick times shown in Figure 5. The average and maximum rms amplitudes in each window are measured and stored in the database along with the time limits of the

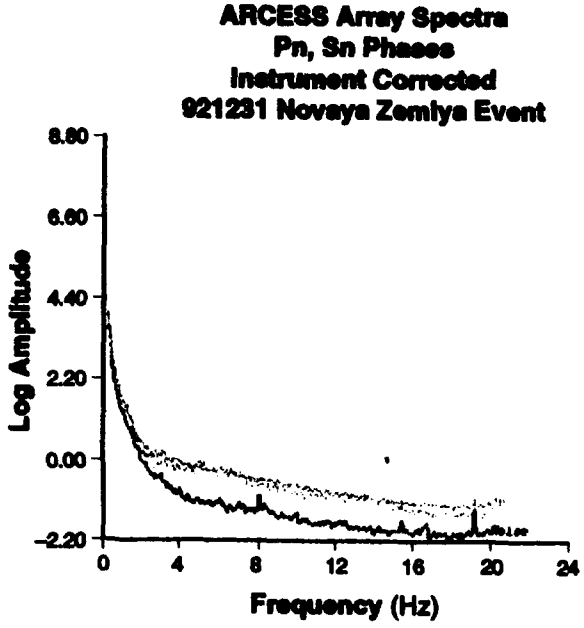

Figure 6a: Array-averaged signal and noise spectra for the 921231 event recorded at ARCESS. Spectra have had ARCESS instrument response removed.

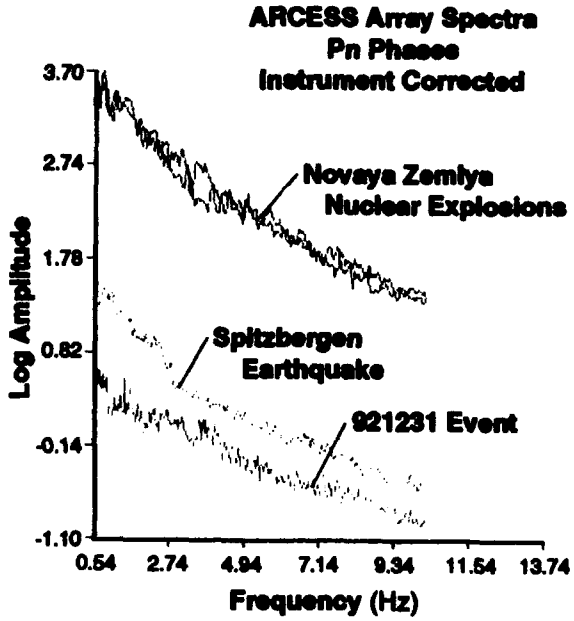

Figure 6b: Comparison of the instrument-corrected spectra for *Pn* for the Novaya Zemlya nuclear explosions, a Spitzbergen earthquake, and the 921231 event.

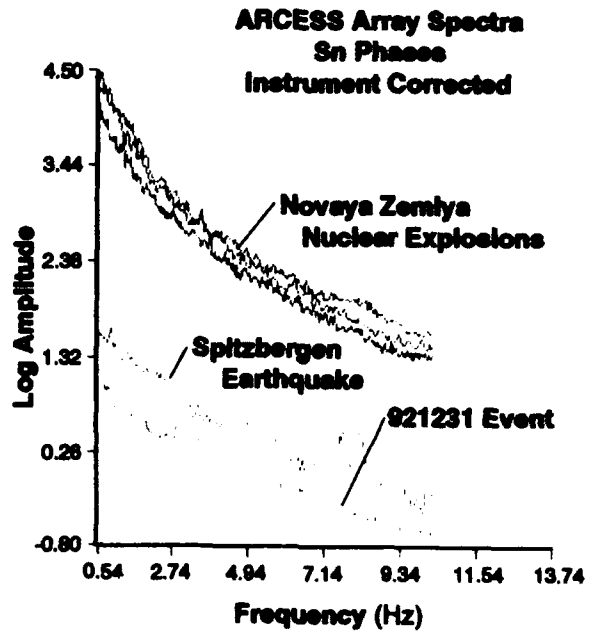

Figure 6c: Comparison of the instrument-corrected spectra for *Sn* for the Novaya Zemlya nuclear explosions, a Spitzbergen earthquake, and the 921231 event.

window. Array-averaged spectra are then computed for each phase, which we will discuss in the next section. For amplitude ratios, we have found the maximum rms amplitude in each phase window to be the best discriminant, rather than the average rms amplitude, because the latter depends critically on the window length which may not always be consistently set.

For all comparative feature analysis, reference events are assigned to *reference regions*, which are geographic regions whose boundaries are set by the average location of the events assigned to the regions. So, for example, the Novaya Zemlya reference region is an area about 50 km in extent, which encloses the IMS locations of the three nuclear explosions which have occurred there since the ARCESS array was installed. The mine sites include the numerous Kola Peninsula mine sites (K1, K3, K4, K5, K8, and K9), identified in the Helsinki bulletin, and one additional one called Kola Zapelyarnyi, the location of two known test charges. Three earthquake regions include the Spitzbergen and Svarlbard regions, defined by the Greenland Sea events, and the Steigen swarm region. Also, the one presumed underwater implosion event, which is believed to be the Komsomolets submarine disaster of 1989 (Baumgardt, 1991b), has been included since it occurred in the same region as the Spitzbergen and Svarlbard earthquakes. This event is assigned to the Svarlbard region. In this study, these regions include a total of about 96 events.

Figure 7a shows a scatter plot versus frequency of the *Pn/Sn* ratios computed from the maximum rms amplitudes in each phase-selection window on each incoherent beam. The frequency ranges printed on the abscissa correspond to the frequency band of each filter. Because there are so many points in the plot, only the average for each event type (earthquake, quarry or mine blast, marine explosion, and nuclear explosion) are plotted as four different symbols, shown in the legend in the upper left part of the plot. Each point has an error bar which is the standard deviation of values for each event type. The triangle with the asterisks superimposed are the computed values for the current event of interest, the 921231 event.

Figure 7a shows that the separation of nuclear explosions from other event types is greatest at high frequencies, beginning at about the 4 to 6 Hz band. Below this frequency band, most of the event types have overlapping error bars. At high frequencies, the event types separate with the nuclear explosions having the highest values, the presumed Komsomolets marine implosion and mine blasts having the next highest, and the earthquakes having the lowest values for *Pn/Sn* ratios. This agrees with the concept that earthquakes generate more *Sn* energy relative to *Pn* energy than explosions and therefore have lower *Pn/Sn* ratios. The nuclear explosions have the highest ratios at high frequencies, even larger than the mine explosions. The best separation is in the 8 to 10 Hz band. The 921231 event falls almost exactly on the average value for all the mine blasts, which is

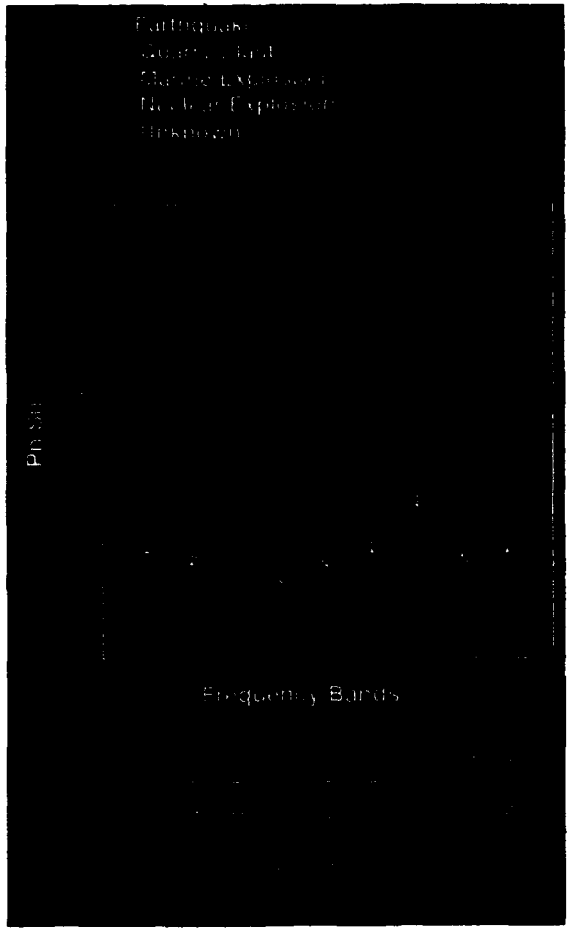

Figure 7a: Plot of the average *Pn/Sn* amplitude ratios measured in 9 frequency bands at ARCESS, using maximum rms measurements, for the reference events shown in Figure 1. The triangle with the asterisks through it indicates the values of the 921231 event. Error bars shows the standard deviations in the values for all events of a given source type.

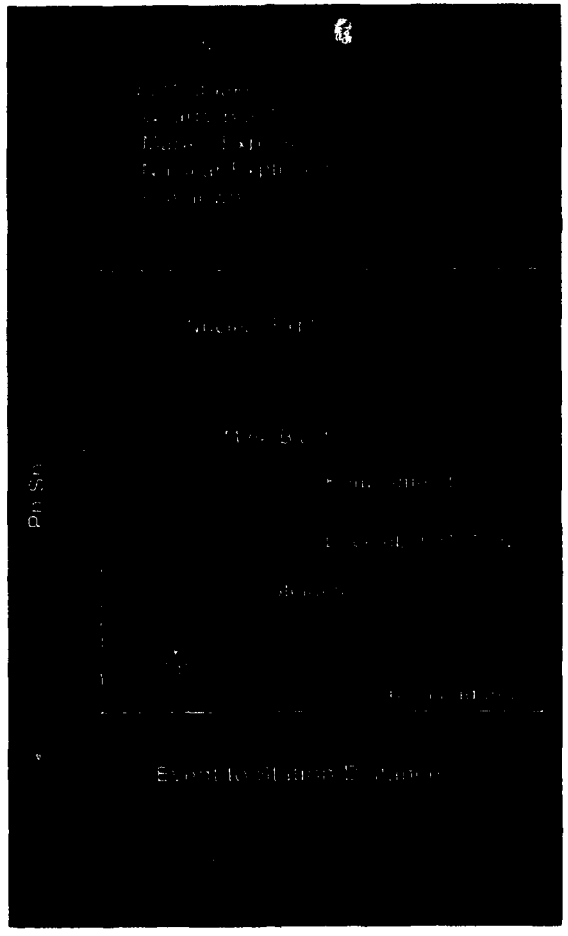

Figure 7b: Scatter plot showing the values of the *Pn/Sn* amplitude ratios in the 8-to-10 Hz band as a function of epicentral distance from ARCESS for all the event types and the 921231 event. Legend in the upper left gives identifies the symbols used in the plot.

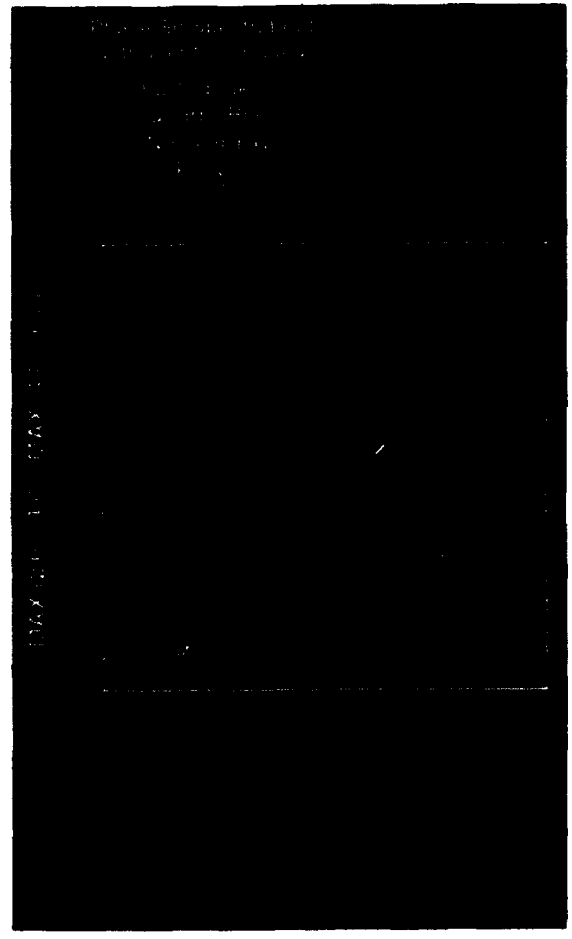

Figure 7c: Scatter plot of *Sn* spectral ratios (2-4 Hz/4-6 Hz) measured at ARCESS as a function of epicentral distance. The 921231 event is the asterisks/triangle overstrike symbol.

well below the ratios observed for the nuclear explosions. However, the ratios only slightly exceed those observed for the earthquakes used in this study.

The problem with comparing amplitude ratios for event types like this is that there may be significant propagation-path differences which could affect these ratios. To examine these more closely, we plot in Figure 7b the *Pn/Sn* amplitude ratios in the 8 to 10 Hz band, which is the most discriminatory band in Figure 7a, as a function of epicentral distance. This plot shows the separation of the nuclear explosions and all other events in the 8 to 10 Hz band. Note, however, that on this plot, the mine explosions and earthquakes are much closer together. Baumgardt (1992) and Baumgardt et al (1992) have studied in detail the separation of mine blasts and earthquakes in this region and have pointed out that mine blasts have much greater variance in this ratio than earthquakes. This was explained as being caused by differences in shear excitation due to rock spalling and fracturing effects in the blasts. The tight clustering of the Steigen earthquakes at around 440 km was noted by Baumgardt et al (1992) and may be accounted for by the fact that these earthquakes occurred as a swarm in the same region and thus, may have had very similar source mechanisms. However, the five Greenland Sea earthquakes, between 900 and 1400 km, have very similar ratios. The reason for this apparent stability of the *Pn/Sn* ratio at high frequency for earthquakes and its large variance for mine explosions is not yet clear but has important implications for interpreting the separability of classes of event types based on this feature.

This plot shows that the 921231 event in question falls in the middle of the range for mine blasts but just barely above the values of the earthquakes in the same distance range as the Novaya Zemlya event. However, the mine blasts are at closer distances (about 400 km) than the Greenland Sea and Novaya Zemlya events (about 900 to 1100 km). So, we cannot rule out the possibility of there being propagation-path differences which might affect these ratios.

From Figures 7a and 7b, we conclude that the 921231 event was probably not a nuclear explosion. However, identifying the event as a conventional blast is still problematic because the ratio is not much higher than those observed for earthquakes in the same distance range, although the ratio is comparable to those of mine blasts at shorter distance ranges and significantly higher than earthquakes in that shorter distance range.

Sn Spectral Ratio Features

Murphy and Bennett (1982), Bennett and Murphy (1986), and Taylor et al (1988, 1989) found that the ratio of low-frequency to high-frequency spectral energy for *Lg* discriminated nuclear explosions and earthquakes in western U.S., with the earthquakes having lower spectral-ra-

tios (higher frequencies) than explosions. Baumgardt et al (1992) found that this discriminant separated blasts and earthquakes in Germany but not in Scandinavia. Taylor and Denny (1991) presented a theoretical argument that *Lg* spectral-ratio discriminant may work if earthquakes and explosions occur at different depths and the explosions occur in a shallow, low-Q medium. Baumgardt et al (1992) have suggested that such conditions may not apply to Scandinavian mine blasts and earthquakes and thus, we would not expect the spectral-ratio discriminant to work in Scandinavia.

A scatter plot of spectral ratios for *Sn* from the 921231 event and other events are shown in Figure 7c. These ratios were computed by taking the maximum spectral densities in the *Sn* spectra in the 2 to 4 Hz and 4 to 8 Hz bands, and ratioing these values. As in the previous plots, the 921231 event is indicated by the triangle and asterisks overstrike symbol. These plots show that the nuclear explosions have higher spectral ratios in *Sn* than for the other event types. The 921231 event has a slightly higher ratio than the earthquakes at the same distance. However, looking at the points in the 200 to 450 km distance range, there appears to be significant overlap in the points for chemical blasts and earthquakes.

The apparent separation in spectral ratio between the nuclear events and all the others may be more due to magnitude differences in the events than in any intrinsic source differences. Looking at the spectra in Figure 6c, it can be seen that there is an enhancement of the 921231 spectrum in the low-frequency band, below about 2.74 Hz. However, this enhancement is caused by noise contamination at low frequency, which can be seen clearly in the comparison of the signal and noise spectra in Figure 6a. This low-frequency enhancement causes the lower spectral ratios for the smaller mine blasts, earthquakes, and the 921231 event compared with the nuclear explosions. These results are consistent with the apparent magnitude scaling in the spectra, as shown in Figure 6c. Thus, we conclude that there appears to be no discrimination of source types in this region based on spectral ratio of *Sn* or any other phase.

DISCRIMINATION ANALYSIS OF THE 860801 NOVAYA ZEMLYA EARTHQUAKE AT NORESS

As mentioned earlier, the small size of the 921231 event precluded our analyzing it at NORESS as we did at ARCESS. Baumgardt (1993) has analyzed the NORESS waveforms from the 921231 event and found that only a single *P*, but no shear waves, were detected. Since we cannot actually study the 921231 event at NORESS for discrimination purposes, we consider instead an earlier, larger event which was recorded at NORESS on August 1, 1986 (860801) and located near the test sites at Novaya Zemlya. At the time this event occurred, only the NORESS ar-

ray was operating. However, we do have the NORESS recordings of the Novaya Zemlya nuclear explosions which can be compared with the 860801 event at NORESS in the same way that we compared the same nuclear explosions with the 921231 event at ARCESS.

The 860801 event was studied in detail by Ryall et al (1987), who considered many signal characteristics of the event recorded at NORESS. Moreover, they relocated the event, using teleseismic data from other stations, to be south of the test site but offshore to the east. Based on an *Ms-mb* analysis at the Hagfors array, the event plotted in between earthquakes and explosions on the *Ms* vs. *mb* plot, but slightly closer to the earthquake population. Subsequent *Ms* vs. *mb* analysis of this event with other stations has placed this event more in the earthquake category (A. Ryall, personal reference). Finally, the event magnitude was about 4.6, which is much too large to be a conventional chemical explosion. Thus, the event appears to have been an earthquake.

Earthquakes are rare at Novaya Zemlya. However, they have been detected by the Kola Scientific Center of the former Soviet Union, now Russia, including this event (W. Leith, personal reference). These earthquakes in the region may result from stresses associated with uplift caused by glacial unloading.

Ryall et al (1987) did not do a *Pn/Sn* analysis of this event and compare it with NORESS recordings of Novaya Zemlya explosions, since these events had not occurred yet. In this section, we reconsider this event, using the same *Pn/Sn* analysis which was done for the ARCESS recording of the 921231 event and compare it to historical events recorded at NORESS.

NORESS Waveforms

Figure 8 shows the locations of the Novaya Zemlya nuclear explosion and several mine blast and earthquake sites along with great circle seismic propagation paths for the events which have been studied at NORESS.

In Figure 9, the NRB1sz channels for the 860801 event and the three Novaya Zemlya explosions are plotted. Note that these traces are broadband with no filtering.

Baumgardt (1990, 1991c) has studied Novaya Zemlya explosions recorded at NORESS and NORSAR and has shown that, like at ARCESS, no direct *Lg* was recorded at NORESS. However, an "early *Lg*" was observed which Baumgardt (1990, 1991c) has explained as being due to an *Sn* to *Lg* mode conversion at the Barents Sea-Kola coastline interface. Direct *Lg* itself seems to have been blocked by the Barents sedimentary basin. The 860801 event shows the same lack of direct *Lg* but the presence of an early *Lg*.

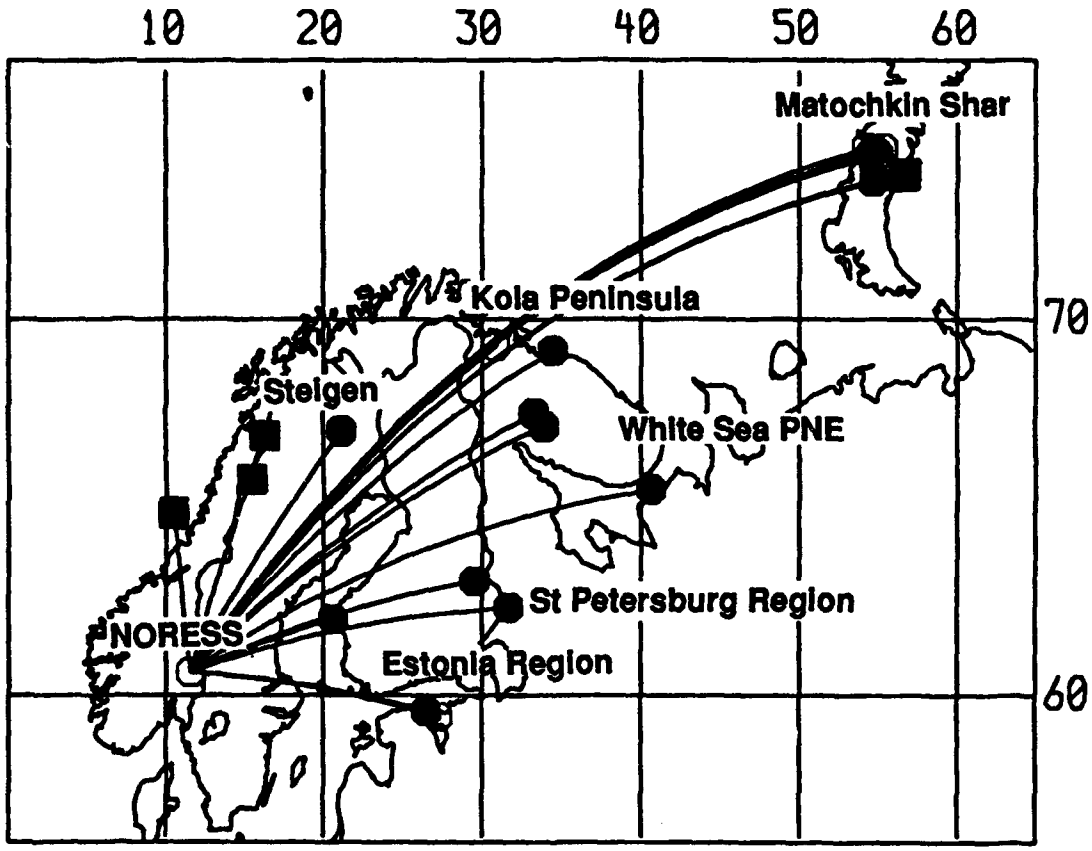

Figure 8: Map showing the locations of the NORESS array and the reference events recorded at NORESS used to characterize the 860801 event. The great circle paths between the Novaya Zemlya events and other reference events to NORESS are shown. Square and circle symbols indicate earthquake and explosion locations, respectively.

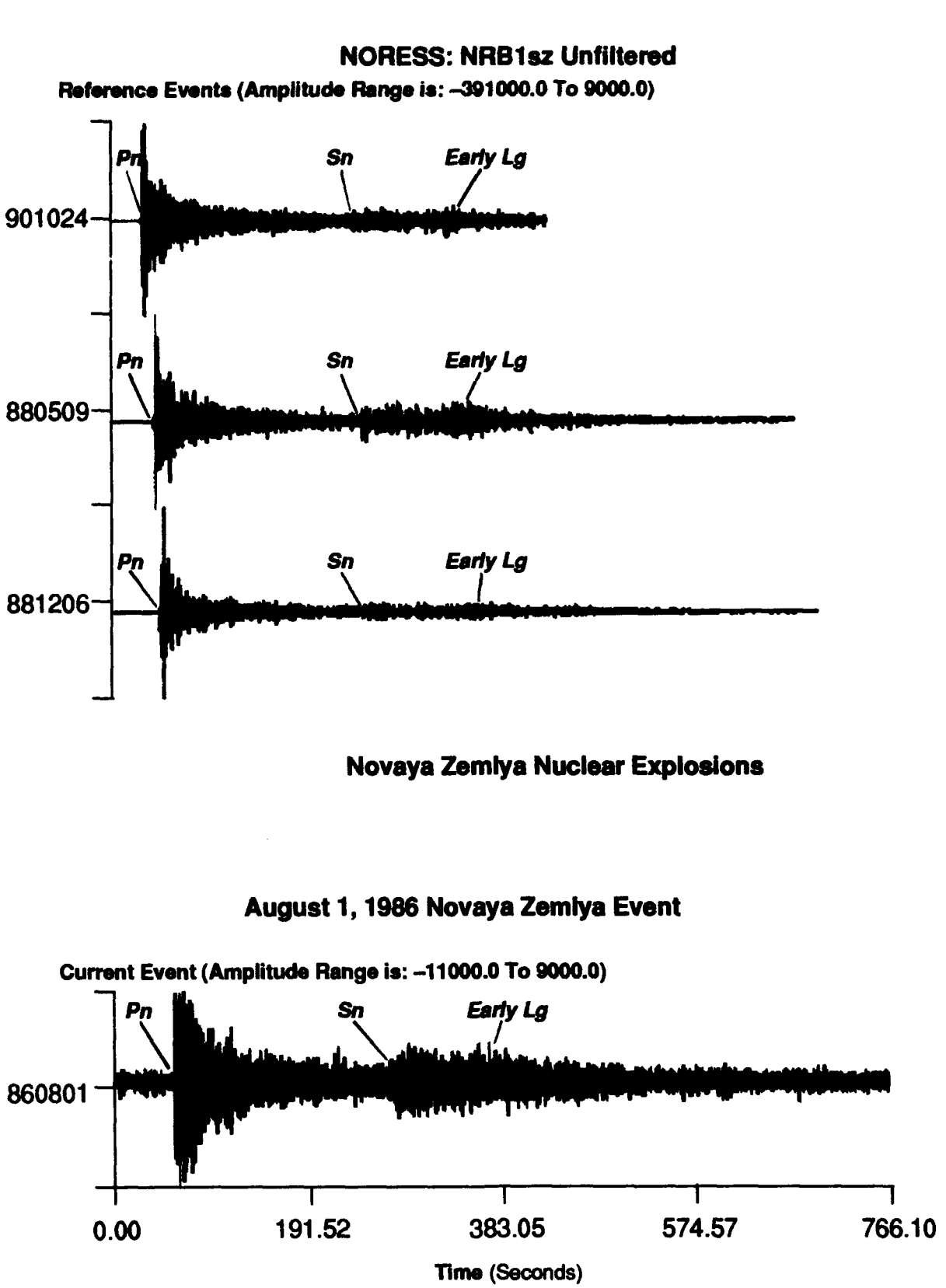

Figure 9: Comparison of unfiltered waveforms recorded on the NORESS NRB1sz channel from the 860801 Novaya Zemlya event (bottom) and the three Novaya Zemlya nuclear explosions.

The 860801 event differs from the nuclear explosions in that it has larger shear waves. To consider if this can be expected for blasts, we compare the event with three other event types in Figure 10. These events, including the 860801 event, have all been filtered in the 2 to 6 Hz band. The top trace is an earthquake in central Norway, the second trace is a small (Ml = 2.8) Kola Peninsula explosion, and the third trace is a presumed peaceful nuclear explosion (PNE) which occurred near the White Sea in northern Russia. The 860801 event looks most like the PNE, both in terms of the impulsiveness and strength of the P relative to the coda and the strength of the shear waves are comparable. In Baumgardt's (1991c) study of this event, he showed that the Lg was not blocked on the White Sea PNE-to-NORESS path since it does not cross any sedimentary basins. Again, based on a subjective comparison of the plots in Figure 8, the 860801 event most resembles a PNE nuclear explosion. However, it should be noted that the epicentral distances of the events in Figure 10 are shorter than that from Novaya Zemlya to NORESS, and the paths all differ in that they do not cross the Barents Basin.

Amplitude Ratio Features

The multispectral incoherent beam analysis and amplitude measurements, described above for ARCESS, were also applied to the NORESS recordings of the 860801 event and other reference events. The reference events include the Novaya Zemlya nuclear explosions, including one which occurred in 1984 prior to the installation of ARCESS (Baumgardt, 1990), the White Sea PNE, mine blasts on the Kola Peninsula which were recorded at NORESS, mine explosions in the St. Petersburg and Estonia regions, and earthquakes in central Sweden, central Norway, and the Steigen region in northern Norway. (Note: In all the analyses, we interpret the first arrival P as Pn, even in the distance range where Pn is not the first arrival. However, in most of these cases, the measurement windows are made long enough so that they include the Pn in the coda. However, for the case of most events beyond about 1000 km, Pn actually refers to direct P.)

Figure 11a shows a plot of Pn/Sn ratios as a function of the filter frequency band. The 860801 event is again plotted as a triangle/asterisks overstrike symbol. This plot shows that the Pn/Sn ratios are lower than those of nuclear explosions but above those for earthquakes and mine blasts. Note that the nuclear explosions do not include the PNE.

The greatest separation of the 860801 event and the nuclear explosions is in the 4 to 6 Hz band. Figure 11b shows a plot of the ratio in this band as a function of distance. This plot shows that the Pn/Sn ratio for the 860801 event is significantly less than the Novaya Zemlya explosions. However, it is comparable to that of the White Sea PNE at 1540 km distance, this in spite of the fact that the PNE was located 800 km closer to NORESS than the Novaya Zemlya. Mine ex-

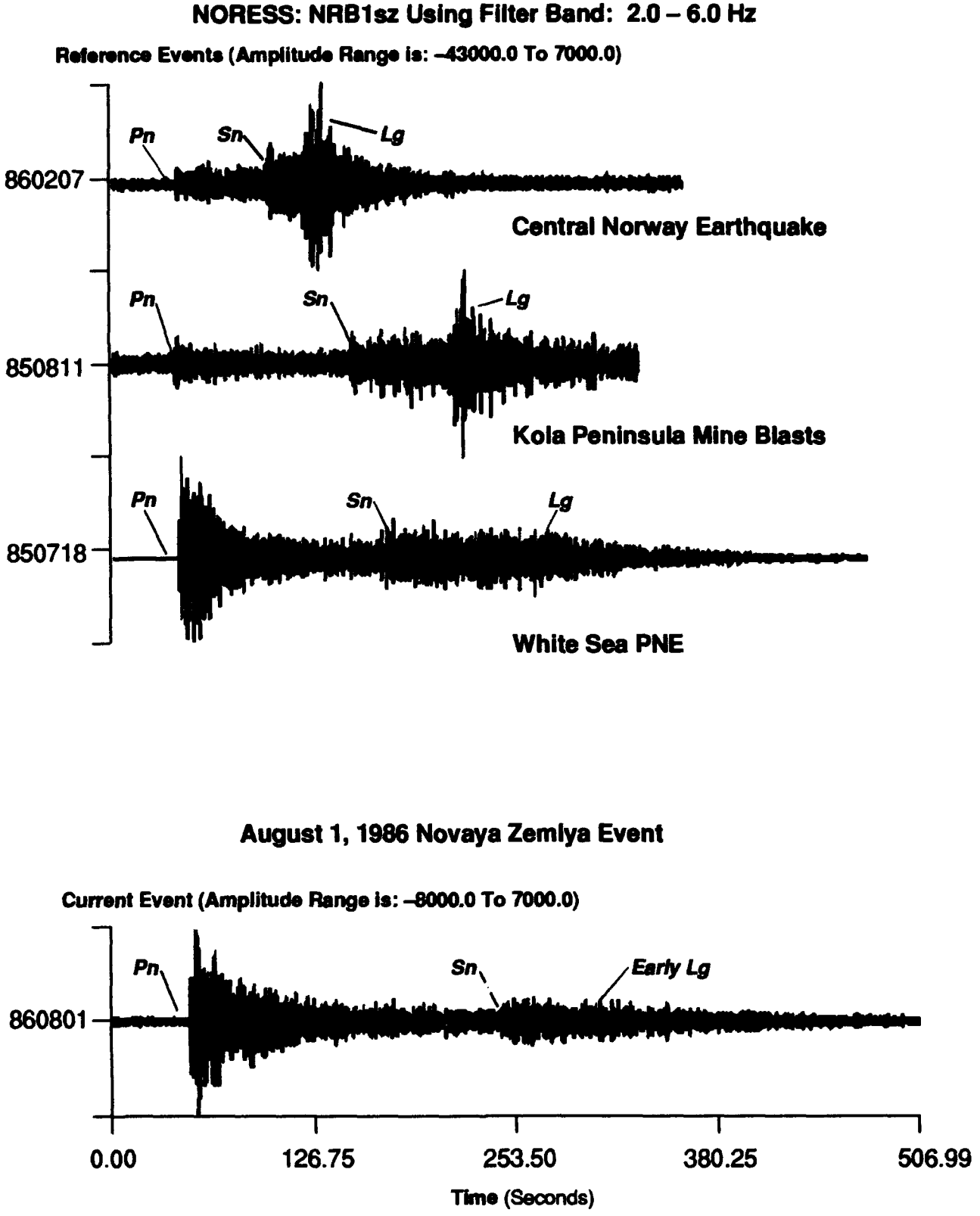

Figure 10: Comparison of 2 - 6 Hz filtered waveforms recorded at the NORESS NRB1sz channel from the 860801 Novaya Zemlya event (bottom) with three reference events.

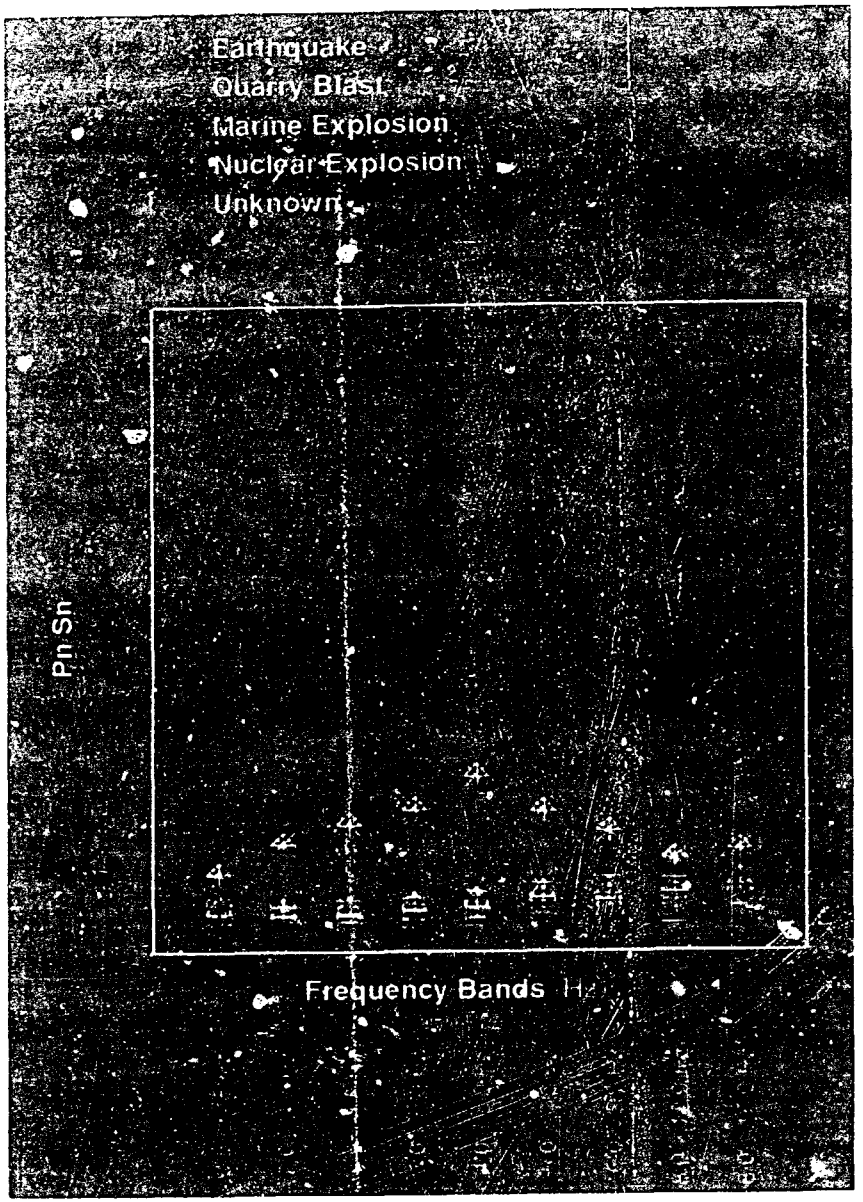

Figure 11a: Plot of the average *Pn/Sn* amplitude ratios measured at NORESS, using maximum rms measurements, for the reference events shown in Figure 8. The triangle with the asterisks through it indicates the values of the 860801 event. Error bars show the standard deviations in the values for all events of a given source type.

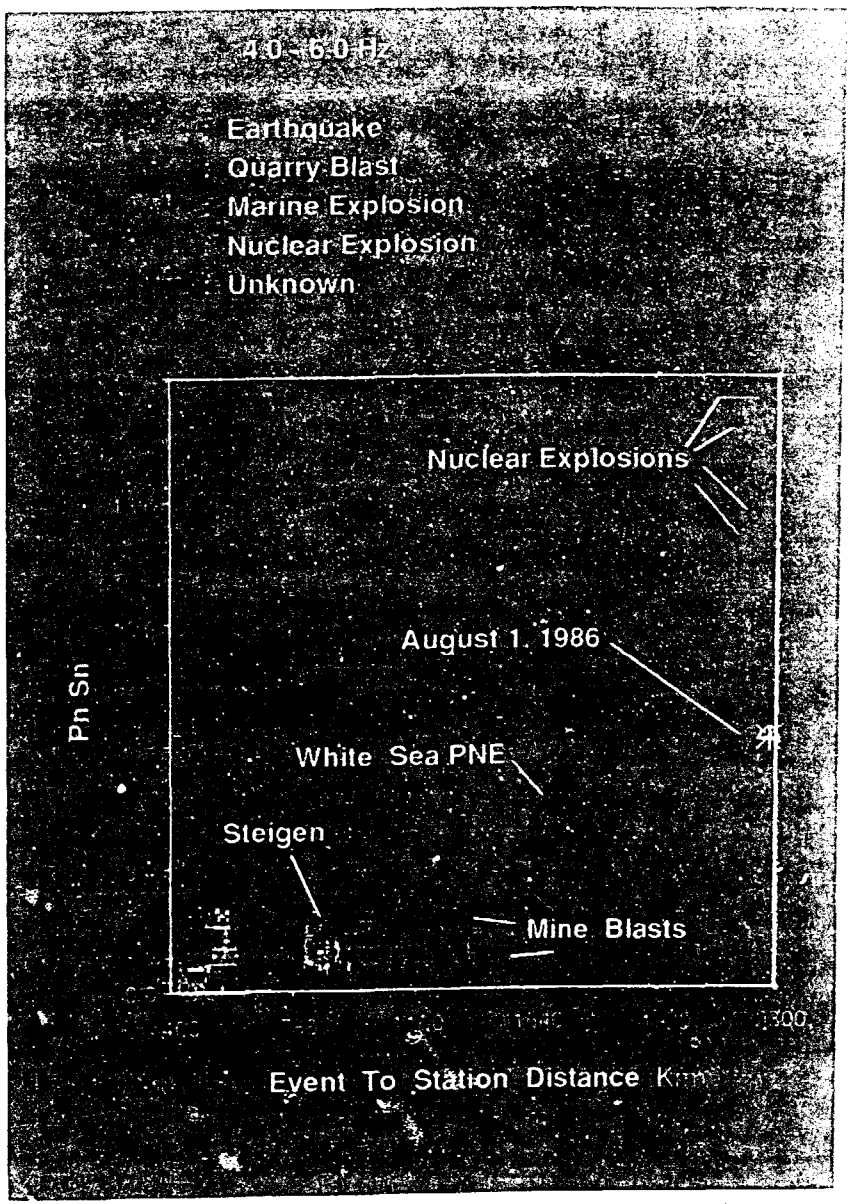

Figure 11b: Scatter plot showing the values of the *Pn/Sn* amplitude ratios in the 4-to-6 Hz band as a function of epicentral distance from NORESS for all the event types and the 860801 event. Legend in the upper left identifies the symbols used in the plot.

plosions have smaller ratios than any of these events and earthquakes at short distances have even smaller ratios, usually less than one.

The problem with these comparisons is the lack of any earthquake data points in the distance range of 1000 to 2300 km. Thus, although the 860801 looks like mine blasts in this distance range, we do not know for sure what an earthquake would look like in this distance range. Second, there is a great gap in observations of any kind in the distance range of 1540 km to 2300 km. We know that *Lg* waves from Novaya Zemlya are blocked by the Barents Sea sedimentary basin in this distance range. However, we are uncertain about what happens to *Sn* waves in this region. Perhaps they are partially blocked in the Barents Sea basin, which may explain the large *Pn/Sn* ratios for the Novaya Zemlya explosions. However, we might also expect *Pn* to be blocked as well, which might stabilize the *Pn/Sn* ratio. To check this, however, data from a known earthquake whose *Sn* waves cross the basin need to be studied.

Spectral Characteristics

Finally, we discuss the spectral characteristics of some of these events. Figure 12a shows the *Pn*, *Sn*, and noise spectra from the 860801 event. These spectra have been corrected for the NORESS instrument response. They show that the signal is quite limited in bandwidth, with the signal disappearing into the noise at about 9 Hz. Furthermore, the spectra are quite simple and, with the exception of some detail in the low-frequency part of the *Pn* spectrum, there are no spectral modulations which may indicate ripple fire or multiple events. The spectra of the Novaya Zemlya nuclear explosions look the same as this event in terms of bandwidth and lack of spectral modulations.

Figure 12b shows a plot of the spectra for the *Pn*, *Sn*, and *Lg* phase from the White Sea PNE. In contrast to all the Novaya Zemlya explosions, this explosion does exhibit spectral modulations in the low-frequency band which appear in all the spectra. Note that the spectral modulations are strongest at low frequency and die out above about 4.48 Hz. Cepstral analysis of these modulations produces a peak at about 0.9 seconds, indicating that these modulations are consistent with a double event delayed in time by about 0.9 seconds. The fact that the modulations do not extend to high frequency, in spite of the fact that the bandwidth for these phases extends beyond 10 Hz, may indicate that these modulations are produced by two shots, a large one and a small one. Because the large shot may have less high-frequency content than the small one, the signals may not correlate beyond a high-frequency limit.

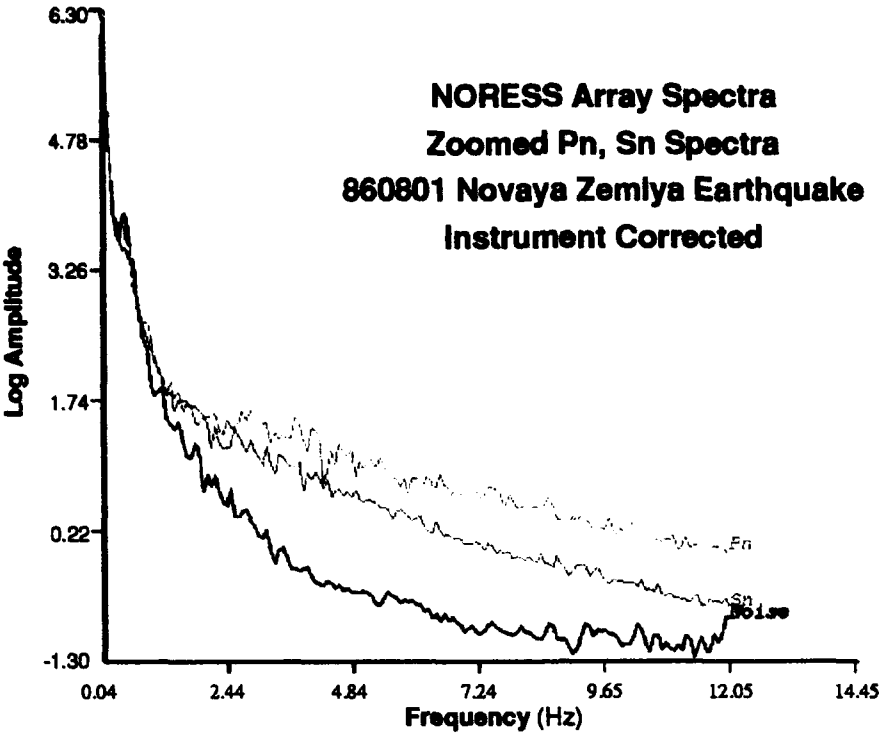

Figure 12a: Array-averaged spectra for signal and noise at NORESS for the 860801 Novaya Zemlya event. Each spectrum has been corrected for the NORESS instrument response.

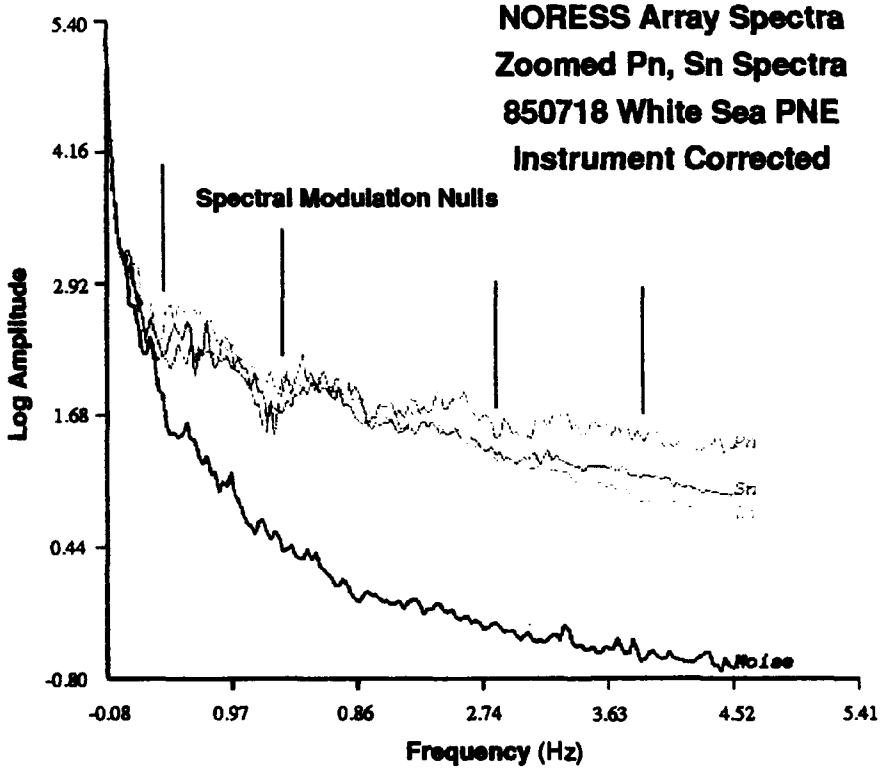

Figure 12b: Instrument-corrected signal and noise spectra for the White Sea PNE recorded at NORESS. These spectra show spectral scalloping in both *Pn*, *Sn*, and *Lg* but not in the noise, indicating that there are two shots with a delay time of about 1 second. The arrows indicate the troughs of the scalloping.

Thus, like the 921231 event, the 860801 was a single event, like the Novaya Zemlya explosions. However, as we have seen in the case of the White Sea event and for other PNEs studied by Baumgardt and Ziegler(1988), many Russian PNES have time-independent spectral modulations indicative of two or more delayed shots. Moreover, it would have been possible to detect at NORESS time-independent spectral modulations caused by multiple sources, had they occurred for the 860801 event, at a distance of 21 degrees, because Baumgardt and Ziegler (1988) observed such effects in PNEs at even greater distances from NORESS and NORSAR.

WERE THE 921231 EVENT AND THE 860801 NOVAYA ZEMLYA EARTHQUAKE SIMILAR?

We now address the following question: Had the 921231 event been large enough so that *Pn/Sn* ratios could be observed at NORESS, would they have been the same as the 860801 event? An affirmative answer to this question would argue strongly that the 921231 event was an earthquake, assuming that the 860801 event was an earthquake. To answer this question, we statistically analyze the *Pn/Sn* ratios of the 921231 and 860801 events relative to the same nuclear explosions which were recorded at both arrays.

The plot of *Pn/Sn* ratios against distance in Figure 11b shows a strong distance dependence in the ratio, caused by differences in attenuation of the *Pn* and *Sn* phases over large distance. The *Sn* phase has stronger attenuation than *Pn*, causing the *Pn/Sn* ratio to decrease exponentially with distance. Thus, to compare the *Pn/Sn* ratios recorded at the ARCESS and NORESS arrays from Novaya Zemlya events, this differential attenuation effect needs to be taken into account.

The distance dependence of attenuation is usually expressed as follows:

$$A_{Pn} = A_{op} e^{-\pi \Delta t_P^*}$$

and

$$A_{Sn} = A_{os} e^{-\pi \Delta t_S^*} \quad ,$$

where A_{Pn} and A_{Sn} are the measured amplitudes of the *Pn* and *Sn* phases, respectively, at an array at distance, Δ, A_{Op}, and A_{OS} are the source excitations of *P* and *S*, respectively, and t_P^* and t_S^* are the attenuation coefficients for *P* and *S* waves, respectively. The ratio of the *Pn* to *Sn* amplitudes can be written:

$$R = \frac{A_{Pn}}{A_{Sn}} = \frac{A_{op}}{A_{os}} e^{+\pi\Delta(t_p^* - t_s^*)},$$

where the exponential distance decay results when $t_p^* < t_S^*$. Consider now the log of the ratios, $LR = \log R$, in order to make the attenuation terms additive. If we difference the logs of the ratios for two events in the same region and at the same distance, Δ, from an array, the additive attenuation terms subtract out, as follows:

$$\log R^1_{NORESS} - \log R^2_{NORESS} = \log R^1_{ARCESS} - \log R^2_{ARCESS}.$$

where $R^i NORESS$ and $R^i ARCESS$ are the *Pn/Sn* amplitude ratios for event i at NORESS and ARCESS, respectively. Thus, the difference log of the *Pn/Sn* ratios for two events in the same region should be the same at both NORESS and ARCESS. If the 921231 event was another type of earthquake like the 860801 event, then we would expect the difference in the logs of the *Pn/Sn* ratios with the nuclear explosions in the same region to be the same at both arrays.

Now, we test the hypothesis that the 921231 and 860801 are the same kind of events. We first difference the *Pn/Sn* ratios in all frequency bands observable at both arrays with the ratios for each nuclear explosion and average the logs of the ratios:

$$\mu_1 = \frac{1}{N_1} \sum_{j=1}^{N_1} \left\{ \sum_{i=1}^{nf} \left[LR^{921231}_{ARCESS}(f_i) - LR^j_{ARCESS}(f_i) \right] \right\}$$

for the ARCESS recordings and

$$\mu_2 = \frac{1}{N_2} \sum_{j=1}^{N_2} \left\{ \sum_{i=1}^{nf} \left[LR^{860801}_{NORESS}(f_i) - LR^j_{NORESS}(f_i) \right] \right\}$$

for the NORESS recordings, where LR refers to the log ratio, $N1$ and $N2$ are the number of nuclear explosions recorded at ARCESS and NORESS, respectively, and nf is the number of frequency bands for which the log *Pn/Sn* amplitude ratios have been measured. Thus, if the 921231 and 860801 events are the same type of sources, then we expect that $\mu 1 = \mu 2$.

Figure 13a shows boxplots of the log ratios in four frequency bands (2-4 Hz, 2.5-4.5 Hz, 3-5 Hz, 4-6 Hz) of the 921231 event at ARCESS and the 860801 event at NORESS alongside the corresponding ratios for the nuclear explosions recorded at the two arrays. These frequency bands were chosen because they are the ones for which both *Pn* and *Sn* have good signal-to-noise ratios at both arrays. For NORESS, four nuclear explosions are plotted, including one in 1984, along with the three explosions that occurred after 1988 and were also recorded at ARCESS. Although

Comparison of Novaya Zemlya Log(Pn/Sn) Ratios at ARCESS and NORESS

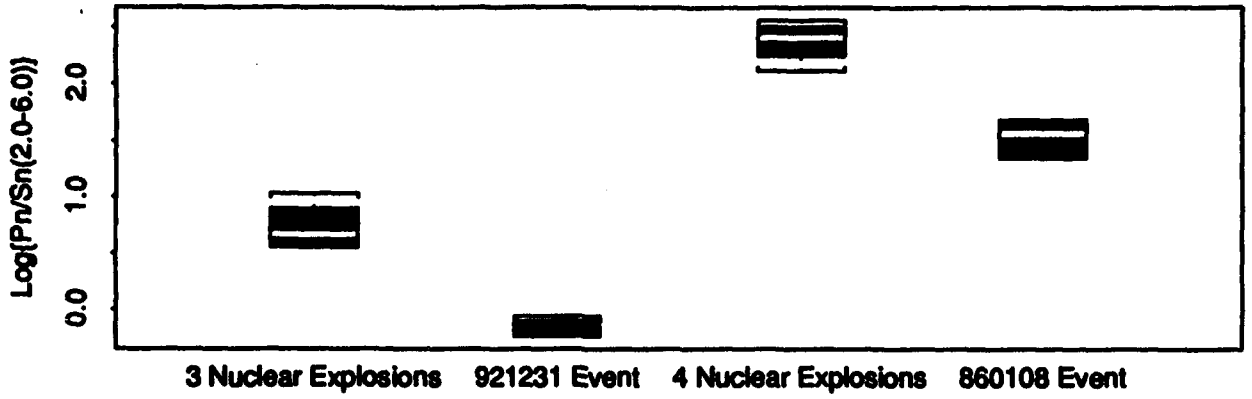

Figure 13a: Boxplots of the log *Pn/Sn* ratios of the 921231 event and three nuclear explosions, measured at ARCESS, and the 860801 event and four nuclear explosions at NORESS. The horizontal white lines indicate the medians of the data and height of each box encloses the first to the third quartiles of the data. The whiskers are plotted at the extreme values.

Comparison of Presumed Earthquake-Explosion Log(Pn/Sn) Ratio Differences

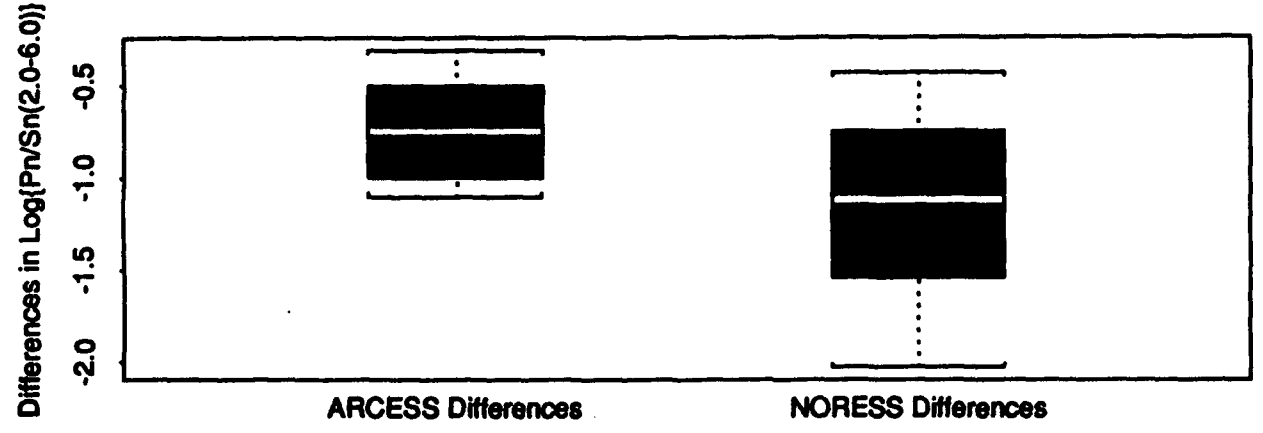

Figure 13b: Boxplots of the differences in the log *Pn/Sn* ratios between the 921231 and 860801 events, recorded at ARCESS and NORESS, respectively, and each of the nuclear explosions recorded at each of the arrays.

the *Pn/Sn* ratios at NORESS are larger than those at ARCESS, because of the differential attenuation effect on *Pn* and *Sn*, the differences in the log ratios appear to be about the same.

We now test whether the means in the differences in the log ratios are the same, i.e., $\mu 1 = \mu 2$. Figure 13b shows box plots of the differences in the log ratios between two events in question and the nuclear explosions at the respective arrays. The white lines in each boxplot are the median values of the difference in ratios. The mean differences, which are nearly the same as the medians, are $\mu 1$ = -0.7 at ARCESS and $\mu 2$ = -1.1 at NORESS. Testing the null hypothesis that $\mu 1 = \mu 2$ using the t test and the nonparametric Wilcoxcon test, we can accept the null hypothesis using the t test at the 98% confidence level and with the Wilcoxcon test at the 96% confidence level. Based on this analysis, we conclude that had the 921231 event been observed at NORESS, it would have had almost the same mean log *Pn/Sn* ratios relative to the nuclear explosions as does the 860801 event. Therefore, if the 860801 was most likely an earthquake, the similarity in relative scaling of log *Pn/Sn* amplitude ratios relative to the nuclear explosions at the two arrays strongly implies that the 921231 event was also an earthquake.

CONCLUSIONS

Our analysis of the waveform features of the 921231 event has shown that the event was probably not a nuclear explosion. Based on the comparison of *Pn/Sn* amplitude-ratio features with historical events, including earthquakes and mine explosions, we conclude that, based on the ARCESS data, the event is consistent with mine blasts on the Kola Peninsula and also resembles earthquakes in the Greenland Sea, although the *Pn/Sn* ratios of the 921231 event are slightly higher than those of the earthquakes. An earthquake identification cannot be ruled out because there are limited earthquakes in the same distance range and none in the actual Novaya Zemlya region, except for the 860801 event, which was only recorded at NORESS.

The event was too small to produce measurable *S* waves at NORESS. However, we reconsidered the 860801 event, which was larger and well recorded at NORESS. Our relative scaling analysis provides indirect evidence that these two events might have been very similar, other than their size, and thus, may have been the same source type. The evidence supports the conclusion that both events were not nuclear explosions, and if the 860801 event was an earthquake, as indicated by other discriminants (e.g., Ryall et al, 1987), then the 921231 was also an earthquake.

This study points up the importance of carefully considering propagation-path differences when trying to compare known explosions and earthquakes with events of unknown identity. If

we compared the 921231 *Pn/Sn* features with Kola mine blasts and Greenland Sea earthquakes while ignoring propagation path differences, the first impression would be that the event was a mine blast. However, the Novaya Zemlya events occurred several hundred kilometers farther from ARCESS than the Kola explosions, and *Sn* probably attenuated more rapidly than *Pn* with distance resulting in *Pn/Sn* ratios increasing with distance.

Novaya Zemlya earthquakes, by virtue of source mechanism differences, might look more like explosions than Greenland Sea earthquakes. The similarity in relative scaling of log *Pn/Sn* ratios that we found for the 921231 event at ARCESS and the 860801 event at NORESS, relative to nuclear explosions, supports this conclusion.

Thus, we conclude that the 921231 event was probably an earthquake which resembled mine blasts in other regions. Analysis of more events, particularly earthquakes, may provide a better understanding of the identification of this event. Further ISEIS analysis of other events in the future, including analysis of earthquakes outside of Scandinavia, will continue to supply more reference events. We expect to process more data from the Spitzbergen array, which is not affected by the propagation anomalies from Novaya Zemlya of the Barents Sea, as in the case of NORESS and ARCESS. Thus, by studying more mine blasts and earthquakes at the Spitzbergen and other Scandinavian arrays and comparing waveform-feature discriminants with the 921231 event, we will be able to better characterize this event and others which may occur at Novaya Zemlya in the future.

REFERENCES

Bache, T.C., S.R. Bratt, J. Wang, R.M. Fung, C. Kobryn, and J.W. Given (1990). The Intelligent Monitoring System, *Bull. Seism. Soc. Am.*, **80**, 1833-1851.

Baumgardt, D.R. (1990). Investigation of teleseismic *Lg* blockage and scattering using regional arrays, *Bull. Seism. Soc. Am.*, **80**, 2261-2281.

Baumgardt, D.R.(1991a). Intelligent Seismic Event Identification System, vol. II: users manual, Final Report, PL-TR-91-2298(II), ENSCO, Inc., Springfield, VA.

Baumgardt, D.R. (1991b). Possible seismic signals from a nuclear submarine accident in the Norwegian Sea, abstract in *EOS*, **72**, 343.

Baumgardt, D.R. (1991c). High-frequency array studies of long range *Lg* propagation and the causes of *Lg* blockage and attenuation in the Eurasian continental craton, Final Report, SAS-TR-91-50, ENSCO, Inc., Springfield, VA.

Baumgardt, D.R.(1992). Investigation of seismic discriminants in Eurasia, SBIR Phase I, Final Report, SAS-TR-92-81, ENSCO, Inc., Springfield, VA.

Baumgardt, D.R. (1993). Regional characterization of mine blasts, earthquakes, mine tremors, and nuclear explosion using the Intelligent Seismic Event Identification System, Final Report, in preparation, ENSCO, Inc., Springfield, VA.

Baumgardt, D.R. and K.A. Ziegler (1988). Spectral evidence of source multiplicity in explosions: application to regional discrimination of earthquakes and explosions, *Bull. Seism. Soc. Am.*, **78**, 1773-1795.

Baumgardt, D.R. and G. B. Young (1990). Regional seismic waveform discriminants and case-based event identification using regional arrays, *Bull. Seism. Soc. Am.*, **80**, 1874-1892.

Baumgardt, D.R., J. Carney, M. Maxson, and S. Carter (1992). Evaluation of regional seismic discriminants using the intelligent seismic event identification system, Semi-Annual Technical Report, SAS-TR-93-38, ENSCO, Inc., Springfield, VA.

Bennett, T.J. and J.R. Murphy (1986). Analysis of seismic discrimination capabilities using regional data from western United States events, *Bull. Seism. Soc. Am.*, **76**, 1069-1086.

Bennett, T.J., B.W. Barker, K.L. McLaughlin, and J.R. Murphy (1989). Regional discrimination of quarry blasts, earthquakes and underground nuclear explosions, Final Report, *GL-TR-89-0114*, S-Cubed, La Jolla, CA.

Bennett, T.J., A.K. Campanella, J.F. Scheimer, and J.R. Murphy (1991). Regional discrimination of Soviet nuclear explosions, earthquakes and mineblasts, *Papers Presented at 13th Annual PL/DARPA Seismic Research Symposium*, 8-10 October 1991, Keystone, CO, 78-84.

Murphy, J.R. and T.J. Bennett (1982). A discrimination analysis of short-period regional seismic data recorded at Toronto Forest Observatory, *Bull. Seism. Soc. Am.*, **72**, 1351-1366.

Ryall, A.S., A. Jurkevics, P.S. Dysart, and J.J. Pulli (1987). Note on seismic discrimination and the 1 August 1986 Novaya Zemlya event, in *Technical Report of the Period 1 October-31 December 1986*, Technical Report C87-01, Center for Seismic Studies, Arlington, VA.

Taylor, S.R. and M.D. Denny (1991). An analysis of spectral differences between Nevada Test Site and Shagan River nuclear explosions, *J. Geophys. Res.*, **96**, 6237-6245.

Taylor, S.R., N.W. Sherman, and M.D. Denny (1988). Spectral discrimination between NTS explosions and western United States earthquakes at regional distances, *Bull. Seism. Soc. Am.*, **78**, 1563-1579.

Taylor, S.R., M.D. Denny, E.S. Vergino, and R.E. Glaser (1989). Regional discrimination between NTS explosions and western U.S. earthquakes, *Bull. Seism. Soc. Am.*, **79**, 1142-1176.

A PRELIMINARY REGIONAL SEISMIC DISCRIMINATION ANALYSIS OF THE NOVAYA ZEMLYA EVENT OF DECEMBER 31, 1992

A Preliminary Regional Seismic Discrimination Analysis of the Novaya Zemlya Event of December 31, 1992

T. J. Bennett
J. R. Murphy
M. E. Marshall
B. W. Barker

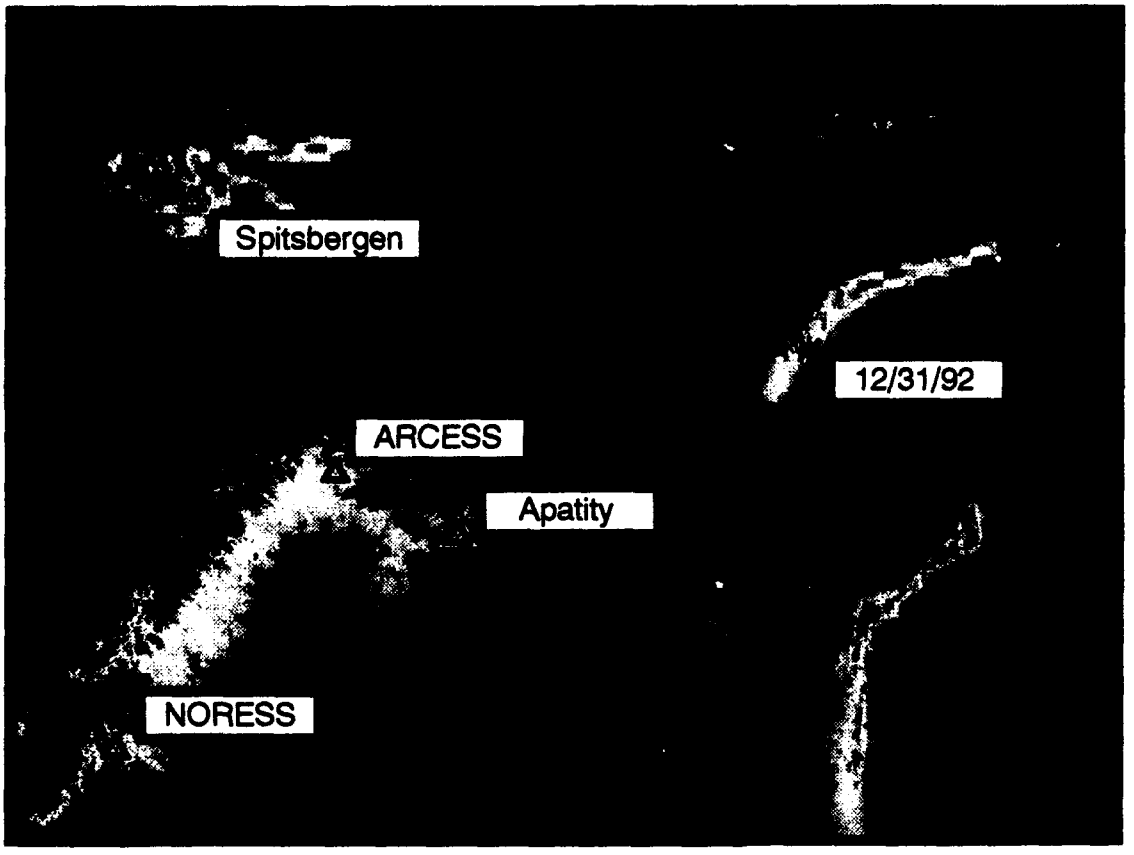

Prepared by: Maxwell Laboratories, Inc., S-CUBED Division

May, 1993

Summary

Although experience with alternative event types from the same source area is extremely limited, seismic evidence appears to support the conclusion that the event at Novaya Zemlya (NZ) on December 31, 1992 was not an underground nuclear explosion test. We have performed a variety of analyses on the regional seismic signals from the subject event which led to this conclusion. The results of these analyses in relation to experience with regional seismic signals from all types of events throughout the world indicate that the event was most likely (1) a natural earthquake, (2) a chemical blast, or (3) a rockburst. However, lacking more specific calibration information from the NZ source area, we are unable to make a definitive distinction between these remaining alternatives. In the following sections we briefly review our regional discrimination experience and then apply it to the available data for the 12/31/92 NZ event.

Background on Regional Seismic Discrimination

Four types of seismic sources are pertinent to the problem of event discrimination: (1) underground nuclear explosions, (2) natural earthquakes, (3) chemical blasts used in mining and construction, and (4) rockbursts related to induced stress release in mines. Interest in lowering the discrimination threshold has focused attention on smaller events for which regional seismic signals provide a key element in the identification process. A long-standing goal of the ARPA research program in nuclear explosion monitoring has been to reduce the identification magnitude threshold to lower levels through utilization of observations at regional seismic stations. Over the years a variety of regional discrimination methods have been proposed as potential techniques for seismic monitoring of underground nuclear explosion testing (cf. Pomeroy et

al., 1982; Blandford, 1981). These different methods have been tested on data samples including alternate source types from many distinct source environments with varying degrees of success. However, the goal of establishing a completely reliable regional discrimination procedure has proven to be elusive because of the complexity of regional signals, their dependence on propagation effects, and incomplete understanding of source influences on regional signal generation. Nevertheless, a basic capability to differentiate seismic source types based on their regional signal character appears to be emerging from the research program.

Experience with regional seismic signals from underground nuclear explosions in the U.S. and former Soviet Union (cf. Bennett et al. 1992) indicates that they normally produce frequency-dependent L_g/P or S/P ratios which are different from those of other seismic source types. The ratios for nuclear explosions are often observed to be one or greater at low frequencies (less than 2 Hz) but drop off rapidly to significantly below one at frequencies above 2 Hz. Figure 1 shows the results of band-pass filter analyses performed on the vertical-component signals at station ARU from a Shagan River underground nuclear explosion ($R \approx 1530$ km) and from an earthquake near the Shagan River test site ($R \approx 1810$ km). In the 0.5 to 2 Hz band the L_g/P ratios are quite similar for the two event types. However, progressing to the higher frequency bands, there appears to be a clear distinction with much larger L_g relative to P for the earthquake than for the nuclear explosion test. The fact that this is a source effect and not related to any path differences is corroborated by similar analyses performed on signals at station GAR from a Lop Nor nuclear explosion test ($R \approx 1590$ km) and a nearly collocated earthquake ($R \approx 1610$ km) as shown in Figure 2. The S/P and L_g/P ratios are observed to be much smaller, particularly at high frequencies, for the underground nuclear explosion.

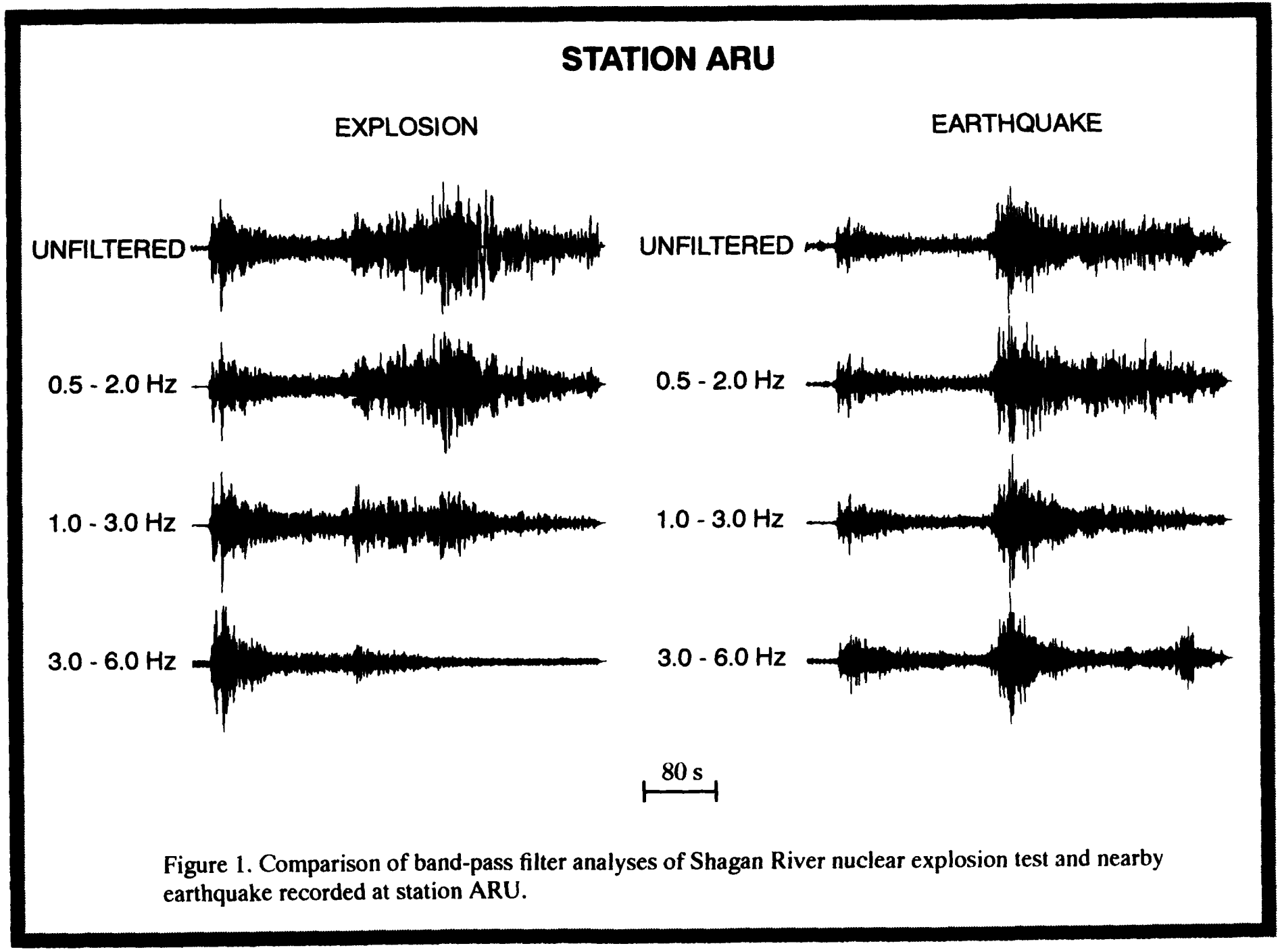

Figure 1. Comparison of band-pass filter analyses of Shagan River nuclear explosion test and nearby earthquake recorded at station ARU.

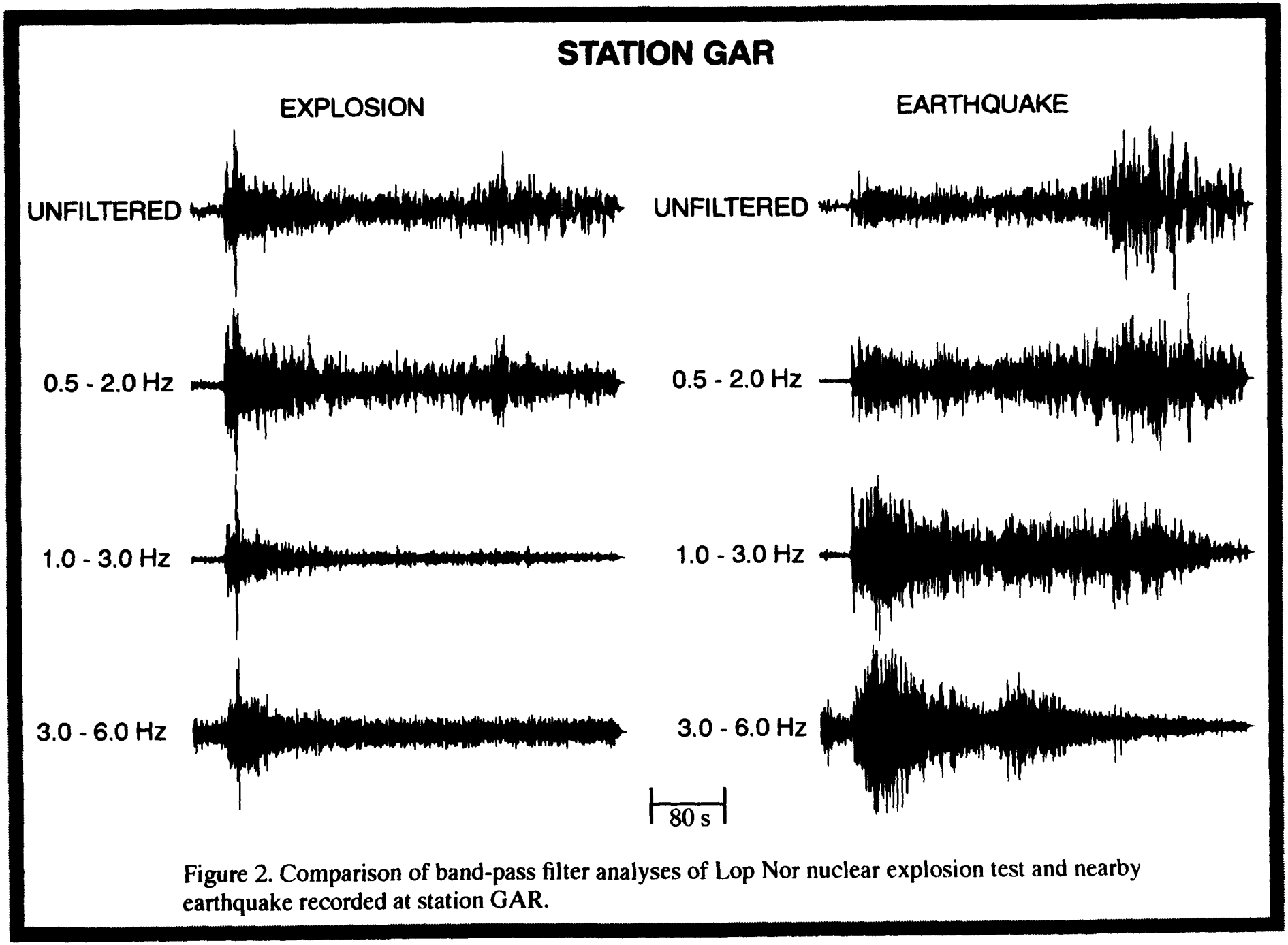

Figure 2. Comparison of band-pass filter analyses of Lop Nor nuclear explosion test and nearby earthquake recorded at station GAR.

Bennett et al. (1992) analyzed the spectral characteristics of the regional phases for a large sample of Shagan River underground nuclear explosions and Eurasian earthquakes recorded at the IRIS stations in the former Soviet Union. This behavior is illustrated in Figure 3 which compares the average L_g/P spectral ratios (vertical component) observed at station ARU from Shagan River underground nuclear explosions and Eurasian earthquakes from the surrounding region. The figure shows the mean ratios for ten Shagan River explosions and for eighteen earthquakes along with plus and minus one sigma bounds about the mean. The ratios are peaked at similar levels near 0.5 Hz, but at high frequencies the nuclear explosion ratios reach and stay at a level well below that of the earthquakes. Our experience with the spectral characteristics of regional signals from the same types of events in the western U.S. (cf. Murphy and Bennett, 1982; Bennett and Murphy, 1986) suggests that similar behavior in the L_g/P spectral ratios occurs there.

With regard to identification of chemical blasts, observations to date indicate several regional seismic discriminant measures which appear to offer some potential for reliable discrimination. These measures include regional signal spectral scalloping, relative excitation of L_g or S versus regional P, and relative excitation of R_g versus other regional phases. Most chemical blasts in this country (and elsewhere) are geometrically dispersed and fired with delays. As a result, we have some experience with seismic signals from time-delayed blasts but almost none with large concentrated chemical blasts. For the former case evidence of ripple firing or extended source duration can sometimes be identified by time-independent spectral scalloping in the regional signals from mine blasts (cf. Baumgardt and Ziegler, 1988; Hedlin et al., 1990), but this requires good S/N over a broad frequency band and may not always be observable (cf. Bennett et al., 1989). Unlike underground nuclear explosion

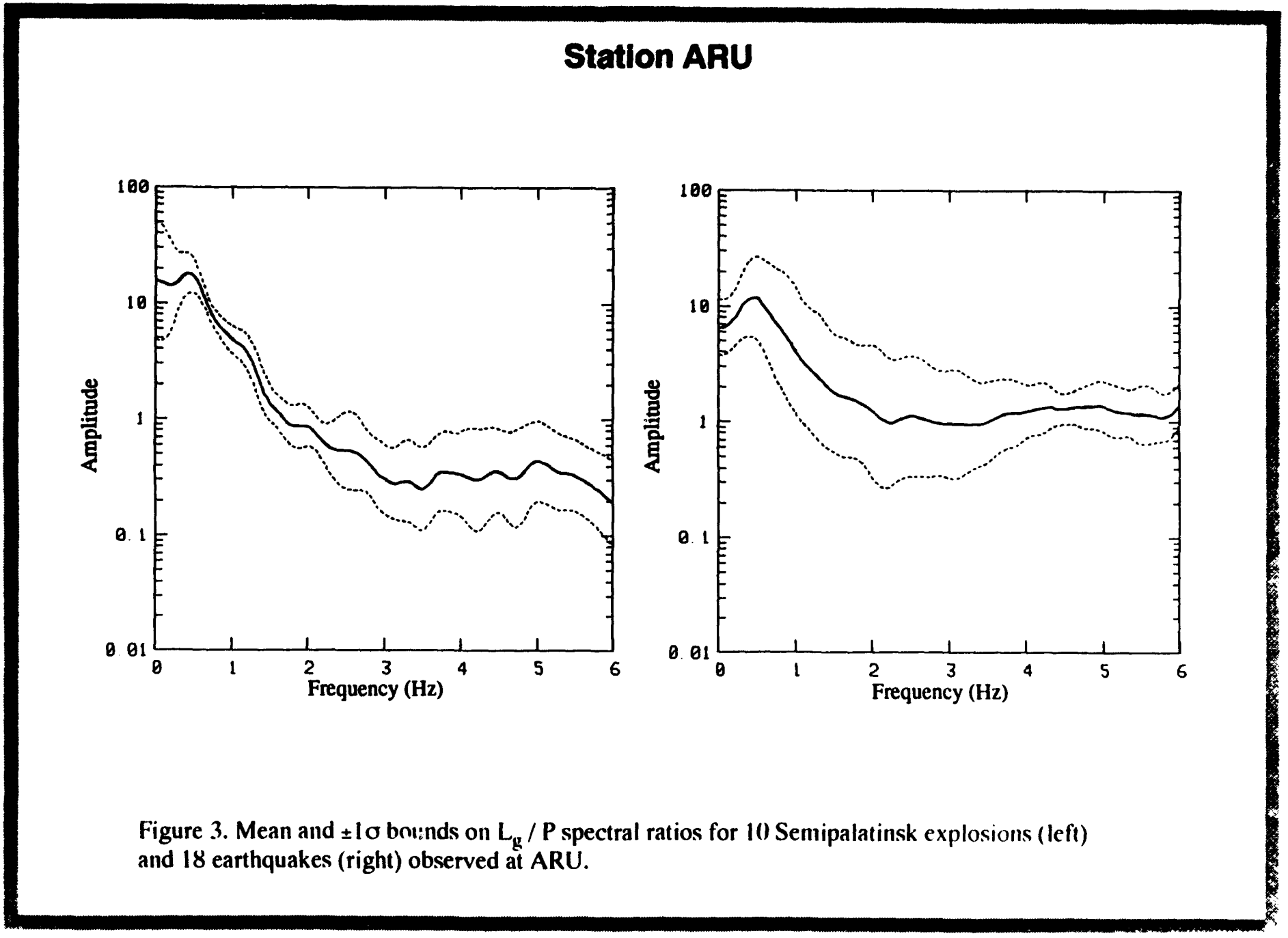

Figure 3. Mean and $\pm 1\sigma$ bounds on L_g / P spectral ratios for 10 Semipalatinsk explosions (left) and 18 earthquakes (right) observed at ARU.

tests, chemical blasts frequently produce L_g/P or S/P ratios more like those of earthquakes (cf. Bennett et al., 1989; 1993), showing less rapid variations with frequency, and remaining at values nearer one at high frequencies. The preliminary indications from theoretical studies (cf. Barker et al., 1993) are that some types of shooting practice may nullify the value of spectral scalloping for discrimination of commercial blasts. Procedures which limit the extent of the source in space or time or which tend to randomize the delays between individual elements would be expected to limit the effectiveness of this discriminant.

The issue of discrimination of underground nuclear explosions from rockbursts has only recently come to attention. Rockbursts occur frequently in mining areas throughout the world, are sometimes large ($M > 5$), may show mechanism complexity, and may be controlled to some degree by mining practice (cf. Bennett et al., 1993). On the other hand, rockbursts often exhibit regional phase seismic signals which are earthquake-like, and this characteristic could be important to their systematic identification. In particular, regional measurements representing the relative excitation of L_g versus P or S versus P are observed to intermingle for rockbursts and earthquakes in several different source areas of the world which have been investigated by Bennett et al. (1993).

Experience with these kinds of observations and spectral analyses of regional signals from all types of events, including nuclear explosions, earthquakes, chemical blasts, and rockbursts, have led us to formulate a working model for regional seismic discrimination. According to this model some commercial blasts should be distinguishable from underground nuclear explosions and earthquakes on the basis of spectral scalloping introduced by the extended duration of the source, under favorable signal-to-noise conditions.

With regard to the relative excitation of L_g versus P or S versus P, the behavior for different source types is schematically illustrated by the sketch in Figure 4. L_g/P or S/P ratios at frequencies near 1 Hz tend to be intermingled for all event types; but at higher frequencies ratios tend to be separated for different source types. High-frequency L_g/P ratios seem to be greatest for earthquakes and rockbursts, somewhat lower for commercial blasts, and significantly lower for underground nuclear explosions. R_g phases are often observable for nuclear explosions, commercial blasts, and rockbursts, but usually not for earthquakes, probably because of the greater focal depth for the latter source type. With some care and appropriate adjustments, it should be possible to extend this model into new areas where experience may be limited to assess seismic identification capability.

Background Information on Novaya Zemlya

On December 31, 1992 a seismic event with a magnitude of 2.26 M_L was located in the vicinity of the Novaya Zemlya nuclear test site. The NORSAR location of the event was at 73.6° N, 55.2° E with a location error ellipse which nearly included the published locations of some of the historical nuclear explosion tests. Master event techniques were subsequently used to relocate the event somewhat to the south and east of the original location (cf. Ryall, 1993). The NZ source region is nearly aseismic in terms of natural earthquake activity. This is illustrated in Figure 5 which shows the seismicity reported in the ARPA Center for Seismic Studies events catalog for the surrounding region during the period from 1957 (the year nuclear testing was initiated at NZ) up to the present. Events thought to be natural earthquakes are shown as black open squares, nuclear explosion tests as red crosses, and the event of 12/31/92 as a black asterisk. With the exception of a single event, there is no reported natural

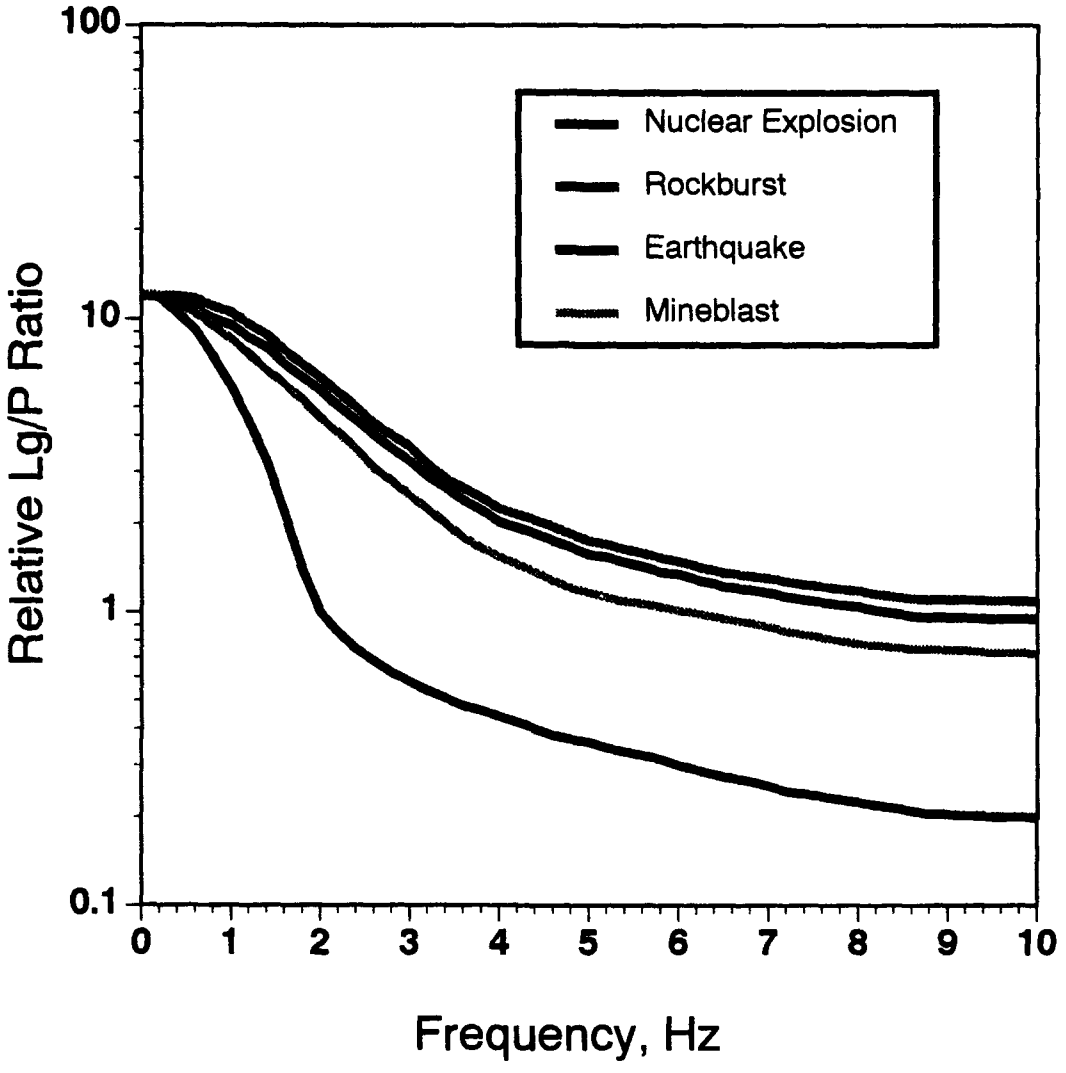

Figure 4. Schematic representation of the empirical model of Lg/P spectral ratio for different seismic source types.

Figure 5. Seismicity in the region surrounding NZ since 1957; nuclear explosions indicated by red crosses, natural earthquakes by black open squares, and the 12/31/92 event by the black asterisk.

earthquake activity within 850 km of the unknown NZ event. The exception is an isolated earthquake which occurred on August 1, 1986. This event had a magnitude of 4.7 m_b and was located at 72.9° N, 55.9° E, just to the south and east within about 60 km of the current event. There is little historical evidence of chemical blasting associated with mining or construction activity in the area; and there have been no reports of rockbursts or stress-release events associated with mining.

Digital seismic waveform data for the 12/31/92 NZ event were recorded at two permanent ARPA regional arrays at ARCESS and NORESS and at two ARPA experimental regional arrays at Spitsbergen and Apatity. Figure 6 shows the locations of these stations relative to the 12/31/92 NZ event. The station ranges from the event are approximately 1060 km, 1150 km, 1170 km, and 2310 km for Apatity, ARCESS, Spitsbergen, and NORESS respectively. All station are located at westerly azimuths from the event, and substantial segments of the propagation paths to all the stations cross the Barents Sea.

Analyses of the December 31, 1992 NZ Event

We performed analyses on the seismic signals recorded at ARCESS, Spitsbergen, NORESS, and Apatity for the 12/31/92 NZ event and offer the following observations based on these analyses and experience with seismic events from other parts of the world. The signals were generally weak at all stations as would be expected from such a small magnitude event at these distances. Bandpass (BP) filter analyses were performed for the recorded waveforms at each station. Figures 7 - 9 show the results of the bandpass filter analyses applied to single-element, vertical-component records from stations at ARCESS, Spitsbergen, and NORESS. The noise level at the Apatity station was high, and we saw no indications of regional signals in the BP filter

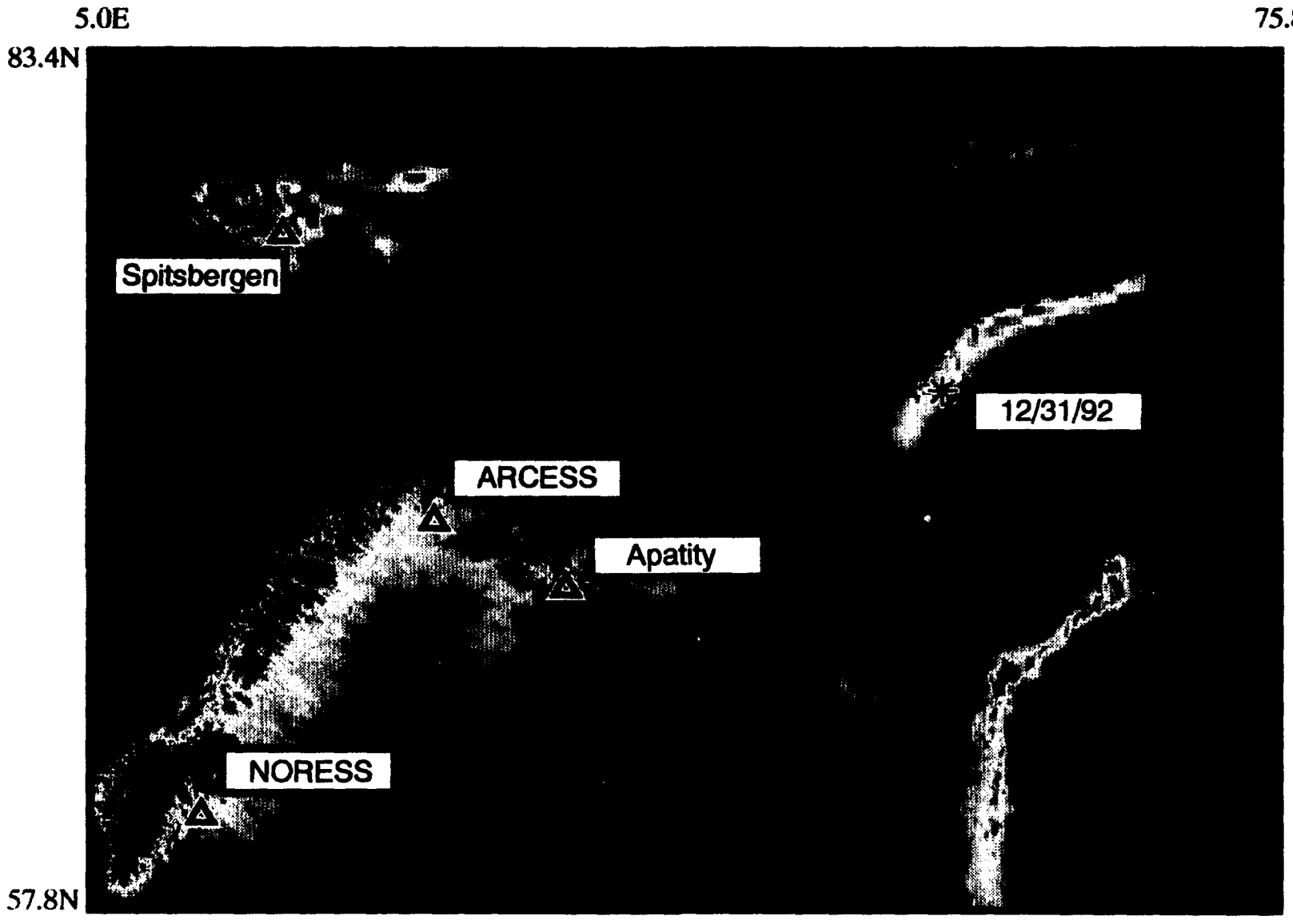

Figure 6. Locations of ARPA regional arrays which recorded digital waveform data for the 12/31/92 event.

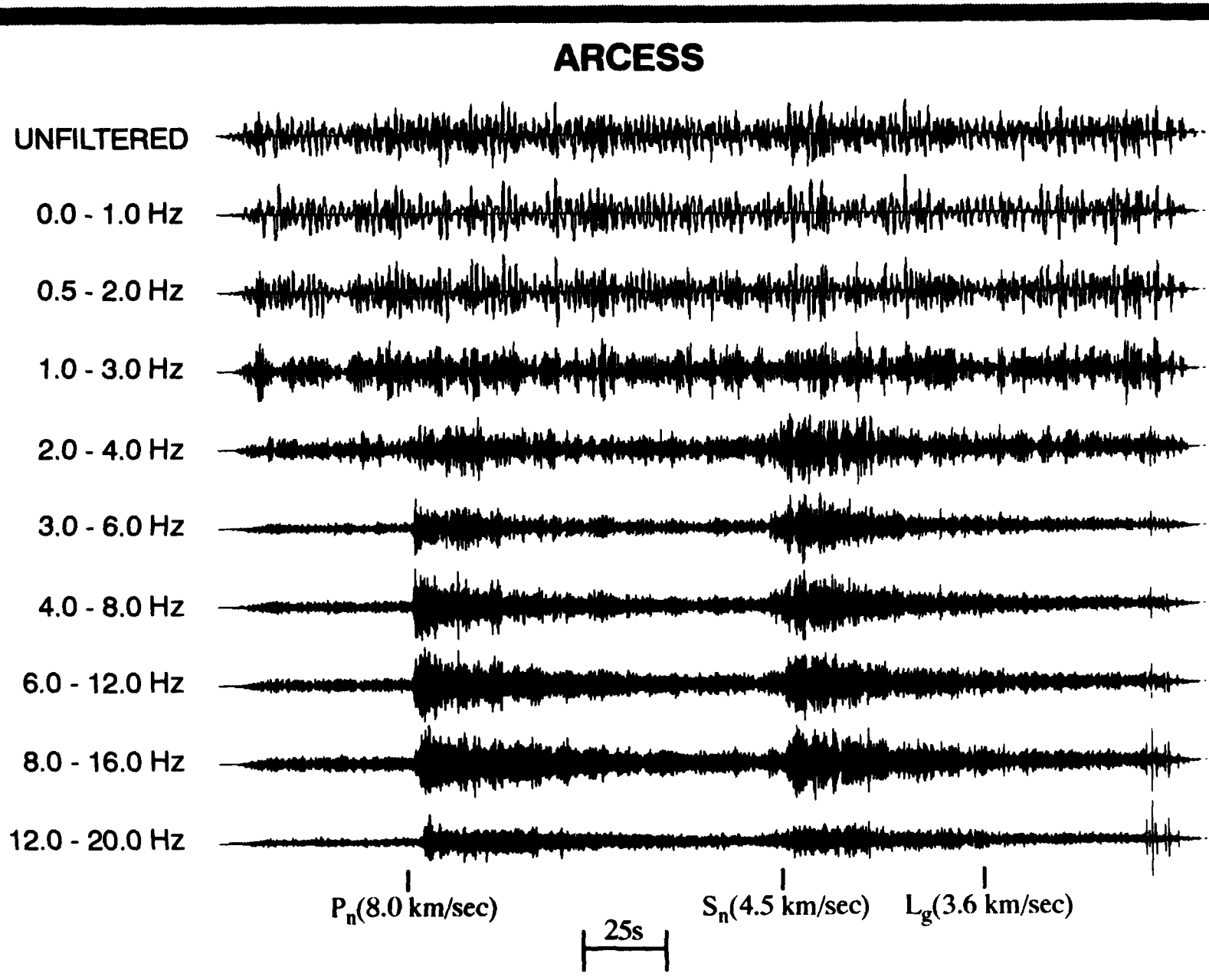

Figure 7. Application of band-pass filter to vertical-component ARA0 recording of the 12/31/92 event.

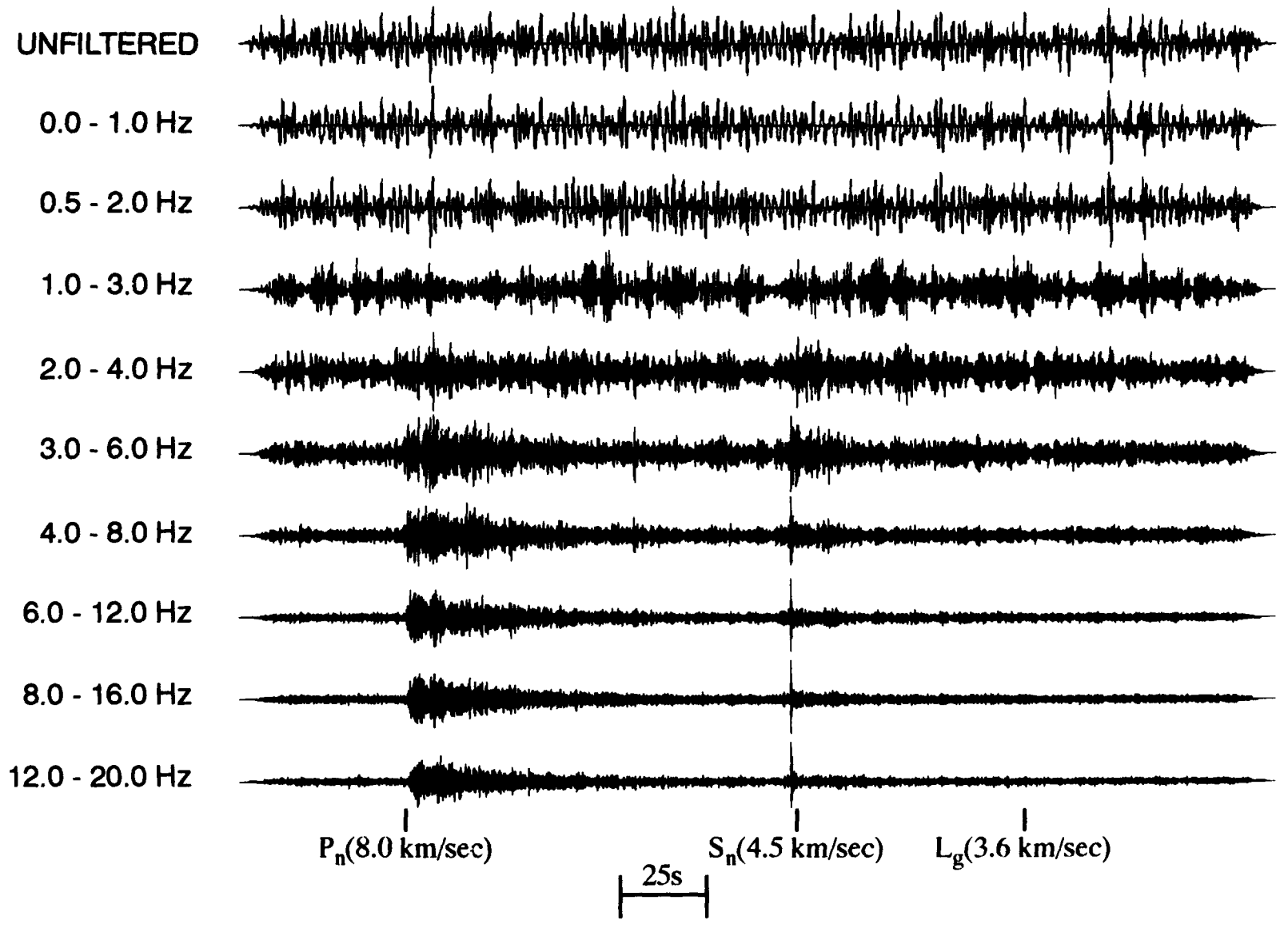

Figure 8. Application of band-pass filter to vertical-component SPB2 recording of the 12/31/92 NZ event.

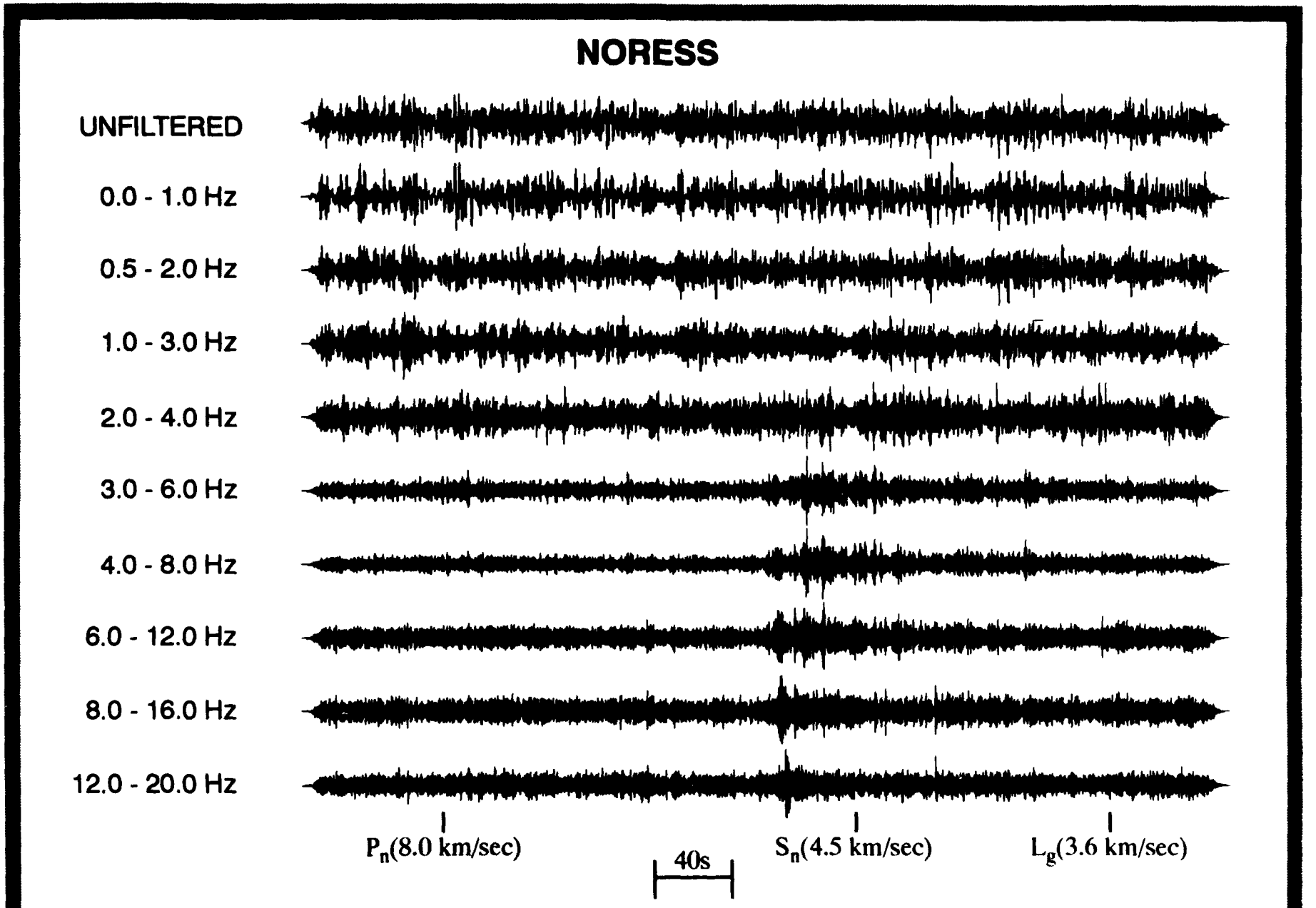

Figure 9. Application of band-pass filter to vertical-component NRD9 recording of the 12/31/92 NZ event.

processing of the APA0 waveforms. The strongest regional signals with useful signal-to-noise levels covering the broadest frequency band were observed at station ARA0. Although the regional signals are not apparent in the lower frequency bands, they do emerge above about 3 Hz and are apparent up to near the Nyquist frequency. The regional P and S signals from the 12/31/92 event appear to show nearly equal amplitudes over the useful frequency band with rather strong complexity and long duration. The SPB2 BP filter analysis in Figure 8 also shows regional P and S signals above about 3 Hz but with somewhat reduced signal-to-noise levels. In addition, while the S signals are roughly equivalent to P up to about 4 Hz, at higher frequencies the regional P dominates S even though the latter is still apparent on the filtered records. At NORESS the regional signals were found to be generally weak. In fact, we reviewed the BP filter results from several channels before finding any evidence of signals on the individual array elements. Figure 9 shows the BP filter analysis of the array element NRD9 where we see indications of regional S and associated coda at frequencies again above 3 Hz. There is little evidence of P at NORESS except in filtered versions of the coherent beams and again only at frequencies above about 3 Hz. The kinds of limitations on the available frequency band of the regional signals cited here would be expected to severely restrict any attempt to utilize spectral scalloping as a discriminant for this event.

On the other hand, at both ARCESS and Spitsbergen spectral ratios of S to P signals appear to provide a potential diagnostic for the 12/31/92 NZ event. In particular, at ARCESS (cf. Figure 7) the S/P ratio remains at or near a value of 1.0 for frequencies from 3 Hz through at least 12 Hz. This behavior contrasts with that seen for underground nuclear explosion tests in many different parts of the world for which the S/P, or L_g/P, ratios fall off rapidly at higher frequencies to

values well below 1.0. The interpretation of the observations at Spitsbergen is somewhat more complicated partly due to a spiky arrival in the S window. At Spitsbergen the general level of the S/P ratios (ignoring the spike) appears to be smaller than at ARCESS. Such differences might be related to propagation path effects, which might be resolved by additional experience; but effects of source radiation pattern on the signals might also be a factor. It should be noted that the regional S phases from the NZ event identified here on the records at ARCESS, Spitsbergen, and NORESS do not seem to be L_g; their associated group velocities are too high. This failure to observe L_g may be related to a transmission path defect producing blockage or severe attenuation of the L_g signals. Nevertheless, our experience suggests that the regional S/P ratios should be diagnostic. The behavior of the S/P spectral ratio seen here for the 12/31/92 event at NZ is typical of that observed for earthquakes, rockbursts, or mineblasts in many source regions for which the observed ratios are often near 1.0 at high frequencies. We would conclude from this that the event is most likely to have been one of these latter source types.

The experience base for seismic event types other than underground nuclear explosions from Novaya Zemlya is extremely sparse. As noted above, natural seismicity is rare within the vicinity of the test site. Construction blasts and rockbursts have also been uncommon or too small to be recorded until the development in recent years of high-quality regional arrays in the area, under ARPA sponsorship. As a result, calibration information in the form of seismic waveform data at relevant regional stations is limited. For this study we have compared the characteristics of the regional signals for the 12/31/92 NZ event with those for a NZ underground nuclear explosion test (10/24/90, m_b = 5.7) recorded at ARCESS. We have also compared NORESS recordings for the

same nuclear test with those for the confirmed earthquake near the NZ test site (8/01/86, m_b = 4.7) and with the NORESS signals for the 12/31/92 NZ event.

Figure 10 shows the comparison of the BP filter analyses of the vertical component records at station ARA0 for the 12/31/92 NZ event and the 10/24/90 NZ underground nuclear explosion. For the 2 - 4 Hz passband the S amplitude level is observed to be somewhat larger than P for both events. However, at higher frequencies, including the 8 - 16 Hz passband shown in Figure 10, the S amplitude level is still larger than P for the 12/31/92 NZ event; but it drops off to less than half the P amplitude for the nuclear explosion. This behavior is somewhat different from that described above for Eurasian events in that the S/P ratio for the nuclear explosion is still above a value of 1.0 at fairly high frequencies (viz 2 - 4 Hz) whereas the Eurasian nuclear explosion S/P ratios fell below 1.0 at frequencies above about 2 Hz. We conclude from this that, while the general trend still holds true that the S/P ratios for nuclear explosions fall below those of other event types at higher frequencies, the frequency band for which the separation can be observed may be regionally dependent. This points out the need for calibration information and a fundamental theoretical understanding of regional phase generation and propagation to allow regional discrimination experience to be transported reliably into new areas.

Figure 11 shows a similar comparison of the BP filter analyses of the NORESS recordings for the 8/01/86 NZ earthquake and the 10/24/90 NZ nuclear explosion. In this case, the S/P ratio is less than 1.0 at all frequencies for both events. The small S signals for the NZ events observed at NORESS appear to be associated with a propagation effect, since the same events often produce larger S signals at other stations (e.g. the 10/24/90 NZ explosion at ARCESS shown in Figure 10). This further emphasizes the need for calibration information to adjust for propagation. Nevertheless, for the nearly common-path

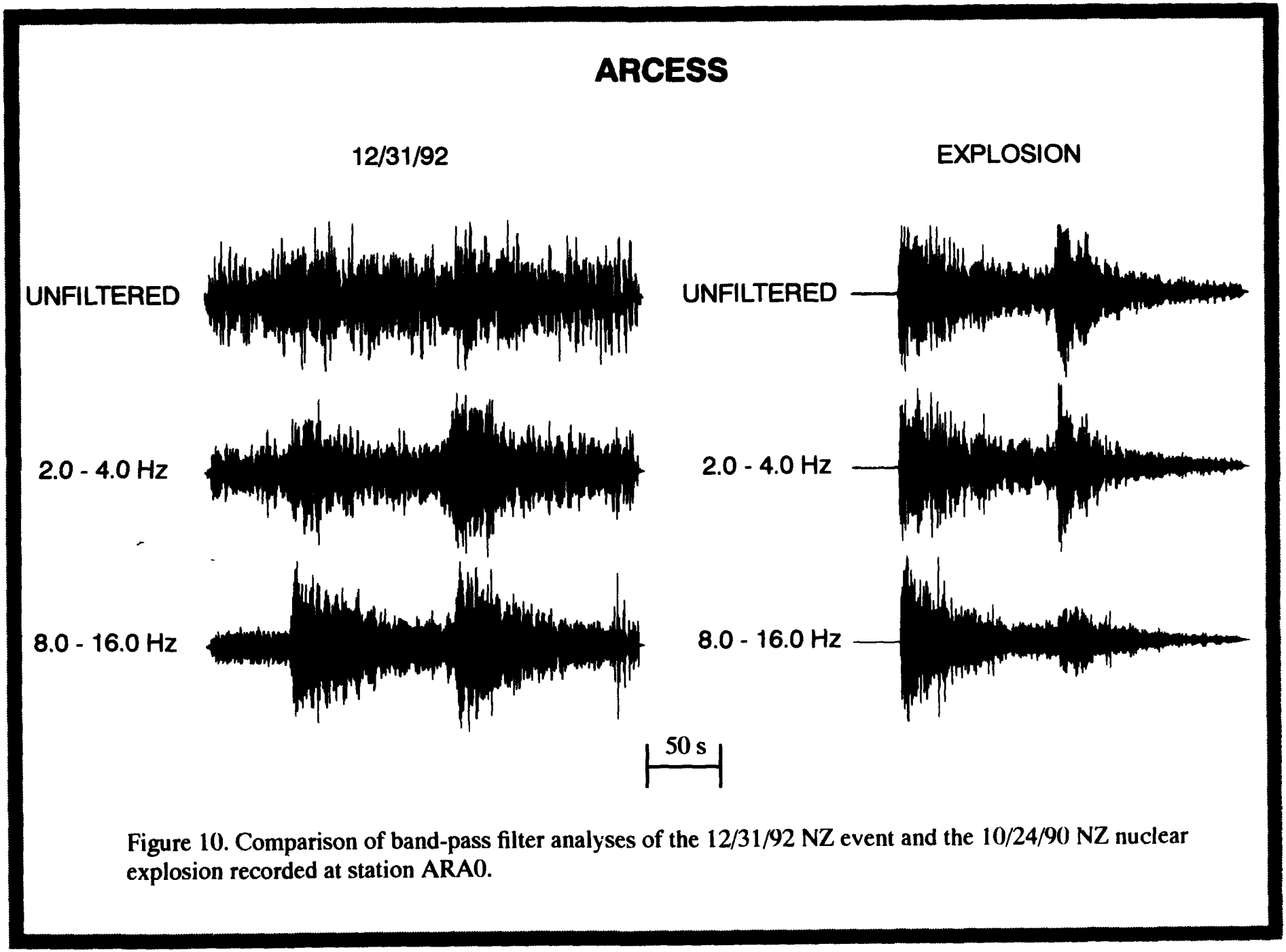

Figure 10. Comparison of band-pass filter analyses of the 12/31/92 NZ event and the 10/24/90 NZ nuclear explosion recorded at station ARA0.

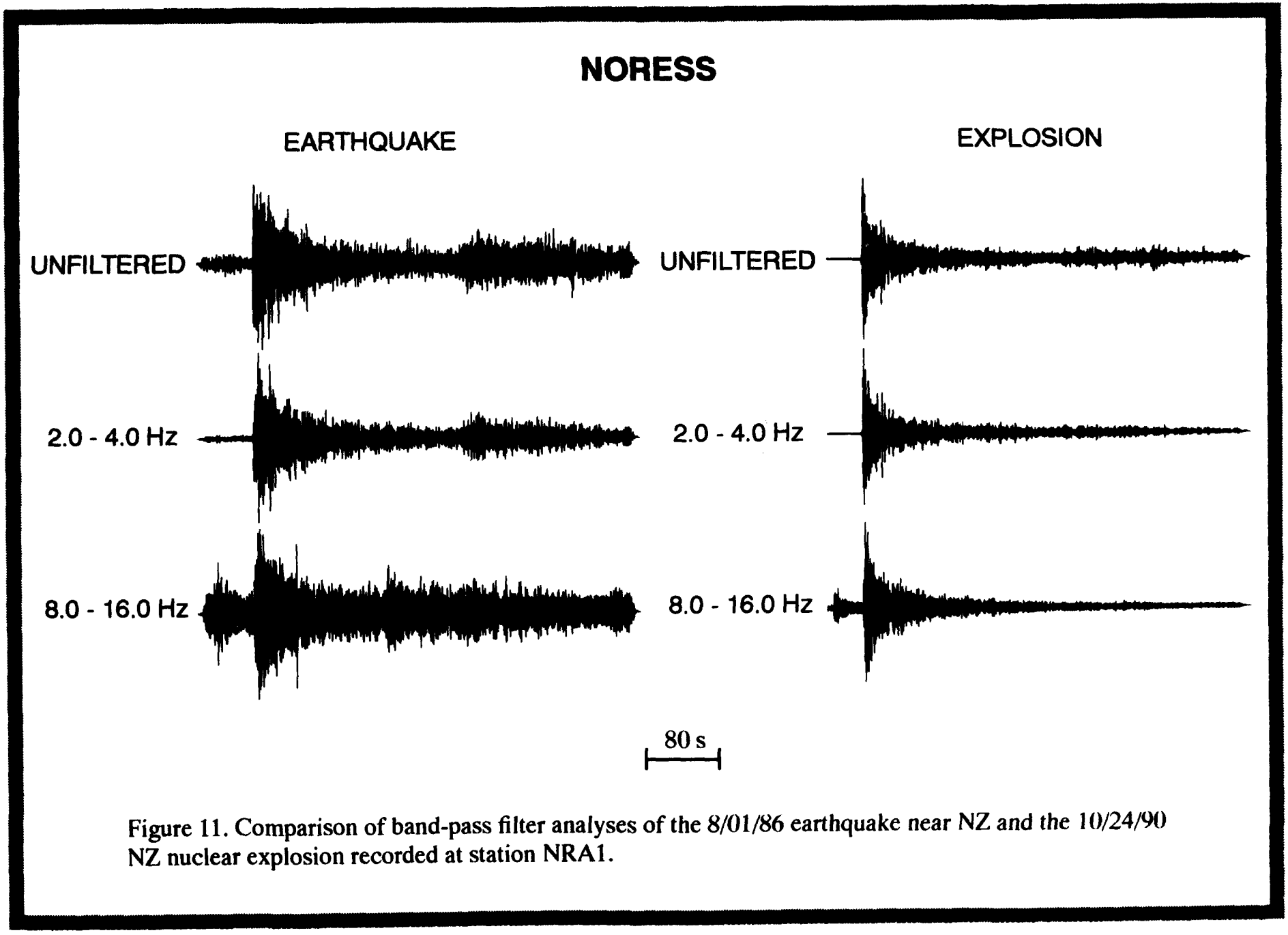

Figure 11. Comparison of band-pass filter analyses of the 8/01/86 earthquake near NZ and the 10/24/90 NZ nuclear explosion recorded at station NRA1.

events in Figure 11, we do see that the S signals are significantly larger, relative to P, for the earthquake than for the nuclear explosion. In particular, for both the "Unfiltered" and 2 - 4 Hz passband, the S/P ratio is at least a factor of two larger for the earthquake. The 8 - 16 Hz passband shows considerable noise contamination for the earthquake record which makes its interpretation questionable. In that band there is no evidence of S in the explosion record, and there may be S which is roughly half the size of P for the earthquake. As described above, the NORESS records (cf. Figure 9) for the 12/31/92 NZ event have very low signal-to-noise levels. As a result, their comparison with similar signals from prior NZ sources is not very persuasive. However, if we assume that the high-frequency arrivals near and after the predicted S time in Figure 9 are real and that the earlier P signals are buried in noise, then the 12/31/92 NZ event would appear to have a high-frequency S/P ratio at NRD9 above 1.0. Such large S/P ratios at high frequencies are more typical of earthquakes and unlike the experience here at NZ or elsewhere for underground nuclear explosion tests.

Conclusions

The observed spectral characteristics of the regional signals from the 12/31/92 NZ event appear to be inconsistent with the event having been an underground nuclear explosion test. However, lacking more specific calibration information from the NZ source region, we are unable to make a definitive distinction between the remaining three alternative source types: (1) earthquake, (2) rockburst, or (3) chemical blast. We base these conclusions on our analyses of the data for the 12/31/92 NZ event described above, experience with regional signal characteristics from all types of seismic events from other

parts of the world, and investigations of the limited data from the relevant stations which are available from prior events in the NZ source region.

References

Barker, T. G., K. L. McLaughlin, and J. L. Stevens (1993). Numerical Simulation of Quarry Blast Sources, S-CUBED Report No. SSS-TR-13859.

Baumgardt, D. R., and K. A. Ziegler (1988). "Spectral Evidence of Source Multiplicity in Explosions: Application to Regional Discrimination of Earthquakes and Explosions,"*Bull. Seism. Soc. Am.*, 78, pp. 1773 - 1795.

Bennett, T. J., and J. R. Murphy (1986). "Analysis of Seismic Discrimination Capabilities Using Regional Data from Western United States Events," *Bull. Seism. Soc. Am.*, 76, pp. 1069 - 1086.

Bennett, T. J., B. W. Barker, K. L. McLaughlin, and J. R. Murphy (1989). Regional Discrimination of Quarry Blasts, Earthquakes, and Underground Nuclear Explosions, S-CUBED Report No. SSS-TR-89-10385, GL Report GL-TR-89-0114, ADA223148.

Bennett, T. J., A. K. Campanella, J. F. Scheimer, and J. R. Murphy (1992). Demonstration of Regional Discrimination of Eurasian Seismic Events Using Observations at Soviet IRIS and CDSN Stations, S-CUBED Report No. SSS-FR-92-13150, PL Report PL-TR-92-2090, ADA253275.

Bennett, T. J., J. F.Scheimer, A. K. Campanella, and J. R. Murphy (1993). Seismic Characteristics of Rockbursts for Use in Discrimination, S-CUBED Report No. SSS-DTR-13792, PL Report PL-TR-93-2059.

Blandford, R. R. (1981). "Seismic Discrimination Problems at Regional Distances," in *Identification of Seismic Source - Earthquake or Underground Explosion*, D. Reidel Publishing Co.

Hedlin, M. A. H., J. B. Minster, and J. A. Orcutt (1990). "An Automatic Means to Discriminate Between Earthquakes and Quarry Blasts," *Bull. Seism. Soc. Am.*, 80, pp. 2143 - 2160.

Murphy, J. R., and T. J. Bennett (1982). "A Discrimination Analysis of Short-Period Regional Seismic Data Recorded at Tonto Forest Observatory," *Bull. Seism. Soc. Am.*, 72, pp. 1351 - 1366.

Pomeroy, P. W., W. J. Best, and T. V. McEvilly (1982). "Test Ban Treaty Verification with Regional Data - A Review," *Bull. Seism. Soc. Am.*, 72, pp. S89 - S129.

Ryall, A. S. (1993). Notes on Analysis of 31 December 1992 NZ Event.

IDENTIFICATION ANALYSIS
OF THE
DEC. 31, 1992
NOVAYA ZEMLYA EVENT

Identification Analysis of the Dec. 31, 1992 Novaya Zemlya Event

Jay J. Pulli and Paul S. Dysart
May 15, 1993

Introduction

This report summarizes the event identification analysis performed on the data for the Dec. 31, 1992 Novaya Zemlya event. Regional data from four arrays were examined for this study. The best data for analysis was provided by the ARCESS array. Spectral features extracted from ARCESS waveforms were input to a backpropagation artificial neural network which was trained on a database consisting of 102 previously identified earthquakes and chemical explosions. The network classified the event as a chemical explosion.

The Data

Data from four regional arrays were available for examination: Apatity, ARCESS, Spitzbergen, and NORESS. The origin determined for this events by Carter, Ryaboy, and Israelson (1993) was 73.455 N, 55.818 E. A map showing this origin and the surrounding stations is shown in *Figure 1*. Array distances and azimuths from this origin are listed in *Table 1*.

Table 1

Array	Distance (deg)	Azimuth (deg)
Apatity	9.47	243
ARCESS	10.31	263
Spitzbergen	10.55	314
NORESS	20.73	256

Apatity

The Apatity array was the closest recording site examined for this event. However, the data were very noisy and not usable for identification. An example of the waveform data is shown in *Figure 2*. The predicted P-wave arrival time is approximately 30 seconds into the waveform; the predicted S-wave arrival time is approximately 150 seconds into the waveform. Neither arrival is apparent on the record. No clear arrivals were seen on other channels or beams. (Some of the channels were dead.) Data from Apatity were not used for the event identification.

ARCESS

Data from the ARCESS array proved to be the most useful for this identification study. An example of the waveform data is shown in *Figure 3*. P- and S-waves are clearly visible on the filtered signals. Lg-waves are not visible. There are some dropouts in the signal near the predicted Lg-wave arrival time, which show up as spikes on the filtered records. These dropouts are present on all channels.

Spitzbergen

The recording at the Spitzbergen array is not as clear as that at ARCESS, but both P- and S-waves are visible in the filtered traces (*Figure 4*). However, the S-wave appears to be of very short duration, and may indicate some sore of signal problem. The data from Spitzbergen were not used in this analysis.

NORESS

The NORESS array is the farthest recording site whos data were examined for this event. Waveform data for the central vertical element are shown in *Figure 5*. The predicted P-wave arrival time is 55 seconds into the waveform, and the S-wave arrival time is approximately 300 seconds into the waveform. The signal at this site is far below the noise; NORESS data were not used in this identification analysis.

Identification Analysis

Description of the Methodology

The methodology used for event identification is termed a *hybrid machine learning* approach. In pure supervised machine learning, data (raw time series, parameters, etc.) from a set of independently identified events (called a *training set*) are used as inputs to an artificial neural network which consists of a number of interconnected *nodes*. Each node represents a nonlinear transfer function whose input consists of the dot product of the incoming data and the associated *weights* which connect each node. During training, a steepest descent approach is used to compute these weights. Training is complete when the the error between the known and computed outputs are below a prescribed level.

Although extremely effective, the pure machine learning approach shares a number of problems with other mathematical modeling techniques. One is that the method treats all inputs equally at the start, so it is sensitive to fitting the identification on irrelevant inputs. A simple example in seismic identification

would be if all of the cases of chemical explosions in the training set occurred at one azimuth, while the earthquakes occurred at another. The network would likely give the greatest weight to event azimuth as the identifying parameter. Another example would be if all of the explosions were of magnitude 2, while the earthquakes spanned a range of magnitudes. Any new event being identified by the network whose magnitude was 2 would likely be identified as an explosion. Another problem is that a large enough network can be trained to fit any distribution of data, regardless of complexity. This may have advantages in some cases, but if outliers exist in the training set, these will be incorporated into the model fit.

To mitigate these problems, the approach we take utilizes techniques from statistics and classical pattern recognition *before* machine learning takes place. The goal is to minimize the number of input parameters, use only relevant parameters, utilize the parameters whose distributions provide the greatest class separability, and minimize the network size. This is accomplished by ranking the parameters in terms of their Mahalanobis Distances (difference in class means divided by sum of class variances), then determining any correlations between parameters, and finally performing a Principal Components Analysis to determine the dimensionality of the data and aid in the design of the network with the smallest number of connections. Hence, the methodology is called hybrid machine learning.

As described in the summary paper by Pulli and Dysart (1992), the final design used for the artificial neural network consists of an input layer with 10 nodes, a single hidden layer with 2 nodes, and an output layer with one node. This network architecture is shown in *Figure 6.*

Identification Analysis

The identification analysis using the backpropagation neural network utilized data only from the ARCESS array. As stated above, only Pn and Sn waves were visible at this array. Spectral parameters were determined using all array elements, with bad channels screened and deleted from the calculation. The values of the six parameters determined are shown in *Table 2.*

Table 2

Pn/ Sn broadband:	0.81	**Pn/ Sn 10-20 Hz:**	0.75
Pn/ Sn 2-5 Hz:	0.76	**Pn cepstral variance:**	0.59
Pn/ Sn 5-10 Hz:	0.89	**Sn cepstral variance:**	0.61

When input to the trained neural network, the event was classified as a chemical explosion. *Figure 7* shows the output of the neural network for the 102 training events as well as the output for the event under study. The Dec. 31 event clearly

falls within the chemical explosion cluster.

Discussion

In a telephone discussion with Dr. Alan Ryall on April 14, we were informed that there was no record of chemical blasting on Novaya Zemlya on the day of the event in question. All non-seismic evidence apparently points toward a natural earthquake as the source type. If this was an actual earthquake, then the question becomes, why did the event identification fail?

One possible reason is that all of the training events used to date have been recorded by the NORESS array, whereas the Dec. 31, 1992 event was both located in a new source area and recorded at another array (ARCESS). Source and propagation effects may be different for this scenario. In addition, Lg waves have proven to be an effective identification tool, at least for the events at NORESS. Lg waves are not observed on the records for this event.

Further insight can be gained by an examination of the six individual parameters extracted for this event. This can be done in two ways. *Figure 8* shows the histograms of each of the six parameters for the training set, as well as the values of each parameter for the event under study. The red columns indicate the number of occurrences of the parameter for chemical explosions, while the green columns are for earthquakes. Ten bins are used to span each range of parameter values. The value of the Pn/Sn broadband spectral ratio falls near the peak in the distribution for chemical explosions. This is also true for the value of the Pn/Sn spectral ratio from 2-5 Hz. The distribution of Pn/Sn spectral ratios from 5-10 Hz is broad for explosions, but this parameter value for the event in question still falls within the range for explosions. The value of the Pn/Sn spectral ratio from 10-20 Hz is well below the peak in the distribution for chemical explosions and fits into the distribution of earthquakes. Cepstral variances for earthquakes are understandably low, while explosions show a broad range of values depending on the amount of ripple firing present in the explosion. The values of Pn and Sn cepstral variances are low for the event under study, and easily fall within the ranges for earthquakes. However, if a single explosive charge were used, the cepstral variance would be low.

Another way of looking at the parameters is with a scatterplot. In this way we see the relationships between the event under study and all other events individually. *Figure 9* shows a scatterplot of Pn/Sn broadband spectral ratios versus Pn/Sn spectral ratios from 2-5 Hz. Red symbols indicate chemical explosions from the training set, green symbols indicate earthquakes, and the blue symbol indicates the event under study. Although there is no clear boundary between the event types, the event under study falls near a large cluster of chemical explosions in the training set. The scatterplot of Pn/Sn for 5-10 Hz versus 10-20 Hz shows

much more overlap, and the event under study falls close to the apparent boundary between explosions and earthquakes. Values of Pn and Sn cepstral variance, shown in *Figure 10* again overlap and the event under study falls near the boundary between the two classes of events.

In summary, it appears that the values of the identification parameters used in our methodology for the Dec. 31, 1992 Novaya Zemlya event fall near the boundary of earthquakes and chemical explosions in our database of independently identified events, with a slight bias toward the explosion side of the distributions. There are no Lg waves available for analysis, and our previous work indicates that these are important for event identification.

References

Carter, J., V. Ryaboy, and H. Israelsson (1993), Location of the event by CSS Staff, in Notes on Analysis of 31 December 1992 NZ Event, A. Ryall, ed.

Pulli, J. and P. Dysart (1992), Analysis and Testing of High-Frequency Regional Seismic Discriminants, Final Report, PL-TR-92-2125

Dec. 31, 1992 NZ Event and Surrounding Stations

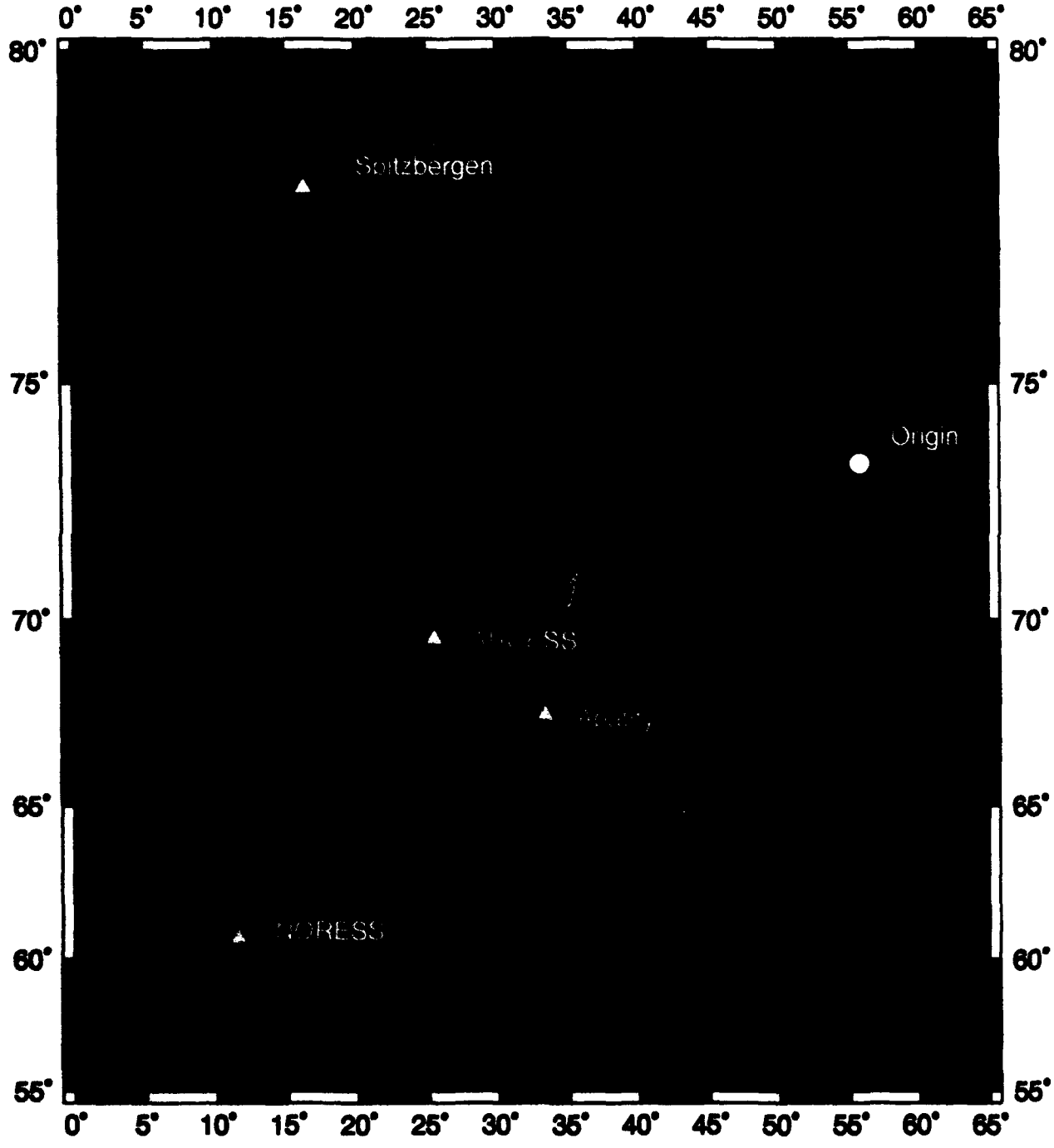

Figure 1

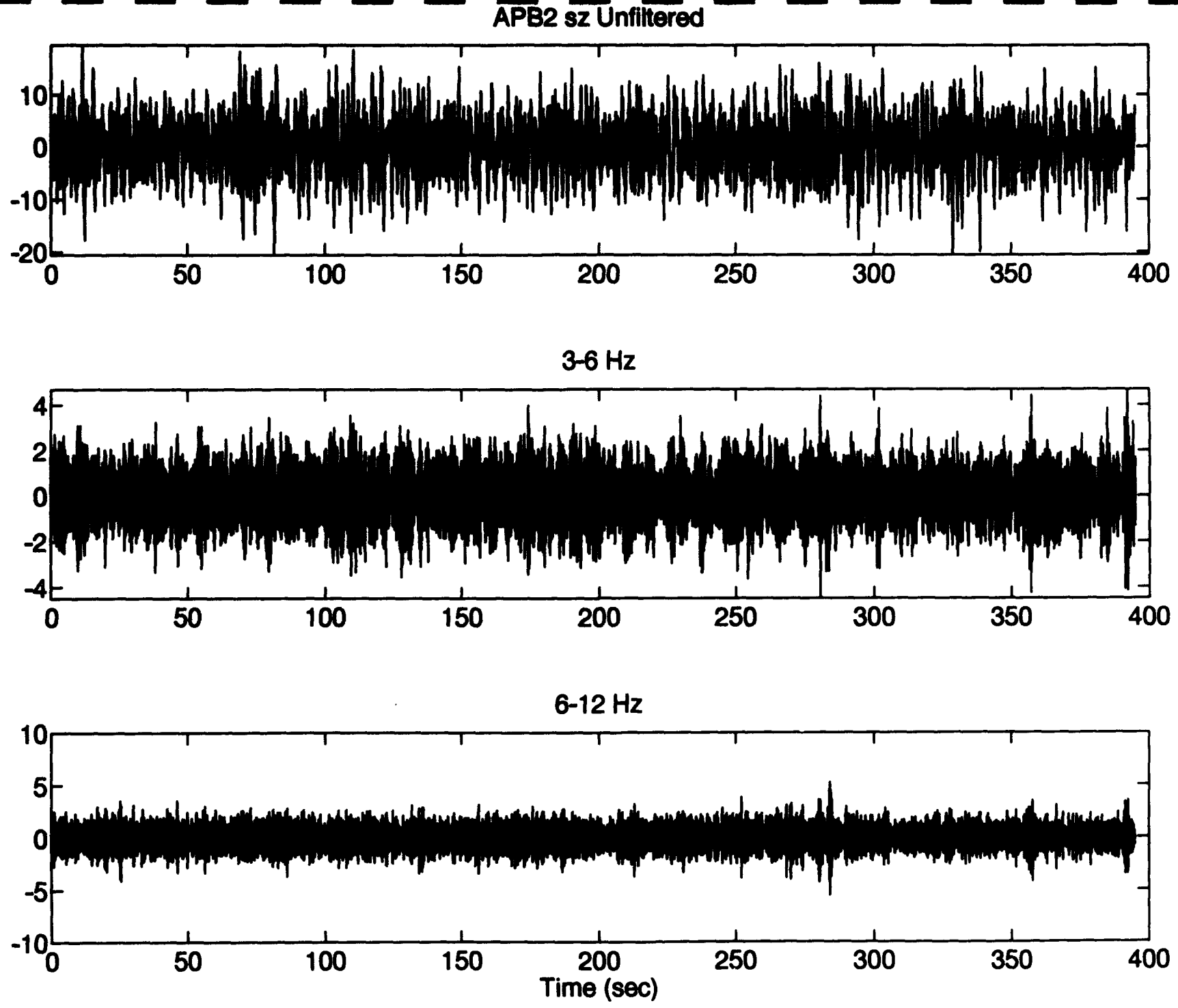
APB2 sz Unfiltered
10
0
-10
-20
0
50
100
150
200
250
300
350
400
3-6 Hz
4
2
0
-2
-4
0
50
100
150
200
250
300
350
400
6-12 Hz
10
5
0
-5
-10
0
50
100
150
200
250
300
350
400
Time (sec)

Figure 2

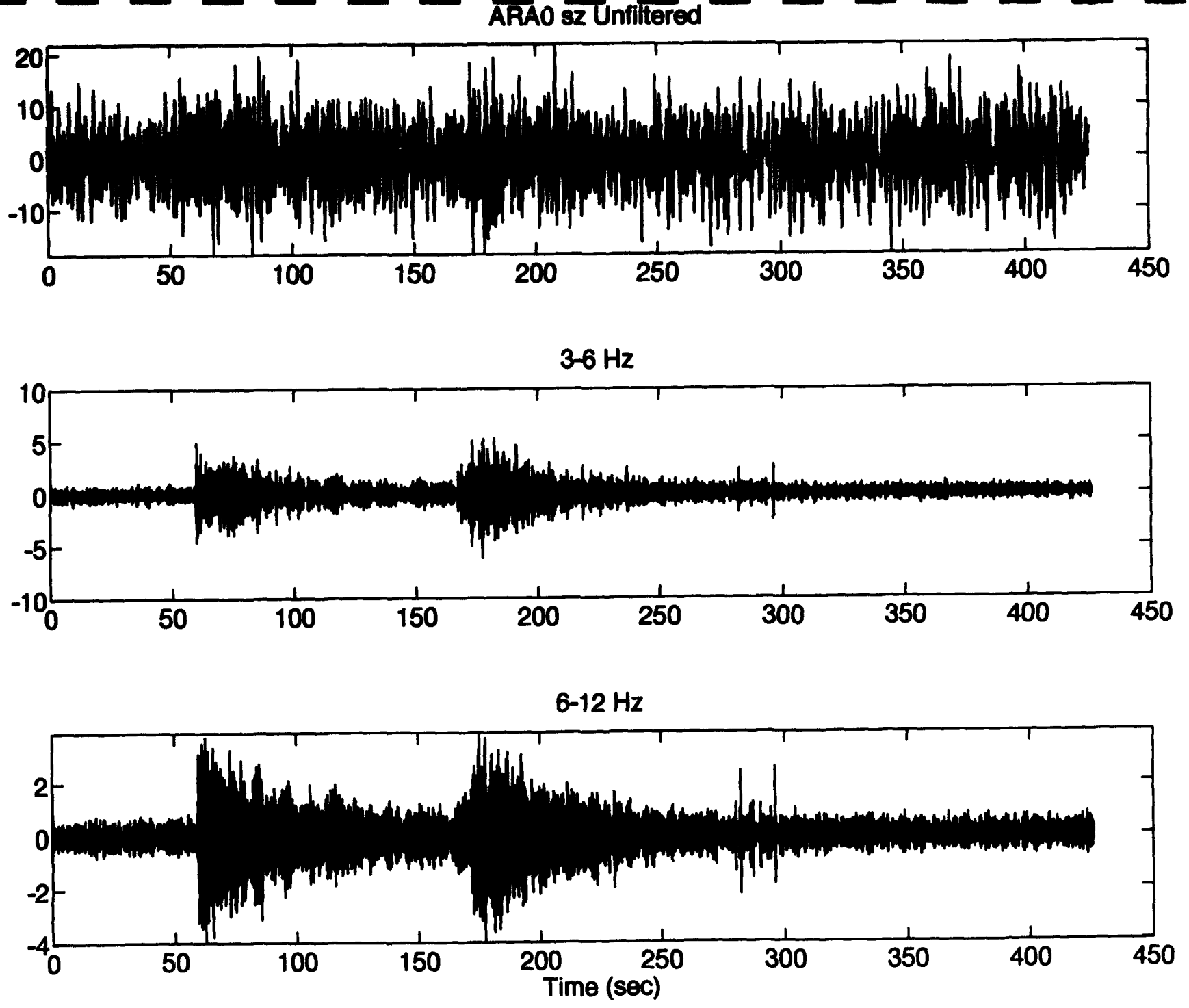
ARA0 sz Unfiltered
20
10
0
-10
0
50
100
150
200
250
300
350
400
450
3-6 Hz
10
5
0
-5
-10
0
50
100
150
200
250
300
350
400
450
6-12 Hz
2
0
-2
-4
0
50
100
150
200
250
300
350
400
450
Time (sec)

Figure 3

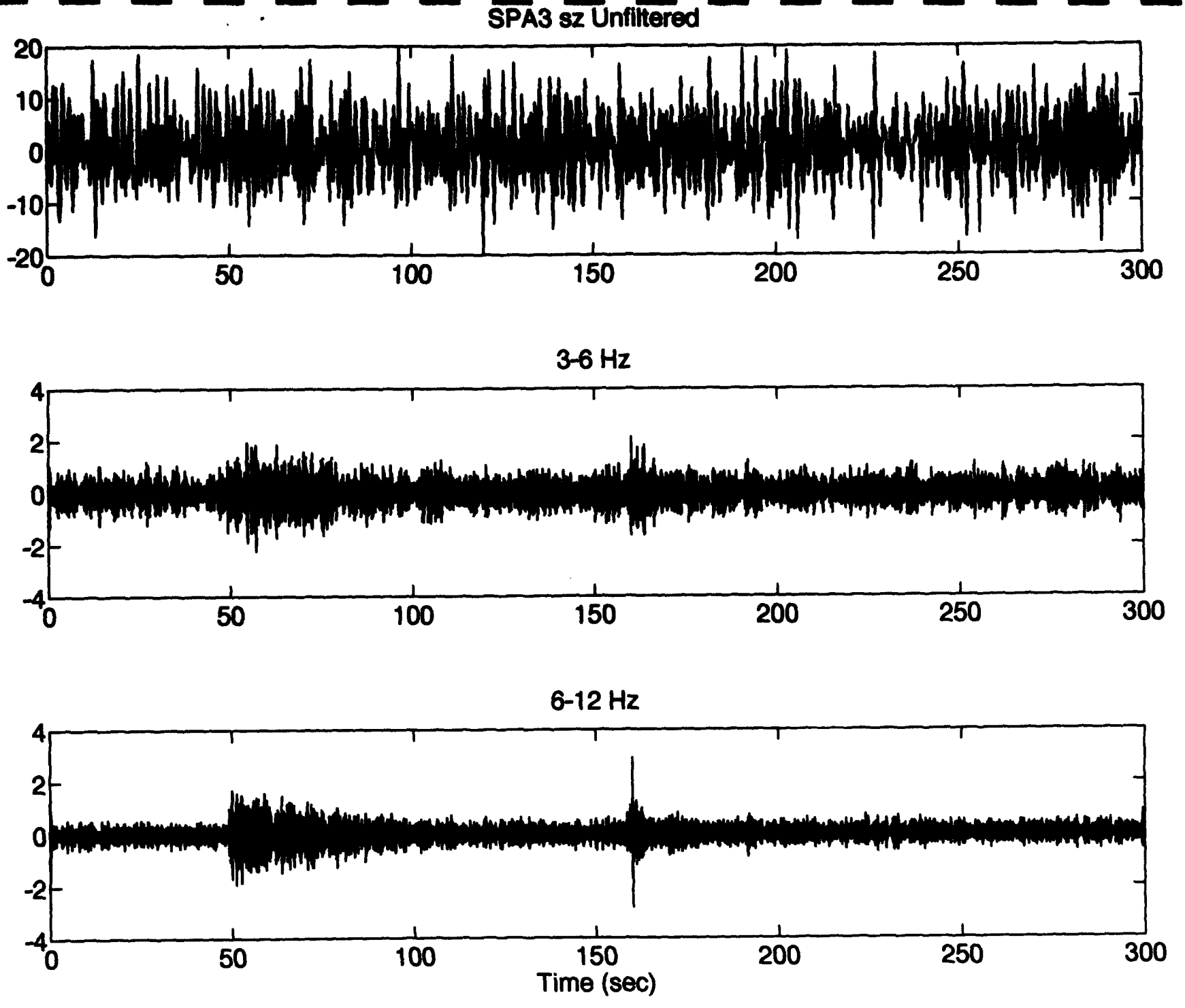
SPA3 sz Unfiltered
20
10
0
-10
-20
0
50
100
150
200
250
300
3-6 Hz
4
2
0
-2
-4
0
50
100
150
200
250
300
6-12 Hz
4
2
0
-2
-4
0
50
100
150
200
250
300
Time (sec)

Figure 4

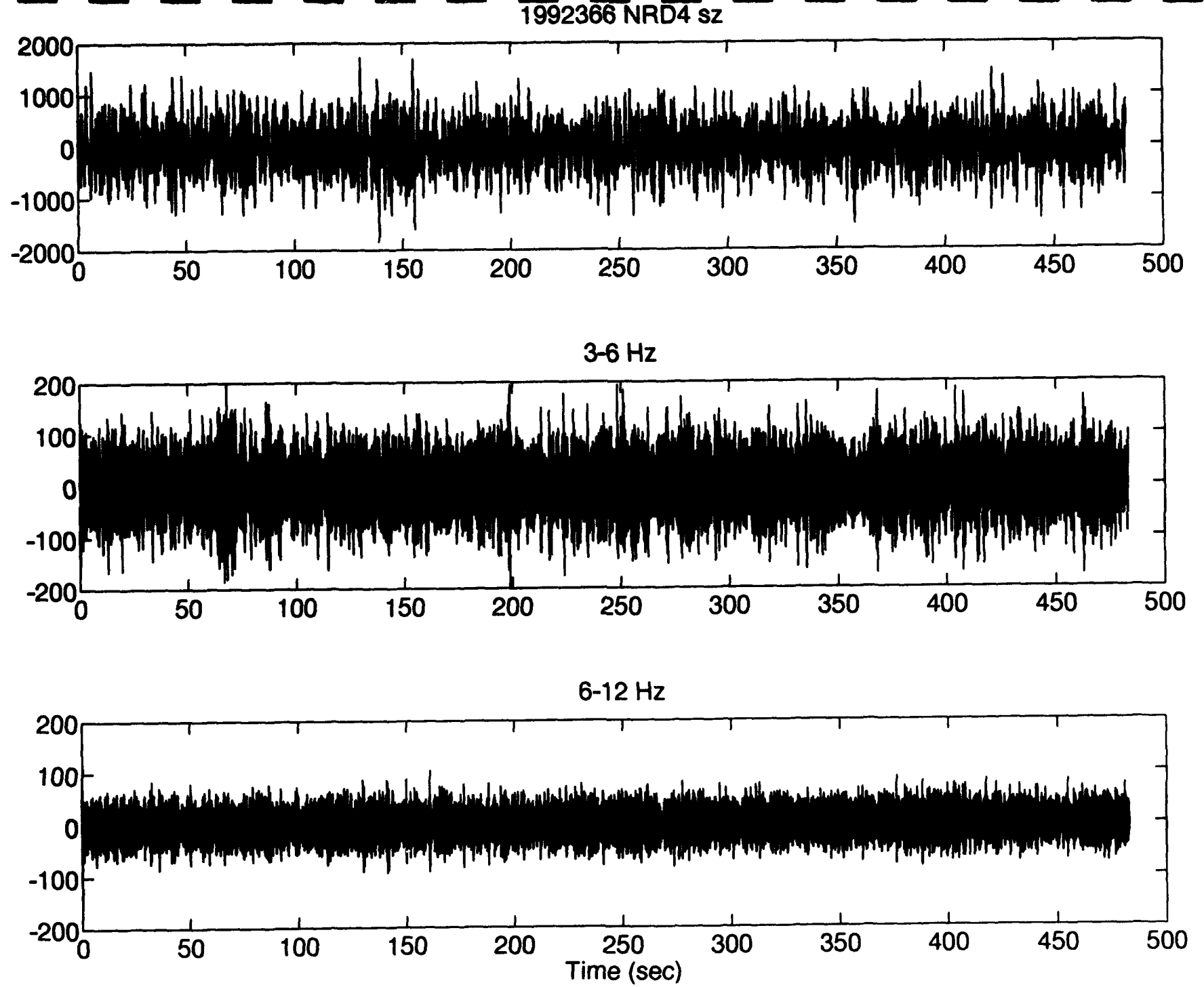
1992366 NRD4 sz
2000
1000
0
-1000
-2000
0
50
100
150
200
250
300
350
400
450
500
3-6 Hz
200
100
0
-100
-200
0
50
100
150
200
250
300
350
400
450
500
6-12 Hz
200
100
0
-100
-200
0
50
100
150
200
250
300
350
400
450
500
Time (sec)

Figure 5

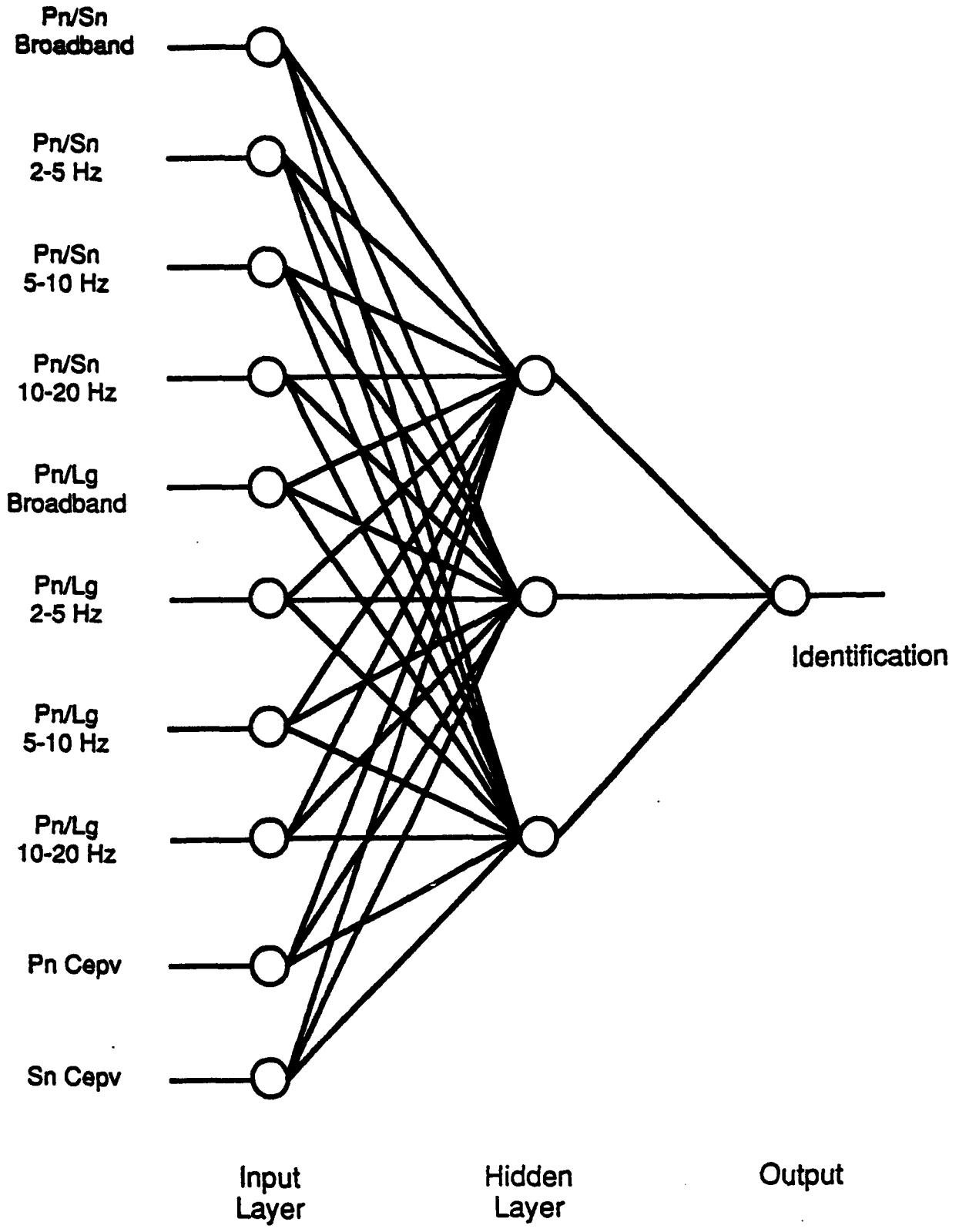
Pn/Sn
Broadband
Pn/Sn
2-5 Hz
Pn/Sn
5-10 Hz
Pn/Sn
10-20 Hz
Pn/Lg
Broadband
Pn/Lg
2-5 Hz
Pn/Lg
5-10 Hz
Pn/Lg
10-20 Hz
Pn Cepv
Sn Cepv
Identification
Input
Layer
Hidden
Layer
Output

Figure 6

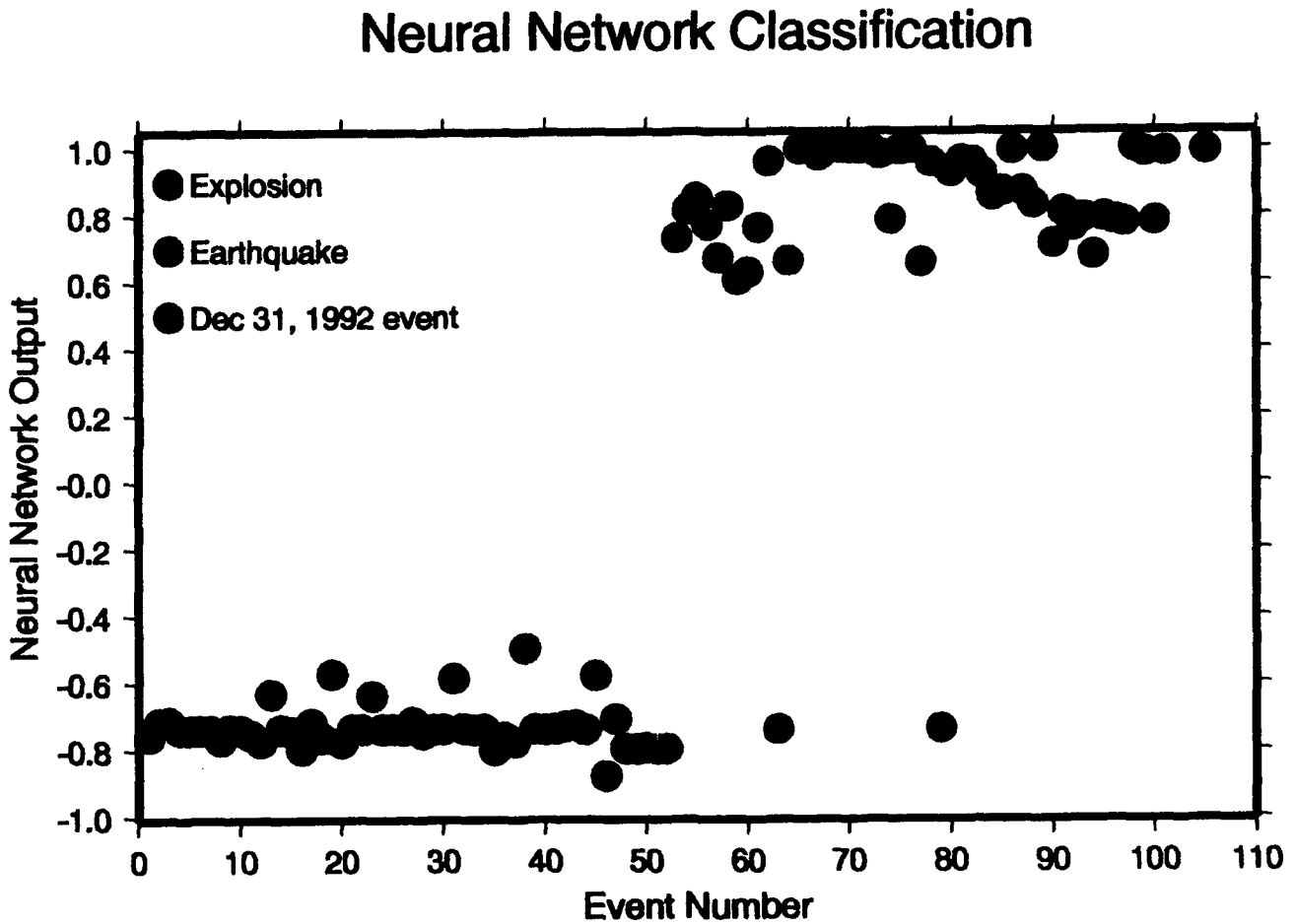
Neural Network Classification
Explosion
Earthquake
Dec 31, 1992 event
Neural Network Output
1.0
0.8
0.6
0.4
0.2
-0.0
-0.2
-0.4
-0.6
-0.8
-1.0
0
10
20
30
40
50
60
70
80
90
100
110
Event Number

Figure 7

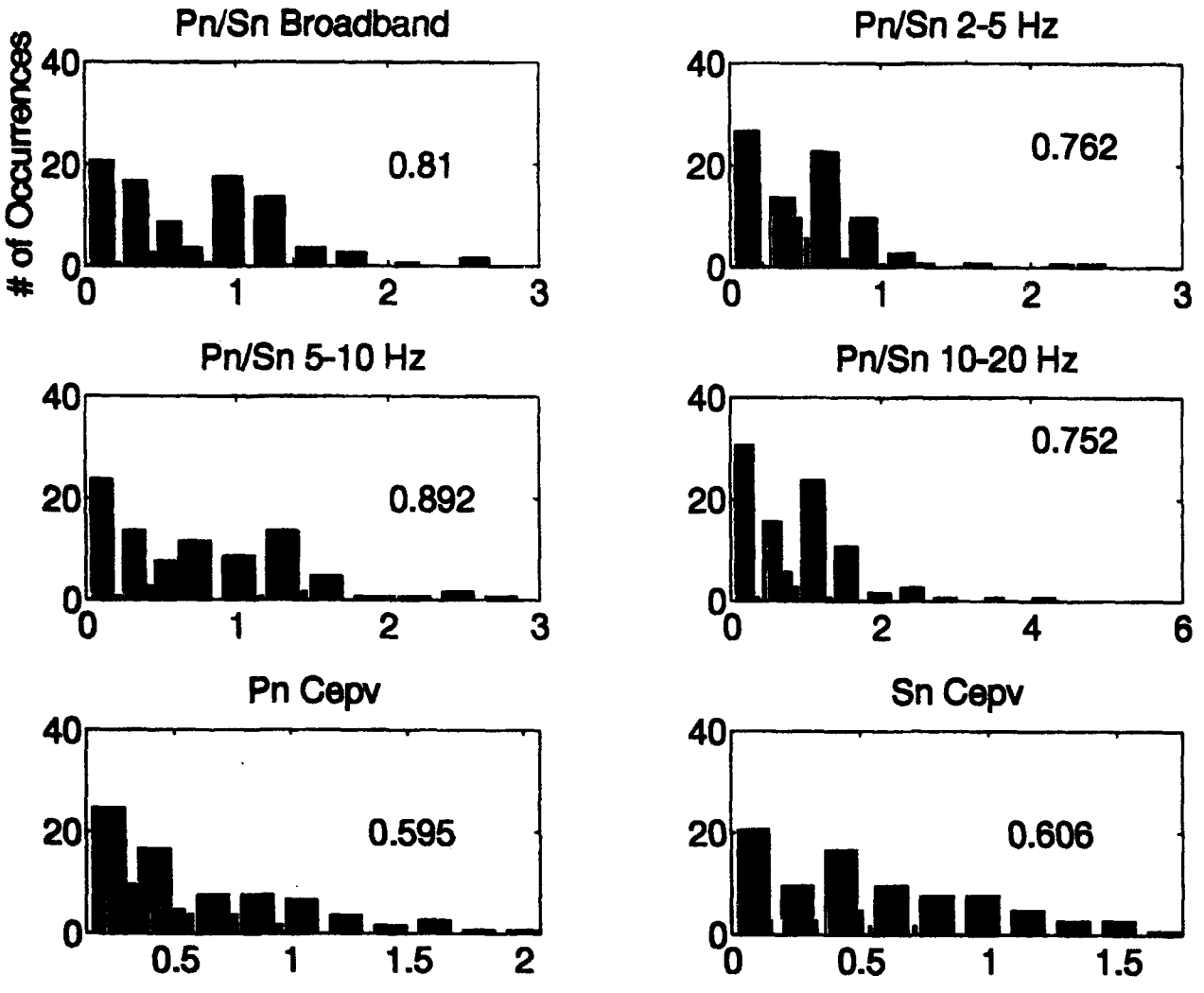
Pn/Sn Broadband
# of Occurrences
0.81
Pn/Sn 2-5 Hz
0.762
Pn/Sn 5-10 Hz
0.892
Pn/Sn 10-20 Hz
0.752
Pn Cepv
0.595
Sn Cepv
0.606

Figure 8

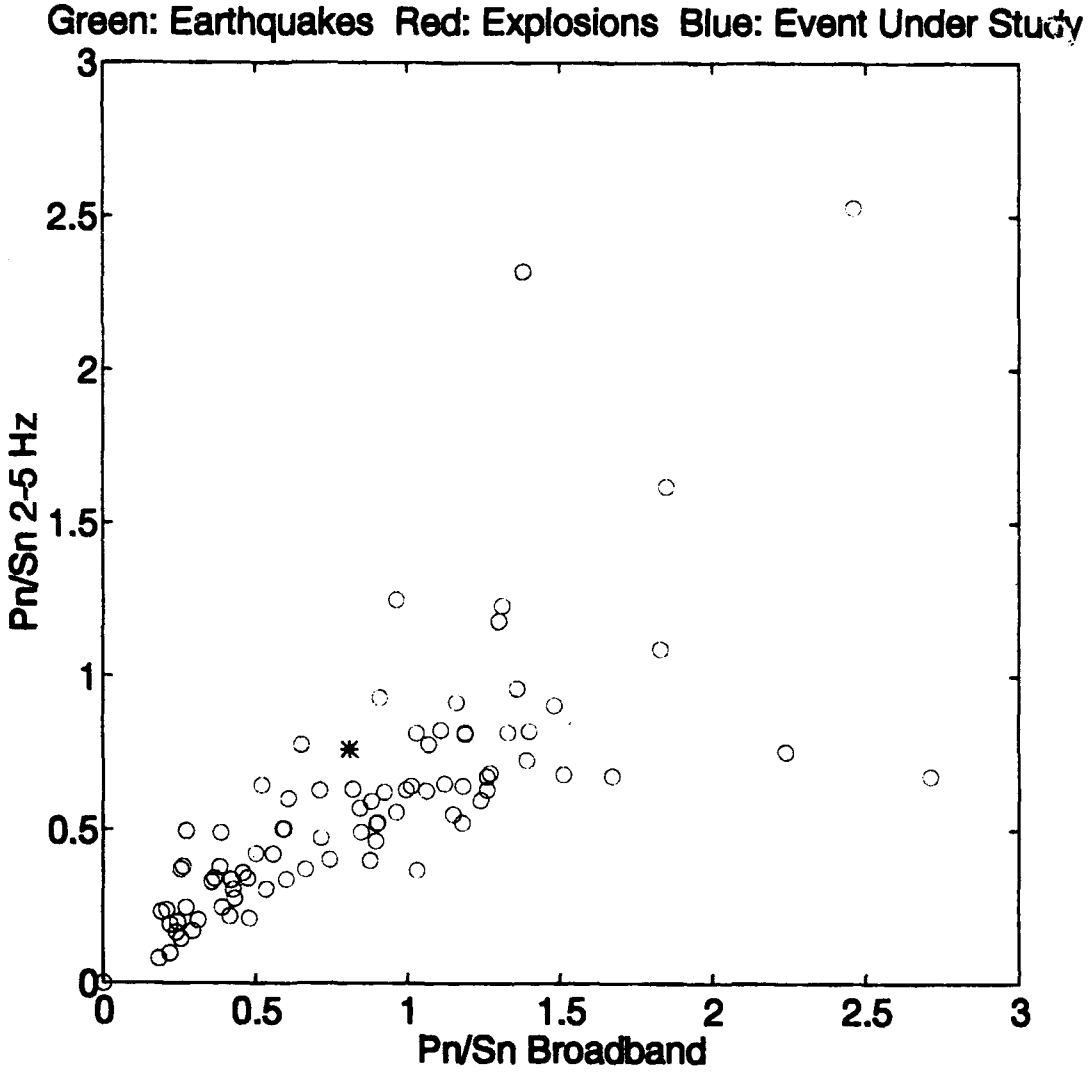
Green: Earthquakes Red: Explosions Blue: Event Under Study
Pn/Sn 2-5 Hz
Pn/Sn Broadband
0
0.5
1
1.5
2
2.5
3

Figure 9

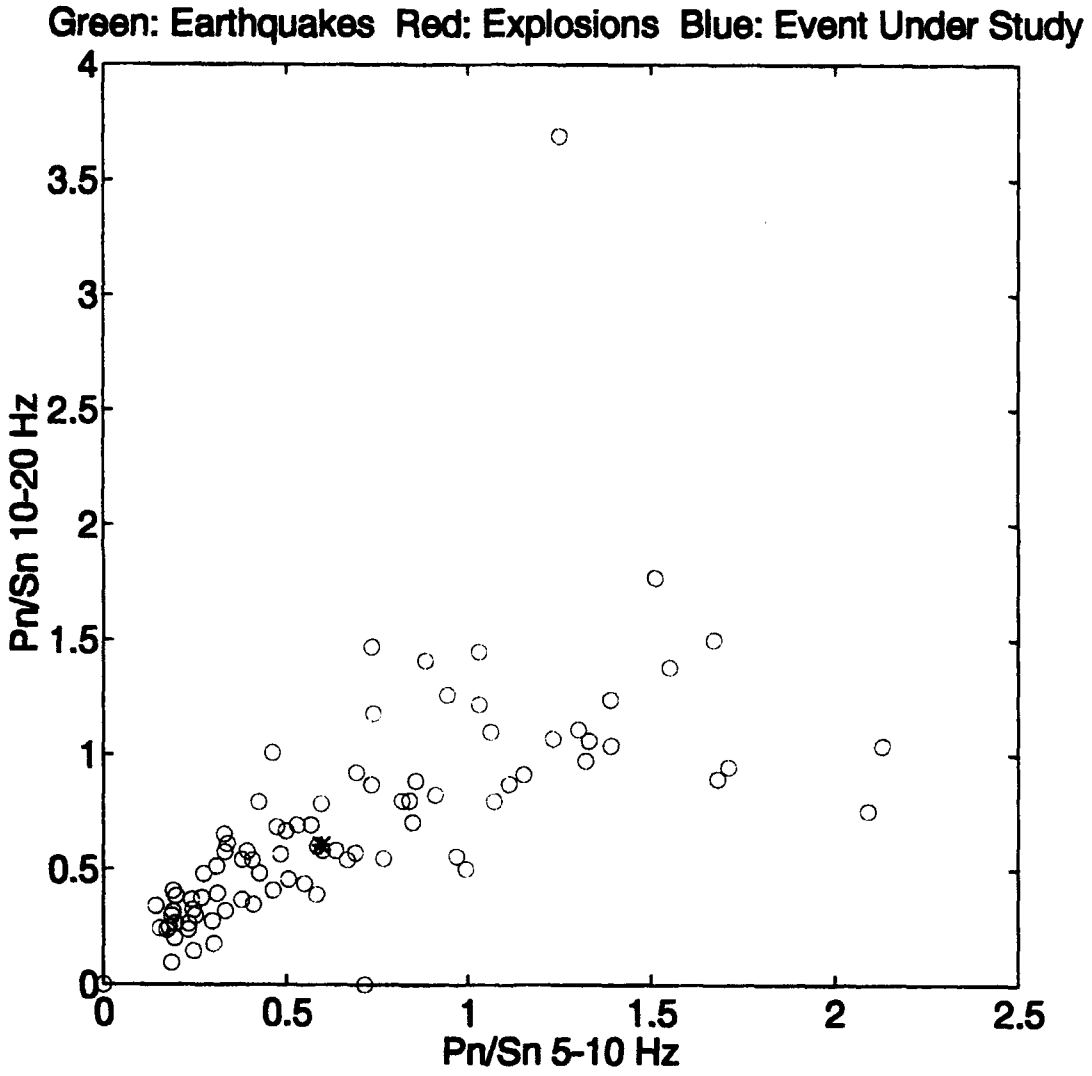
Green: Earthquakes Red: Explosions Blue: Event Under Study
Pn/Sn 10-20 Hz
Pn/Sn 5-10 Hz
0
0.5
1
1.5
2
2.5
3
3.5
4

Figure 10

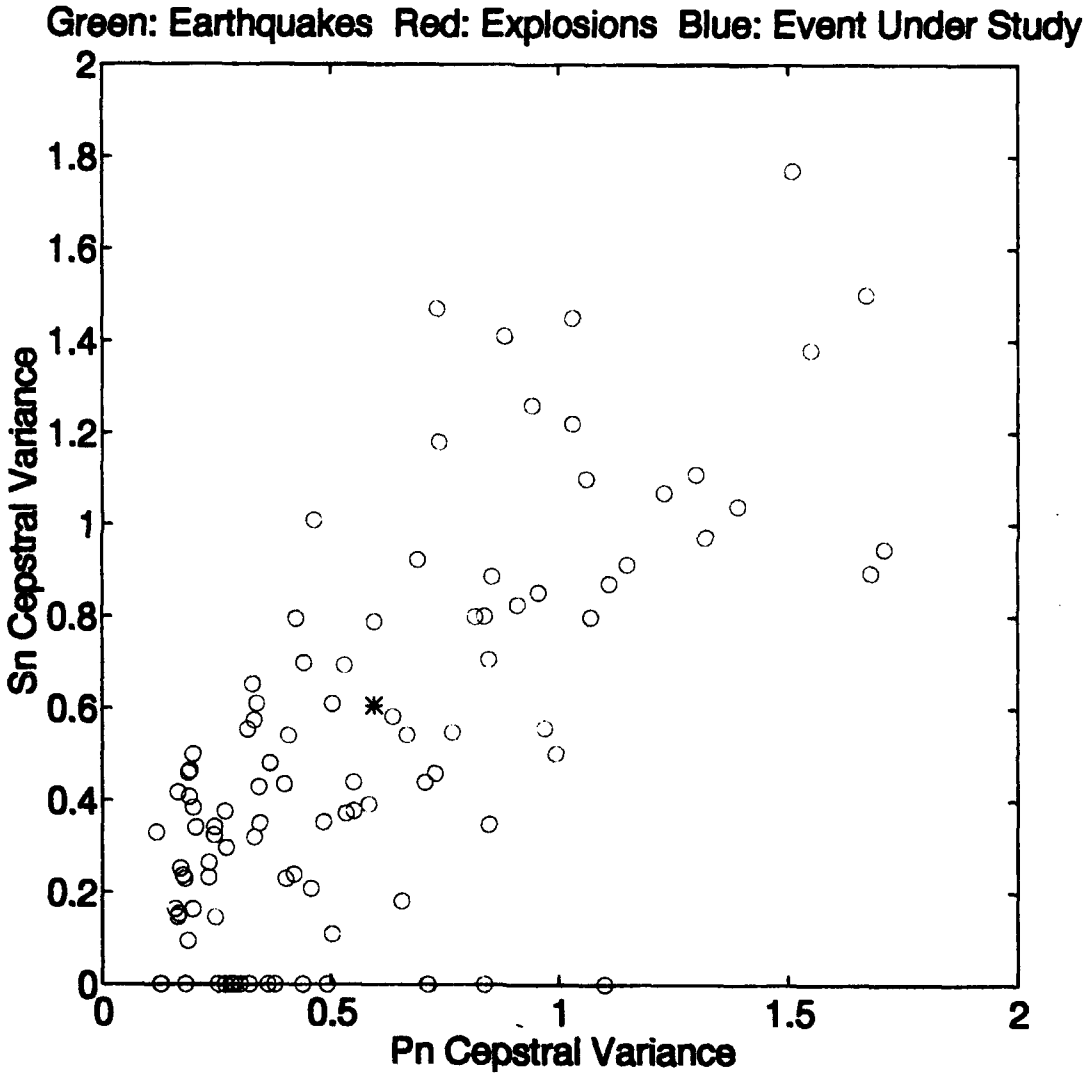
Green: Earthquakes Red: Explosions Blue: Event Under Study
Sn Cepstral Variance
Pn Cepstral Variance
0
0.2
0.4
0.6
0.8
1
1.2
1.4
1.6
1.8
2
0
0.5
1
1.5
2

Figure 11

EVENT IDENTIFICATION ANALYSIS OF THE NOVAYA ZEMLYA EVENT ON 31 DECEMBER 1992 USING OUTLIER AND CLASSIFICATION LIKELIHOOD RATIO TESTS

Copy No. _____ MRC-R-1449

Technical Report

Event Identification Analysis of the Novaya Zemlya Event on 31 December 1992 using Outlier and Classification Likelihood Ratio Tests

Mark D. Fisk, MRC
Henry L. Gray, SMU

June 1993

Sponsored by: Defense Advanced Research Projects Agency
Nuclear Monitoring Research Office

Issued by: Phillips Laboratory Under
Contract No. F19628-90-C-0135

Prepared by: MISSION RESEARCH CORPORATION
735 State Street, P. O. Drawer 719
Santa Barbara, CA 93102

Event Identification Analysis of the Novaya Zemlya Event on 31 December 1992 using Outlier and Classification Likelihood Ratio Tests

Mark D. Fisk
Mission Research Corporation
735 State Street
Santa Barbara, CA 93102

and

Henry L. Gray
Southern Methodist University
Department of Statistical Science
Dallas, TX 75275

1. INTRODUCTION

Using seismic amplitude ratios recorded at ARCESS, we have performed statistical tests of hypothesis in order to assess the identification of an event at Novaya Zemlya (NZ) on 31 December 1992. Based on origin analysis by the Intelligent Monitoring System (Bache et al., 1990), this was a small regional event (M_L 2.26) occurring at origin time 12/31/92 09/29:24 (GMT), latitude 73.58 and longitude 55.21. We will refer to this event by its origin identification number, ORID=361575.

The methods used in our analysis are based on the likelihood ratio for outlier detection and classification. These methods were developed at MRC and SMU (Baek et al., 1992, 1993) and are generalizations of previously well-established discrimination procedures based on the likelihood ratio (e.g., Anderson, 1984; Seber, 1984; Johnson and Wichern, 1988). The tests were applied to event 361575 using training data for previous nuclear explosions, earthquakes and quarry blasts with similar (but not identical) paths to ARCESS. The data sets were provided to us by Baumgardt (1993), who also used them to classify this event using an alternative classification approach.

The remainder of this report is organized as follows. In Section 2 we describe the training sets and the discriminants used in the analysis, and present novel graphical displays of the discriminants as a means to better visualize the multivariate data. In Section 3 we provide brief descriptions of the statistical methods used to classify event 361575, as well as preliminary training set analyses applied to the data to ensure that the appropriate assumptions, required by the discriminant analysis methods, hold. In Section

4 we present the results of the discriminant analysis tests and in Section 5 we provide our conclusions and recommendations for further analysis.

2. Training Data Sets and Discriminants

The feature data (discriminants) used here were obtained from seismic waveform analysis performed by Baumgardt (1993) using the Intelligent Seismic Event Identification System (ISEIS) (e.g., Baumgardt et al., 1991). They consist of Pn/Sn ratios of maximum amplitude in five frequency bands, 4-6, 5-7, 6-8, 8-10, and 8-16 Hz (which we denote Pn/Sn[max;8-16], for example) recorded by ARA0. Data for four events at NZ were provided, three of which are known nuclear explosions (EXs) and the fourth is the event in question. For comparison we also used Pn/Sn[max] in the same five frequency bands for 53 quarry blasts (QBs) occurring in the Kola Peninsula region, 24 earthquakes (EQs) occurring in the Steigen region, and 5 EQs occurring in the direction of the Mid-Atlantic Ridge.

A map of the event and seismic array locations is shown in Figure 1. The green circles represent the EQs in the Steigen region of Norway (lower left) and in the direction of the Mid-Atlantic Ridge (upper center). The blue squares show the locations of the Kola Peninsula QBs. The red triangles represent the 3 previous EXs at NZ, and the yellow star depicts the location of the event at NZ on 31 December 1992. Last, the white circle shows the location of ARCESS.

A scatter plot of the amplitude ratios for all of these events is shown in Figure 2. The legend in the upper lefthand corner associates the markers with the event types; event 361575 is listed as RU for regional unknown. The five frequency bands in which the ratios were computed are listed along the bottom. It is evident that the ratios for event 361575 are significantly different than those for either the NZ EXs or the Steigen EQs in all frequency bands. There are some bands for which 361575 has Pn/Sn values similar to the Mid-Atlantic Ridge EQs (e.g., 4-6, 5-7 and 8-10 Hz), while it has noticeably different values in the 6-8 and 8-16 Hz bands. The Pn/Sn values for event 361575 are consistent with those of the Kola QBs in all frequency bands.

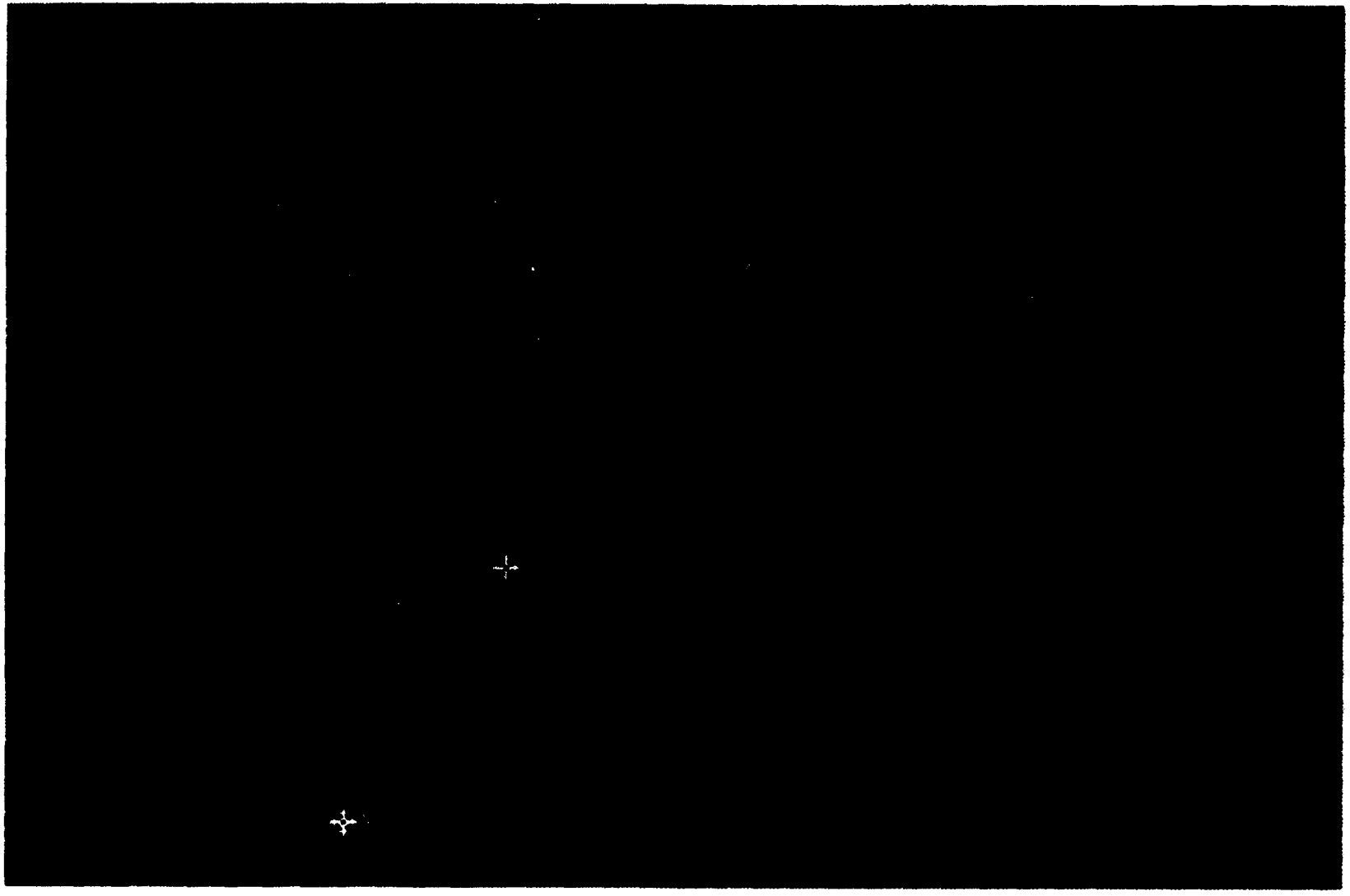

Figure 1. Map showing event and seismic array locations used in event identification analysis of Novaya Zemlya event 361575.

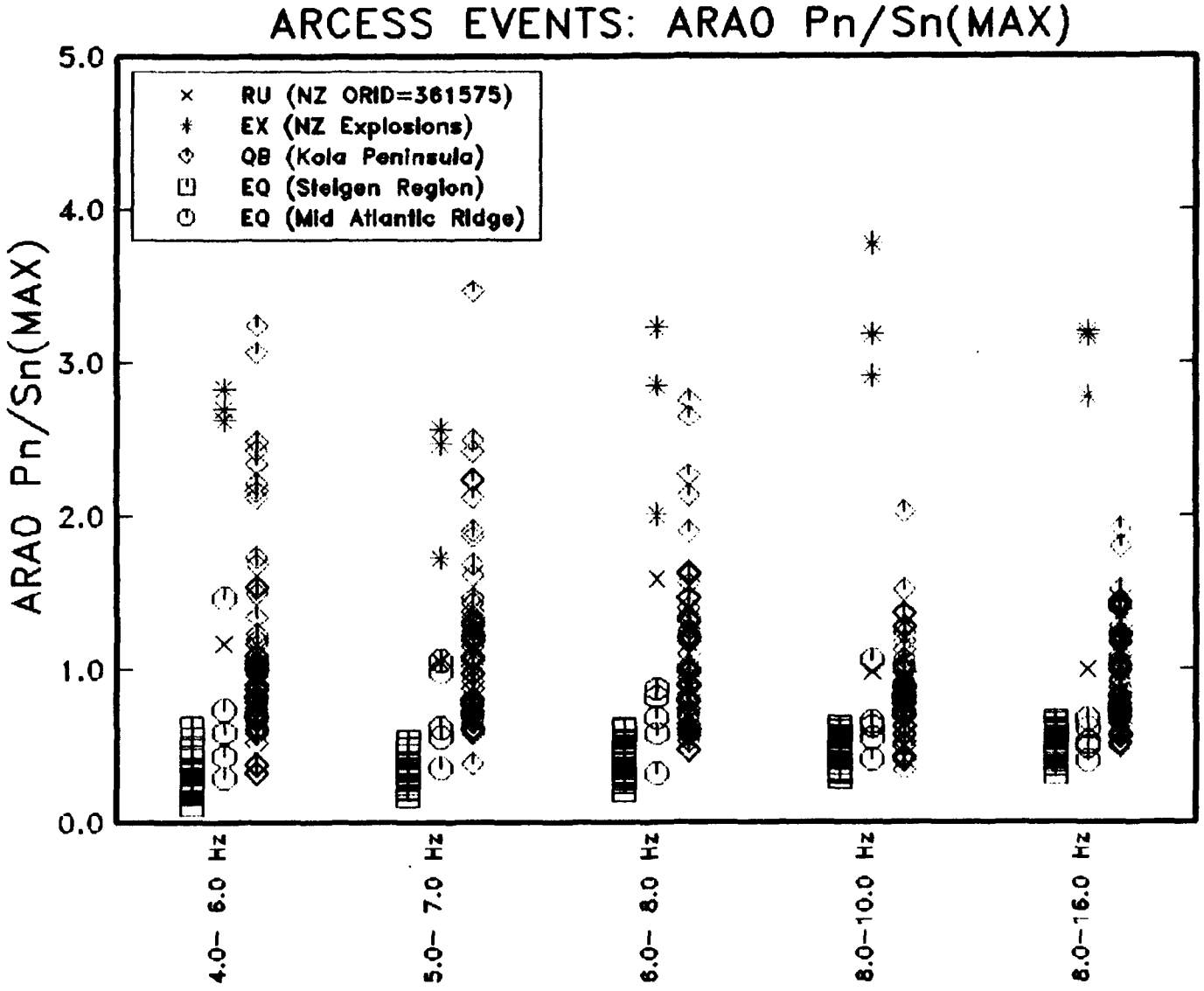

Figure 2. Scatter plot of Pn/Sn maximum amplitude ratios in five frequency bands for all seismic events used here.

We have also generated Andrews' Fourier plots as a means to visualize how the multivariate discriminants compare as a whole. Andrews (1972) suggested a useful technique to represent multivariate data as a 2-dimensional plot using a Fourier series expansion. For each event, the coefficients of the series are the values of the discriminants that have been standardized so that all discriminants have the same overall mean and standard deviation computed over all of the events; this prevents a single discriminant from completely dominating the plot.

The Andrews' plots for all of the events considered here are shown in Figures 3. Only four of the amplitude ratios were used as coefficients of the Fourier series; they are listed in the upper lefthand legend. The line types and colors for the various types of events are given in the righthand legend. Note that the curve for event 361575 is significantly different than those for previous NZ EXs, as well and Steigen and Mid-Atlantic Ridge EQs, while it is quite similar to a number of the curves for Kola QBs. To clarify this, Figure 4 shows a comparison for all but the Kola QBs and Figure 5 shows a comparison for only event 361575 and the Kola QBs. Note that the curve for 361575 does look similar to the curve for one of the Mid-Atlantic Ridge EQs in the middle of the plot. This is due to the fact that the values of Pn/Sn are nearly identical in the 5-7 Hz band (cf. Figure 2). Overall, however, the curves do look different. From Figure 5 it is clear that event 361575 has very similar amplitude ratios to the Kola QBs in all of the frequency bands.

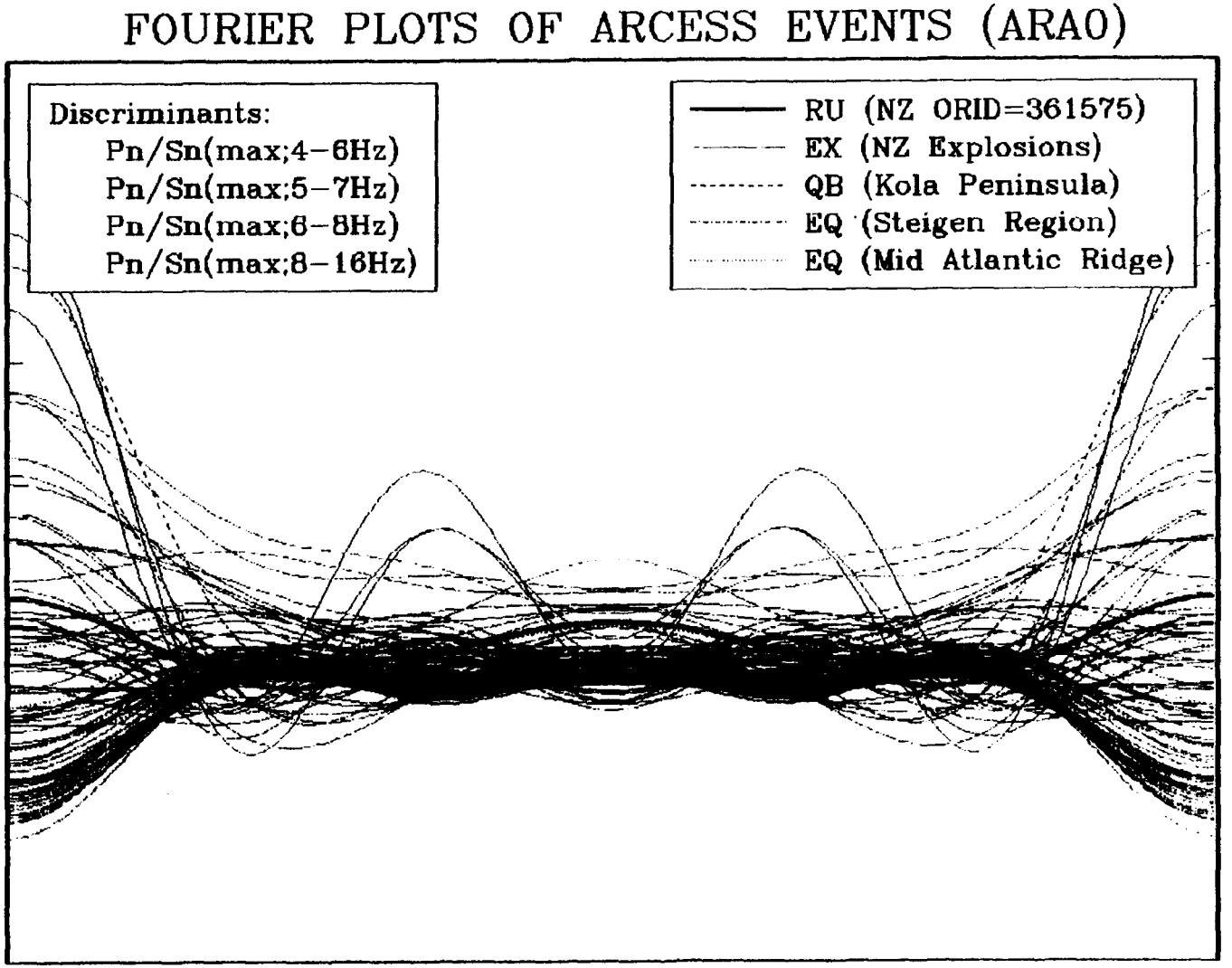

Figure 3. Andrews' plots for all events used in this study. The discriminants used as coefficients of the Fourier series are given in the lefthand legend and the line types and colors associated with the various event types are given in the righthand legend.

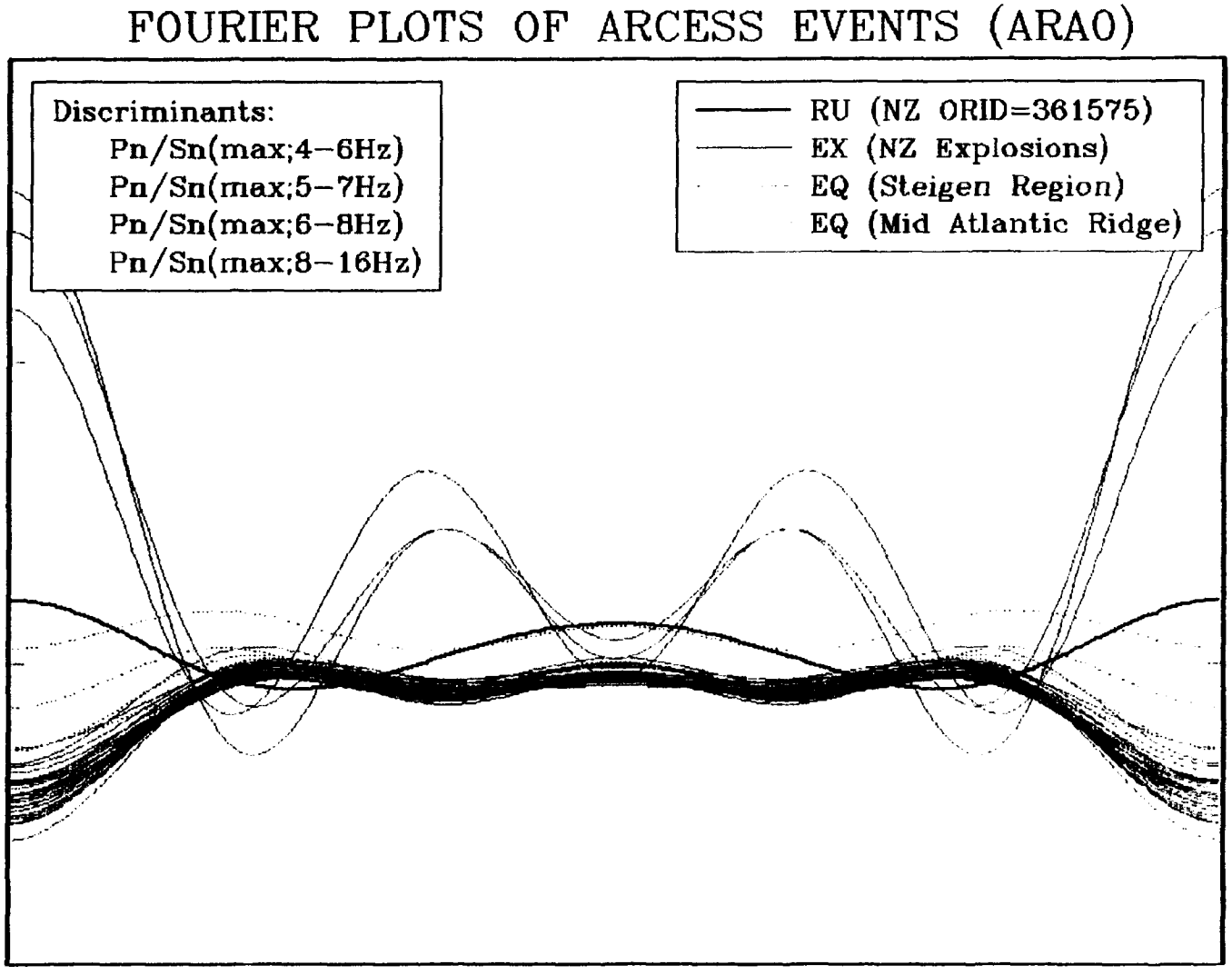

Figure 4. Andrews' plots for all events except the Kola quarry blasts.

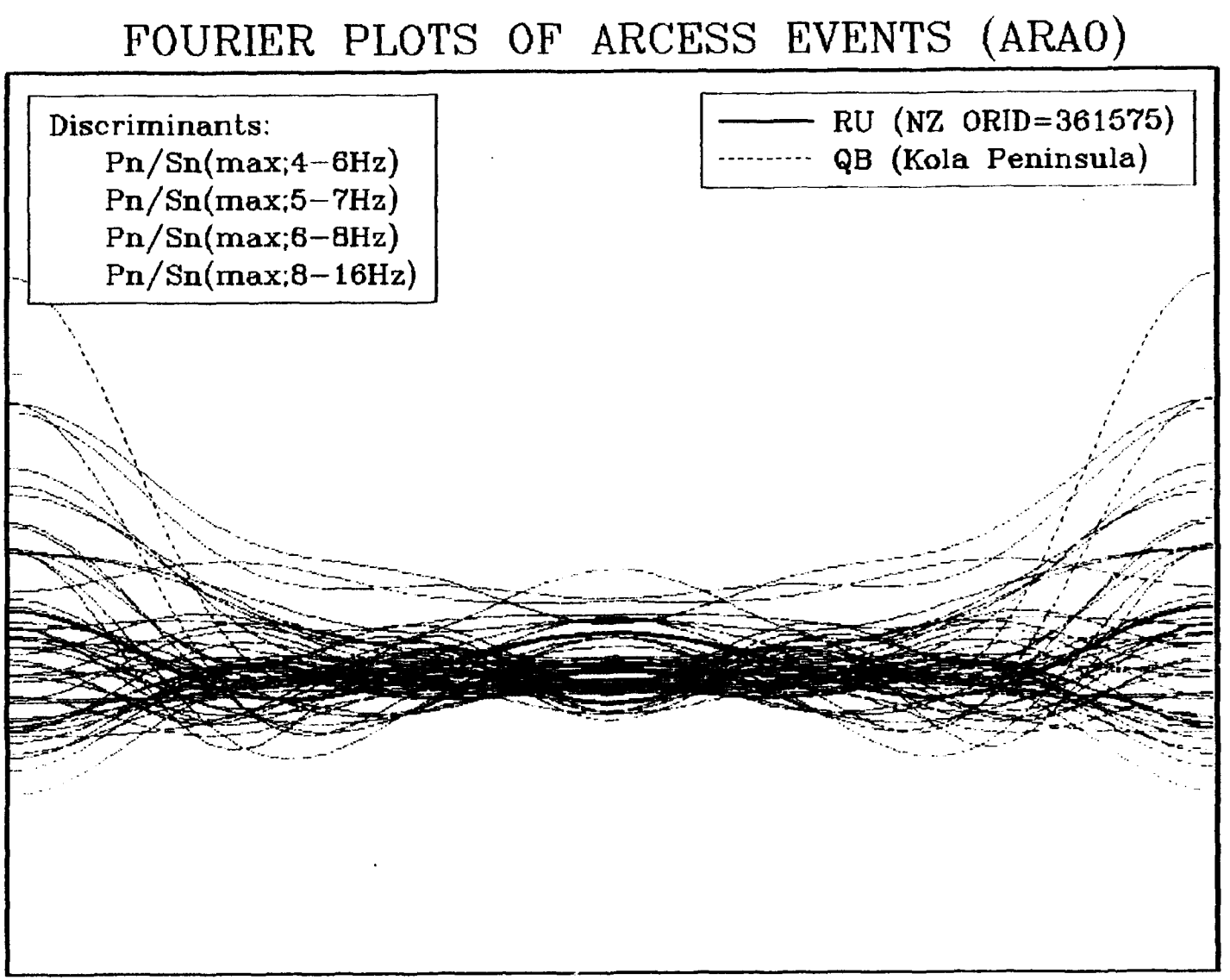

Figure 5. Andrews' plots for event 361575 and the Kola quarry blasts.

3. METHODS

3.1. Discriminant Analysis Methods

Among the crucial statistical issues associated with seismic event identification are the availability of useful training sets and the complicated statistics of discriminants. Data sets for new regions of interest may be extremely limited. Path differences often prohibit direct application of training sets to classification in new regions. Ground-truth data sets are being established, but progress is relatively slow. In addition, discriminants rarely have normal distributions, and the distribution type and covariance structure typically differ from one event type to the next (e.g., Baumgardt, 1992; Baumgardt et al., 1992). Some very useful discriminants are in fact discrete rather than continuous. Combinations of these issues have limited useful application of many statistical classification methods in the past. It is vital, however, for monitoring applications that these issues are all addressed with statistical rigor so that classification accuracy can be optimized and so that estimated error rates have precise meaning; improper treatment of discriminant distributions can lead to misclassifications and biased estimates of error rates.

To address these issues, MRC and SMU (Baek et al., 1992, 1993) have developed statistical methods for classification and outlier detection. The methods, based on the generalized likelihood ratio (GLR) and the bootstrap technique, have considerable flexibility to rigorously treat a mixture of continuous (e.g., amplitude and spectral ratios, spectral and cepstral variances, etc.) and discrete (e.g., presence of cepstral peaks, seismicity, deep/shallow, offshore/onshore, etc.) features, normal or non-normal statistics, equal or unequal covariance matrices, and different distribution functions for different event types. (For detailed presentations of the methods, see Baek et al., 1992, 1993; Gray et al., 1993. There is also extensive literature on the likelihood ratio methodology. For reviews, see Anderson, 1984; Seber, 1984; Johnson and Wichern, 1988).

The GLR outlier test is particularly useful for situations with training data limited to one class. Here a hypothesis test is used to determine whether an event belongs to the same population as the training data or not. For example, when monitoring a new region there may only be a handful of previously recorded events. In fact, we may not even know what the event type is for a particular set. The GLR outlier test can still be applied to flag peculiar events that are not "business as usual." A related application of the outlier test is to test training sets which lack ground-truth for possible contamination. In this way,

peculiar events can be flagged for further expert analysis or corroboration with bulletins, etc. Thus, the GLR outlier test allows monitoring to be performed under conditions for which minimal information is available.

The test statistic on which the outlier test is based is given by the ratio of the maximized likelihood computed under the null hypothesis that the event belongs to the same class as the training set, to the maximized likelihood computed under the alternative hypothesis that the event does not belong to this class. Small values of the ratio indicate that the event is an outlier. The bootstrap technique (Efron, 1979, 1982) is used to set the critical value of the test such that the false alarm rate is fixed. Figure 6 shows a schematic of this procedure, where the distribution of the likelihood ratio is obtained by bootstrapping. The critical value is set such that there are only $100\alpha\%$ of the EQs in the tail that would be rejected falsely, where α is the significance level of the test.

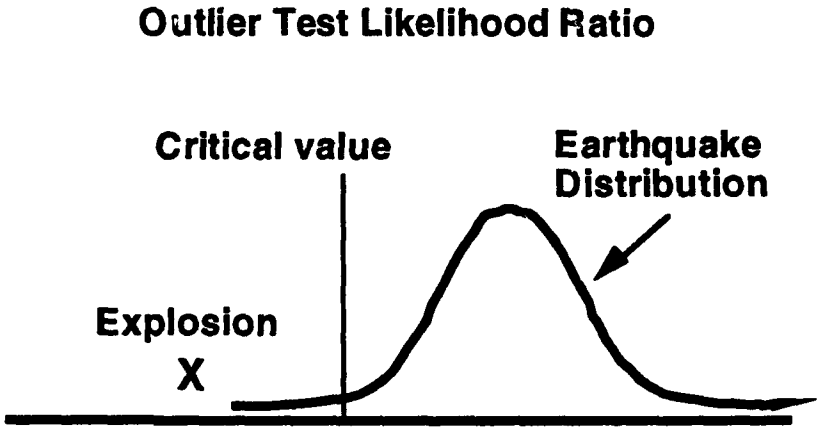

Figure 6. Schematic illustrating the outlier test based on the likelihood ratio test.

For situations where more training data are available, the GLR classification method is an improved procedure to optimize classification accuracy. In this case, training data for all available classes are used and the event in question is allocated into one of two or more classes. (Our classification routine treats only two populations at present, so we adopt a sequential testing procedure to determine in which of the classes event 361575 belongs.) In addition to proper treatment of the discriminant distributions, the Bootstrap GLR method allows the overall cost of misclassification to be minimized or, alternatively, the false alarm rate associated with misclassifying a particular type of event to be controlled, e.g., the percentage of actual nuclear explosions that are identified incorrectly. The latter

case is a particularly important aspect, since for most monitoring applications we want to limit the number of undetected nuclear explosions to a very small number.

The test statistic for classification is similar except that now it is given by the ratio of the maximized likelihood computed under the null hypothesis that the event belongs to one of the classes, to the maximized likelihood computed under the alternative hypothesis that the event belongs to the other class. Small values of the likelihood ratio indicate that the event does not belong to the first class. The bootstrap technique is used here as well to set the critical value of the test such that the false alarm rate is fixed. Figure 7 shows a schematic of this procedure. The distribution on the right is obtained by bootstrapping, where the new event is sampled from the EX population, while the distribution on the left is obtained by sampling the new event from the EQ population. The critical value is set such that there are only $100\alpha\%$ of the EXs in the tail that would be rejected falsely.

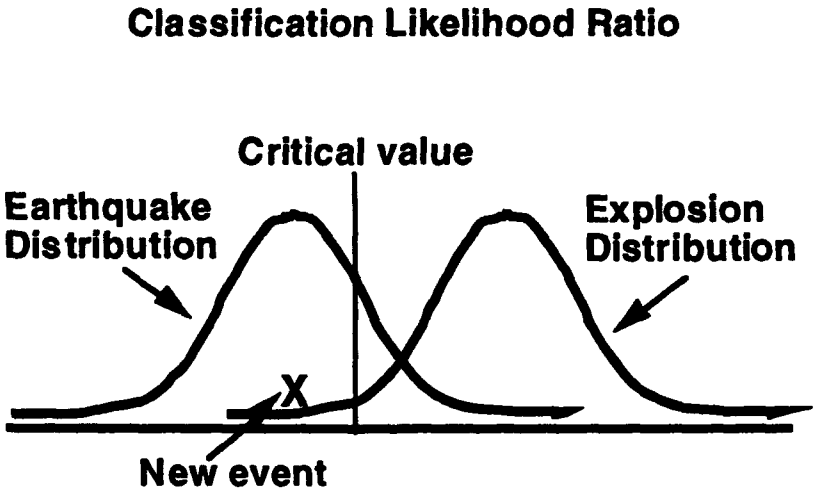

Figure 7. Schematic illustrating classification based on the likelihood ratio test.

It is important to understand what the results of these tests of hypothesis mean at a given significance level. Intuitively, the outlier test determines whether the event is similar or significantly different than the events in the training set, based on the discriminant values of the event being tested relative to the distribution of the training data. If the hypothesis is rejected, the outlier test makes no statement as to which other class of events the tested event might belong. The significance level is the probability that an event is rejected as belonging to the class of events in the training sample when it should not be rejected, i.e., when it actually belongs to the same population as the training sample.

For example, if an event is rejected as belonging to the class of nuclear explosions at the 0.025 significance level, then we can say that this event has been rejected as a nuclear explosion with a 2.5% probability of it being rejected falsely. Thus, if an event is rejected at a small significance level, the probability that a mistake was made is small. Unfortunately, the significance level of the test does not have a simple relation to the probability that the event was accepted when it should not have been. This probability depends on the unknown distribution of the other type of event.

The classification test is similar in that it determines whether the event in question should be rejected as belonging to a particular class of events, based on the training data. In this case, however, the test makes use of training data for two event types, allowing the event to be classified preferentially as one or the other type of event. The significance level, now set with respect to one of the two classes, is still the probability that a new event is rejected as belonging to that particular class when the event should not be rejected.

For example, suppose we use both nuclear explosion and earthquake training data to classify an event in question. If the event is rejected as belonging to the class of nuclear explosions, with the significance level set at 0.025 with respect to the explosion class, then we can say that the probability of rejecting this event falsely as a nuclear explosion is 2.5%. Thus the event is classified in this case as looking more like an earthquake than an explosion with only 2.5% probability of it actually being an explosion. As before, the significance level does not have a simple relation to the probability that the event is correctly identified as an earthquake given that it actually was an earthquake. (However, this probability can be estimated straightforwardly, based on the critical value of the test and the distribution of the discriminants for the EQ class.)

Furthermore, a rejection that it was an explosion does not mean that the event could not be of some other type not included in the training set, only that its classification as an earthquake is preferred to classification as an explosion in this example. However, the test does make a strong statement about the event not being an explosion. So in this sense, rejections of hypothesis at fixed significance level are much more meaningful in order to say that an event is not of a given type than it is to say that the event belongs to a particular class.

3.2. Preliminary training set analyses

Since the statistics of most discriminants in general are quite complicated and the validity of classification results depend on their proper treatment, we apply several tests to training sets to determine whether necessary assumptions hold. Although the Bootstrap GLR methods do not require that features are normally distributed, implementation of the tests simplify greatly if this assumption is made. In most cases, however, discriminants do not obey normal statistics. To remedy this situation we first apply two hypothesis tests to determine whether the data are normal. The Wilk-Shapiro test (Shapiro and Wilk, 1965) is powerful for detecting skewed distributions and the Anderson-Darling test (Anderson and Darling, 1954) is powerful for detecting long-tailed distributions. If the data are rejected by either test at fixed significance level, then the features are transformed using Box-Cox transformations. Special cases of Box-Cox transformations are the square root and the logarithm. In general, the procedure automatically finds a power-law transformation that maximizes the normal likelihood function of the transformed data. Once transformed, the data sets are tested again for normality. Although these transformations do not ensure normality in every case, we found that all of the features used here are accepted as normal after applying the transformations.

An example of this analysis is shown in Figure 8. The histogram plots are of Pn/Sn[max; 4-6 Hz] values for the Steigen EQs (left) and Kola QBs (right). The lower frames were produced before the feature values were transformed and the upper frames correspond to the values after applying the Box-Cox transformation. The legends in each frame give the results of the tests for normality. Before applying the transformation, the distributions for both the EQs and QBs are skewed and, hence, normality was rejected. The skew has been removed from the transformed variable and normality is now accepted. Quantile-Quantile (Q-Q) plots for the same case are shown in Figure 9. Q-Q plots are useful for visualizing whether data obey normal statistics. If the data are approximately normal, the values of the sample quantiles computed from the data (red squares) should correspond to the quantiles of a normal distribution (line). Figure 9 shows that the transformed data are normal to a good approximation. Similar results were also obtained for the other discriminants used in our analysis.

Robust application of classification tests also depend on whether covariance matrices for the features are equal for the various event types. If sample sizes are small or covariance matrices are not significantly different, using a classification method based on a pooled

estimate of a single covariance matrix is more robust. If the covariance matrices are significantly different, estimating separate covariance matrices leads to a classification test with greater power (e.g., Seber, 1984). Thus, we have implemented and applied a hypothesis test based on the F-distribution to determine whether covariance matrices are equal. Because there were only 3 events in the NZ EX training set, the covariance matrices were treated as equal for all tests involving this set. For classification into Kola QB or Steigen/Mid-Atlantic Ridge EQ classes, the covariance matrices were found to be unequal and, hence, were treated accordingly in the classification test.

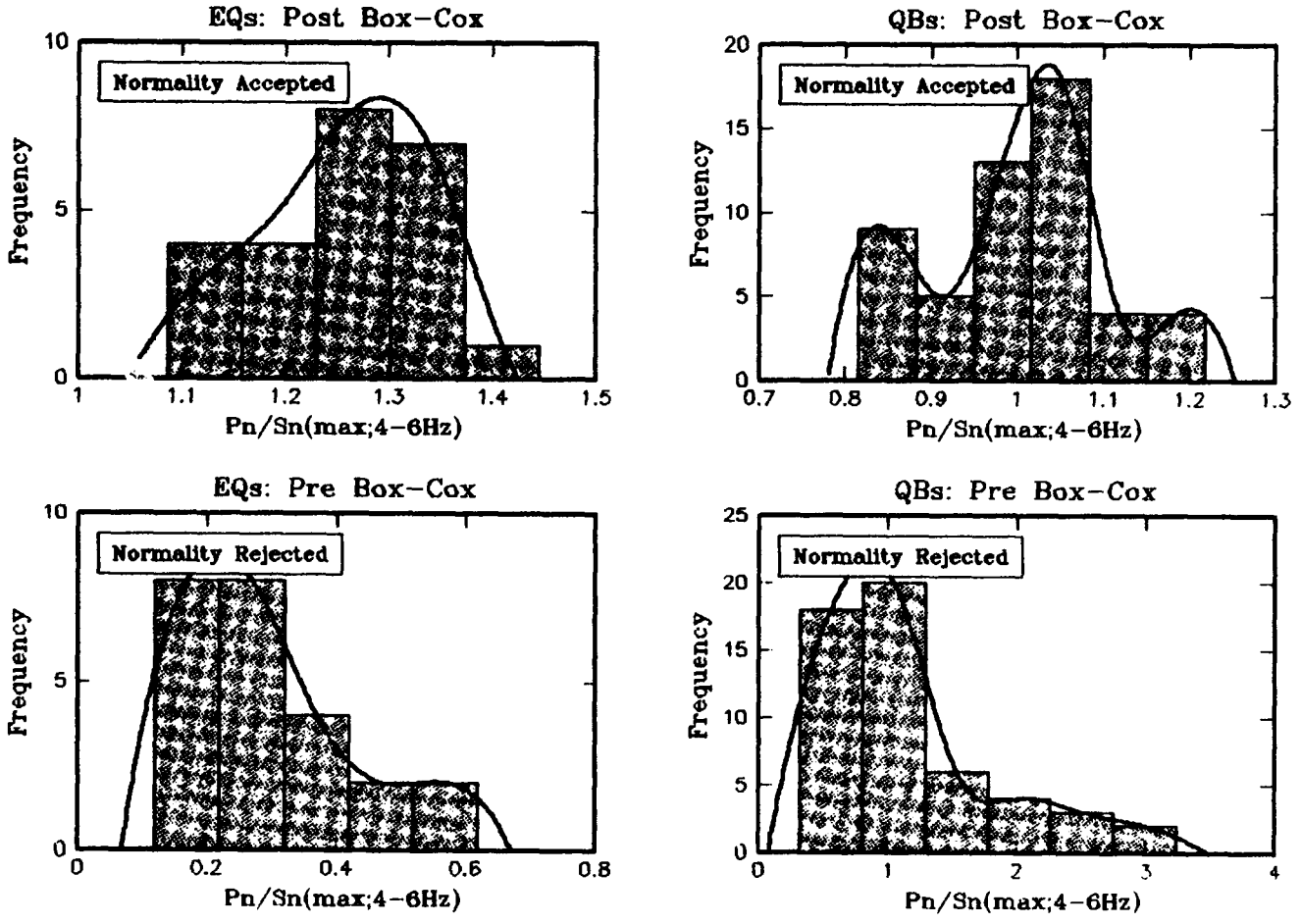

Figure 8. Histogram plots of Pn/Sn[max; 4-6 Hz] for Steigen EQs (left) and Kola QBs (right), before (lower) and after (upper) applying the Box-Cox transformation. The legends in each frame contain the results of the tests for normality.

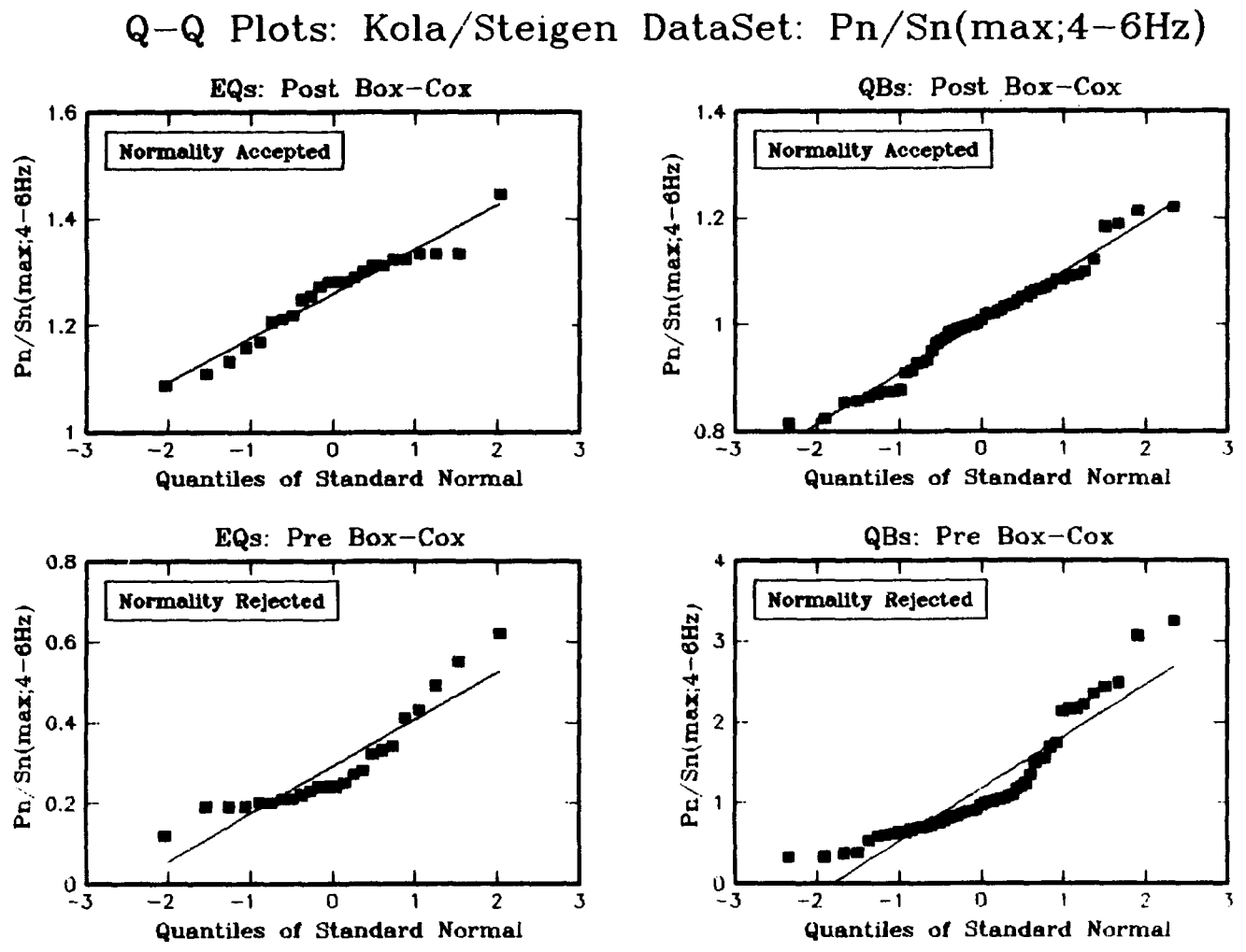

Figure 9. Q-Q plots of Pn/Sn[max; 4-6 Hz] for Steigen EQs (left) and Kola QBs (right), before (lower) and after (upper) applying the Box-Cox transformation. The legends in each frame contain the results of the tests for normality.

4. RESULTS

After first performing the preliminary training set analysis just described, we performed the following tests of hypothesis on event 361575:

Outlier Tests:

- Outlier Test #1: tested as an outlier of the NZ EX population
- Outlier Test #2: tested as an outlier of the Kola QB population
- Outlier Test #3: tested as an outlier of the Steigen EQ population
- Outlier Test #4: tested as an outlier of the Mid-Atlantic Ridge population

Classification Tests:

- Classification Test #1: classified into NZ EX or Kola QB populations
- Classification Test #2: classified into Kola QB or the combined EQ populations

For the classification tests we also considered the Steigen and Mid-Atlantic Ridge EQs separately and found that the results remain roughly the same. We also examined the range of significance levels for which we reject a particular hypothesis. For some cases the limiting significance levels at which particular hypotheses were rejected were much higher than commonly acceptable. Recall that if an event is rejected at a relatively high significance level, the probability that an error was made is accordingly high. Although the standard testing approach is to fix the significance level, this analysis provides useful information regarding the range of significance levels for which a particular hypothesis is rejected or accepted. Last, we also provide classification results using the same GLR method, but setting the classification rule such that the overall misclassification rate is minimized.

4.1. Outlier Test Results

Outlier Test #1. Since the training sample size of NZ EXs is so small, the number of features that can be used is two or less; otherwise, the sample covariance matrix used in the likelihood ratio of the outlier test is singular. In fact, Seber (1984) recommends that only one discriminant be used for such small samples since it is very difficult to obtain a reasonable estimate of a correlation coefficient. Thus using only ARA0 Pn/Sn[max;8-16] for the 3 NZ EXs, event 361575 was tested and rejected as an EX at the 0.025 significance level. In fact it is also rejected at the 0.015 significance level. This is significant statistical evidence that event 361575 is different than previous NZ EXs.

Outlier Test #2. Using the outlier test trained on 53 Kola QBs with 5 features, ARA0 Pn/Sn[max] at 4-6, 5-7, 6-8, 8-10 and 8-16 Hz, event 361575 is accepted as a Kola QB at the 0.025 significance level. It is rejected only if the significance level is greater than or equal to 0.34. This means that we would reject 361575 as belonging to the same population as Kola QBs only if we are willing to falsely reject 1 out of 3 actual Kola QBs as not being a Kola QB. So for a wide range of reasonable significance levels the evidence is insufficient to reject the hypothesis that this event is from the same population as Kola QBs.

Outlier Test #3. Using the outlier test trained on 24 Steigen EQs with the same 5 features as in the previous test, event 361575 is rejected as a Steigen EQ at the 0.025 significance level. This is strong statistical evidence that 361575 is not from the same population as Steigen EQs.

Outlier Test #4. As for the first test, the training sample size of 5 Mid-Atlantic Ridge EQs is small. Using only ARA0 Pn/Sn[max;8-16] for these 5 EQs, event 361575 is not rejected as a Mid-Atlantic Ridge EQ at the 0.025 significance level, but is at the 0.035 significance level and above. This suggests that event 361575 is different than previous Mid-Atlantic Ridge EQs, with a 0.035 probability that an actual Mid-Atlantic Ridge EQ would be falsely rejected.

Results are represented graphically in Figure 10 for the 4 outlier tests. The distributions shown are smoothed histograms of the likelihood ratio (LR) obtained by bootstrapping the corresponding training set. The vertical lines shown correspond to critical values of the tests for various significance levels given in the lowest legend. The LR for event 361575 is denoted by the red triangle marker. The training set and discriminants are listed in the upper legends. Figure 10 clearly shows that the LR for event 361575 is in the tails of the EX and EQ LR distributions, while it lies roughly in the middle of the LR distribution for the Kola QBs.

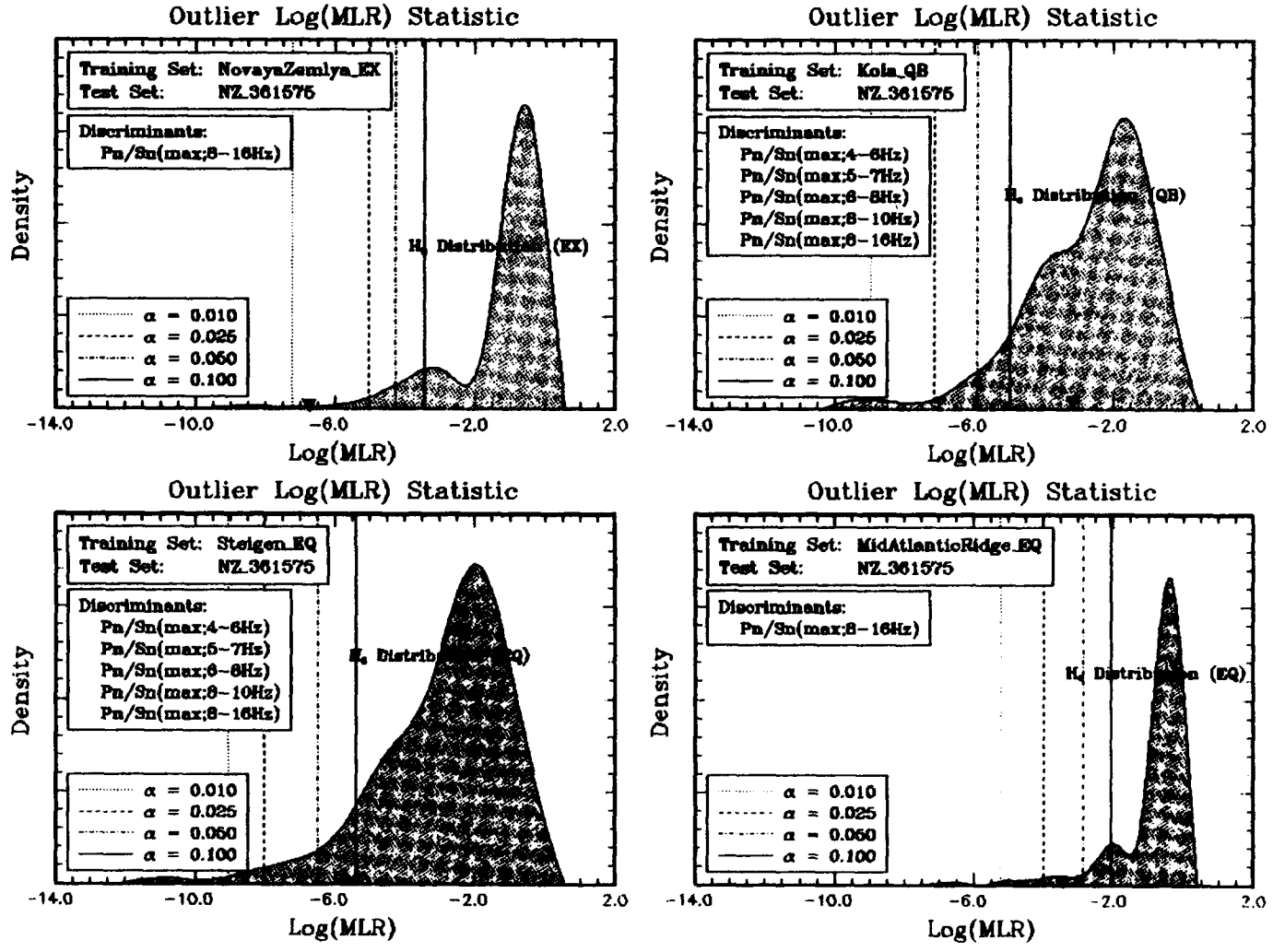

Figure 10. Graphical representation of the four GLR outlier tests. The distributions shown are smoothed histograms of the likelihood ratio (LR) obtained by bootstrapping the corresponding training data. The vertical lines represent critical values of the test for various significance levels listed in the lowest legend. The LR for event 361575 is depicted by the red triangle.

4.2. Classification Test Results

Classification Test #1. Using the GLR classification test trained on the 3 NZ EXs and 53 Kola QBs with ARA0 Pn/Sn[max] at 4-6, 5-7, 6-8 and 8-16 Hz, event 361575 is rejected as an NZ EX at the 0.025 significance level. It is also rejected at the 0.01 significance level. This is strong statistical evidence that 361575 is not from the same population as NZ EXs, with preferred classification as a Kola QB. (Note that the assumption of equal covariance matrices was used for this test. This allowed a pooled estimate of the covariance matrix to be computed for the four features using all 56 samples.)

Classification Test #2. Since event 361575 was classified as a Kola QB in the first of these tests, it was then tested as belonging to either the Kola QB or the combined Steigen/Mid-Atlantic Ridge EQ sets. Using the GLR classification test, based on these training sets and the same four features, event 361575 is rejected as an EQ at the 0.025 significance level, set with respect to the EQs. It is also rejected at the 0.01 significance level of falsely rejecting an EQ. Again, this is strong statistical evidence that 361575 is not from the same population as the Steigen or Mid-Atlantic Ridge EQs; classification as a Kola QB is preferred. It does not imply that event 361575 could not also belong to some other class of events that are not included in the training sets.

Results of these tests are represented graphically in Figure 11. The distributions shown are smoothed histograms of the LR, bootstrapped from the training data, where the H_0 (null) distribution corresponds to LRs if the new event is from the first population and the H_1 (alternative) distribution corresponds to LRs if the new event is from the second population. As for the graphical representations of the outlier tests, the critical values of the tests for various significance levels are depicted by the vertical lines. The thick vertical line is the value of the LR which minimizes the total misclassification rate. Classification based on minimizing overall misclassifications also allocate 361575 to the QB population.

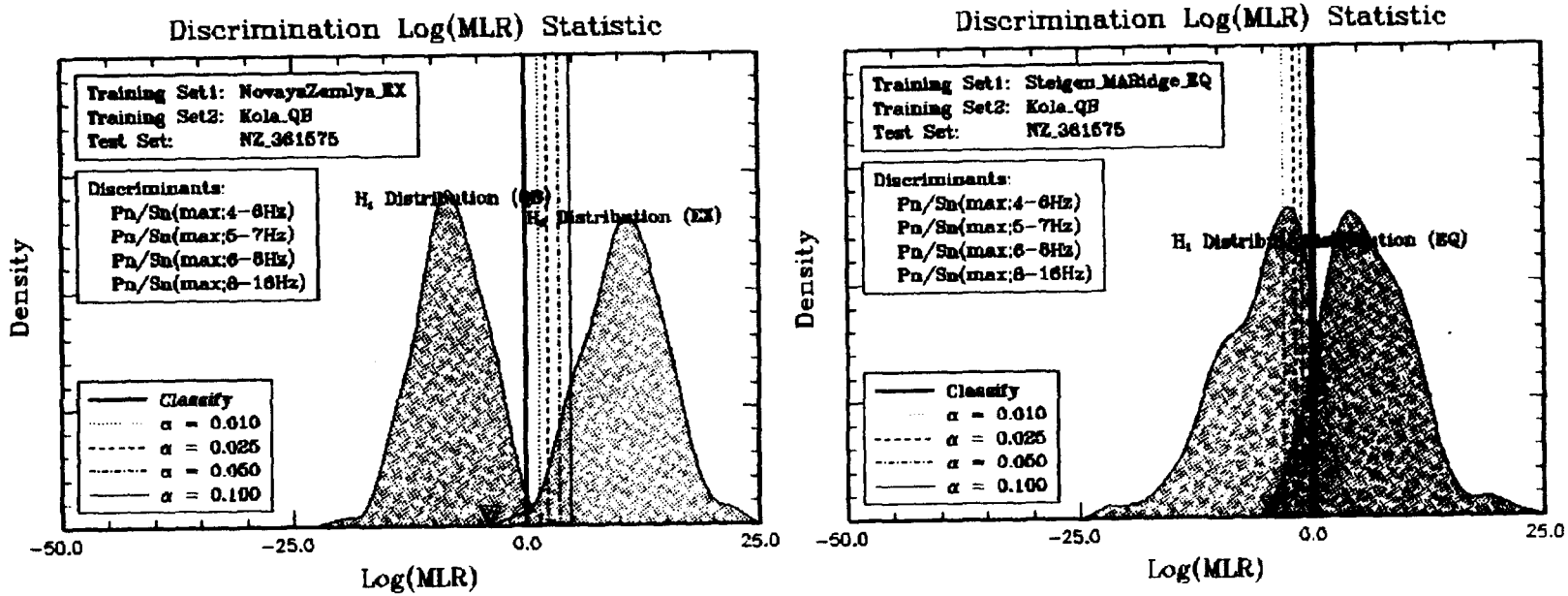

Figure 11. Graphical representation of the GLR classification tests. The distributions shown are smoothed histograms of the LR obtained by bootstrapping. The vertical lines represent critical values of the test for various significance levels listed in the lowest legend. The thick vertical line corresponds to the critical value which minimizes the total misclassification rate. The LR for event 361575 is depicted by the red triangle.

5. CONCLUSIONS AND RECOMMENDATIONS

With the exception of the outlier test, trained on Pn/Sn[max;8-16] for the 5 Mid-Atlantic Ridge EQs, the results show that event 361575 is rejected statistically, by all of the tests at 0.025 significance as belonging to the EX or EQ populations. In most cases, these results also held for smaller significance levels, e.g., 0.01 for both of the classification tests. Event 361575 is also rejected as a Mid-Atlantic Ridge EQ if we are willing to accept a false alarm rate of 3.5% or larger.

The outlier and classification results also show that there is insufficient evidence to reject event 361575 as belonging to the Kola QB population for all of the relevant tests at 0.025 significance. Classification based on minimizing the total misclassification rate clearly allocates event 361575 to the QB population. Thus, based on these tests and the training data for the three classes considered, event 361575 is classified as belonging to the Kola QB population.

Note that these results do not imply that this event was necessarily a QB, only that this classification is strongly preferred over the alternatives and there is insufficient evidence to reject it as a Kola QB, based on the training data. Since we do not know the actual distribution from which this event was produced, we cannot estimate the probability that the event was classified as a Kola QB when it might, in fact, be something else. Thus, the strongest conclusion that we can draw, based on the data, is that event 361575 was not a nuclear explosion similar to others at NZ nor an earthquake similar to those in the Steigen region or in the direction of the Mid-Atlantic Ridge.

Although our quantitative measures are substantially different, our qualitative results are the same as those of Baumgardt (1993), who also concluded, based on a neural net approach and a similar set of discriminants, that event 361575 looks most like a Kola QB. This is not surprising since the training sets are effectively the same and no matter how the amplitude ratios for event 361575 are examined, plotted or statistically tested, they look similar to the Kola QB amplitude ratios.

A key question remaining to be answered is whether these discriminants based on the observed seismic signals are truly characteristic of the source. Our results should be tempered by the caveat that there may be significant path differences to ARCESS from the various regions which warrant investigation. For example, Pn/Sn[max] ratios for explosions differ dramatically for the NZ to ARCESS path as compared to the NZ to

NORESS path. Even though all discriminants were obtained from signals recorded on a common instrument at ARCESS for our study, relatively small path differences could yield different results for the tests comparing event 361575 to Kola or Steigen events.

Note, however, that our outlier test based on the 3 NZ EXs is not subject to this caveat as are the tests using data from other regions performed by us and others. Thus until path differences can be investigated suitably, this test may provide the only reliable statistical evidence that event 361575 was not a nuclear test. Even so, a larger nuclear explosion training set for NZ events is desired to strengthen our conclusions. Furthermore, as noted by Ryall (1993) and Sereno (1993), this result should also be tempered by the caveat that, even if event 361575 was a nuclear explosion, there are likely to be significant differences in the signal generated by that event as compared to those generated by the three known nuclear explosions at NZ, based simply on source size. This issue also warrants future investigation.

As a final comment, the relatively limited set of discriminants used here does not take full advantage of the generalized likelihood ratio approach which can also treat interesting discrete discriminants (contextual features and others) such as offshore/onshore, seismicity, presence of cepstral peaks, etc. It is not clear whether these features would provide additional useful information but they could certainly be included in our procedure for more complete analysis.

REFERENCES

Anderson, T.W. (1984). An Introduction to Multivariate Analysis, Second Edition, John Wiley and Sons, Inc., New York.

Anderson, T.W. and D.A. Darling (1954). A Test of Goodness-of-Fit, *J. Am. Stat. Assoc.*, 49, 765-769.

Bache, T.C., S.R. Bratt, J. Wang, R.M. Fung, C. Kobryn and J.W. Given (1990). The Intelligent Monitoring System, *Bull. Seism. Soc. Am.*, **80**, 1833-1851.

Baek, J., H. L. Gray, and W. A. Woodward (1992). A Generalized Likelihood Ratio Test in Outlier Detection or Script Matching, submitted to *J. Am. Stat. Assoc.*, Southern Methodist University.

Baek, J., H. L. Gray, W. A. Woodward and M.D. Fisk (1993). A Bootstrap Generalized Likelihood Ratio Test in Discriminant Analysis, submitted to *J. Am. Stat. Assoc.*, Southern Methodist University.

Baumgardt, D.R. (1992). Investigation of Seismic Discriminants in Eurasia, Final Technical Report SAS-TR-92-81, ENSCO, Inc., Springfield, VA.

Baumgardt, D.R. (1993). Private Communication.

Baumgardt, D.R., J. Carney, M. Maxson and S. Carter (1992). Evaluation of Regional Discriminants using the Intelligent Seismic Event Identification System, Semi-Annual Technical Report SAS-TR-93-38, ENSCO, Inc., Springfield, VA.

Baumgardt, D.R., G. Young and K. Ziegler (1991). Design and Development of the Intelligent Seismic Event Identification System: Design Considerations and Processing for Regional Event Identification. Technical Report PL-TR-91-2211, Phillips Laboratory, Hanscom AFB, MA.

Fisk, M.D., G.L. Gray and G.D. McCartor (1993). Applications of Generalized Likelihood Ratio Tests to Seismic Event Identification, MRC-R-1444, to appear as a Phillips Laboratory Techical Report, Mission Research Corp., Santa Barbara, CA.

Gray, H.L., W. A. Woodward, G.D. McCartor and M.D. Fisk (1993). A Bootstrap Generalized Likelihood Ratio Test in Discriminant Analysis, to appear in *Proceedings of the Fifteenth Annual Seismic Research Symposium*, Phillips Laboratory, Hanscom AFB, MA.

Johnson, R.A. and D.W. Wichern (1988). Applied Multivariate Statistical Analysis, Prentice Hall, New Jersey.

Ryall A., (1993). Private Communication.

Seber, G.A.F. (1984). Multivariate Observations, John Wiley, New York.

Sereno, T.J. (1993). Private Communication.

Shapiro, S.S. and M.B. Wilk (1965). An Analysis of Variance Test for Normality (Complete Samples), *Biometrika*, 52, 591-611.